ISSN 0140-3818
SSSU 46

WIND TUNNEL INVESTIGATION OF THE INFLUENCE OF PROPELLER LOADING ON SHIP RUDDER PERFORMANCE

A.F. Molland and S.R. Turnock

Ship Science Report No. 46

March 1991

ISSN 0140-3818
SSSU 46

WIND TUNNEL INVESTIGATION OF THE INFLUENCE OF PROPELLER LOADING ON SHIP RUDDER PERFORMANCE

A.F. Molland and S.R. Turnock

Ship Science Report No. 46

March 1991

WIND TUNNEL INVESTIGATION OF THE INFLUENCE OF PROPELLER LOADING ON SHIP RUDDER PERFORMANCE

by

A.F.Molland and S.R.Turnock

Ship Science Report No 46

University of Southampton

March 1991

SUMMARY

A detailed investigation has been carried out into the interaction between a ship rudder and propeller combination. The tests used the 11' x 8' low speed wind tunnel at the University of Southampton. This report presents results for a series of three All-Movable rudders with the same mean chord of 667mm and NACA0020 sections, but with varying aspect ratio and taper ratio. A four-bladed, 800mm diameter, adjustable pitch propeller was used. This propeller is a modified version of the Wageningen B4.40 series. Open-water results for the modified design were validated against published data.

The test consisted of a series of parametric studies into the effect of the longitudinal distance between the propeller and rudder, propeller thrust loading, rudder aspect ratio, and rudder taper ratio. A five-component strain-gauge dynamometer was used to measure lift, drag and three moments on the rudder and a rotating strain gauge dynamometer the developed thrust and torque of the propeller. In addition, both spanwise and chordwise pressure distributions were measured on the rudder surface. Propeller revolutions were varied between 0 and 3,000 rpm and tunnel wind speeds up to 20m/s were used.

Results are presented in the form of non-dimensional coefficients of lift(C_L), drag(C_D), spanwise(CP_s) and chordwise(CP_c) position of the centre of pressure variation with incidence for the rudder. The influence of rudder on propeller performance is given in terms of non-dimensional thrust(K_T) and torque(K_Q) coefficient variation with advance ratio (J). The surface pressure measurements on the rudder are presented as both a spanwise distribution of the local lift coefficient (C_L) and as a surface pressure distribution.

Principal findings of the work were that: increasing propeller thrust loading increased rudder sideforce while delaying stall. For constant rpm the presence of the rudder alters the propellers developed thrust and torque characteristic. Changes in the longitudinal separation of the rudder and propeller had only a minimal effect on the sideforce characteristics of the rudder. The information presented should be of considerable use in numerically modelling the flow interaction and in the development of more advanced ship manoeuvring simulations.

TABLE OF CONTENTS

LIST OF FIGURES

LIST OF TABLES

NOMENCLATURE

A	-	Rudder Area (m^2)
AR_g	-	Rudder Geometric Aspect Ratio
c	-	Mean Rudder Chord (m)
s	-	Rudder Span (m)
c_{tip}	-	Rudder Tip Chord (m)
c_{root}	-	Rudder Root Chord (m)
D	-	Propeller Diameter (m)
Nc	-	Corrected rpm
Nm	-	Measured rpm
n	-	revolutions per second
Uo	-	Freestream Wind speed (m/s)
d	-	Aerodynamic Drag (N)
L	-	Aerodynamic Lift (N)
N	-	Normal Force (N)
Mx	-	Aerodynamic Moment about x-axis (Nm)
My	-	Aerodynamic Moment about y-axis (Nm)

Mz	-	Aerodynamic Moment about z-axis (Nm)
V	-	Vertical Distance of Dynamometer Measurement Centre to Rudder Root (m)
W	-	Horizontal Distance of Dynamometer Rudder Stock From Rudder Leading Edge (m)
X	-	Longitudinal Separation of Rudder Leading Edge and propeller plane of rotation (m)
Y	-	Longitudinal Separation of Rudder Stock and propeller plane of rotation
Q	-	Torque (Nm)
T	-	Thrust (N)
V_L	-	Rudder Dynamometer Lift Voltage (μ v)
V_D	-	Rudder Dynamometer Drag Voltage (μ v)
V_{Mz}	-	Rudder Dynamometer M_z Voltage (μ v)
V_{Mx}	-	Rudder Dynamometer M_x Voltage (μ v)
V_{My}	-	Rudder Dynamometer M_y Voltage (μ v)
V_{Dp}	-	Scanivalve Dynamic Pressure Voltage (v)
V_P	-	Scanivalve Port Voltage (v)
V_{Po}	-	Scanivalve Zero Wind Voltage (v)
V_Q	-	Torque balance output voltage (μ v)
V_{Qo}	-	Torque dynamic zero voltage (μ v)
V_{Qs}	-	Torque Supply Voltage (v)
V_T	-	Thrust balance output voltage (μ v)
V_{To}	-	Thrust dynamic zero voltage (μ v)
V_{Ts}	-	Thrust supply voltage (v)
C_Q	-	Torque calibration slope (Nm/μ v)
C_T	-	Thrust calibration slope (N/μ v)
C_l	-	Lift coefficient per unit span
C_L	-	Non-dimensional Lift (sideforce)
C_N	-	Normal force per unit span
C_d	-	Drag coefficient per unit span
C_D	-	Non-Dimensional drag
CP_c	-	Chordwise centre of pressure
CP_s	-	Spanwise centre of pressure
C_{Mz}	-	Non-dimensional Moment about rudder stock
C_{Mx}	-	Non-dimensional moment about rudder root chord
C_{My}	-	Non-dimensional moment about y axis
C_p	-	Non-Dimensional Pressure Coefficient
K_T	-	Thrust Coefficient ($T/\rho\ n^2D^4$)
K_Q	-	Torque Coefficient ($Q/\rho\ n^2D^5$)
η	-	Efficiency ($J\ K_T/2\pi\ K_Q$)
J	-	Advance Ratio (V/nD)
ρ	-	Air Density (Kg/m3)

1. INTRODUCTION

A propeller upstream of a ship rudder accelerates and rotates the inflow onto the rudder. Additionally the ship rudder both blocks and diverts the flow arriving at the propeller. The physical modelling of these interactions is, at present, limited by the availability of good experimental data for a wide range of representative ship rudder and propeller combinations.

This report presents results from a detailed wind tunnel investigation into the performance of a series of rudders downstream from a propeller. The experiments were carried out in the University of Southampton's 11' x 8' low-speed wind tunnel. The use of air as a working fluid rather than water eases significantly the measurement of data and the test procedures. Propeller cavitation cannot be studied, but this is not considered a significant factor in the context of the current investigation.

The aim of this report is to provide a comprehensive presentation of the results obtained in four weeks of tunnel testing carried out in March and August of 1990. Section 2 details the rudder and propeller models used. The test rig design and the tests carried out are described in Section 3. Sections 4 and 5 respectively detail the data reduction and its presentation. Section 6 discusses the results and conclusions and recommendations drawn from the test results are presented as Section 7.

2. DESCRIPTION OF MODELS

2.1 Rudders

A series of three all-movable rudders, all with a mean chord of 667mm and a NACA 0020 section, were manufactured for these tests. A detailed description of the method of manufacture of the rudder models is given in Turnock [1]. Table I presents the particulars for each of the rudders and Figure 1 their overall dimensions. Rectangular Rudder No. 3 is Rudder No 2 with a 200mm extension attached to its tip to increase its span to 1.2m. All three models had pressure tappings to give complete coverage of the

rudder surface, as detailed in figure 1. The pressure tappings were manufactured using the technique developed by Molland [2]. This consists of mounting small-bore plastic tubing in routed grooves running from rudder root to tip. The rudder surface is made smooth by filling over the tube/groove and 1mm diameter holes are drilled through into the tube at the desired span-wise locations. One end of each tube is sealed and the other attached to a port of a rotary pressure transducer (scanivalve). Only one hole on a tube is exposed at a time the others being sealed with clear adhesive tape.

For the tests carried out all three rudders had a roughness strip with its leading edge attached at a distance of 5.7% chord from the leading edge of the chord on both sides of the rudder. The roughness strips were manufactured from 12mm wide double-sided tape densely covered with 100 Grade carborundum grit(0.15mm diameter).

2.2 Propeller

A representative propeller design, based on the Wageningen B4.40 series, was chosen. A four-bladed propeller with a diameter of 800mm and a blade area ratio of 0.4 was manufactured. Modifications were made to the basic Wageningen design. These modifications are detailed in Turnock [3] and consisted of altering the blade root shape to allow an adjustable pitch design with four separate blades and a split hub, removing rate and decreasing blade sweep to reduce centripetal loading moments at the root, and increasing the hub/diameter ratio from 0.167 to 0.25. Overall propeller details are summarised in Table II. Figure 2 shows a comparison of the modified blade shape and the basis Wageningen B4.40.

The split hub was manufactured from aluminium alloy and a positive clamping action allows the four blades to be rotated to the desired pitch ratio setting. The four blades were manufactured using hybrid carbon/glass fibre composite laid up in the same split female mould to produce identical blades. The production of the composite blades is detailed in Molland and Turnock [4] and the machining of the split female mould in Turnock [3]. Figure 3 shows views of the four blades, split hub and the final assembly.

The hub nose cone was made from glass fibre and its dimensions and those of the hub are given in Turnock [1]. In appearance the hub/blade root region is very similar to that of a typical controllable pitch propeller.

3. APPARATUS AND TESTS

3.1 General

The tests were carried out in the 11' x 8' low-speed wind tunnel at the University of Southampton. The overall rig for testing the interaction of ship rudder and propellers is shown in Figure 4. The rig consists of two independent units which allow free-stream(open-water) tests to be carried out independently on rudders and propellers as well the investigation of their interaction.

3.2 Rudder Rig/Dynamometer

A simple modification to the rig originally developed for determining the free stream performance of semi-balanced skeg rudders (Molland [5]) was required to allow for its use in the University of Southampton's 11' x 8' low speed wind tunnel. This consisted, as shown in Figure 5, of a welded steel extension piece fitted between the cast steel pedestal attached to the floor and the five-component strain gauge dynamometer. The dynamometer, the design and calibration of which is given in Molland [6], allows the forces and moments on both all-movable and semi-balanced skeg rudders to be measured. The rudder and/or skeg stems are bolted directly to the dynamometer. The dynamometer is levelled and adjusted vertically so that there is a small gap of approximately 2.5mm (0.004c) between the rudder root and the working section floor.

3.3 Propeller Rig

Figure 6. shows a side view of the propeller rig installed in the 11' x 8' wind tunnel. The installation process is described in Turnock[1]. The tests detailed in this report were carried out with the propeller's axis of rotation 600mm above the wind tunnel floor and in the flow direction. The propeller rotates anti-clockwise when viewed from aft (looking

upstream). The aerofoil fairing around the propeller drive shaft support tubes and drive belt has a NACA63040 profile with a chord of 550mm and 25% maximum thickness. The trailing edge of the fairing is located 0.5 of the propeller diameter (400mm) upstream of the propeller's plane of rotation. The fairing around the propeller drive shaft has a diameter equal to the minimum hub diameter(180mm). The hub cone and nose cone have an identical profile, the dimensions of which are given in Turnock[1].

An in-line strain gauge dynamometer mounted close to the propeller was used to measure the delivered thrust and torque. The design and static calibration of this dynamometer is detailed in Molland and Turnock[7]. The two measurement components of the dynamometer are connected via a slip-ring assembly to Fylde Bridge balance units with a built in stabilised power supply. The bridge balance output voltage is measured directly (without amplification) using a Schlumberger Minate Digital Voltmeter. Data acquisition is controlled by a Research Machines personal computer and results stored on a 3.5" floppy disk for subsequent analysis.

A Fuji Variable Frequency Inverter is used to control the 30kw electric motor. The propeller rpm can be continuously varied in small discrete steps between 0 and 3000 rpm. The controller has a voltage output proportional to its output supply frequency and hence propeller rpm. This voltage is recorded to give the propeller rpm for a given measurement of thrust and torque.

Tests were carried out at four windspeeds of 5m/s, 10m/s, 15m/s, and 20m/s. This speed was set using the wind tunnel speed controller and measured using a Betz manometer. For given propeller revolutions the wind speed controller was varied as necessary to compensate for the windspeed imparted by the propeller.

3.4 Data Acquisition System

The large number of individual data readings required the use of an automated system for data acquisition. The system used is based on that developed for measuring the performance of 2-D aerofoil sections (Turnock[8]). A schematic of the data acquisition

system is shown in Figure 7.

Data is recorded from the six-component strain-gauge dynamometer which measures the forces and moments acting on the rudder. The propeller's torque and thrust are measured using the in-line strain gauge dynamometer. The propeller revolutions are measured indirectly via a voltage proportional to frequency generated by the Electric Motor Controller. This was modified in subsequent tests whereby revs. were obtained from a shaft drive tachometer. Pressure measurements over the surface of the rudder are obtained using a compressed air stepping Scanivalve which for each step exposes each of four differential pressure transducers to one of 36 input ports. This allows pressure data to be measured from a maximum of 144 individual pressure tubes.

The measurement component of the system is an accurate digital voltmeter connected to one of 15 input channels. The voltmeter and input channels are controlled by software running on a Research Machines Nimbus via an IEEE connection. The stepping of the scanivalve is also controlled via an RS232c system connected to the PC. The computer provides data storage and backup through the use of twin floppy disk drives. For the March 1990 tests two of the four pressure transducers were used and in August 1990 all four transducers were used.

3.4.1 System Hardware

The data acquisition hardware used for the rudder and propeller rig was mainly existing equipment with well documented performance. The individual system components are described in Turnock[8] and the overall layout for data flow is given in Figure 7. Plug-socket connections and wiring boxes were used to allow rapid wiring of the system and to minimise problems with bad connections.

3.4.2 Acquisition Software

The software used for acquiring data and controlling the devices connected to the Nimbus PC is based on that developed for the 2-D aerofoil tests (Turnock[8]).

Executable programs were developed using the PROPASCAL dialect of Pascal as a wide variety of procedures were available for driving the devices connected to the PC.

To ease subsequent data analysis a flexible menu driven system was used to allow the operator to define which particular subset of data was to be recorded. A graphical screen display was used to allow monitoring of the data acquired and to produce pressure plots on the screen. A single data file was created for each data recording session which contained all the information necessary to analyse the data. This data was stored in ASCII format and allowed a readable hardcopy to be made immediately after each test.

3.5 Tests

3.5.1 General

Results are reported from two sessions of testing in the 11' x 8' low-speed wind tunnel. The sessions consisted of 10 and 9 working days respectively. Running of the tunnel was restricted to between 9 am and 5 pm. Figure 9 (b) shows a dimensioned layout of the test setup for the rudder and propeller combination.

The basic propeller/rudder tests were carried out at a nominal Reynolds number of $0.4*10^6$, based on a free stream velocity of 10m/s. Velocities induced by the propeller at the higher thrust loadings led to effective Reynolds numbers of up to $1.0x10^6$ over much of the rudder based on rudder chord. English[14] indicated that a satisfactory Reynolds number, based on propeller diameter and rpm, to avoid scaling problems would be greater than $1.4x10^6$. The lowest rpm used in these tests was 800 rpm which for an 800mm diameter propeller gives a Reynolds number over the rudder of $1.53x10^6$.

3.5.2 March 1990

The first session in the tunnel was primarily for commissioning of the rudder and propeller rig. Tests were carried out using Rudder No. 1 in both an all-movable and

semi-balanced skeg configuration in the ahead configuration. Only one longitudinal separation with an X/D of 0.34 was used. The propeller was set to a pitch ratio of 0.95 for the whole series of tests. The results for the semi-balanced skeg configuration of Rudder No.1 are the subject of a separate report (Molland and Turnock [12]). A detailed survey of rudder surface pressure measurements were carried out on Rudder No 1 in its All-Movable configuration. These were conducted at a windspeed of 10m/s and propeller revolutions of 800, 1470, and 2150 rpm. Rudder incidence was varied in the range of -30° to 30°. Rudder force and propeller torque and thrust measurements were taken for a wider range of wind speeds (5m/s to 20m/s) and rudder incidence.

3.5.3 August 1990

A detailed parametric investigation of rudder longitudinal separation and rudder aspect ratio was carried out in the second wind tunnel session. All tests were carried out in the ahead condition. At a constant wind speed of 10m/s and for propeller rpm of 800, 1470, and 2100 all-movable rudder's No.2 and No.3 were tested at three longitudinal separations corresponding to X/D = 0.30, 0.39, and 0.52. Surface pressure and rudder force measurements were made at a nominal rudder incidence of -30°, 20°, -10°, 0°, 10°, 20°, and 30°. Rudder forces were additionally measured at rudder incidences between -35° and 40°. Propeller torque and thrust measurements were also recorded for all test points.

In addition to the parametric study, a free stream rudder investigation and open-water propeller tests were carried out. In each case, the redundant part of the rig was completely removed from within the tunnel working section.

A series of tests were carried out with nominal zero wind speed (J=0). This corresponds to the bollard condition and the case of low-speed manoeuvring. These results are presented in a separate report, (Molland & Turnock[13]).

4. DATA REDUCTION AND CORRECTIONS

4.1 Introduction

The software controlling the data acquisition generated a data file for each individual test. Data was stored as ASCII text which allowed a direct transcription of all data recorded to be obtained. The data recorded were the unprocessed voltages read from the voltmeter. The hard copy allowed 'by hand' verification checks to be made of the software used to analyse the test data files. The format of the test data file is described in Appendix 1. The data file format was designed to ease the subsequent analysis.

A suite of specific programs were written to manage the large amount of test data acquired from the two wind tunnel sessions. This allows effective interrogation of the database of test results to be carried out. The process of obtaining the desired information is illustrated in Figure 8. Data reduction has been divided into the three distinct tasks of rudder forces, rudder surface pressures, and propeller thrust and torque. The data reduction of the three categories is detailed in the following sections.

4.2 Rudder Forces

The five components of the rudder dynamometer are reduced using the method described in detail in Molland[6]. For each force component, the supply voltage Vs (v) and no-load voltage Vo (μv) are recorded for each test. With these, the measured bridge offset voltage V_T is recorded and then scaled to give a voltage V proportional to the applied force at the original calibrated supply voltage Vc:

$$V = (V_T - Vo) \times (\frac{Vs}{Vc})$$

The original calibration of the dynamometer (Molland[6]) quantified the interaction between the five components of the balance. The matrix expression given below uses the interaction matrix and incorporates the calibration constants to give the Lift and

Drag in Newtons, and the three Moments Mz, Mx, and My in Newton Metres.

$$\begin{bmatrix} L \\ d \\ M_z \\ M_x \\ M_y \end{bmatrix} = \begin{bmatrix} 0.338035 & -1.188x10^{-03} & -3.952x10^{-04} & -1.484x10^{-03} & -3.2605x10^{-03} \\ 2.12x10^{-05} & 0.252512 & -6.659x10^{-04} & 1.6823x10^{-03} & -9.901x10^{-04} \\ -1.82x10^{-04} & 2.845x10^{-04} & 3.9367x10^{-02} & 1.344x10^{-04} & 3.2x10^{-04} \\ 7.002x10^{-04} & -2.37x10^{-05} & -3.4036x10^{-03} & 6.3492x10^{-02} & 2.049x10^{-04} \\ -3.3x10^{-06} & 6.333x10^{-04} & 1.47x10^{-05} & -3.008x10^{-04} & 4.8468x10^{-02} \end{bmatrix} \begin{bmatrix} V_L \\ V_D \\ V_{Mz} \\ V_{Mx} \\ V_{My} \end{bmatrix}$$

Where V_L, V_D, V_{Mz}, V_{Mx} and V_{My} are the scaled and offset voltages in microvolts for the five dynamometer components.

For the results presented in this report only all-movable rudders were tested and, therefore, the forces measured are in the direction of the wind-tunnel axes. The appropriate sign conventions are illustrated in Figure 9. The non-dimensional coefficient form of the forces are obtained as shown:

$$C_L = \frac{L}{\frac{1}{2}\rho\, Uo^2 A}$$

$$C_D = \frac{d}{\frac{1}{2}\rho\, Uo^2 A}$$

$$C_{Mz} = \frac{M_z}{\frac{1}{2}\rho\, Uo^2 A\, c}$$

$$C_{Mx} = \frac{M_x}{\frac{1}{2}\rho\, Uo^2 A\, s}$$

$$C_{My} = \frac{M_y}{\frac{1}{2}\rho\, Uo^2 A\, s}$$

where ρ is the tunnel air density (kg/m3), Uo the free stream velocity (m/s), s the rudder span, c the mean rudder chord, and A the total rudder area (A = s .c). The position of the centre of pressure on the rudder in the spanwise and chordwise directions are obtained as follows:

$$CP_c = \left(\frac{M_z}{N} + W \right) \times \frac{100}{c}$$

$$CP_s = \left(\frac{M_N}{L} - V \right) \times \frac{100}{s}$$

where W is the distance of the dynamometer rudder stock from the leading edge and V the distance from the dynamometer measurement centre to the rudder root.

No corrections were made to the values of non-dimensional coefficients thus determined as effects such as tunnel blockage for the 11' x 8' working section were found to have a negligible effect for the rudder size and propeller diameter tested.

4.3 Surface Pressure

The four differential pressure transducers used in conjunction with the rotary scanivalve give a maximum of 144 individual pressure measurements for any test. The no-wind

pressure transducer output voltage V_{Po} was measured at the beginning of each test. The reference pressure connected to all four transducers was the static line of the main wind tunnel pitot-static probe. This line was also connected to one input port for each transducer to give a 'real' zero pressure difference value V_{Po}. The pitot line was connected to another input port to give a voltage V_{Dp} proportional to the total tunnel dynamic pressure.

For each pressure port measurement V_P, the non-dimensional pressure coefficient C_p is obtained directly as:

$$C_p = \frac{V_P - V_{Po}}{V_{Dp}}$$

This expression does not require an explicit value for the calibration constant of the particular pressure transducer, since the transducer has a linear response.

As the location of each pressure measurement on the rudder surface is known, integration of C_p around the chord of the rudder for a constant span allows the local non-dimensional Normal Force coefficient C_N to be calculated. This integration was carried out using a quadratic numerical procedure similar to Simpson's rule with variable spacing.

4.4 Propeller Forces

Manual calculation checks on propeller rpm were carried out using a handheld optical tachometer and compared with the value measured from the motor controller. Using a regression analysis the following correction to measured rpm was obtained:

$$N_c = 1.04N_m - 6.8\times10^{-06} N_m^2$$

where Nc and Nm are the corrected and measured rpm respectively. This expression was used to modify all the measured revolution speeds.

The static calibration carried out on the Torque-Thrust dynamometer gave a linear response to loading of both thrust and torque with negligible interactions (Molland and Turnock[7]). The calibration for both channels was carried out with a supply voltage of 7 volts. The slope constant (C_T) for the thrust channel was 0.0903 N/μv and for the torque channel (C_Q) of 0.01284 Nm/μv. The propeller is separated from the dynamometer by a short shaft supported on two axially unconstrained roller bearings. When the propeller is rotating these give minimal torque and thrust losses. However, when stationary, frictional resistance in these bearings is enough to produce spurious no-load voltages.

To overcome this problem a dynamic dynamometer zeroing procedure was developed. This method was based on the zero windspeed characteristic of the propeller where the Thrust (or Torque) is proportional to the square of the speed of revolution. At the beginning and end of each test run, the thrust and torque output voltages were measured for three rpm; typically 350, 650, and 1000. Using a least-squares linear regression (Kreyszig[9]) the true dynamometer 'zero' voltage at 0 rpm is found. The method was found to give good, repeatable data.

For each individual torque and thrust measurement both the balance output voltages, V_Q and V_T (μv), as well as the balance supply voltage, V_{Qs} and V_{Ts} (v), were recorded. This gives the measured thrust T (N) and torque Q (Nm) as:

$$T = (V_T - V_{To}) \times (\frac{V_{Ts}}{7.0}) \times C_T$$

$$Q = (V_Q - V_{Qo}) \times (\frac{V_{Qs}}{7.0}) \times C_Q$$

where V_{To} and V_{Qo} are the relevant dynamic zero voltages, the 7.0 is the value of calibration supply voltage in volts and C_T, C_Q are the calibration slopes.

Using the relevant windspeed V (m/s) and n (revs/sec) the advance ratio J is calculated as:

$$J = \frac{V}{n\,D}$$

where D is propeller diameter. The non-dimensional thrust coefficient(K_T) and torque coefficient(K_Q) are given by

$$K_T = \frac{T}{\rho\, n^2\, D^4}$$

$$K_Q = \frac{Q}{\rho\, n^2\, D^5}$$

where ρ is the air density. The propeller efficiency η is:

$$\eta = (\frac{J}{2\pi}) \times (\frac{K_T}{K_Q})$$

5. PRESENTATION OF DATA

The notation of rudder incidence and coefficients used in the presentation is given in Figure 9(a). The propeller rotates in an anti-clockwise direction when viewed from aft as shown in the diagram. Care must be taken to relate this correctly to the direction of positive rudder sideforce and rudder incidence.

The results of the tests are presented graphically. Figures 10 to 28 show force coefficients, centre of pressure chordwise(as a percentage of mean chord from its leading edge) and centre of pressure spanwise(percentage of span from rudder root) versus rudder angle of attack. The data are presented in terms of J values rather than directly as thrust loadings (K_T/J^2). This is to eliminate ambiguity between the use of the nominal free-stream (open water) thrust loading and the actual thrust loading in the presence of the rudder. The latter is larger than that in the freestream for the same free stream J value. For completeness, free stream propeller K_T and K_Q values are presented in Figure 52. Figures 53 to 55 quantify the influence of the rudder and longitudinal separation on the experimentally measured propeller thrust coefficient K_T, which may include spinner loading effects.

In Figures 29 to 51 the distribution of local chordwise two-dimensional normal force coefficients over the complete rudder span are shown for the range of rudder incidence tested. The C_N presented is for unit chord, not actual chord (0.667). It is assumed that the local C_N at the root is equal to that at the next inboard section and that at the rudder tip C_N is zero.

The rudder surface pressure distributions for the three all-movable rudders are given as Figures 56 to 76 and are for the three Advance Ratios of 0.35, 0.51 and 0.94 tested. Each figure presents the pressure distribution at each spanwise station for the range of rudder incidences tested. The spanwise stations are numbered as shown in figure 1 which includes the actual spanwise location. The section nearest to the rudder root is at the bottom of the figure and that near the tip at the top. The columns of pressure plots are presented in order from left to right of increasing rudder incidence from -30° to +30°. The x-axis of the individual pressure plots is given as a percentage of the local chord

between 0 and 100%. The y-axis is in terms of C_p, with the convention of negative pressure in the positive (upward) direction. The y-scale increment is held constant at 5 for all plots. The dotted line represents , as per the axis convention of figure 9, the pressures on the positive y side of the rudder and the solid line those on the negative y side.

Appendix 2 tabulates all the rudder dynamometer data obtained, averaged and used in the presentation of results.

6. DISCUSSION OF RESULTS

6.1 Rudders in Freestream

Figure 10 presents free stream results for Rudders No. 2 and 3 together with those obtained for the similar although swept rudder tested in the same rig and reported in Goodrich & Molland [10].

The results are very similar providing a validation of the set up and data acquisition procedures for the current tests. Also, the small increase in C_L with increase in aspect ratio between Rudders No. 2 and No. 3 is as expected from low aspect-ratio wing theory.

Figure 11 presents free stream results for Rudder No 2. It includes the influence of Reynolds Number, indicating that there is only a small effect, except on stall angle which is delayed slightly with increasing Reynolds No.

6.2 Propeller in Freestream

Dimensions and particulars of the propeller are given in Table II. In all the current tests the propeller pitch ratio was set at a mean pitch ratio of 0.95, and the freestream performance characteristics for this pitch ratio are shown in Figure 52.

Further details of the propeller free stream characteristics, including the results for

different pitch settings and the influence of Reynolds' Number , are given in Molland and Turnock[11].

6.3 Rudder and Propeller Combination

6.3.1 Reynolds Number Effects

Figure 12 shows the influence of Reynolds Number on the performance characteristics of all-movable Rudder No. 2 at X/D = 0.30. Results for two wind speeds of 10m/s and 20m/s are shown at an advance ratio of J = 0.71. The 10m/s results have been linearly interpolated from the rudder characteristics of J = 0.94 and J = 0.51. Close agreement between the curves for C_L, C_D, and CP_c indicates that scale effects should be negligible. The slight discrepancy of CP_s probably results from the interpolation procedure.

6.3.2 Influence of Thrust Loading on Rudder Characteristics

Figs. 13 to 19 show the results for C_L, C_D, CP_c, and CP_s to a base of rudder angle for different thrust loading (K_T/J^2) and rudder-propeller longitudinal separation (X/D). The results are for the three all-movable rudders Nos 1,2 and 3.

C_L: There is an increase in lift-curve slope with increase in propeller thrust loading as would be expected. There is a significant delay in stall compared with results obtained in the free-stream where stall occurs at approximately $\pm 20°$ (e.g. fig. 11). The stall angle is no longer the same for positive and negative incidence, stall occurring later for positive incidence. This results in a greater value of maximum sideforce (lift) at positive incidence. The angle of stall and therefore C_{Lmax} increases with propeller thrust loading (decreasing advance ratio).

C_D: The rudder drag coefficient between $-10°$ and $+10°$ is in a similar region for the three advance ratios tested. As rudder incidence is further increased the drag component due to lift increases rapidly for the lower advance ratios. The rudder drag at zero incidence does not consistently follow the trend of increasing drag with increasing thrust loading, although for a given rudder-propeller separation the trend is the same for rudder's 1, 2 and 3 (eg figs. 13, 15 and 18).

CP_c: For both positive and negative rudder incidence CP_c moves forward with increasing thrust loading. At high advance ratio (J = 0.94) CP_c is slightly aft of the freestream position of the chordwise centre of pressure, whereas at the low advance ratio (J = 0.35) it is well forward. There does not appear to be any pronounced asymmetry between CP_c for negative and positive rudder incidence.

CP_s: For positive rudder angles, CP_s moves outboard (towards rudder tip) with increasing propeller thrust loading, whereas for negative rudder angles CP_s moves inboard (towards rudder root). At high advance ratios CP_s is almost identical to that in the free-stream position.

6.3.3 Influence of rudder-propeller separation

Figs. 20 to 22 show for rudder No. 2 and figs. 23 to 25 for rudder No. 3 the influence on rudder characteristics for a given advance ratio J on changing the longitudinal separation of rudder and propeller. Overall, the effect on rudder lift of changing the separation is very small. This is not the result predicted by simple momentum theory which suggests that the increasing induced velocity due to increasing separation should increase side-force. Although the differences in lift-curve are small, the value does increase with separation, and as advance ratio decreases the changes are more noticeable. The separation appears to influence stall; the greater the separation the lower the stall angle.

Altering the longitudinal separation has a more profound influence on the rudders drag characteristics, especially at low advance ratio. In general, the greater the separation the lower the drag. Both the spanwise and chordwise position of the centre of pressure do not appear to alter with changes in longitudinal separation.

6.3.4 Comparison between the Three All-Movable Rudders

Figures 26 to 28 compare Rudders 1, 2 and 3 at the same longitudinal separation of the rudder stock and propeller plane of rotation (X/D=0.34 for Rudder No 1 and X/D=0.39 for rudder's 2 and 3) for given values of J.

Overall, the changes in C_L between the three rudders is small. This is an interesting result when rudders 2 and 3 are compared since free stream results would indicate an increase in lift curve slope for rudder No 3 (with ARg = 3.6) in freestream of about 5% to 7% compared with rudder No 2 (with ARg = 3.0). It is apparent that the accelerated flow over the rudder in the way of the propeller slipstream dominates the flow and, for the same chord value, the influence of aspect ratio is unlikely to be significant, especially at high thrust loadings. It should be noted that at high advance ratio (low thrust loading) the difference in lift-curve slope is of the right order of magnitude, however progressive increases in thrust loading reduce the lift-curve slope of rudder No.3 below that of rudder No. 2. The taper of rudder No. 1 results in an asymmetric performance for positive and negative rudder incidence. At positive incidence rudder no. 2 has greater lift than that of rudder No. 1 and the reverse is true for negative incidence. This appears to be due to the rotational nature of rudder inflow onto the rudder differing over its span and interacting with the taper of rudder No. 1.

The drag characteristic is not strongly influenced by rudder shape although rudder No.1 has a more asymmetric performance. The drag of rudder No. 2 is greater than that of rudder No. 3 following low-aspect ratio theory.

Changes in CP_c and CP_s for Rudders 2 and 3 are not large. For all three J values CP_s is seen to decrease for Rudder No 3. This is perhaps not surprising on account of the dominating effect of the propeller slipstream (mentioned earlier) and the fact that the propeller and rudder tip coincide for rudder No. 2 (fig. 9(b)). For positive incidence, the spanwise centre of pressure alters between Rudders 1 and 2 more than for negative incidence. Although for Rudder No. 3 the magnitude of movement of CP_s is similar but in opposite directions.

6.4 Spanwise Distribution of Local Normal Force Coefficient

Figure 29 and 30 show the free stream spanwise distribution of local normal force coefficient of Rudders No 2 and 3. These are identical to the free-stream distributions obtained by Molland[2] and verify the pressure measurement procedure. The increase

in lift at the rudder tip caused by the tip vortex is apparent at higher values of rudder incidence.

Figures 31 to 42 , for Rudder No.2, show the local normal force coefficient to a base of span for the three values of longitudinal separation at advance ratios J of 0.35, 0.51, and 0.94. The influence on the force distribution of the increase in thrust loading can clearly be seen. At high J values the force coefficient outside of the impinging propeller slipstream is of the same order as that within the slipstream whereas at low J values the slipstream local force coefficients dominate the loading on the rudder.

For Rudder 3, in Figures 43 to 51, a similar pattern of results is illustrated for the same separations and J values, although in this case at the outer 20% of the rudder span a free-stream behaviour is observed. Comparison of the local force distributions for Rudders 2 and 3 shows very similar shaped curves within the slipstream of the propeller.

6.5 Rudder Pressure Distributions

In figure 56 to 76 the chordwise variation in local pressure coefficient with incidence, thrust loading, and longitudinal separation for different spanwise positions is given for all three all-movable rudders. In general the results are of a similar nature. The high leading edge values of C_p for high thrust loading arise from the use of freestream velocity in the calculation of C_p. The plots are given for completeness and to allow the comparison of theoretical results for surface pressure distributions. Global integration of the rudder surface pressure distributions gives a good comparison with the forces measured on the rudder dynamometer. Representative points to illustrate this good agreement are shown in figure 15.

6.6 Influence of Rudder on Propeller Thrust Loading

The results presented in Figures 12 to 51 are for three values of advance ratio J. These advance ratios, for a given pitch ratio, have a known open-water thrust coefficient K_T. However, Figures 53 to 55 show the influence of both the rudder type and longitudinal separation on the measured propeller thrust coefficient at zero incidence compared with

the propeller open-water characteristics, given in Figure 52. It is noted that the propeller thrust augment increases with decreasing separation. In Figure 55 it can be seen that Rudder No. 1 has a larger affect on the propeller thrust than Rudder No 2 and that the influence of Rudder No 3 is small. This suggests that it is the position of the rudder tip relative to the propeller which affects the thrust augment.

7. CONCLUSION AND RECOMMENDATIONS

7.1 There is an increase in lift-curve slope with increase in thrust loading; this follows reasonably well documented trends. It should be noted that the increases were less than those predicted by simple momentum theory.

7.2 There is a significant increase in stall angle, compared with free stream, when the rudder is working aft of the propeller. The stall characteristics are not symmetrical for positive and negative incidence.

7.3 Changes in lift characteristics due to changes in rudder taper and aspect ratio when working aft of a propeller do not appear to be significant since the accelerated flow over the rudder in way of the propeller slipstream tends to dominate the flow, especially as advance ratio decreases. Therefore, the percentage of the rudder covered by the propeller's slipstream will control the generation of sideforce.

7.4 Chordwise centre of pressure, CP_c, moves forward with increasing thrust loading, and, apart from high advance ratios, is forward of the freestream CP_c. Its behaviour is symmetrical for positive and negative incidence.

7.5 Spanwise centre of pressure, CP_s, moves inboard (towards rudder root) for negative incidence and outboard (towards rudder tip) for positive incidence. The magnitude of the movement depends on the geometry of the rudder. For the symmetrical case where there is equal area of rudder either side of the propeller race the magnitude of movement of CP_s is the same for a given advance ratio.

7.6 The test results indicate that changes in rudder-propeller longitudinal separation for fixed advance ratios tend to have a relatively small influence on rudder characteristics, although there is an indication of a very small increase in lift-curve with increasing separation. However, it is also seen that stall angle for a given advance ratio decreases with increasing separation. It should be noted that as the rudder is moved closer to the propeller there is an induced increase in propeller thrust, the magnitude of which will depend on rudder section shape and thickness, and actual longitudinal separation. The effect of this induced change in K_T on the slipstream will therefore work in the opposite sense to the assumed acceleration in the slipstream for a fixed K_T. It is concluded that the two effects will tend to cancel each other for a fixed value of J for the propeller.

7.7 The test rig was newly constructed for the purpose of propeller and propeller/rudder interaction investigations. The results reported on, which include those derived during the commissioning period, indicate the ability of the rig to produce repeatable and reliable data.

7.8 The chordwise local normal force distributions and surface pressure measurements provide a valuable resource for the validation of mathematical models of ship rudder and propeller interactions and provide an insight into the fundamental physics of the flow over the rudder.

7.9 The results reported are part of on-going research. Further work has been carried out into the influence of propeller pitch, lateral separation of propeller and rudder, vertical separation of propeller and rudder, and this will be fully detailed in subsequent reports.

ACKNOWLEDGEMENTS

The work described in this report covers part of a research project funded by the S.E.R.C./M.O.D. through the Marine Technology Directorate Ltd. under research grant Ref No GR/E/65289.

REFERENCES

1. Turnock, S.R., "A Test Rig For The Investigation of Ship Propeller/Rudder Interactions", Ship Science Report No. 45, University of Southampton, November 1990.

2. Molland, A.F., "Pressure Distribution Investigation of a Semi-Balanced Ship Skeg-Rudder", Ship Science Report No. 5/81, University of Southampton, October 1980.

3. Turnock, S.R.," Computer aided Design and Numerically Controlled Manufacture of a Split mould for a Composite Model Ship Propeller", University of Southampton, Ship Science Report 42, December 1990.

4. Molland, A.F.,& Turnock, S.R.," The Design and Construction of Propeller Blades in Composite Materials for a Wind Tunnel Model". University of Southampton, Ship Science Report 41, October 1990.

5. Molland, A.F.,"The Free-Stream Characteristics of a Semi-Balanced Ship Skeg-Rudder", University of Southampton, Ship Science Report 3/77, May 1977.

6. Molland, A.F." The Design, Construction and Calibration of a five-component strain gauge wind tunnel dynamometer " , University of Southampton, Ship Science Report 1/77, Nov. 1976.

7. Molland, A.F., & Turnock, S.R.," The Design, Construction and Calibration of a Thrust and Torque Dynamometer for a Wind Tunnel Propeller Model", University of Southampton, Ship Science Report 44, October 1990.

8. Turnock, S.R., " Two-Dimensional Wind Tunnel Tests of SSS Series 1 Structurally Efficient Aerofoils for Wind Turbines", University of Southampton, Ship Science Report 38, June 1989.

9. Kreyszig, E.:" Advanced Engineering Mathematics". J. Wiley and Sons, 5th Edition, 1983.

10. Goodrich, G.J.,& Molland, A.F.,"Wind Tunnel Investigation of Semi-Balanced Ship Skeg-Rudders", pp285-307 Trans. R.I.N.A., Vol.121, 1979.

11. Molland, A.F., & Turnock, S.R.," Wind Tunnel Test Results for a Model Ship Propeller Based on a Modified Wageningen B4.40 ", University of Southampton, Ship Science Report 43, December 1990.

12. Molland, A.F., & Turnock, S.R., " The performance of a ship semi-balanced skeg rudder behind a propeller", University of Southampton, Ship Science Report, under preparation.

13. Molland, A.F., & Turnock, S.R., "Preliminary zero and low-speed tests on a model ship rudder-propeller combination", University of Southampton, Ship Science Report, under preparation.

14. English, J.W., & Bain, D.C., "Some manoeuvring devices for use at zero and low ship speed." Trans. N.E.C.E.I.S., Vol. 88, 1971/72.

APPENDIX 1: TEST DATA FILE FORMAT

Data was stored in ASCII format to allow direct hard copy to be made of the test data. Information is categorised into 10 different types and a marker used to identify a particular data category. In the subsequent data analysis a TurboPascal program was written to extract Rudder Dynamometer, Rudder pressures and Propeller Thrust/Torque by simply reading through the data file and using the markers to identify the data category. The format of the different categories were as follows, the comments in [square brackets] have subsequently been added.

```
0:Configuration
   0    MARKER
 RUDDER AND PROPELLER INTERACTIONS
     8      7        [Number of integer, Number of real constants]
    16    TestNo
    23    Day
     8    Month
  1990    Year
    15    Time - Hours
    32    Time - Minutes
     4    Propeller Blades  [Number of]
     1    Identity of Pressure Tappings
  -10.0000  Rudder Angle ( degrees)
  -10.0000  Skeg Angle (degrees)
 1000.0000 Rudder Span (mm)
    1.0000  Propeller Pitch Ratio
  800.0000 Propeller Diameter (mm)
  323.0000 Rudder-Propeller Distance (mm)
  600.0000 Propeller Axis Height Above Wind Tunnel floor
1:Test Conditions
   1    MARKER
  764.999980  tunnel atmospheric pressure (mm Hg)
   25.999999  tunnel atmospheric temperature (deg Celsius)
```

0.000000 tunnel dynamic pressure (mm H2O)

2:Channel Supply Voltages

2 MARKER

7 Number of channels

2 Number of readings

Channel	Voltage	S.D.	supply volts channels	Corrected
13	7.003300	0.001259	0.000000	0.000000
14	7.006200	0.001199	0.000000	0.000000
15	6.981500	0.000000	0.000000	0.000000
16	7.000000	0.000000	0.000000	0.000000
17	11.000001	0.000000	0.000000	0.000000
18	7.000000	0.000000	0.000000	0.000000
19	7.000000	0.000000	0.000000	0.000000

3:Wind Off Voltages

3 MARKER

14 Number of channels

2 Number of readings

Channel	Voltage	S.D.	windoff channels	Corrected
2	-0.000283	0.000000	0.000000	0.000000
3	-0.000135	0.000001	0.000000	0.000000
4	0.000042	0.000002	0.000000	0.000000
5	0.000011	0.000001	0.000000	0.000000
6	0.000094	0.000000	0.000000	0.000000
7	0.000046	0.000000	0.000000	0.000000
8	-0.000309	0.000000	0.000000	0.000000
9	-0.001044	0.000001	0.000000	0.000000
10	-0.000658	0.000001	0.000000	0.000000
11	-0.001822	0.000001	0.000000	0.000000
12	-0.000785	0.000264	0.000000	0.000000
13	7.003250	0.001259	0.000000	0.000000
14	7.006150	0.001199	0.000000	0.000000
15	6.985400	0.000000	0.000000	0.000000

4: Scanivalve Pressures

4 MARKER

4 34 Number of Channels and Ports

6 Number of readings

666.999990 Rudder Chord (mm)

69.999998 Spanwise position(mm)

Scani	Port	Voltage	S.D.	Scanivalve	[chord %]
1	0	-0.001046	0.000001	5.4	(static)
1	1	-0.000973	0.000001	72.4	(pitot)
1	2	-0.000978	0.000001	68.7	0.0 RUDDER
1	3	-0.001069	0.000001	-15.6	2.5 RUDDER
1	4	-0.001077	0.000001	-23.3	5.0 RUDDER
1	5	-0.001085	0.000001	-30.4	10.0 RUDDER
1	6	-0.001085	0.000001	-30.5	20.0 RUDDER
1	7	-0.001081	0.000001	-26.9	30.0 RUDDER
		[continued to]			
4	31	-0.000759	0.002040	11.0	100.0 RUDDER
4	32	-0.000759	0.002040	11.2	100.0 RUDDER
4	33	-0.000758	0.002040	11.4	100.0 RUDDER

5: Thrust/Torque

5 MARKER

2 Number of channels

6 Number of readings

Channel	Voltage	S.D.	Torque-Thrust channels	Corrected
2	0.000124	0.000023	0.0	0.0
3	0.000143	0.000001	0.0	4.965957

6: Propeller RPM

6 MARKER

1 Number of channels

6 Number of readings

Channel	Voltage	S.D.	RPM channel	Corrected
1	1.436733	0.001508	1436.733300	0.000000

7: Rudder Dynamometer

7 MARKER

5 Number of channels

6 Number of readings

Channel	Voltage	S.D.	Rudder-dynamometer channels	Corrected
4	0.000139	0.000008	9.977194	9.939999
5	-0.000021	0.000003	-1.692538	-9.348303
6	0.000036	12.080254	-9.228590	-35.958361
7	0.000349	12.080224	210.150160	17.306989
8	-0.000142	0.000001	-45.485398	0.017539

8:End of Test Run

8 MARKER

8 End of File

9: Comment

9 comment

FORCES ON EXTENDED ALL_MOVABLE

10: Change of wind speed

10 new wind speed

10.0

11: Change of Rudder Incidence

11 New All-Movable Incidence

-10.0000

APPENDIX 2: TABULATED RUDDER DYNAMOMETER DATA

Rudder No.2 Freestream Characteristic 10m/s

Angle	V	RPM	C_L	C_N	C_D	C_{mz}	C_{mx}	C_{my}	CP_c	CP_s
-25.40	10.00	1041.50	-0.8802	-0.700	0.222	0.004	-0.9498	0.1868	29.112	56.614
-22.90	10.00	1041.50	-0.9286	-0.779	0.196	0.012	-0.9851	0.1709	27.735	54.509
-20.40	10.00	1041.50	-1.0006	-0.889	0.140	0.036	-1.0181	0.1246	23.981	50.849
-15.40	10.00	1041.50	-0.8110	-0.760	0.083	0.029	-0.8100	0.0789	24.312	49.210
-10.40	10.00	1041.50	-0.5241	-0.508	0.039	0.028	-0.5091	0.0399	21.776	47.261
-5.40	10.00	1041.50	-0.2621	-0.260	0.013	0.013	-0.2555	0.0226	22.228	47.276
-0.40	10.00	1041.50	-0.0127	-0.013	0.006	-0.003	-0.0103	0.0103	75.650	41.520
4.60	10.00	1041.50	0.2357	0.234	0.016	-0.018	0.2314	0.0185	18.386	47.911
9.60	10.00	1041.50	0.4714	0.458	0.039	-0.033	0.4713	0.0352	19.108	49.283
14.60	10.00	1041.50	0.7710	0.723	0.093	-0.035	0.7656	0.0749	22.787	49.148
19.60	10.00	1041.50	0.9645	0.862	0.140	-0.046	0.9677	0.1186	22.004	49.985
22.10	10.00	1041.50	0.9952	0.853	0.183	-0.034	1.0116	0.1488	24.003	51.399
24.60	10.00	1041.50	0.9282	0.753	0.219	-0.022	0.9666	0.1758	25.542	53.885

Rudder No. 2 Free stream 25 m/s

Angle	V	RPM	C_L	C_N	C_D	C_{mz}	C_{mx}	C_{my}	CP_c	CP_s
-25.40	25.00	1041.50	-0.8062	-0.836	0.251	0.002	-0.5751	0.2571	29.661	53.524
-22.90	25.00	1041.50	-0.8588	-0.877	0.222	0.005	-0.6084	0.2383	29.375	53.421
-20.40	25.00	1041.50	-0.9847	-0.983	0.171	0.043	-0.6650	0.1772	25.584	50.127
-15.40	25.00	1041.50	-0.8020	-0.797	0.091	0.059	-0.5242	0.0975	22.554	48.034
-10.40	25.00	1041.50	-0.5354	-0.535	0.049	0.046	-0.3450	0.0535	21.452	47.080
-5.40	25.00	1041.50	-0.2715	-0.273	0.025	0.026	-0.1726	0.0286	20.449	46.199
-0.40	25.00	1041.50	-0.0155	-0.016	0.018	0.002	-0.0079	0.0204	18.905	34.948
4.60	25.00	1041.50	0.2345	0.236	0.025	-0.022	0.1538	0.0276	20.467	48.150
9.60	25.00	1041.50	0.4902	0.491	0.048	-0.043	0.3208	0.0512	21.136	48.034
14.60	25.00	1041.50	0.7521	0.751	0.091	-0.058	0.4960	0.0931	22.228	48.535
19.60	25.00	1041.50	1.0060	0.999	0.153	-0.063	0.6717	0.1596	23.678	49.410
22.10	25.00	1041.50	0.9046	0.915	0.205	-0.017	0.5921	0.2094	28.136	48.208
24.60	25.00	1041.50	0.8085	0.837	0.244	-0.004	0.5535	0.2461	29.516	50.803

Rudder No. 2 Free stream 32 m/s

Angle	V	RPM	C_L	C_N	C_D	C_{mz}	C_{mx}	C_{my}	CP_c	CP_s
-25.40	29.00	1041.50	-0.7677	-0.592	0.237	0.000	-0.8196	0.2537	29.918	53.676
-22.90	29.00	1041.50	-0.8045	-0.660	0.209	0.010	-0.8536	0.2154	27.682	53.539
-20.40	29.00	1041.50	-0.9015	-0.788	0.163	0.024	-0.9306	0.1753	25.438	51.141
-15.40	29.00	1041.50	-0.8001	-0.747	0.092	0.040	-0.7845	0.0978	22.041	47.711
-10.40	29.00	1041.50	-0.5311	-0.513	0.050	0.030	-0.5153	0.0539	21.211	47.078
-5.40	29.00	1041.50	-0.2693	-0.266	0.025	0.017	-0.2580	0.0289	20.652	46.293
-0.40	29.00	1041.50	-0.0190	-0.019	0.018	0.001	-0.0140	0.0198	20.544	31.706
4.60	29.00	1041.50	0.2296	0.227	0.024	-0.014	0.2275	0.0271	20.610	48.534
9.60	29.00	1041.50	0.4842	0.469	0.048	-0.028	0.4784	0.0506	21.043	48.326
14.60	29.00	1041.50	0.7435	0.697	0.089	-0.038	0.7381	0.0920	21.726	48.633
19.60	29.00	1041.50	0.9915	0.882	0.154	-0.040	0.9990	0.1602	23.148	49.565
22.10	29.00	1041.50	0.8616	0.724	0.198	-0.015	0.8707	0.2057	26.915	49.701
24.60	29.00	1041.50	0.7675	0.597	0.243	-0.001	0.7900	0.2556	29.750	50.919

Rudder No.3 Free stream 10m/s

Angle	V	RPM	C_L	C_N	C_D	C_{mz}	C_{mx}	C_{my}	CP_c	CP_s
-25.40	10.00	1041.50	-0.8742	-0.694	0.224	0.011	-1.0580	0.2179	27.239	54.505
-22.90	10.00	1041.50	-0.9477	-0.799	0.189	0.018	-1.1368	0.1862	25.907	53.187
-20.40	10.00	1041.50	-0.9876	-0.876	0.143	0.031	-1.1305	0.1458	23.670	49.441
-17.90	10.00	1041.50	-0.9179	-0.838	0.114	0.036	-1.0408	0.1066	22.254	48.908
-15.40	10.00	1041.50	-0.8114	-0.758	0.091	0.031	-0.9143	0.0866	22.552	48.353
-10.40	10.00	1041.50	-0.5406	-0.523	0.050	0.026	-0.6031	0.0477	21.034	47.585
-5.40	10.00	1041.50	-0.2601	-0.257	0.025	0.014	-0.3005	0.0268	20.155	49.684
-0.40	10.00	1041.50	0.0202	0.020	0.022	0.001	-0.0113	0.0157	41.553	-75.502
4.60	10.00	1041.50	0.2858	0.283	0.025	-0.013	0.2759	0.0196	22.037	39.148
9.60	10.00	1041.50	0.5506	0.533	0.056	-0.025	0.5631	0.0407	21.568	42.555
14.60	10.00	1041.50	0.8211	0.771	0.092	-0.031	0.8786	0.0780	22.847	45.280
17.10	10.00	1041.50	0.9358	0.858	0.125	-0.034	0.9936	0.1043	22.762	44.982
19.60	10.00	1041.50	1.0294	0.919	0.153	-0.034	1.1060	0.1366	23.288	45.688
22.10	10.00	1041.50	0.9995	0.853	0.193	-0.022	1.1049	0.1784	25.372	47.724
24.60	10.00	1041.50	0.4765	0.307	0.304	0.014	0.4824	0.2935	38.485	42.781

Rudder No. 3 Free stream 25m/s

Angle	V	RPM	C_L	C_N	C_D	C_{mz}	C_{mx}	C_{my}	CP_c	CP_s
-25.40	25.00	1041.50	-0.8251	-0.849	0.242	0.004	-0.5652	0.2902	29.536	53.680
-22.90	25.00	1041.50	-0.8632	-0.877	0.210	0.017	-0.6011	0.2526	27.990	54.779
-20.40	25.00	1041.50	-0.9379	-0.936	0.163	0.030	-0.6007	0.2095	26.769	49.896
-15.40	25.00	1041.50	-0.8564	-0.849	0.087	0.064	-0.5309	0.1079	22.430	47.607
-10.40	25.00	1041.50	-0.5694	-0.568	0.046	0.048	-0.3504	0.0582	21.585	47.073
-5.40	25.00	1041.50	-0.2977	-0.298	0.022	0.026	-0.1786	0.0310	21.240	45.558
-0.40	25.00	1041.50	-0.0143	-0.014	0.016	0.001	-0.0074	0.0206	20.766	38.632
4.60	25.00	1041.50	0.2508	0.252	0.022	-0.024	0.1547	0.0285	20.627	47.186
9.60	25.00	1041.50	0.5234	0.523	0.045	-0.046	0.3242	0.0541	21.209	47.437
14.60	25.00	1041.50	0.8018	0.798	0.086	-0.062	0.4996	0.1014	22.231	47.814
19.60	25.00	1041.50	1.0224	1.013	0.147	-0.060	0.6529	0.1777	24.108	49.431
22.10	25.00	1041.50	0.8670	0.878	0.199	-0.021	0.5782	0.2386	27.575	52.101
24.60	25.00	1041.50	0.7931	0.817	0.231	-0.007	0.5314	0.2893	29.105	52.727

Rudder No. 1 X/D = 0.34 J = 0.94

Angle	V	RPM	C_L	C_N	C_D	C_{mz}	C_{mx}	C_{my}	CP_c	CP_s
-30.40	10.00	779.86	-0.9470	-1.044	0.449	0.009	-0.6650	0.2980	34.514	51.860
-25.40	10.00	779.09	-1.4090	-1.412	0.324	0.096	-0.9260	0.2210	28.608	48.460
-20.40	10.00	779.57	-1.2770	-1.254	0.165	0.082	-0.7820	0.1510	28.832	45.103
-10.40	10.00	778.99	-0.6570	-0.651	0.029	0.055	-0.3760	0.0430	26.886	40.501
-0.40	10.00	779.39	-0.0580	-0.059	0.018	-0.006	-0.0140	0.0130	45.260	5.910
19.60	10.00	781.47	0.9630	0.936	0.085	-0.163	0.7090	0.1310	18.016	58.526
24.60	10.00	784.12	1.0830	1.106	0.290	-0.110	0.7430	0.2480	25.440	52.979
29.60	10.00	784.14	1.1890	1.238	0.413	-0.112	0.7830	0.3190	26.370	50.208

Rudder No. 1 X/D = 0.34 J = 0.51

Angle	V	RPM	C_L	C_N	C_D	C_{mz}	C_{mx}	C_{my}	CP_c	CP_s
-30.40	10.00	1418.79	-2.6620	-2.735	0.867	0.266	-1.7680	0.5970	25.671	49.318
-25.40	10.00	1419.48	-2.4310	-2.458	0.612	0.264	-1.5540	0.4240	24.628	46.996

-20.40	10.00	1420.84	-1.9590	-1.952	0.333	0.216	-1.2170	0.2590	24.343	45.567
-10.40	10.00	1417.39	-0.7940	-0.817	0.198	0.186	-0.5300	0.1080	12.611	48.697
-0.40	10.00	1418.22	-0.0370	-0.038	0.087	0.043	0.0450	0.0390	-77.974	-135.432
9.60	10.00	1423.45	0.7560	0.750	0.029	-0.125	0.6540	0.0600	18.657	69.826
19.60	10.00	1423.00	1.6170	1.601	0.232	-0.222	1.2830	0.2220	21.517	62.673
24.60	10.00	1423.21	2.0880	2.089	0.457	-0.250	1.6350	0.3760	23.408	61.148
29.60	10.00	1423.52	2.3700	2.388	0.662	-0.219	1.8520	0.6650	26.204	63.674

Rudder No. 1 X/D = 0.34 J = 0.35

Angle	V	RPM	C_L	C_N	C_D	C_{mz}	C_{mx}	C_{my}	CP_c	CP_s
-30.40	10.00	2129.53	-4.1080	-4.256	1.408	0.462	-2.7060	0.9540	24.534	48.698
-25.40	10.00	2131.38	-3.6690	-3.723	0.953	0.435	-2.2940	0.6530	23.686	45.676
-20.40	10.00	2130.63	-3.0280	-3.041	0.580	0.405	-1.8550	0.4080	22.073	44.345
-10.40	10.00	2127.32	-1.5210	-1.518	0.123	0.262	-0.8330	0.1160	18.140	37.886
-0.40	10.00	2127.68	-0.1040	-0.105	0.076	0.062	0.0950	0.0360	-23.378	-107.509
9.60	10.00	2132.82	1.0680	1.066	0.080	-0.199	1.0090	0.0980	16.744	77.316
19.60	10.00	2132.90	2.3840	2.386	0.418	-0.388	2.0080	0.3700	19.115	66.955
24.60	10.00	2132.65	3.0520	3.082	0.739	-0.408	2.5070	0.5910	22.142	64.431
29.60	10.00	2133.07	3.8070	3.847	1.087	-0.463	3.0980	0.9000	23.337	64.077

Rudder No. 1 X/D = 0.34 J = 0.27

Angle	V	RPM	C_L	C_N	C_D	C_{mz}	C_{mx}	C_{my}	CP_c	CP_s
-30.40	10.00	2709.10	-5.6610	-5.903	2.016	0.753	-3.8875	1.4350	17.233	51.607
-25.40	10.00	2716.30	-4.7688	-4.913	1.410	0.698	-3.2299	1.0122	15.779	50.729
-20.40	10.00	2706.10	-3.8948	-3.973	0.925	0.636	-2.5960	0.6385	13.972	49.344
-10.40	10.00	2700.60	-1.9034	-1.918	0.252	0.424	-1.1410	0.1774	7.890	42.694
-0.40	10.00	2706.80	-0.1236	-0.125	0.132	0.111	0.1544	0.0519	-59.594	-141.222
9.60	10.00	2709.40	1.5359	1.558	0.261	-0.219	1.5482	0.1917	15.937	82.537
19.60	10.00	2835.40	3.5087	3.605	0.894	-0.540	3.1475	0.6955	15.019	71.212
24.60	10.00	2837.60	4.4242	4.566	1.306	-0.661	3.8716	1.0556	15.503	69.214
29.60	10.00	2836.10	5.4392	5.686	1.938	-0.729	4.6486	1.5320	17.174	66.888

Rudder No. 2 X/D = 0.30 J = 0.94

Angle	V	RPM	C_L	C_N	C_D	C_{mz}	C_{mx}	C_{my}	CP_c	CP_s
-35.40	10.00	795.03	-0.8780	-1.075	0.620	-0.097	-0.6480	0.3240	39.036	49.056
-30.40	10.00	792.39	-0.9525	-1.029	0.410	-0.060	-0.7015	0.2195	35.851	52.079
-20.40	10.00	791.06	-0.8930	-0.910	0.213	0.004	-0.6400	0.1165	29.582	52.835
-10.40	10.00	790.51	-0.5080	-0.510	0.058	0.019	-0.3425	0.0290	26.239	49.507
-0.40	10.00	792.85	-0.0010	-0.001	0.030	-0.009	-0.0080	0.0180	873.953	820.763
9.60	10.00	792.28	0.5045	0.508	0.063	-0.052	0.3180	0.0410	19.742	45.520
19.60	10.00	791.50	1.0125	1.022	0.205	-0.061	0.6720	0.1230	24.004	48.455
29.60	10.00	790.86	1.4040	1.450	0.465	-0.018	0.9635	0.2765	28.748	49.700
39.60	10.00	795.03	1.0390	1.253	0.710	0.054	0.8380	0.4790	34.292	58.432

Rudder No. 2 X/D = 0.30 J = 0.51

Angle	V	RPM	C_L	C_N	C_D	C_{mz}	C_{mx}	C_{my}	CP_c	CP_s
-35.40	10.00	1433.22	-2.7650	-2.905	1.124	-0.168	-1.6370	0.7310	35.767	43.015
-30.40	10.00	1433.58	-2.6065	-2.662	0.819	0.064	-1.7750	0.5530	27.578	50.519
-20.40	10.00	1432.43	-1.7240	-1.740	0.356	0.087	-1.1390	0.2395	24.992	48.636
-10.40	10.00	1432.63	-0.8675	-0.874	0.114	0.064	-0.5365	0.0755	22.709	44.434
-0.40	10.00	1433.00	-0.0160	-0.017	0.056	-0.008	0.0360	0.0430	77.877	-254.819
9.60	10.00	1431.95	0.8335	0.842	0.118	-0.085	0.6395	0.0855	19.917	59.056
19.60	10.00	1434.71	1.6775	1.703	0.366	-0.109	1.2530	0.2520	23.585	56.779
29.60	10.00	1430.94	2.4695	2.554	0.823	-0.082	1.8550	0.5650	26.768	56.591
39.60	10.00	1433.22	2.7300	3.211	1.738	0.137	1.9170	1.1260	34.238	50.855

Rudder No. 2 X/D =0.30 J = 0.35

Angle	V	RPM	C_L	C_N	C_D	C_{mz}	C_{mx}	C_{my}	CP_c	CP_s
-35.40	10.00	2080.12	-4.0770	-4.467	1.974	-0.010	-2.6400	1.2840	30.198	47.318
-30.40	10.00	2078.43	-3.7610	-3.929	1.354	0.161	-2.4890	0.9100	25.877	48.864
-20.40	10.00	2079.72	-2.6095	-2.640	0.557	0.215	-1.6850	0.3820	21.861	47.361
-10.40	10.00	2078.12	-1.2935	-1.304	0.174	0.129	-0.7655	0.1290	20.083	42.030
-0.40	10.00	2078.72	-0.0150	-0.016	0.076	-0.010	0.1160	0.0610	93.958	-762.443
9.60	10.00	2078.22	1.2000	1.212	0.174	-0.151	1.0115	0.1245	17.541	66.510
19.60	10.00	2079.18	2.3925	2.422	0.500	-0.236	1.9350	0.3660	20.215	62.854

29.60	10.00	2078.18	3.6215	3.744	1.203	-0.225	2.8790	0.8785	23.995	60.959
34.60	10.00	2080.12	4.2650	4.509	1.758	-0.137	3.3670	1.2320	26.938	59.478
39.60	10.00	2080.12	4.4040	4.722	2.084	-0.129	3.6200	1.6410	27.248	63.727

Rudder No. 2 X/D = 0.39 J = 0.94

Angle	V	RPM	C_L	C_N	C_D	C_{mz}	C_{mx}	C_{my}	CP_c	CP_s
-35.40	10.00	792.73	-0.9170	-1.057	0.534	-0.115	-0.6280	0.3050	40.860	47.640
-30.40	10.00	792.12	-1.2885	-1.362	0.494	-0.034	-0.9725	0.2930	32.489	55.065
-20.40	10.00	792.57	-1.0615	-1.068	0.213	0.041	-0.7345	0.1200	26.201	50.818
-10.40	10.00	793.68	-0.4975	-0.502	0.073	0.030	-0.3405	0.0335	23.860	50.348
-0.40	10.00	789.51	-0.0410	-0.041	0.005	-0.014	-0.0120	0.0105	11.743	0.398
9.60	10.00	792.87	0.5315	0.537	0.077	-0.046	0.3345	0.0540	21.556	45.623
19.60	10.00	794.16	0.9840	1.005	0.235	-0.045	0.6685	0.1365	25.595	49.677
29.60	10.00	792.96	1.4365	1.479	0.465	-0.012	0.9825	0.2775	29.165	49.520
34.60	10.00	792.73	1.6310	1.702	0.634	0.017	1.1070	0.3530	30.966	47.813
39.60	10.00	792.73	1.2180	1.445	0.795	0.089	0.7980	0.4870	36.122	46.497

Rudder No. 2 X/D = 0.39 J = 0.51

Angle	V	RPM	C_L	C_N	C_D	C_{mz}	C_{mx}	C_{my}	CP_c	CP_s
-35.40	10.00	1436.73	-2.0220	-2.320	1.159	-0.209	-1.2370	0.7540	38.998	44.789
-30.40	10.00	1435.49	-2.4075	-2.522	0.881	-0.046	-1.5605	0.5775	31.810	47.467
-20.40	10.00	1434.08	-1.8335	-1.839	0.345	0.116	-1.1965	0.2255	23.696	47.757
-10.40	10.00	1434.69	-0.8695	-0.873	0.098	0.072	-0.5510	0.0630	21.816	45.902
-0.40	10.00	1434.54	0.0115	0.011	0.053	-0.003	0.0375	0.0210	29.510	-119.736
9.60	10.00	1434.99	0.8600	0.868	0.121	-0.077	0.6490	0.0795	21.147	57.737
19.60	10.00	1434.68	1.7905	1.808	0.361	-0.107	1.3005	0.2460	24.035	54.830
29.60	10.00	1435.42	2.5505	2.614	0.802	-0.068	1.8750	0.5450	27.362	55.169
34.60	10.00	1436.73	2.7380	2.927	1.185	0.059	2.0180	0.8230	32.002	55.228
39.60	10.00	1436.73	2.6780	3.081	1.596	0.135	1.8840	1.0960	34.351	52.303

Rudder No. 2 X/D = 0.39 J = 0.35

Angle	V	RPM	C_L	C_N	C_D	C_{mz}	C_{mx}	C_{my}	CP_c	CP_s
-35.40	10.00	2146.30	-4.5190	-4.781	1.895	0.082	-2.8890	1.1770	28.277	46.008
-30.40	10.00	2146.07	-4.1920	-4.238	1.230	0.250	-2.7630	0.8245	24.091	48.578
-20.40	10.00	2144.25	-2.8425	-2.851	0.535	0.242	-1.8145	0.3620	21.508	46.586
-10.40	10.00	2144.78	-1.3940	-1.391	0.111	0.139	-0.8280	0.0765	20.027	42.022
-0.40	10.00	2144.67	-0.0520	-0.052	0.016	-0.006	0.1190	-0.0030	40.595	-244.870
9.60	10.00	2145.35	1.2505	1.251	0.109	-0.147	1.0655	0.0805	18.241	67.592
19.60	10.00	2145.75	2.5830	2.595	0.482	-0.252	2.0455	0.3540	20.286	61.338
29.60	10.00	2145.40	3.9215	3.997	1.188	-0.265	3.0630	0.8600	23.367	59.763
34.60	10.00	2146.30	4.3200	4.403	1.493	-0.260	3.5290	1.1760	24.087	63.636
39.60	10.00	2146.30	4.6950	5.011	2.187	-0.059	3.6880	1.8100	28.802	62.223

Rudder No. 2 X/D = 0.52 J = 0.94

Angle	V	RPM	C_L	C_N	C_D	C_{mz}	C_{mx}	C_{my}	CP_c	CP_s
-30.40	10.00	792.92	-0.9645	-1.050	0.432	-0.071	-0.6975	0.2250	36.690	50.641
-20.40	10.00	790.59	-1.0745	-1.075	0.194	0.033	-0.7500	0.0990	26.981	51.140
-10.40	10.00	792.13	-0.5475	-0.551	0.067	0.023	-0.3705	0.0210	25.874	49.342
-0.40	10.00	792.61	-0.0170	-0.017	0.036	-0.010	-0.0190	0.0130	89.539	96.307
9.60	10.00	789.57	0.5280	0.536	0.096	-0.051	0.3570	0.0390	20.457	49.251
19.60	10.00	793.99	1.0030	1.017	0.217	-0.059	0.6725	0.1100	24.184	48.378
29.60	10.00	791.71	1.4020	1.448	0.463	-0.018	0.9855	0.2595	28.747	50.547
34.60	10.00	791.42	1.1720	1.315	0.617	0.046	0.8580	0.5410	33.458	59.592

Rudder No. 2 X/D = 0.52 J = 0.51

Angle	V	RPM	C_L	C_N	C_D	C_{mz}	C_{mx}	C_{my}	CP_c	CP_s
-35.40	10.00	1433.64	-2.1330	-2.602	1.490	-0.175	-1.5980	0.9780	36.728	54.356
-30.40	10.00	1433.74	-2.6755	-2.693	0.762	0.078	-1.8535	0.4905	27.102	51.095
-20.40	10.00	1430.36	-1.8095	-1.826	0.373	0.125	-1.2205	0.2115	23.144	49.224
-10.40	10.00	1434.77	-0.9170	-0.917	0.082	0.063	-0.5780	0.0380	23.103	45.253
-0.40	10.00	1433.67	-0.0375	-0.038	0.007	-0.017	0.0175	-0.0025	73.620	-66.570

9.60	10.00	1430.93	0.8220	0.828	0.103	-0.087	0.6375	0.0475	19.526	59.373
19.60	10.00	1434.10	1.6905	1.706	0.336	-0.117	1.2580	0.1995	23.091	55.915
29.60	10.00	1433.93	2.5295	2.590	0.791	-0.086	1.8935	0.5205	26.684	55.984
34.60	10.00	1433.64	2.7790	2.978	1.216	0.101	2.2320	1.0650	33.385	64.495
39.60	10.00	1433.64	2.2330	2.713	1.557	0.216	1.7830	1.3050	37.957	63.807

Rudder No. 2 X/D = 0.52 J = 0.35

Angle	V	RPM	C_L	C_N	C_D	C_{mz}	C_{mx}	C_{my}	CP_c	CP_s
-35.40	10.00	2079.45	-4.0650	-4.543	2.123	-0.339	-2.7420	1.5670	37.443	51.674
-30.40	10.00	2078.85	-3.9490	-3.999	1.172	0.192	-2.6030	0.7520	25.185	48.173
-20.40	10.00	2079.55	-2.7660	-2.751	0.456	0.213	-1.7575	0.2705	22.267	45.794
-10.40	10.00	2079.75	-1.3950	-1.381	0.053	0.119	-0.8310	0.0235	21.365	41.971
-0.40	10.00	2079.47	-0.0405	-0.041	-0.046	-0.010	0.1045	-0.0445	75.348	-452.711
9.60	10.00	2080.43	1.1750	1.174	0.092	-0.145	1.0100	0.0405	17.669	67.926
19.60	10.00	2080.20	2.3905	2.392	0.419	-0.246	1.9265	0.2815	19.690	62.323
29.60	10.00	2079.13	3.7250	3.802	1.139	-0.251	2.9360	0.7765	23.399	59.744
34.60	10.00	2079.45	4.7210	4.945	1.866	-0.103	3.8790	1.4550	27.896	63.763
39.60	10.00	2079.45	3.7600	4.488	2.496	0.342	3.0780	2.0390	37.616	64.306

Rudder No. 3 X/D = 0.30 J = 0.94

Angle	V	RPM	C_L	C_N	C_D	C_{mz}	C_{mx}	C_{my}	CP_c	CP_s
-30.40	10.00	789.22	-1.1560	-1.238	0.476	-0.062	-0.7915	0.2730	34.952	51.731
-20.40	10.00	790.58	-1.0945	-1.098	0.206	0.033	-0.6945	0.1230	26.966	48.645
-10.40	10.00	790.30	-0.5115	-0.516	0.071	0.026	-0.3250	0.0395	24.785	48.787
-0.40	10.00	791.37	-0.0110	-0.011	0.008	-0.017	-0.0035	0.0125	457.956	-58.405
9.60	10.00	790.15	0.5390	0.543	0.074	-0.058	0.3265	0.0395	19.281	45.872
19.60	10.00	789.25	1.0840	1.093	0.213	-0.070	0.6715	0.1160	23.566	46.968
29.60	10.00	789.33	1.2400	1.310	0.468	-0.001	0.7745	0.2615	29.892	46.798

Rudder No. 3 X/D = 0.39 J = 0.51

Angle	V	RPM	C_L	C_N	C_D	C_{mz}	C_{mx}	C_{my}	CP_c	CP_s
-30.40	10.00	1431.02	-2.6410	-2.706	0.845	0.046	-1.5940	0.5215	28.313	45.987
-20.40	10.00	1431.05	-1.7425	-1.760	0.363	0.077	-1.0175	0.2275	25.583	44.115
-10.40	10.00	1430.98	-0.8520	-0.860	0.124	0.055	-0.4790	0.0790	23.680	41.838
-0.40	10.00	1430.38	-0.0175	-0.018	0.057	-0.015	0.0225	0.0350	115.635	-137.005
9.60	10.00	1430.86	0.7930	0.802	0.124	-0.089	0.5290	0.0700	18.863	51.918
19.60	10.00	1431.09	1.6335	1.657	0.352	-0.111	1.0810	0.2080	23.321	51.090
29.60	10.00	1431.57	2.4335	2.519	0.817	-0.058	1.6145	0.4945	27.707	50.873

Rudder No. 3 X/D = 0.52 J = 0.35

Angle	V	RPM	C_L	C_N	C_D	C_{mz}	C_{mx}	C_{my}	CP_c	CP_s
-30.40	10.00	2076.25	-3.5270	-3.694	1.289	0.107	-2.0150	0.7740	27.079	43.060
-20.40	10.00	2076.65	-2.4425	-2.481	0.547	0.161	-1.3520	0.3315	23.491	41.163
-10.40	10.00	2077.47	-1.2275	-1.240	0.179	0.110	-0.6340	0.1210	21.098	37.474
-0.40	10.00	2076.58	-0.0510	-0.051	0.076	-0.024	0.0560	0.0535	75.098	-122.834
9.60	10.00	2076.65	1.0500	1.062	0.161	-0.152	0.7450	0.1020	15.609	56.197
19.60	10.00	2076.92	2.2135	2.243	0.468	-0.227	1.5265	0.2955	19.861	54.004
29.60	10.00	2077.40	3.3565	3.504	1.184	-0.168	2.3215	0.7545	25.166	53.666

Rudder No. 3 X/D = 0.39 J = 0.94

Angle	V	RPM	C_L	C_N	C_D	C_{mz}	C_{mx}	C_{my}	CP_c	CP_s
-30.40	10.00	792.45	-1.1530	-1.211	0.430	-0.062	-0.7340	0.2470	35.075	47.949
-20.40	10.00	792.08	-1.1835	-1.175	0.188	0.034	-0.7250	0.1140	27.127	46.654
-10.40	10.00	790.91	-0.5635	-0.564	0.055	0.022	-0.3340	0.0365	26.092	44.883
9.60	10.00	791.31	0.5200	0.522	0.057	-0.063	0.3315	0.0310	17.823	49.035
19.60	10.00	791.12	1.0220	1.025	0.187	-0.069	0.6605	0.1040	23.272	49.538
29.60	10.00	791.71	1.1420	1.211	0.441	0.008	0.7045	0.2410	30.666	45.787

Rudder No. 3 X/D = 0.39 J = 0.51

Angle	V	RPM	C_L	C_N	C_D	C_{mz}	C_{mx}	C_{my}	CP_c	CP_s
-35.40	10.00	1435.40	-1.9300	-2.164	1.020	-0.159	-1.2930	0.6910	37.338	52.642
-30.40	10.00	1434.13	-2.4830	-2.599	0.903	-0.066	-1.4840	0.5510	32.488	45.435
-20.40	10.00	1433.14	-1.8415	-1.842	0.331	0.087	-1.0660	0.2090	25.241	43.641
-10.40	10.00	1433.09	-0.9130	-0.914	0.087	0.050	-0.4990	0.0620	24.542	40.373
-0.40	10.00	1433.15	-0.0500	-0.050	0.024	-0.018	0.0150	0.0190	70.809	-47.508
9.60	10.00	1433.48	0.7780	0.782	0.088	-0.091	0.5315	0.0505	18.350	53.467
19.60	10.00	1432.97	1.6750	1.681	0.305	-0.126	1.1190	0.1845	22.508	51.811
29.60	10.00	1432.87	2.5205	2.595	0.815	-0.046	1.6645	0.5085	28.206	50.857
34.60	10.00	1435.40	2.5920	2.718	1.031	0.138	1.6150	0.7440	35.048	49.856
39.60	10.00	1435.40	1.9730	2.261	1.161	0.167	1.3040	0.8810	37.354	54.702

Rudder No. 3 X/D = 0.39 J = 0.35

Angle	V	RPM	C_L	C_N	C_D	C_{mz}	C_{mx}	C_{my}	CP_c	CP_s
-35.40	10.00	2081.90	-4.0470	-4.132	1.438	0.015	-2.3180	1.1260	29.623	46.924
-30.40	10.00	2079.52	-3.7975	-3.829	1.094	0.150	-2.1580	0.7040	26.070	43.332
-20.40	10.00	2079.22	-2.5605	-2.559	0.459	0.176	-1.4225	0.2835	23.114	41.359
-10.40	10.00	2079.02	-1.2760	-1.274	0.107	0.095	-0.6565	0.0745	22.533	37.158
-0.40	10.00	2078.97	-0.0740	-0.074	0.005	-0.025	0.0485	0.0095	66.406	-82.670
9.60	10.00	2079.13	1.0175	1.018	0.088	-0.147	0.7400	0.0555	15.529	58.006
19.60	10.00	2079.62	2.2335	2.244	0.416	-0.225	1.5435	0.2565	19.959	54.063
29.60	10.00	2079.07	3.5760	3.622	1.038	-0.232	2.4660	0.6710	23.587	53.773
34.60	10.00	2081.90	4.0800	4.119	1.339	-0.139	2.8400	0.9860	26.598	55.767
39.60	10.00	2081.90	4.1910	4.528	2.037	0.072	2.8510	1.4230	31.579	53.956

Rudder No. 3 X/D = 0.52 J = 0.94

Angle	V	RPM	C_L	C_N	C_D	C_{mz}	C_{mx}	C_{my}	CP_c	CP_s
-35.40	10.00	792.52	-1.1170	-1.169	0.446	-0.131	-0.6600	0.3100	41.228	46.808
-30.40	10.00	791.90	-1.0885	-1.160	0.437	-0.062	-0.7475	0.2405	35.274	51.501
-20.40	10.00	792.12	-1.1565	-1.147	0.180	0.036	-0.7330	0.0990	26.815	48.365

-10.40	10.00	790.73	-0.5610	-0.561	0.053	0.023	-0.3445	0.0210	26.011	46.509
-0.40	10.00	792.75	0.0060	0.006	0.023	-0.010	-0.0005	0.0100	523.356	54.608
9.60	10.00	791.86	0.5535	0.555	0.057	-0.060	0.3395	0.0305	19.199	46.634
19.60	10.00	792.92	1.0745	1.074	0.182	-0.072	0.6905	0.1020	23.241	49.218
29.60	10.00	789.99	1.2275	1.294	0.459	0.016	0.7400	0.2590	31.204	45.030
34.60	10.00	792.52	0.9540	1.072	0.505	0.022	0.5990	0.3200	32.009	48.295

Rudder No. 3 X/D =0.52 J = 0.51

Angle	V	RPM	C_L	C_N	C_D	C_{mz}	C_{mx}	C_{my}	CP_c	CP_s
-35.40	10.00	1433.64	-1.8010	-2.183	1.233	-0.163	-1.1070	0.6230	37.434	43.321
-30.40	10.00	1432.47	-2.4430	-2.524	0.823	0.006	-1.5100	0.4855	29.756	46.756
-20.40	10.00	1431.95	-1.8605	-1.849	0.302	0.088	-1.0935	0.1820	25.223	44.307
-10.40	10.00	1433.67	-0.9165	-0.913	0.065	0.053	-0.5120	0.0375	24.246	41.355
-0.40	10.00	1432.30	-0.0385	-0.038	0.011	-0.015	0.0110	0.0050	69.338	-44.281
9.60	10.00	1432.97	0.8020	0.803	0.073	-0.091	0.5340	0.0400	18.704	51.809
19.60	10.00	1433.51	1.7110	1.709	0.287	-0.124	1.1240	0.1725	22.726	50.788
29.60	10.00	1429.36	2.5530	2.626	0.824	-0.036	1.6505	0.4900	28.566	49.291
34.60	10.00	1433.64	2.2940	2.459	1.005	0.068	1.5530	0.6830	32.751	53.176
39.60	10.00	1433.64	1.8390	2.239	1.289	0.164	1.2410	0.8500	37.306	52.349

Rudder No. 3 X/D = 0.52 J = 0.35

Angle	V	RPM	C_L	C_N	C_D	C_{mz}	C_{mx}	C_{my}	CP_c	CP_s
-35.40	10.00	2079.45	-3.4120	-3.801	1.761	-0.299	-1.9020	1.0320	37.844	41.927
-30.40	10.00	2079.55	-3.6570	-3.736	1.151	0.132	-2.1470	0.6435	26.443	43.699
-20.40	10.00	2078.35	-2.5800	-2.562	0.412	0.176	-1.4475	0.2410	23.146	41.639
-10.40	10.00	2077.80	-1.2470	-1.235	0.050	0.098	-0.6510	0.0270	22.058	37.697
-0.40	10.00	2078.15	-0.0780	-0.078	-0.045	-0.024	0.0425	-0.0240	60.822	-70.376
9.60	10.00	2078.13	1.0550	1.051	0.068	-0.155	0.7550	0.0365	15.279	56.780
19.60	10.00	2078.30	2.2800	2.273	0.373	-0.229	1.5610	0.2340	19.886	53.563
29.60	10.00	2077.63	3.5260	3.564	1.009	-0.199	2.3830	0.6360	24.412	52.376
34.60	10.00	2079.45	3.9130	4.099	1.546	-0.102	2.6960	0.9540	27.485	52.781
39.60	10.00	2079.45	3.1120	3.718	2.071	0.269	2.1400	1.3600	37.221	53.086

Table I Particulars of Three All-Movable Rudder Models

Rudder Number	1	2	3
Mean Chord c mm	667	667	667
Span S mm	1000	1000	1200
Geometric Aspect Ratio AR_G	1.50	1.50	1.80
Taper Ratio C_T/C_R	0.80	1.0	1.0
Thickness/Chord Ratio t/c	0.20	0.20	0.20
Section	NACA0020 Root and Tip with square tips		

Table II Overall Modified Wageningen B4.40 Series Propeller Details

Number of Blades	4
Range of revolutions rpm	0 to 3000
Diameter mm	800
Boss Diameter (max) mm	200
Mean Pitch Ratio	0.95 (set for tests)
Blade Area Ratio	0.40
Rake (deg)	0°
Blade Thickness Ratio t/D	0.050
Sections shape	Based on Wageningen B series
Blade Outline shape	Based on Wageningen but with reduced skew

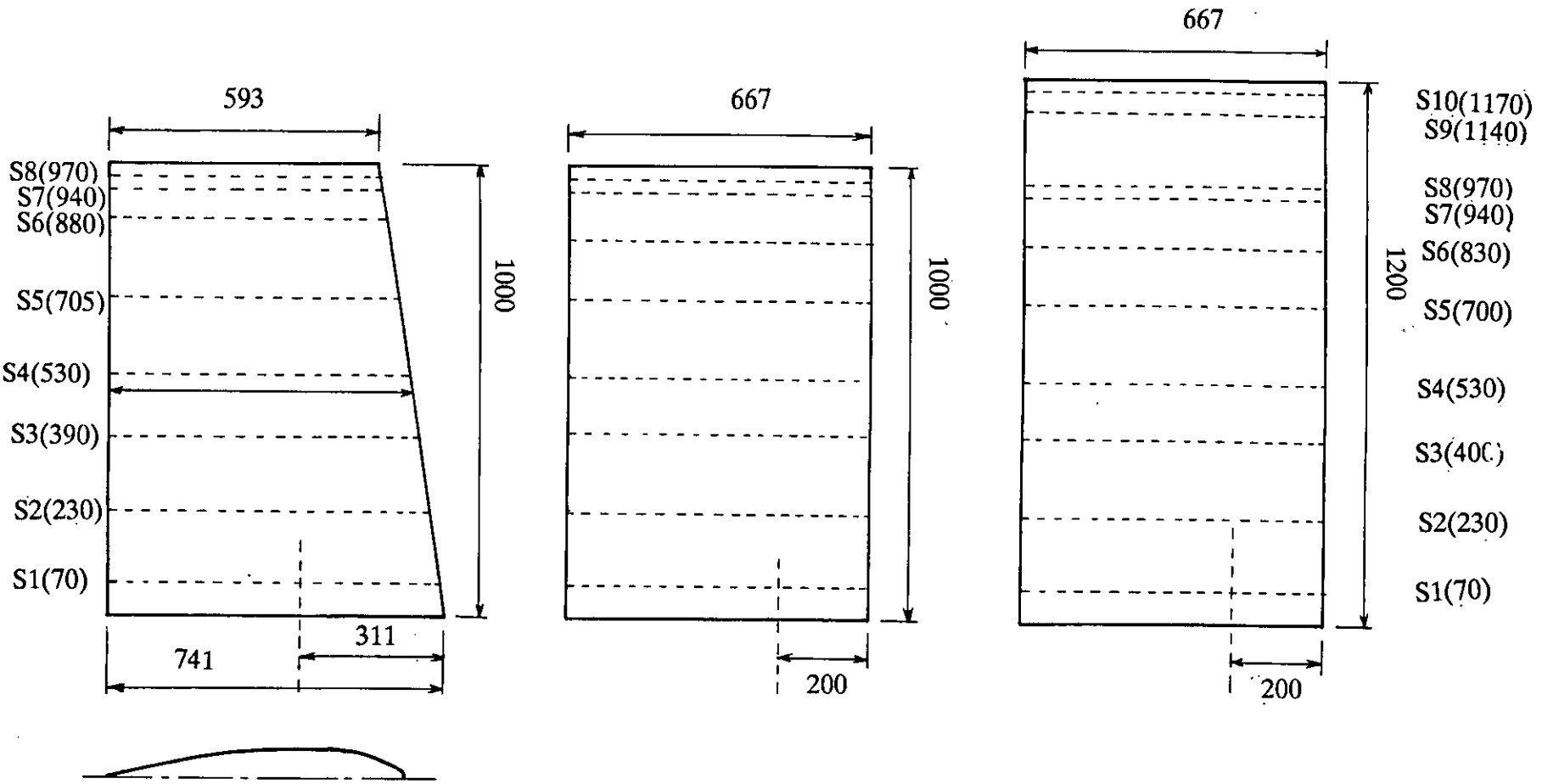

SECTION: NACA 0020 For All Rudders

Chordwise position of tappings (%c from L.E.):
0, 2.5, 5, 10, 20, 30, 40, 50, 60, 70, 80, 90, 95

All dimensions in mm

Figure 1 Dimensions of Three All-Movable Rudder Models

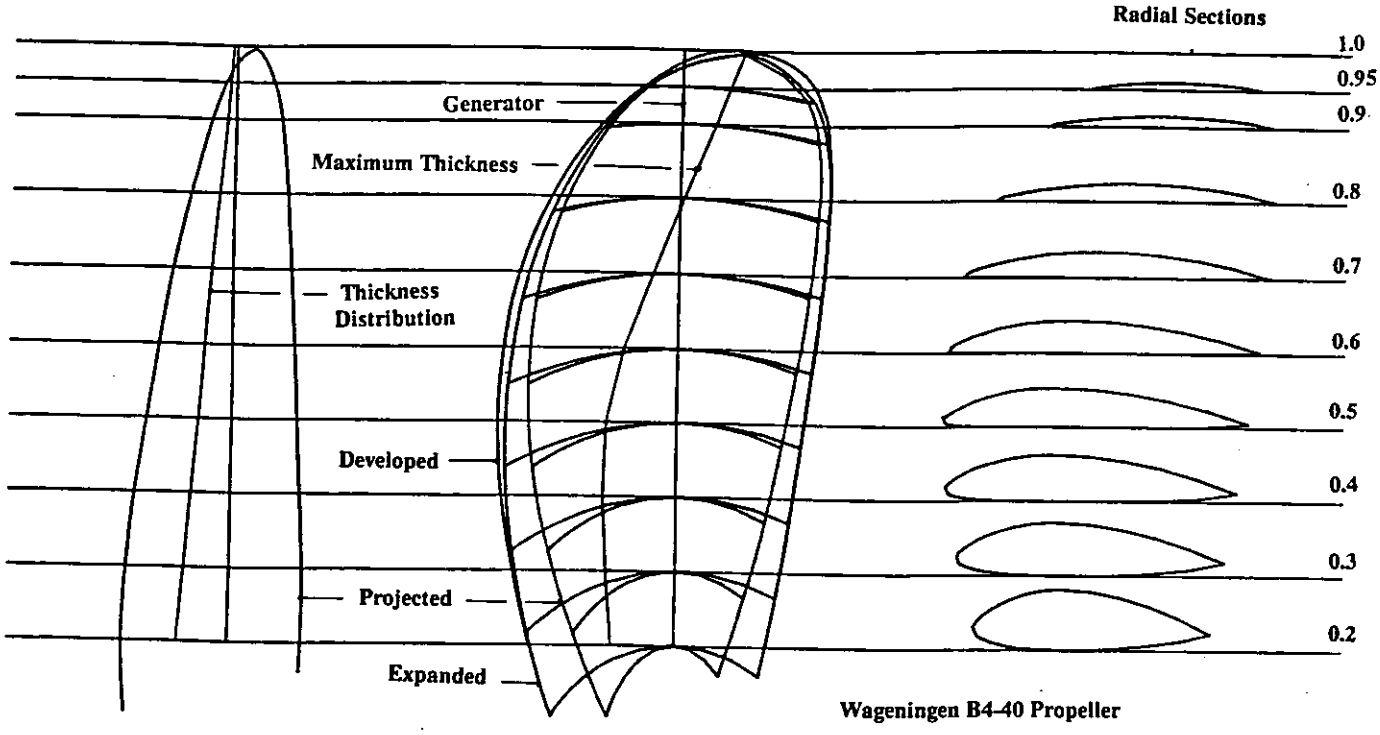

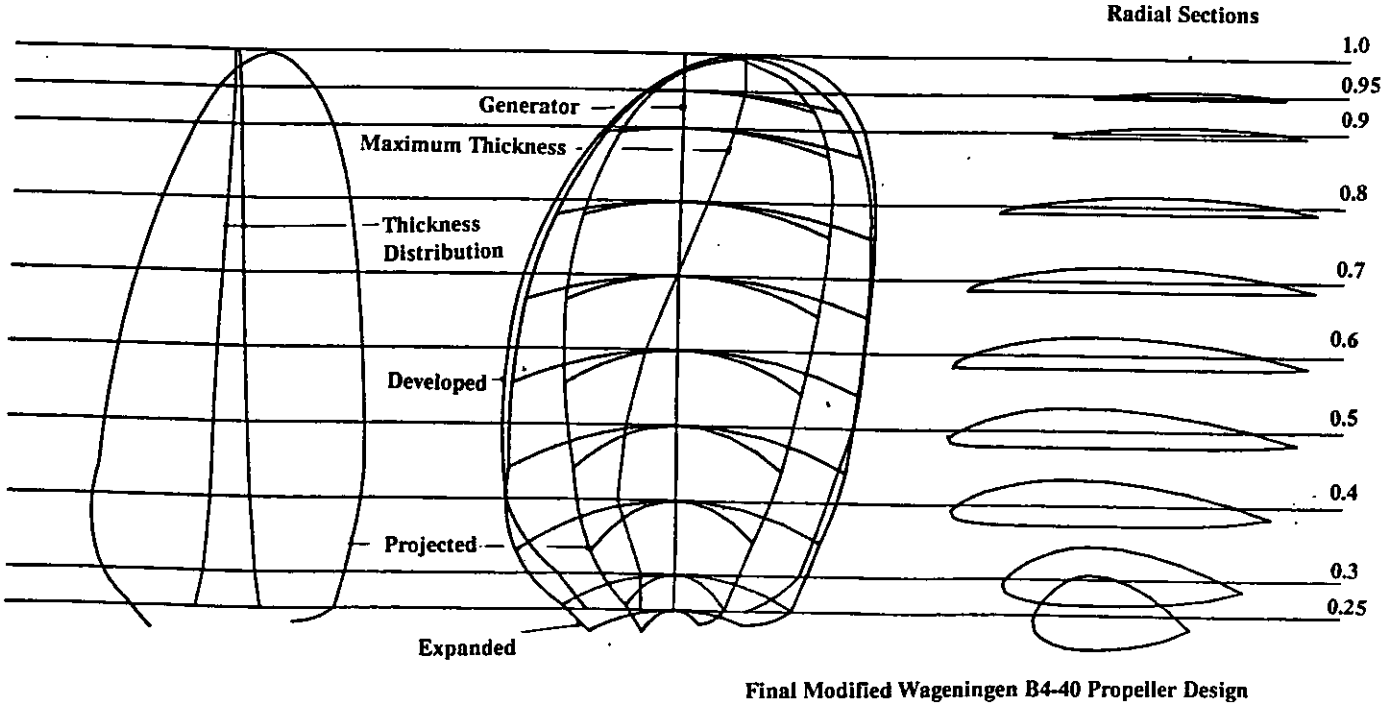

Figure 2 Comparison of Basis and Modified Wageningen B4.40 Propeller

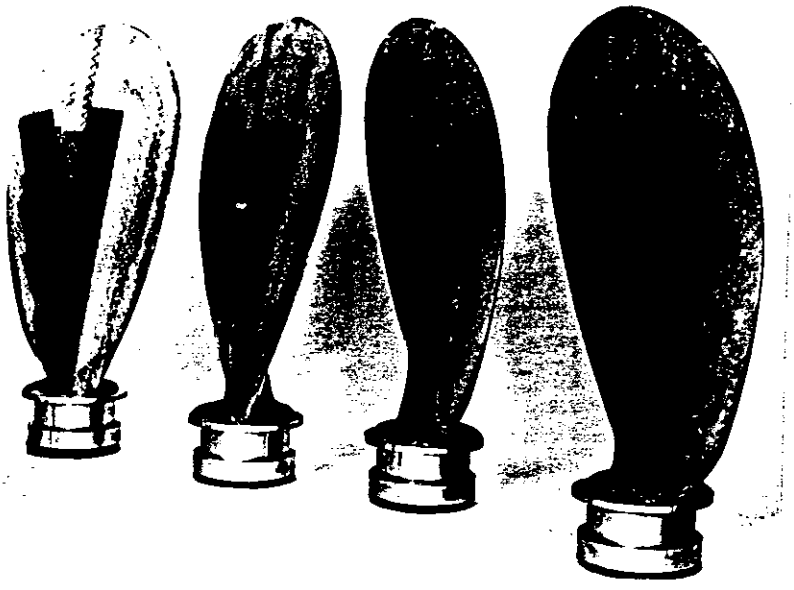

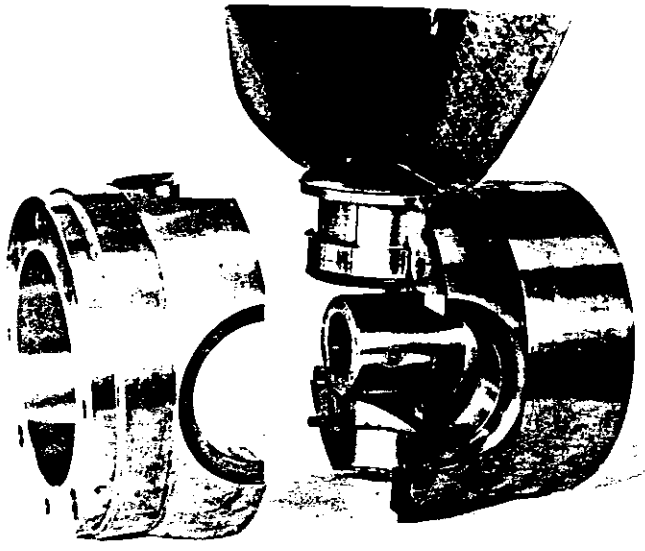

Figure 3 Views of Propeller Blades, Hub and final Assembly

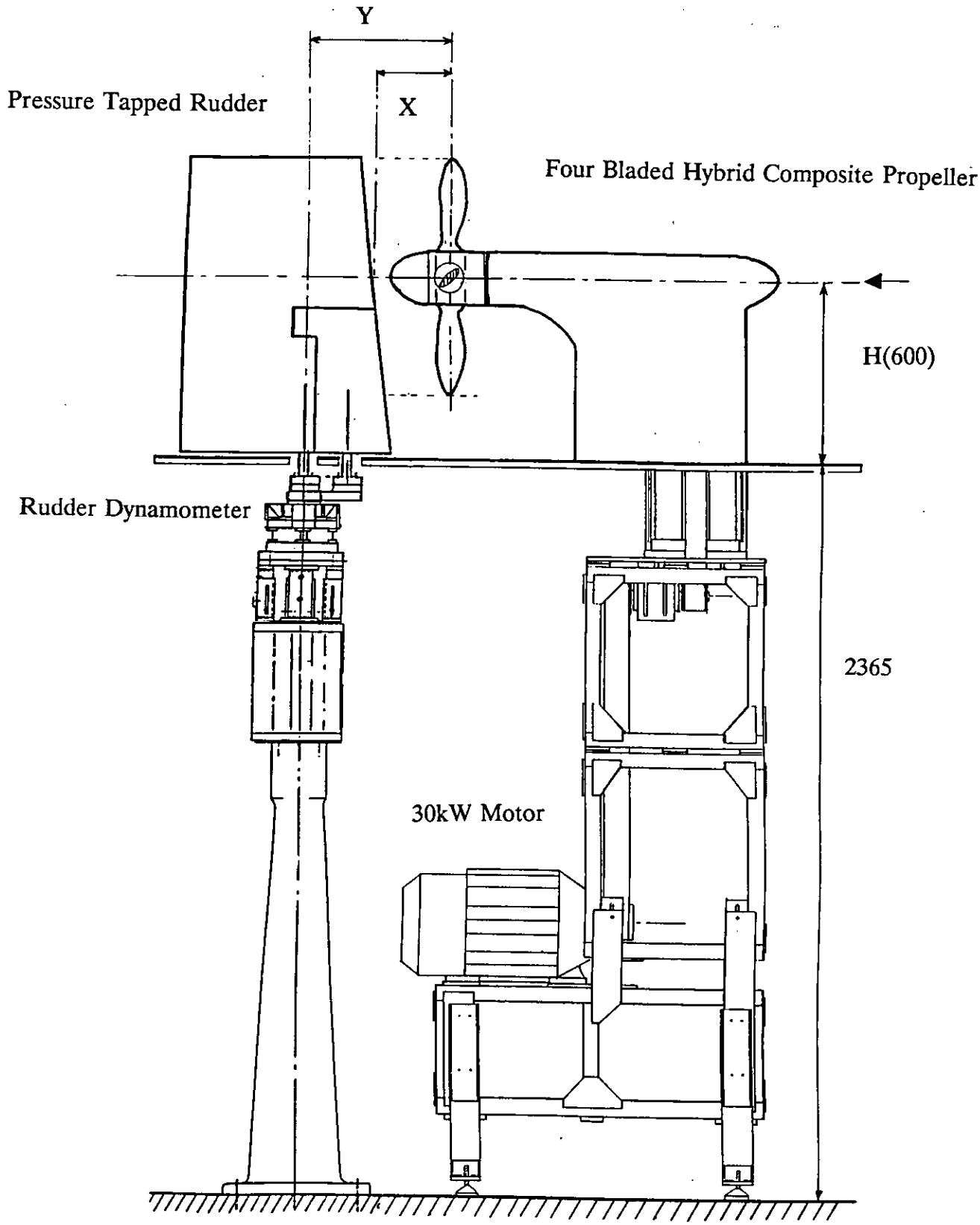

Figure 4 Overall Test Rig for Investigation of Rudder and Propeller Interaction

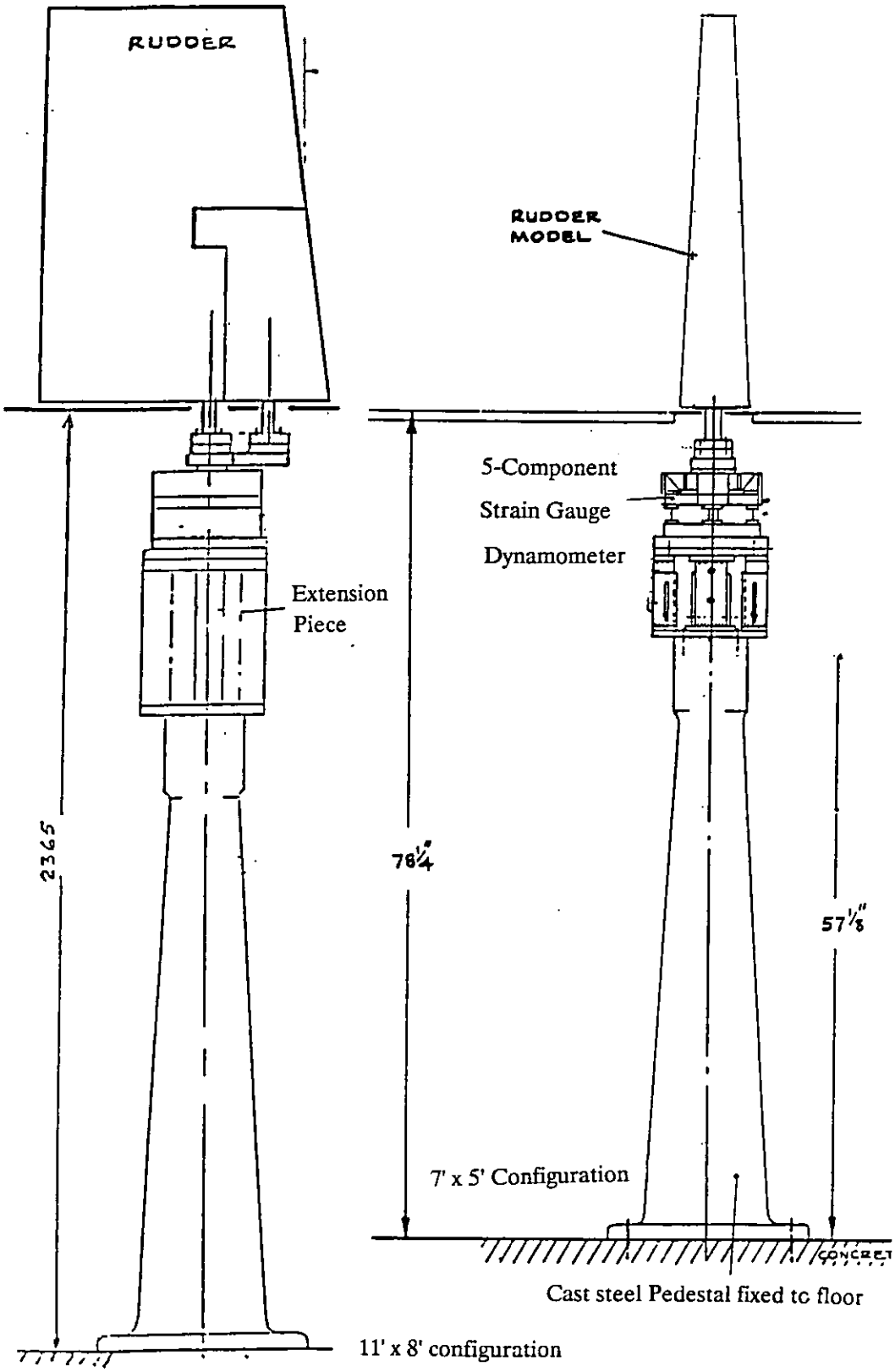

Figure 5 Modification to Original Rudder Test Rig

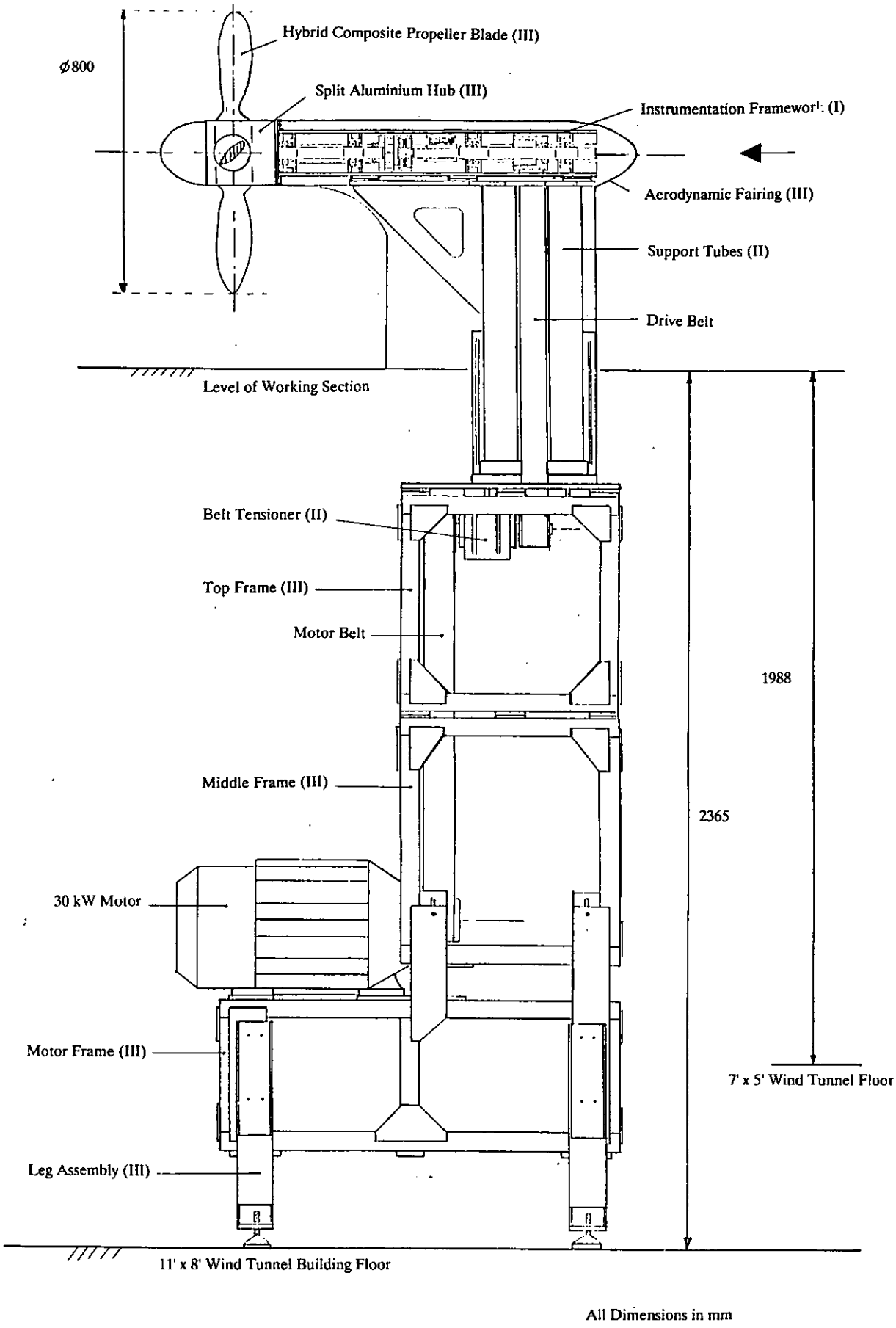

Figure 6 Side View of Installed Propeller Rig

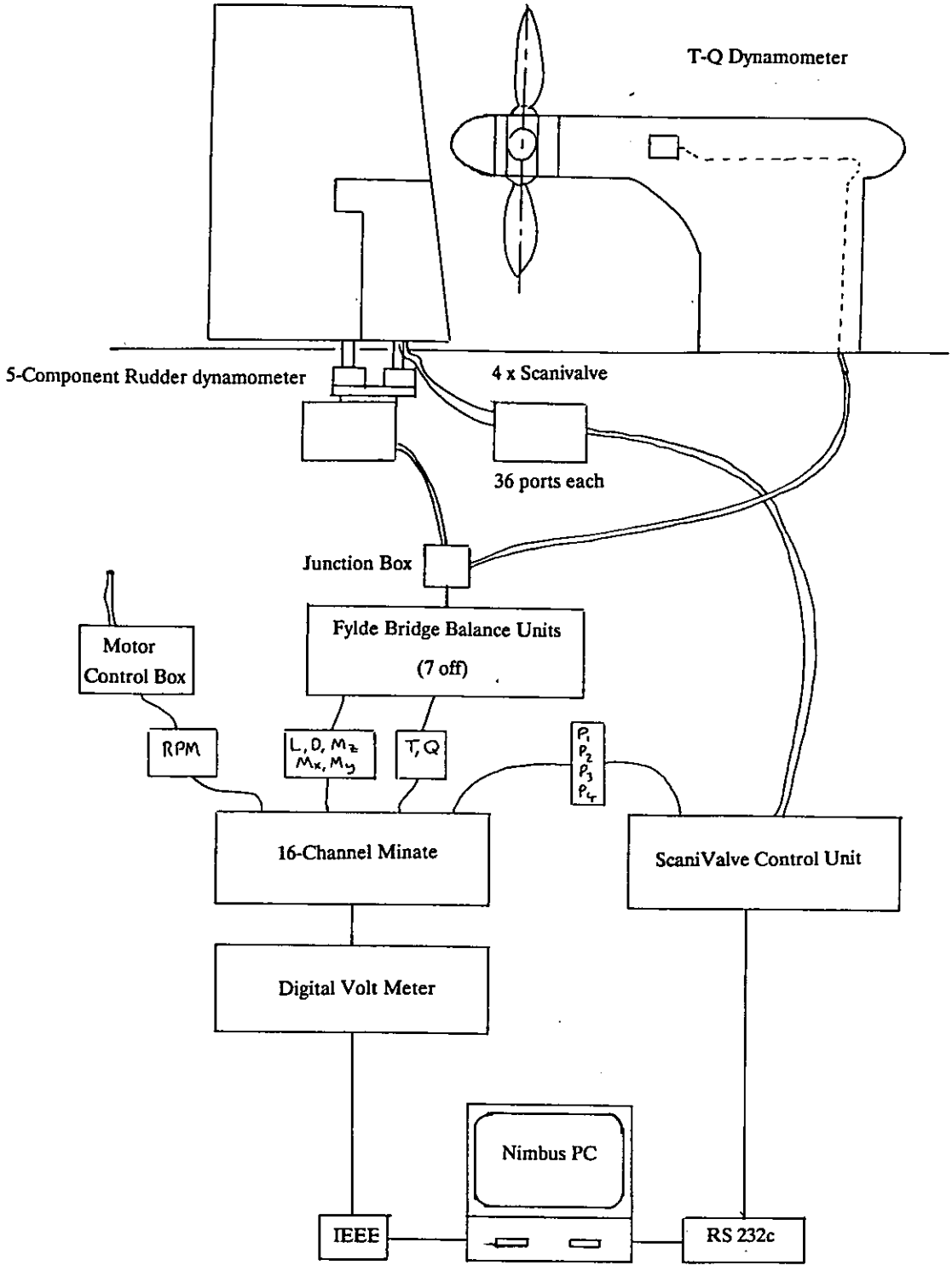

Figure 7 Schematic of Data Acquisition System

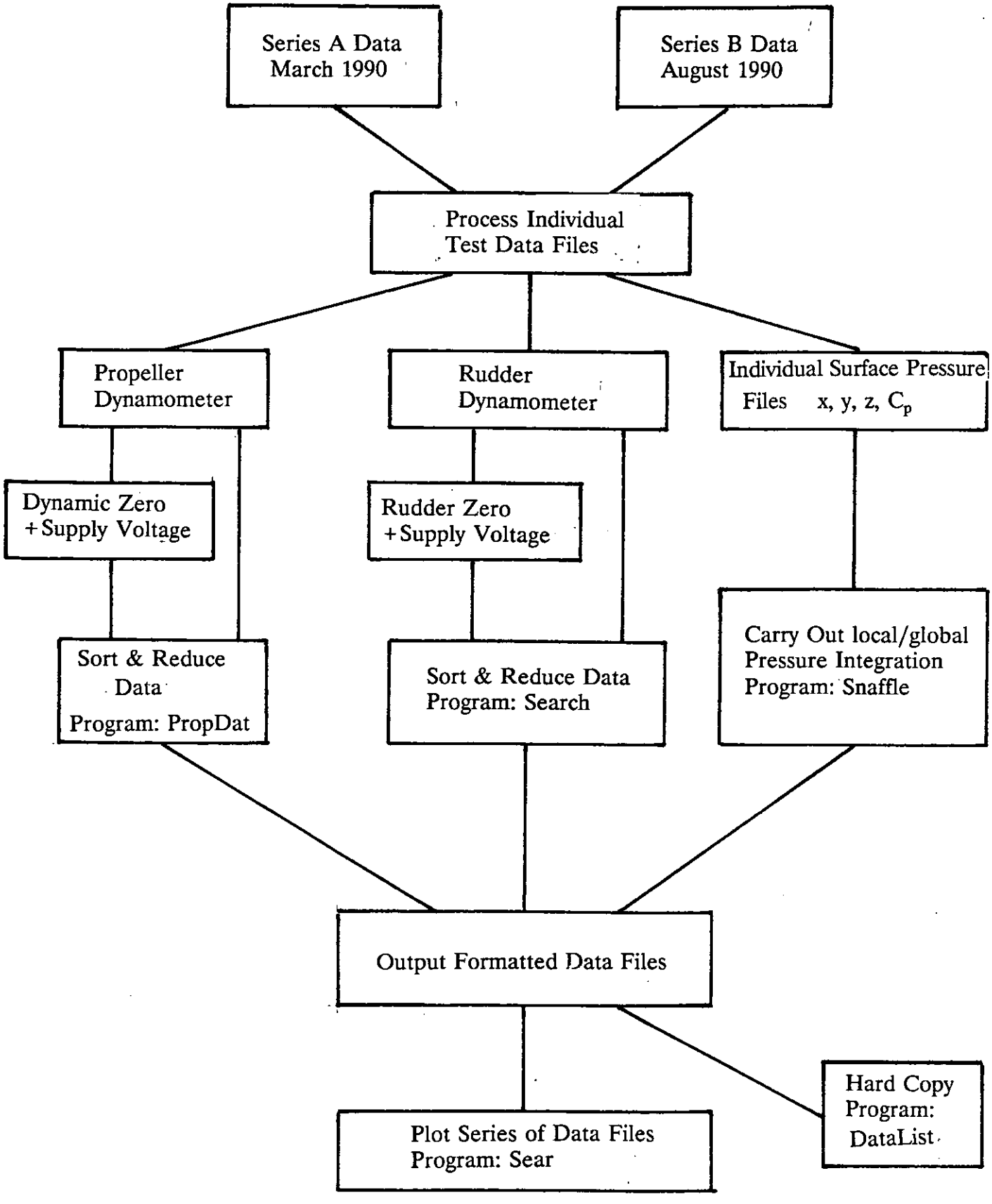

Figure 8 Schematic of Data Analysis Process

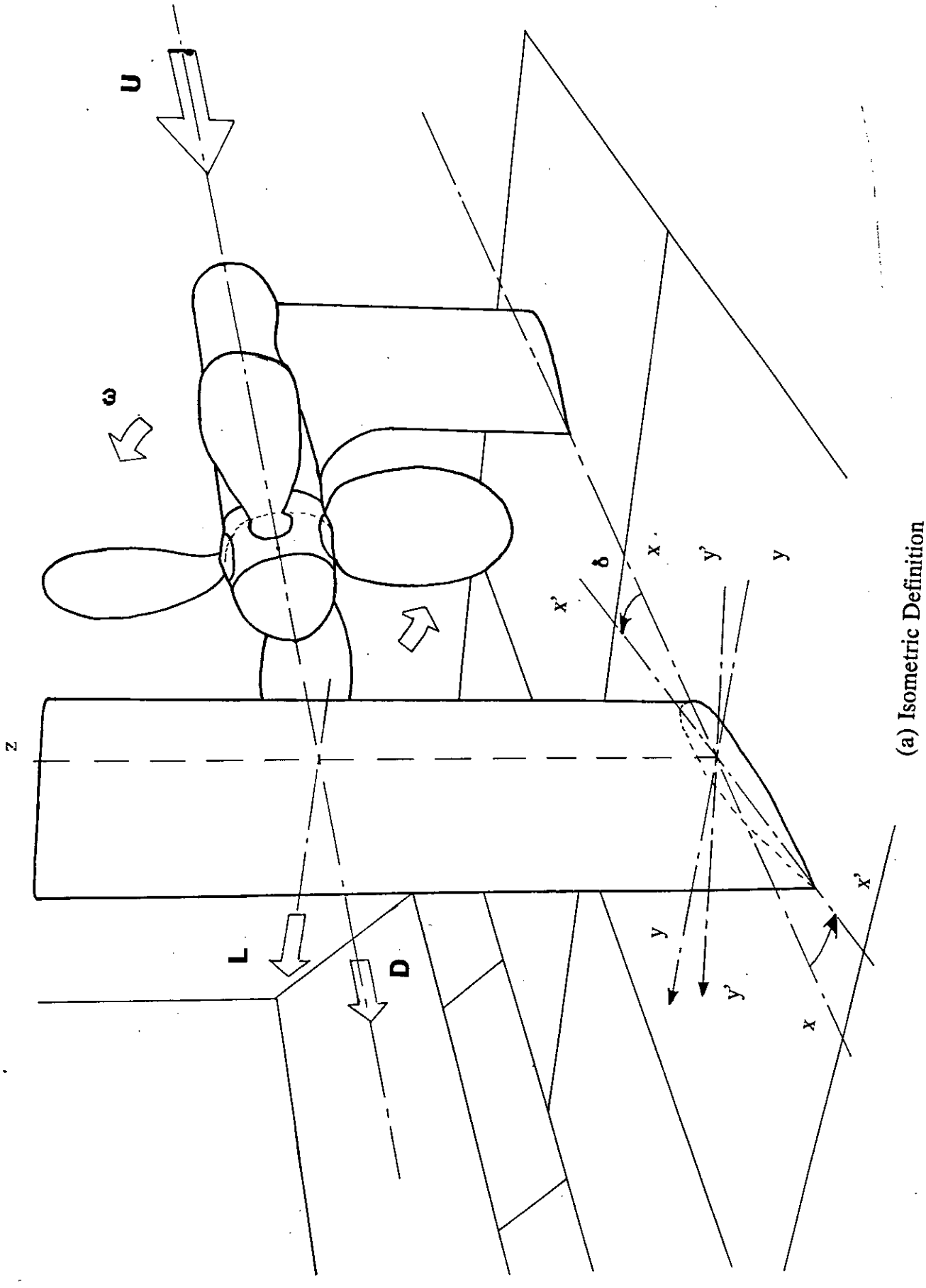

Figure 9 Rudder and Propeller Test Definition 9(a) Isometric Definition

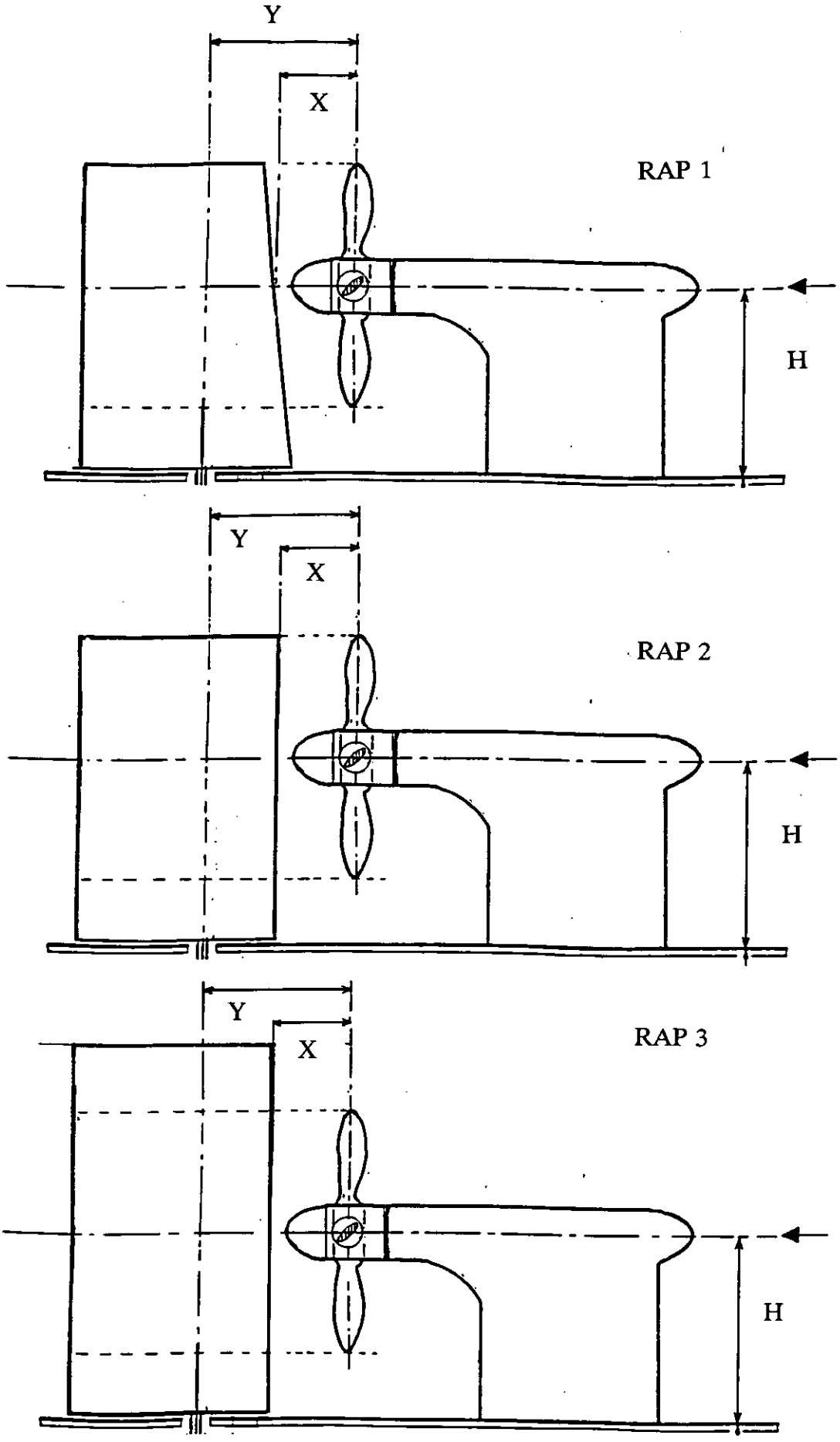

Figure 9(b) Configuration Geometries

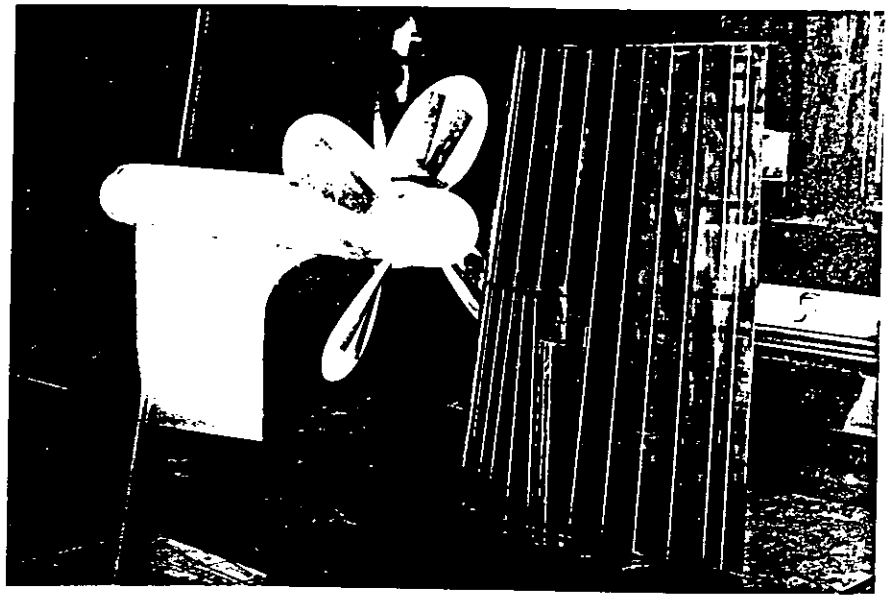

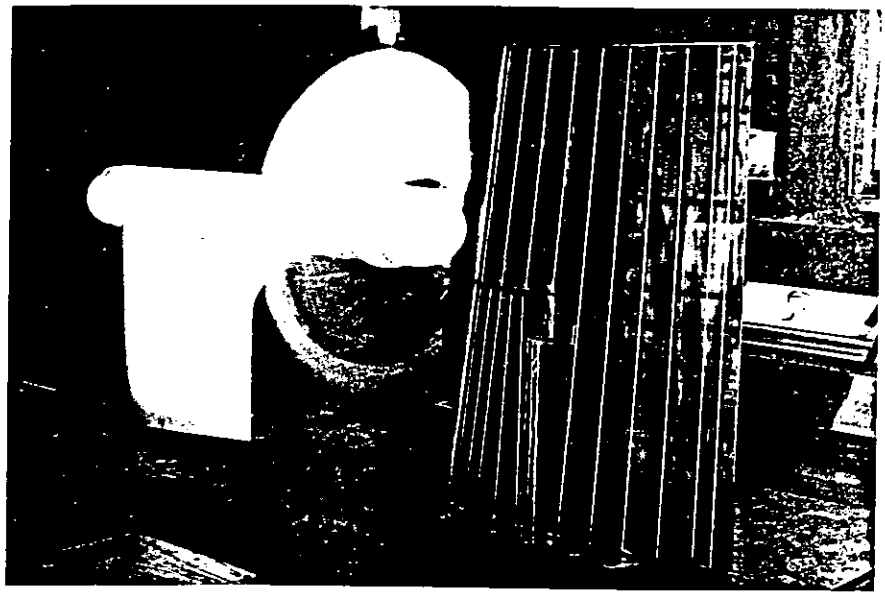

Figure 9(c) Views of rig

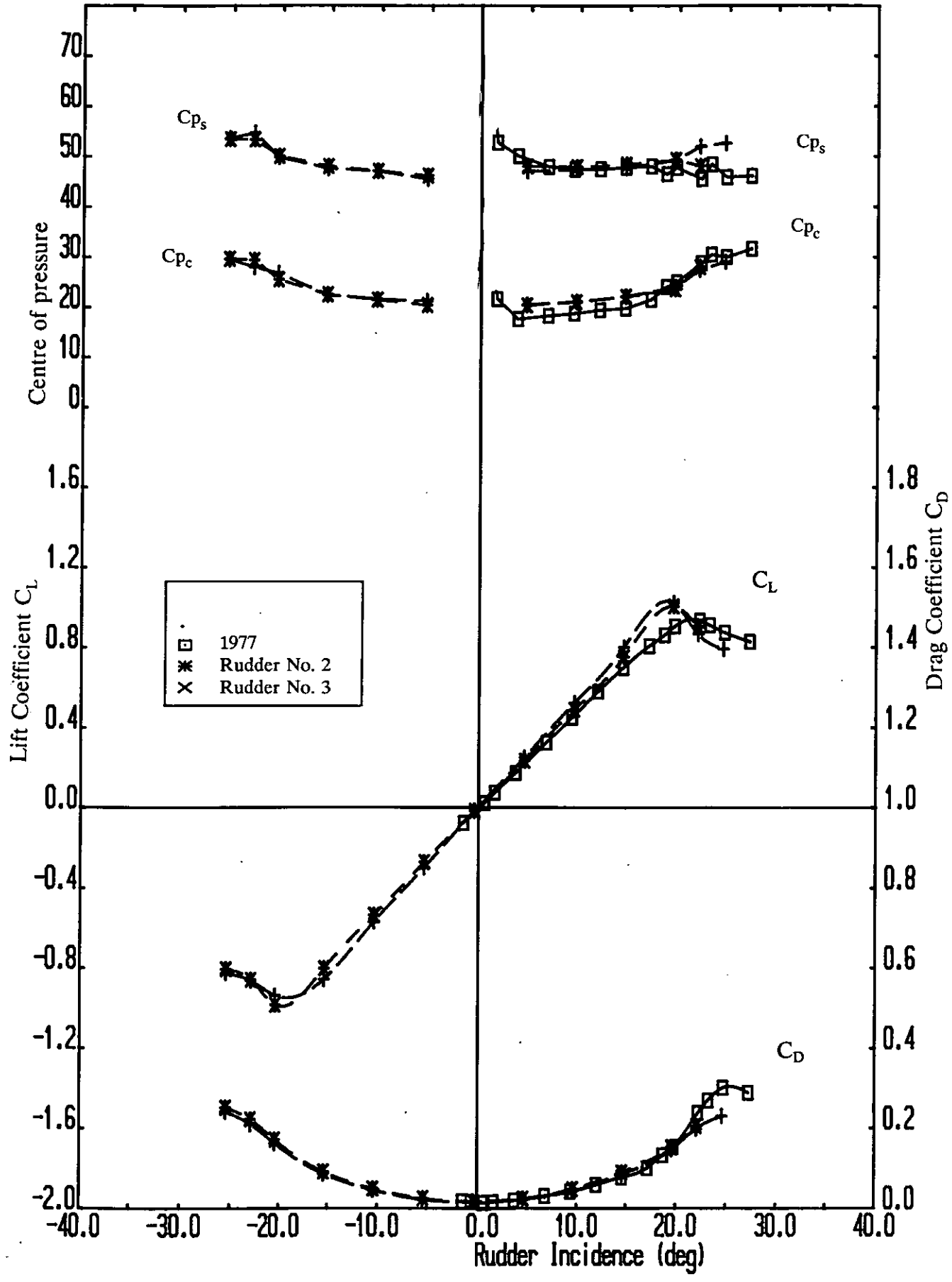

Figure 10 Comparison of Rudder Free Stream Characteristic between 1977 and 1990

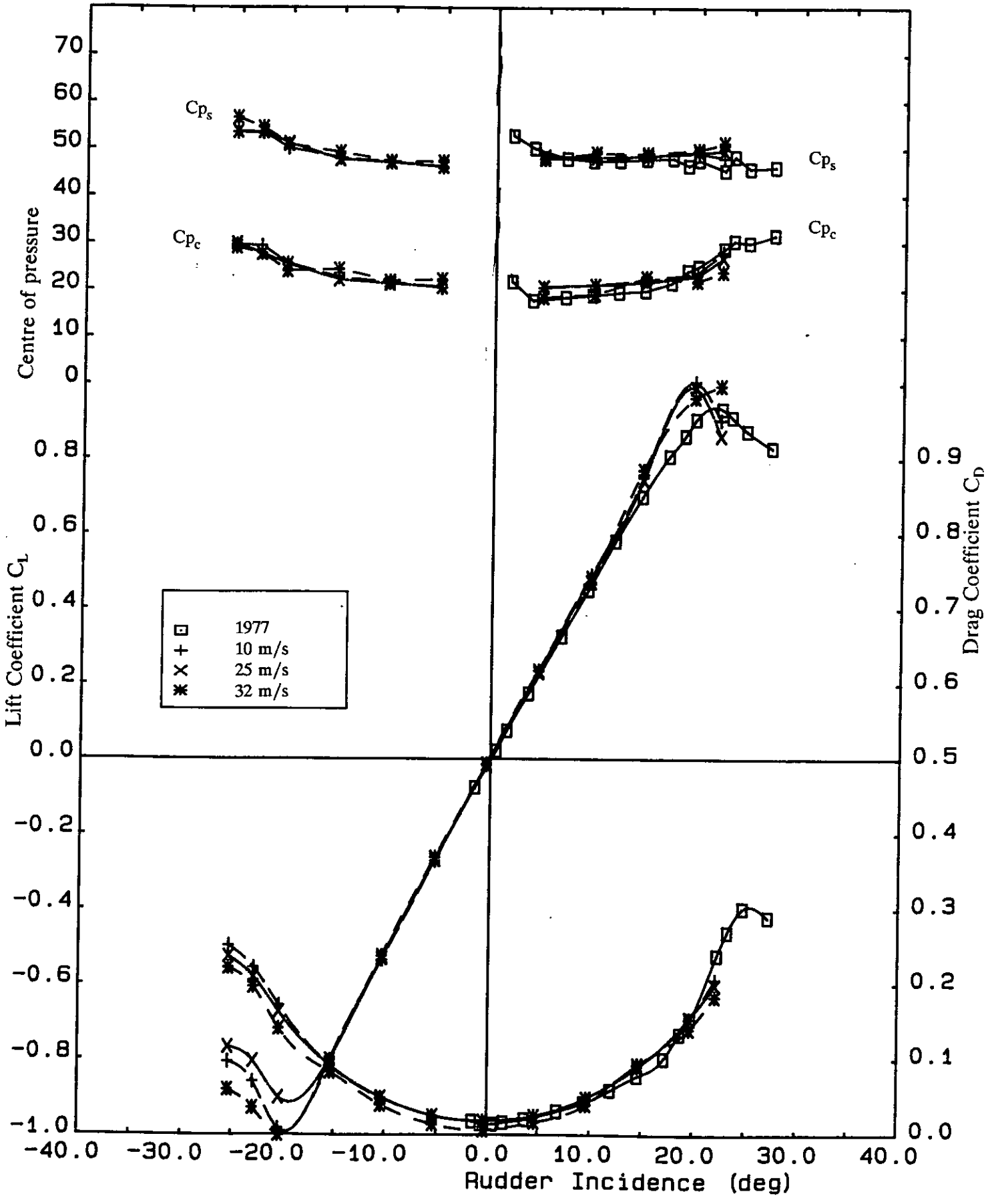

Figure 11 Effect of Reynolds Number on the freestream Characteristic All-Movable Rudder No. 1

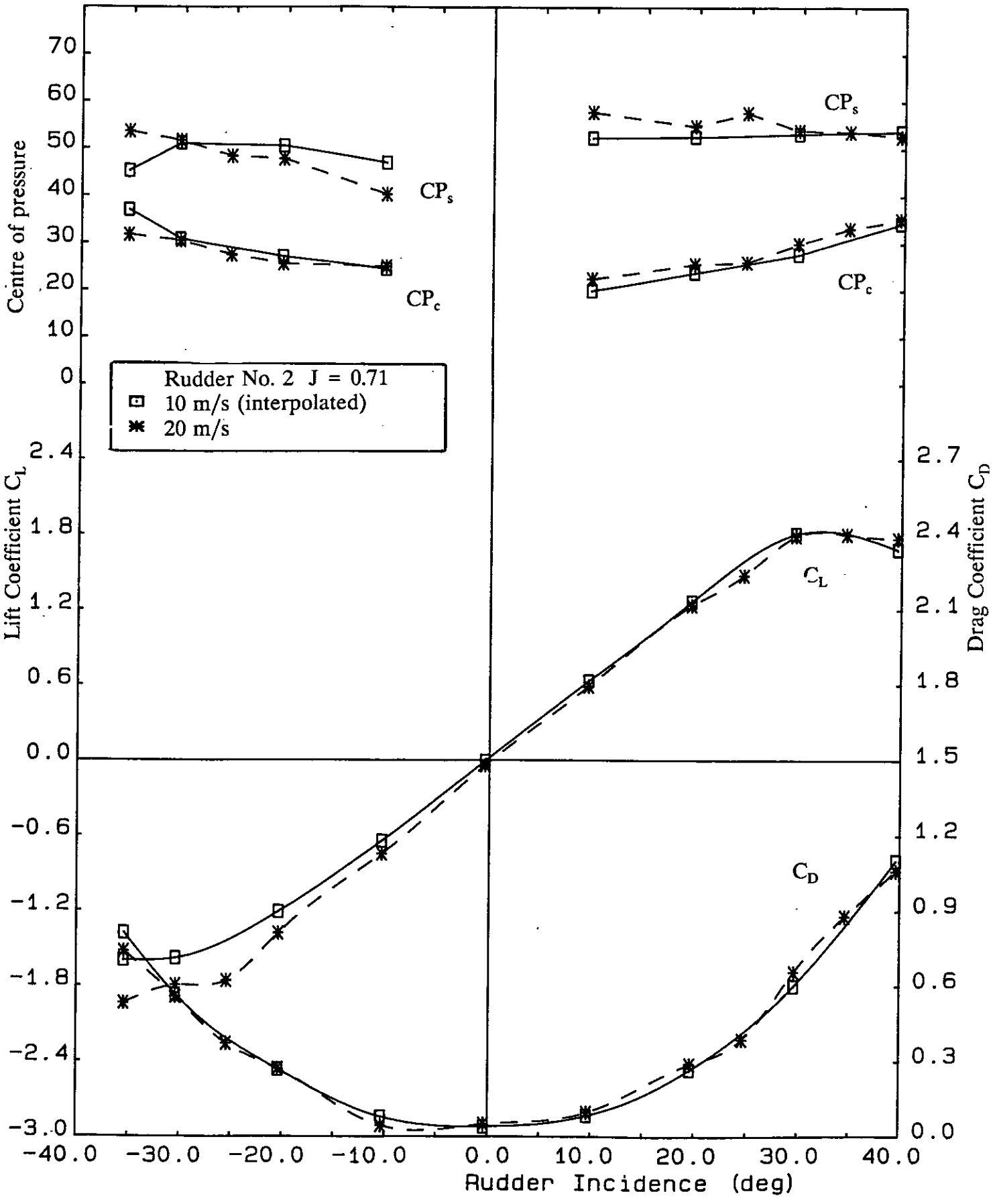

Figure 12 Influence of Reynolds Number on Rudder performance aft of Propeller

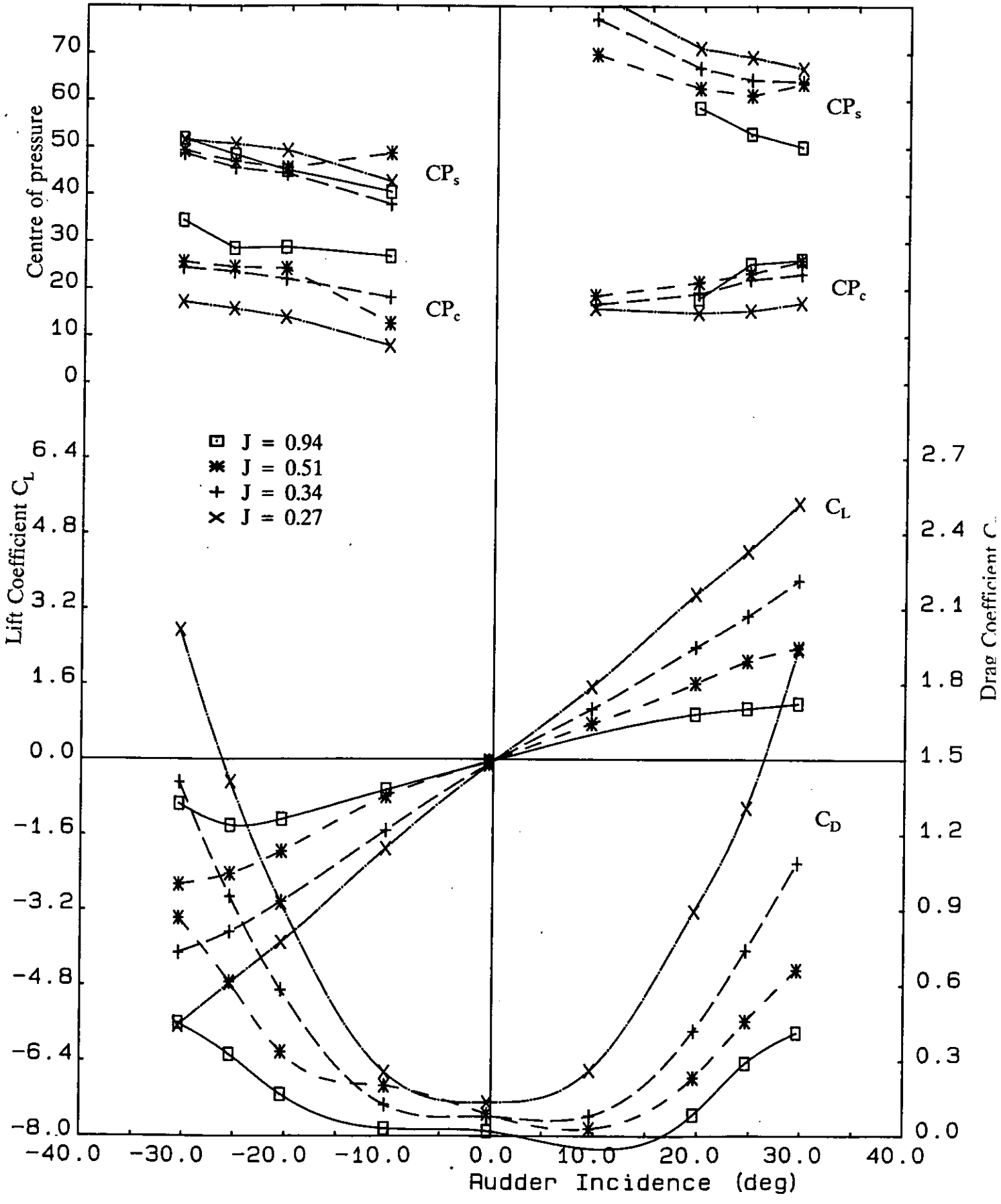

Figure 13 Variation of All-Movable Rudder No.1 performance Characteristics for three propeller advance ratios

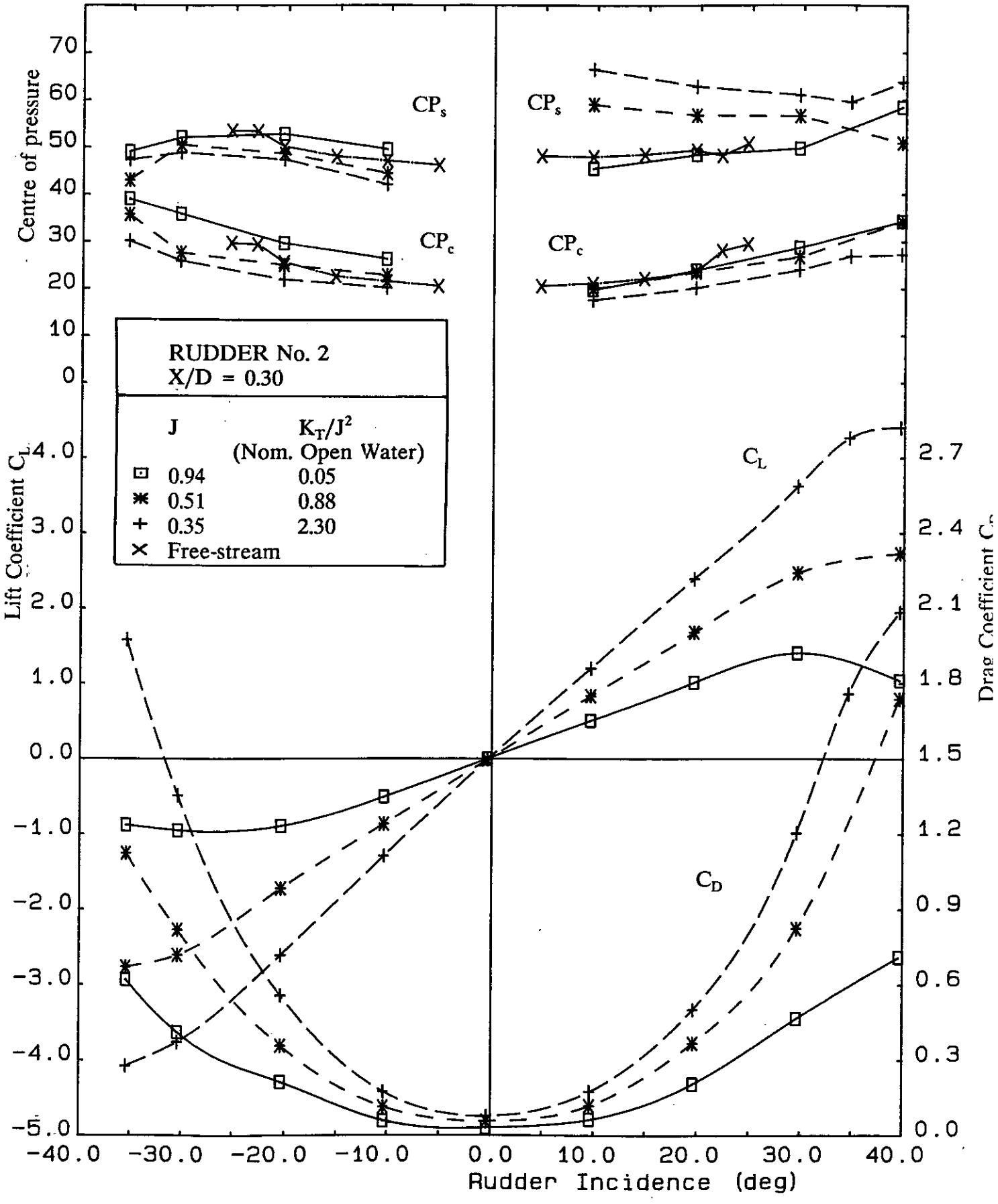

Figure 14 Variation of All-Movable Rudder No.2 performance Characteristics for three propeller advance ratios at a longitudinal separation X/D=0.3

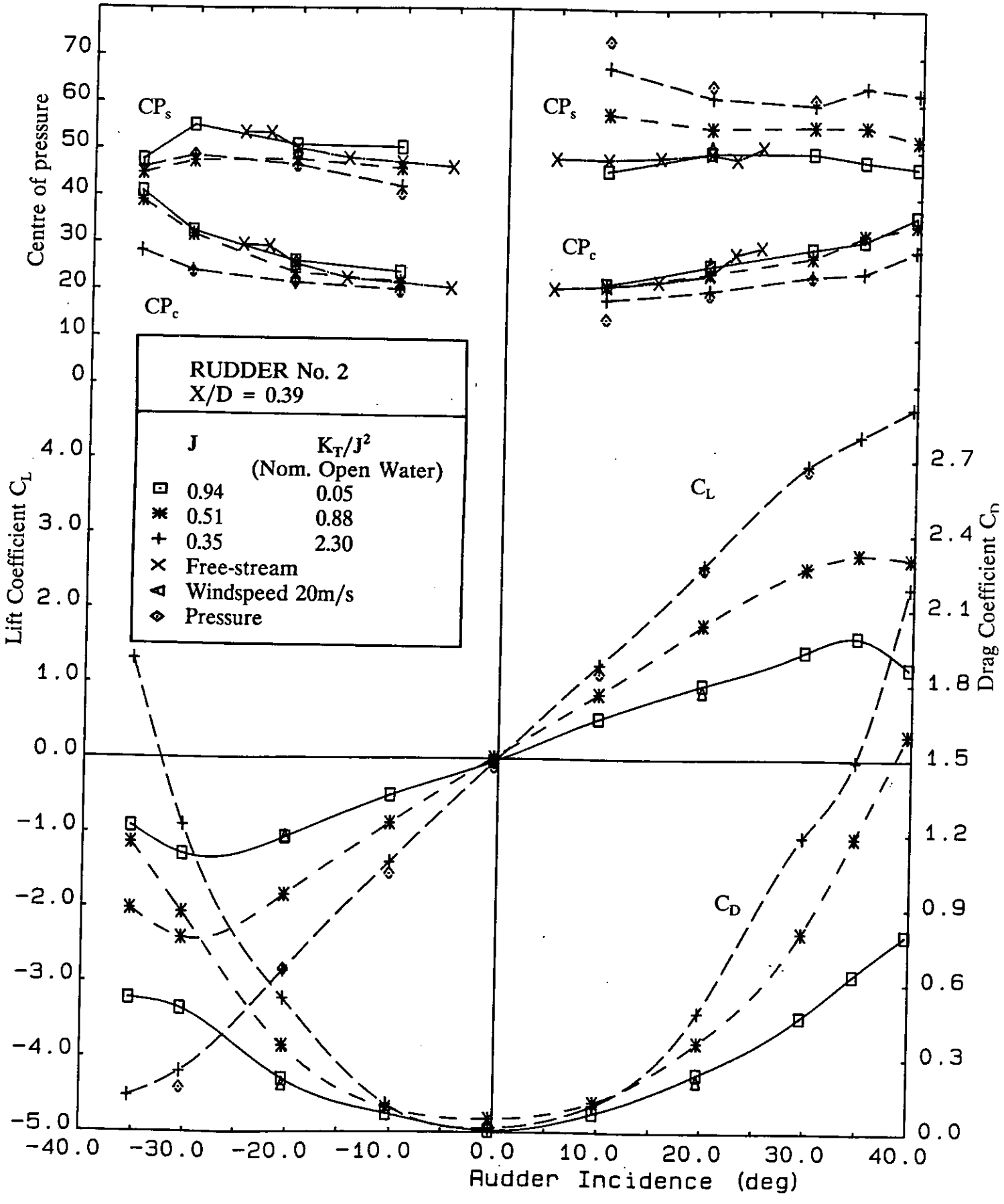

Figure 15 Variation of All-Movable Rudder No.2 performance Characteristics for three propeller advance ratios at a longitudinal separation X/D=0.39

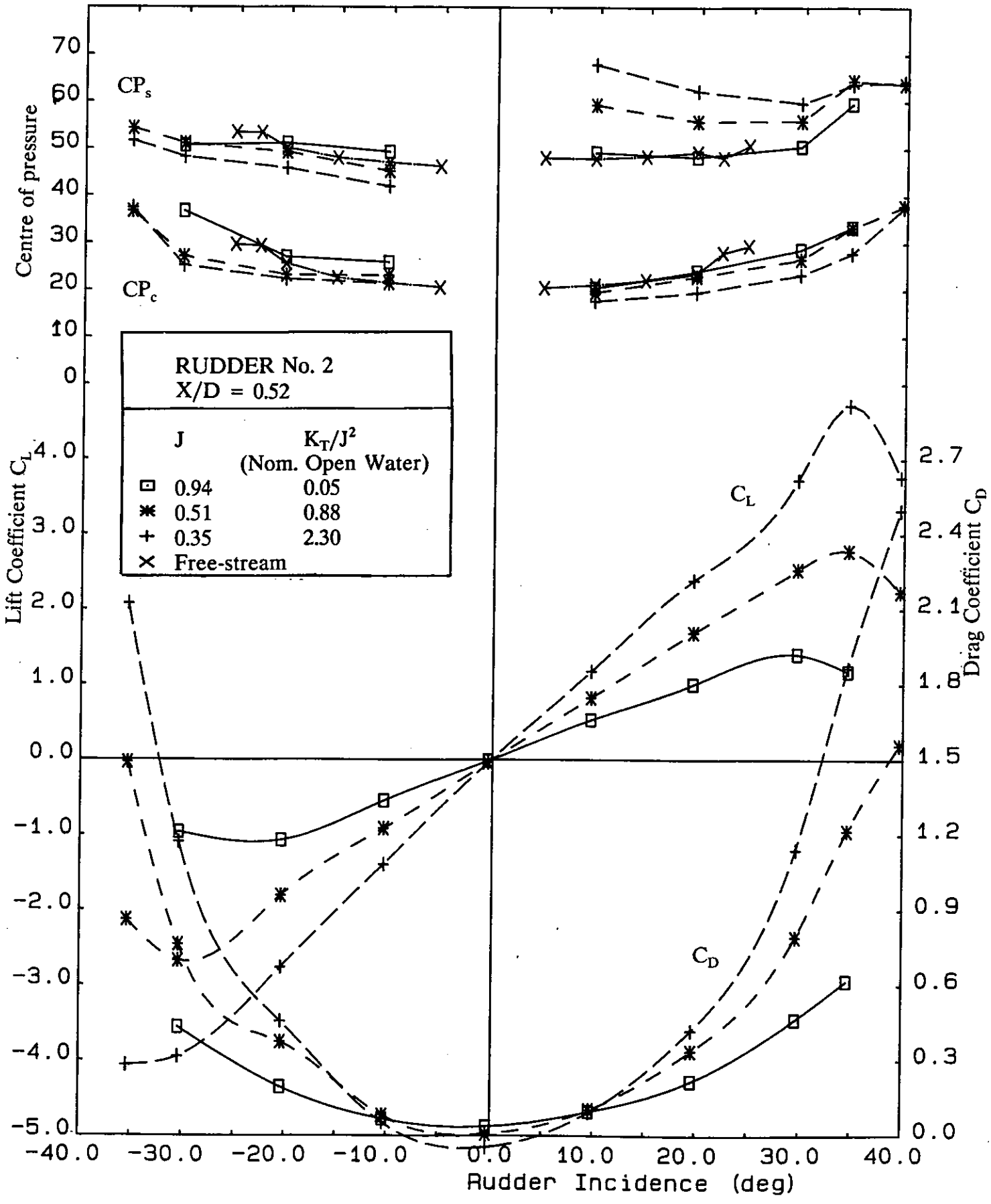

Figure 16 Variation of All-Movable Rudder No.2 performance Characteristics for three propeller advance ratios at a longitudinal separation X/D=0.53

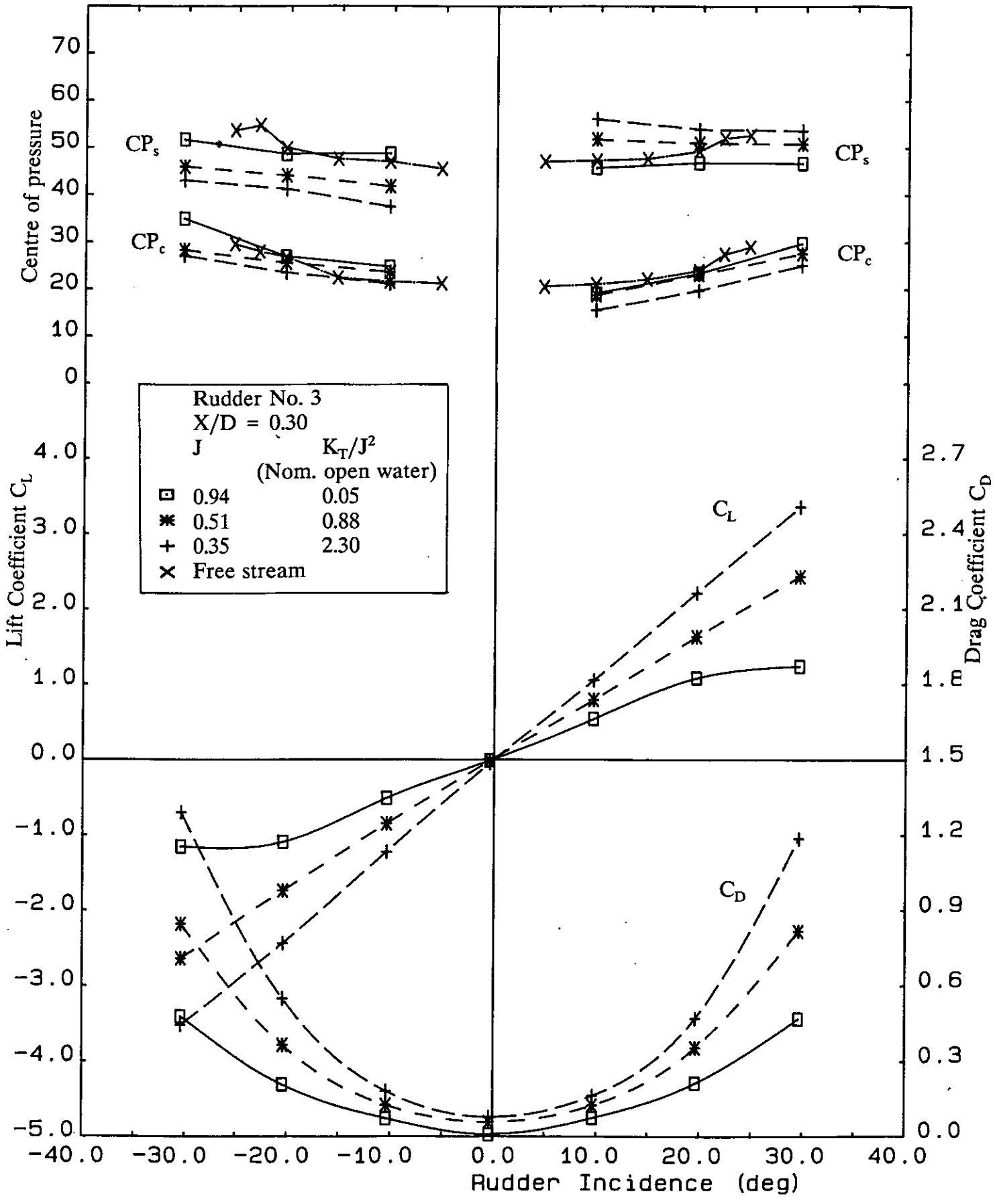

Figure 17 Variation of All-Movable Rudder No.3 performance Characteristics for three propeller advance ratios at a longitudinal separation X/D=0.3

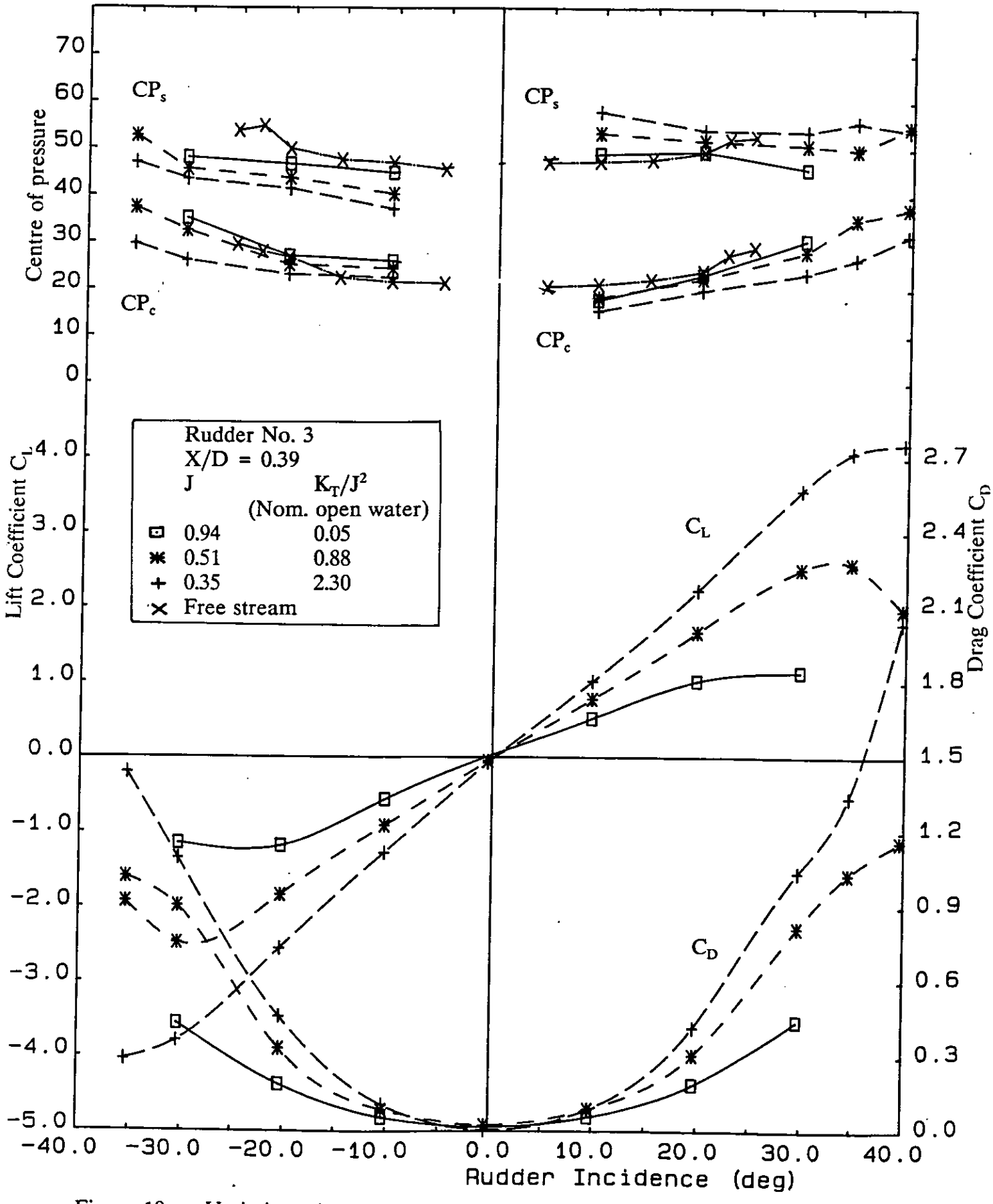

Figure 18 Variation of All-Movable Rudder No.3 performance Characteristics for three propeller advance ratios at a longitudinal separation X/D=0.39

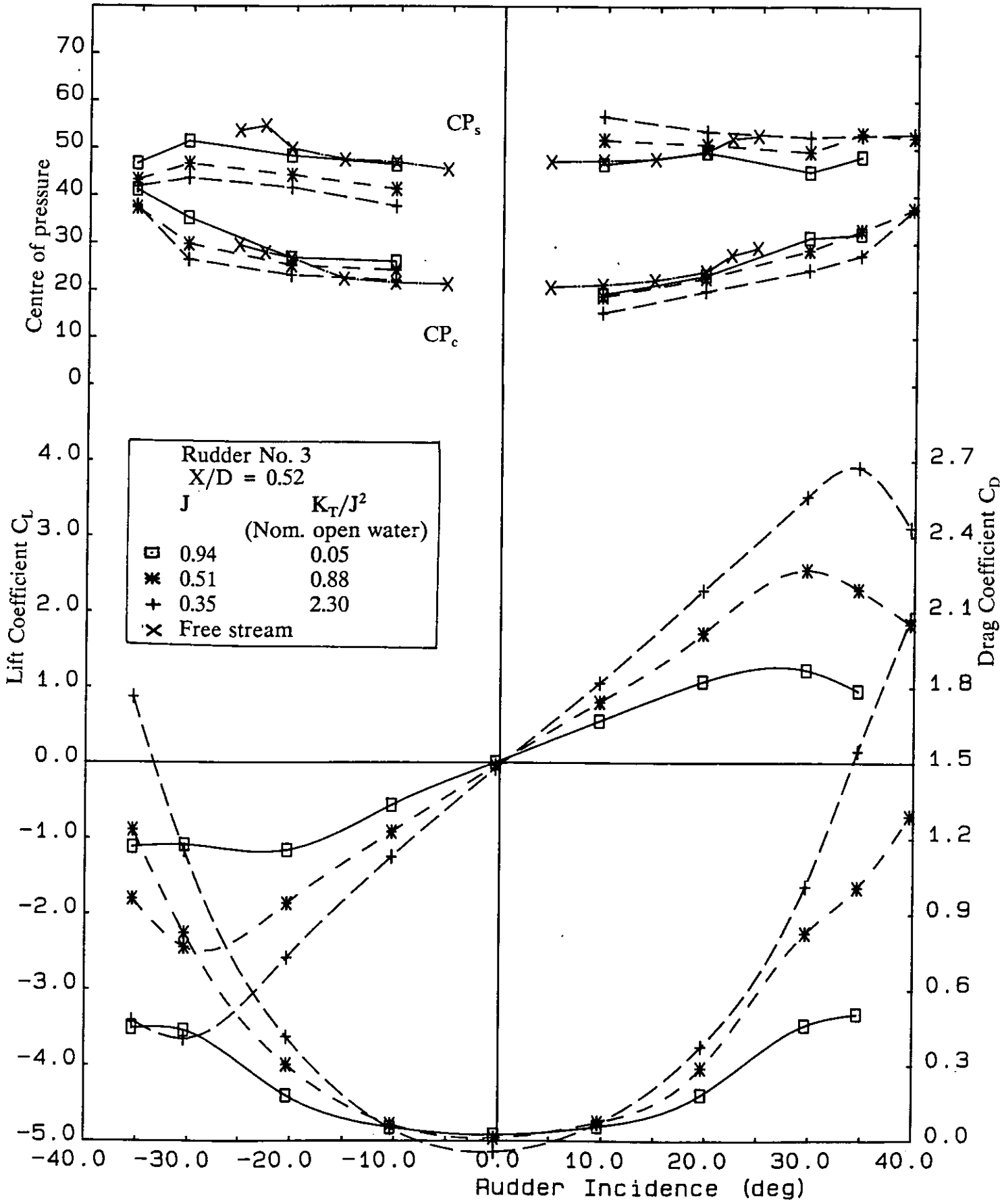

Figure 19 Variation of All-Movable Rudder No.3 performance Characteristics for three propeller advance ratios at a longitudinal separation X/D=0.52

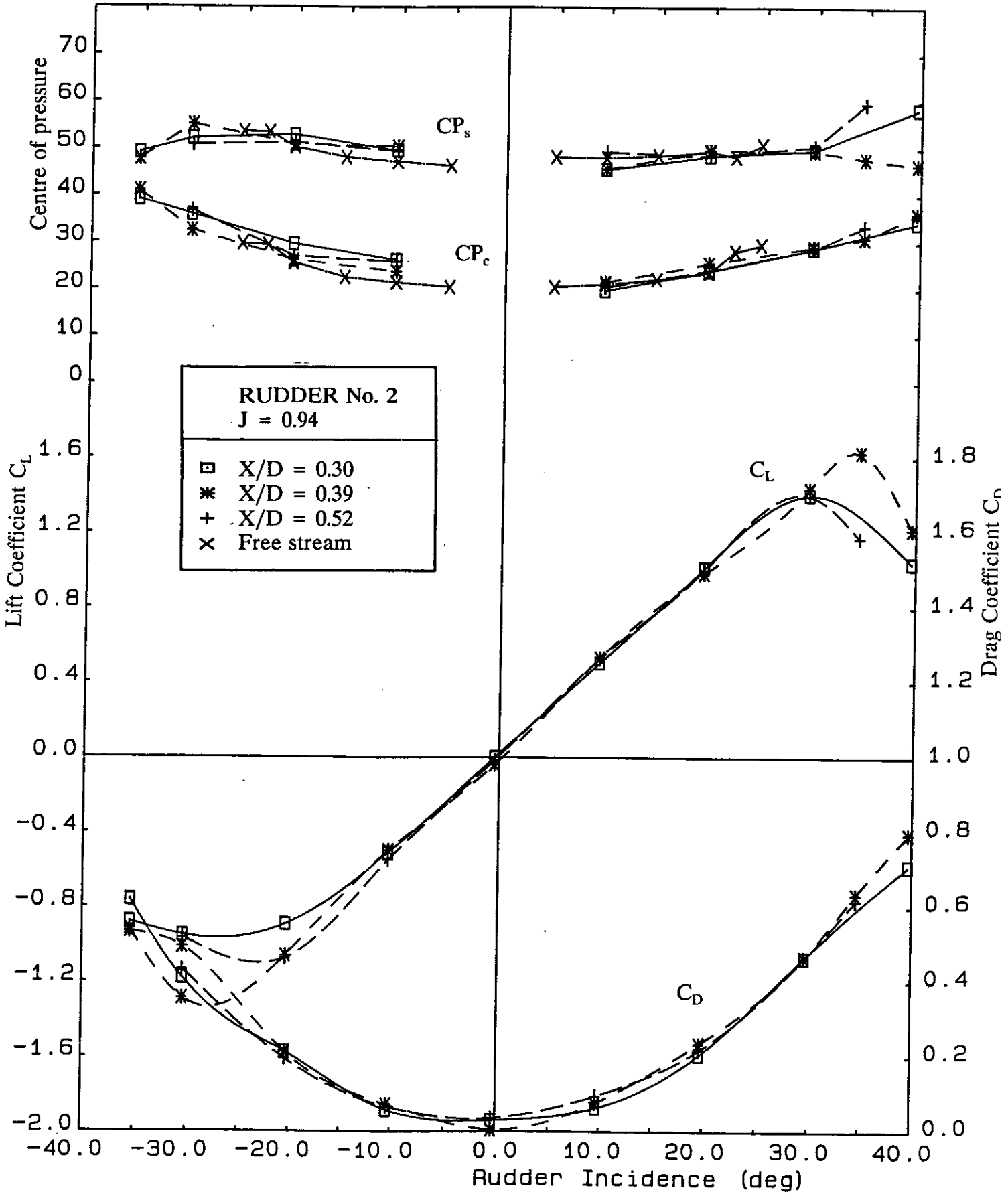

Figure 20 Effect of Longitudinal Separation on the Performance Characteristic of All-Movable Rudder No.2 with a propeller advance ratio of 0.94

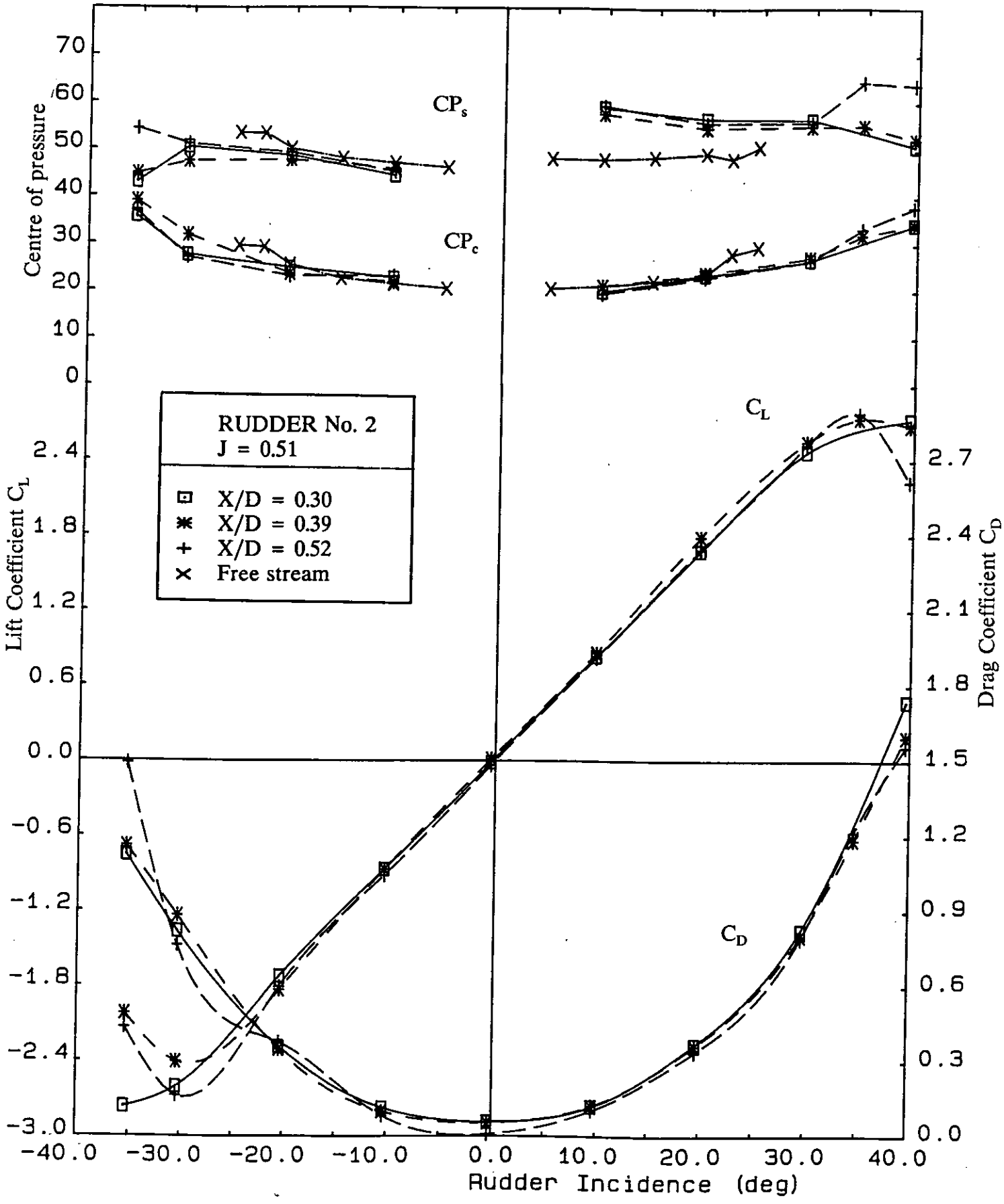

Figure 21 Effect of Longitudinal Separation on the Performance Characteristic of All-Movable Rudder No.2 with a propeller advance ratio of 0.51

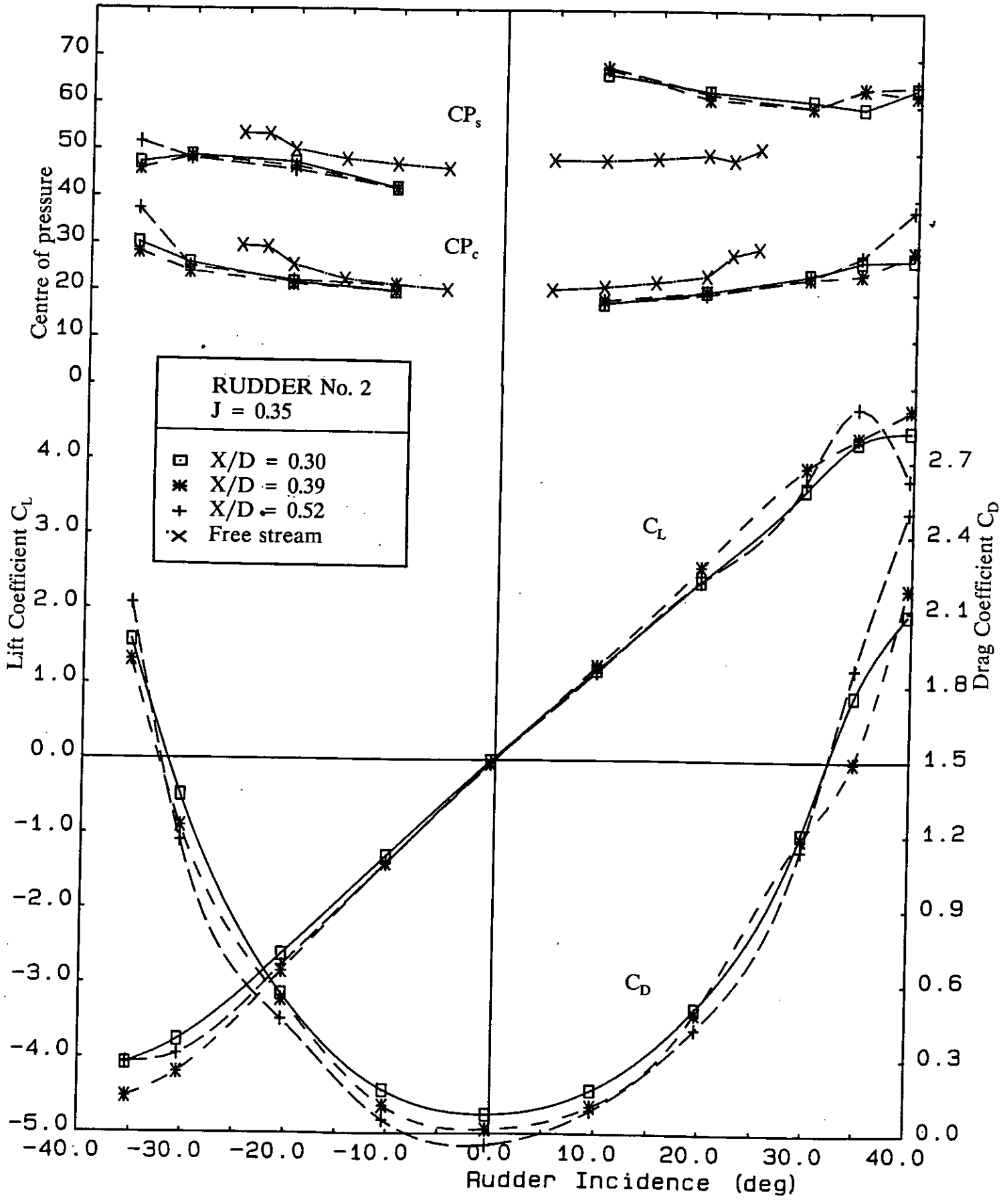

Figure 22 Effect of Longitudinal Separation on the Performance Characteristic of All-Movable Rudder No.2 with a propeller advance ratio of 0.35

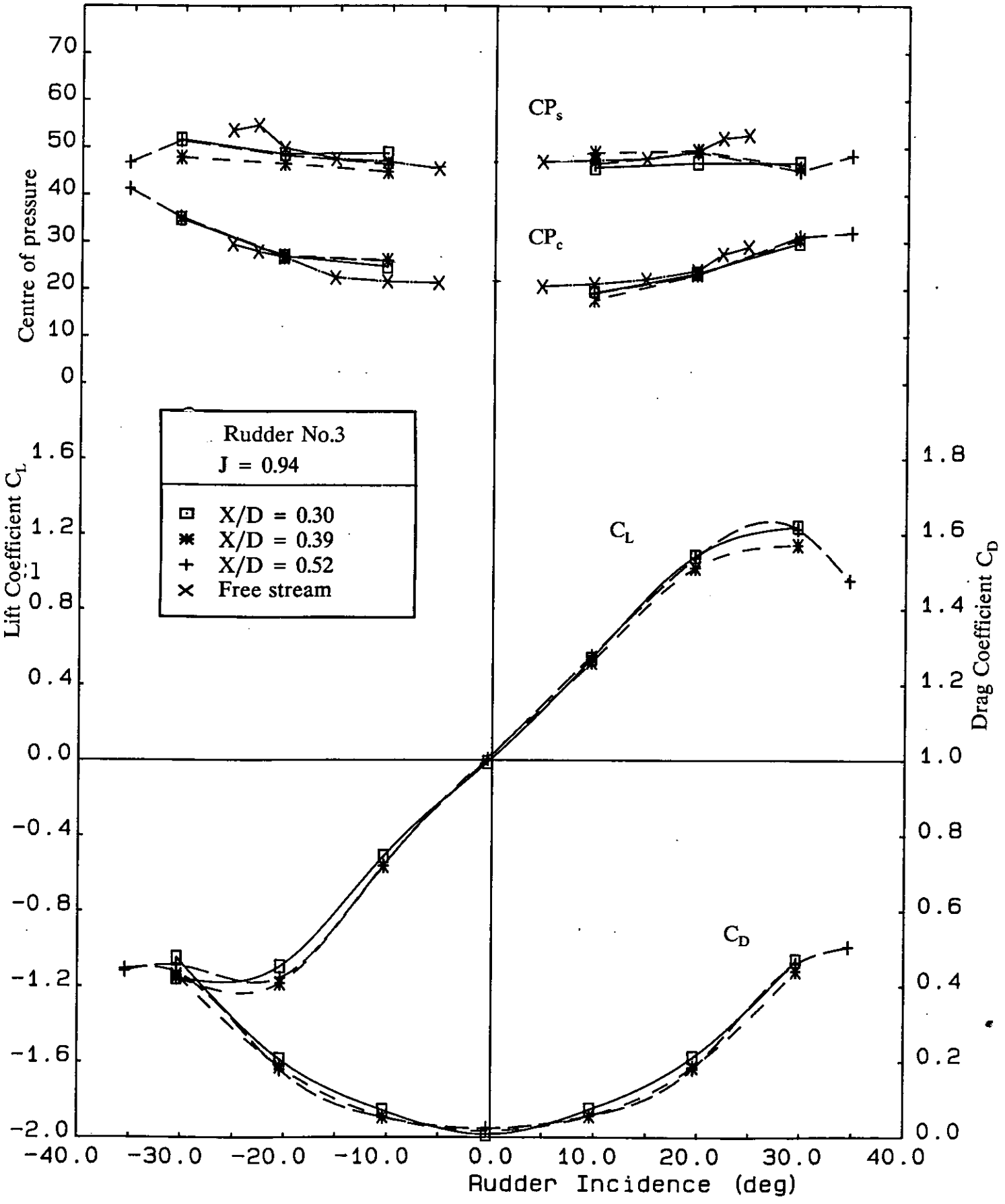

Figure 23 Effect of Longitudinal Separation on the Performance Characteristic of All-Movable Rudder No.3 with a propeller advance ratio of 0.94

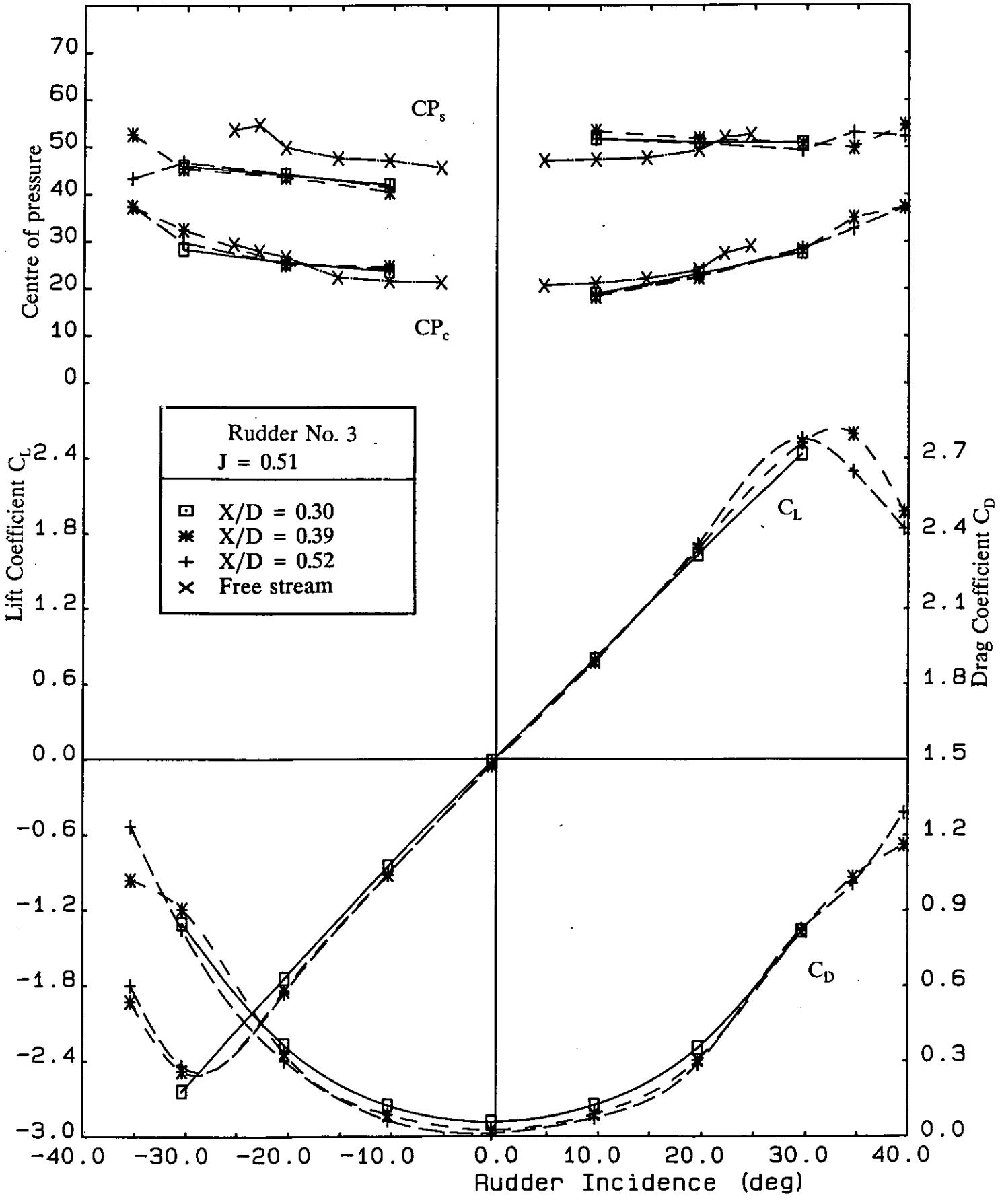

Figure 24 Effect of Longitudinal Separation on the Performance Characteristic of All-Movable Rudder No.3 with a propeller advance ratio of 0.51

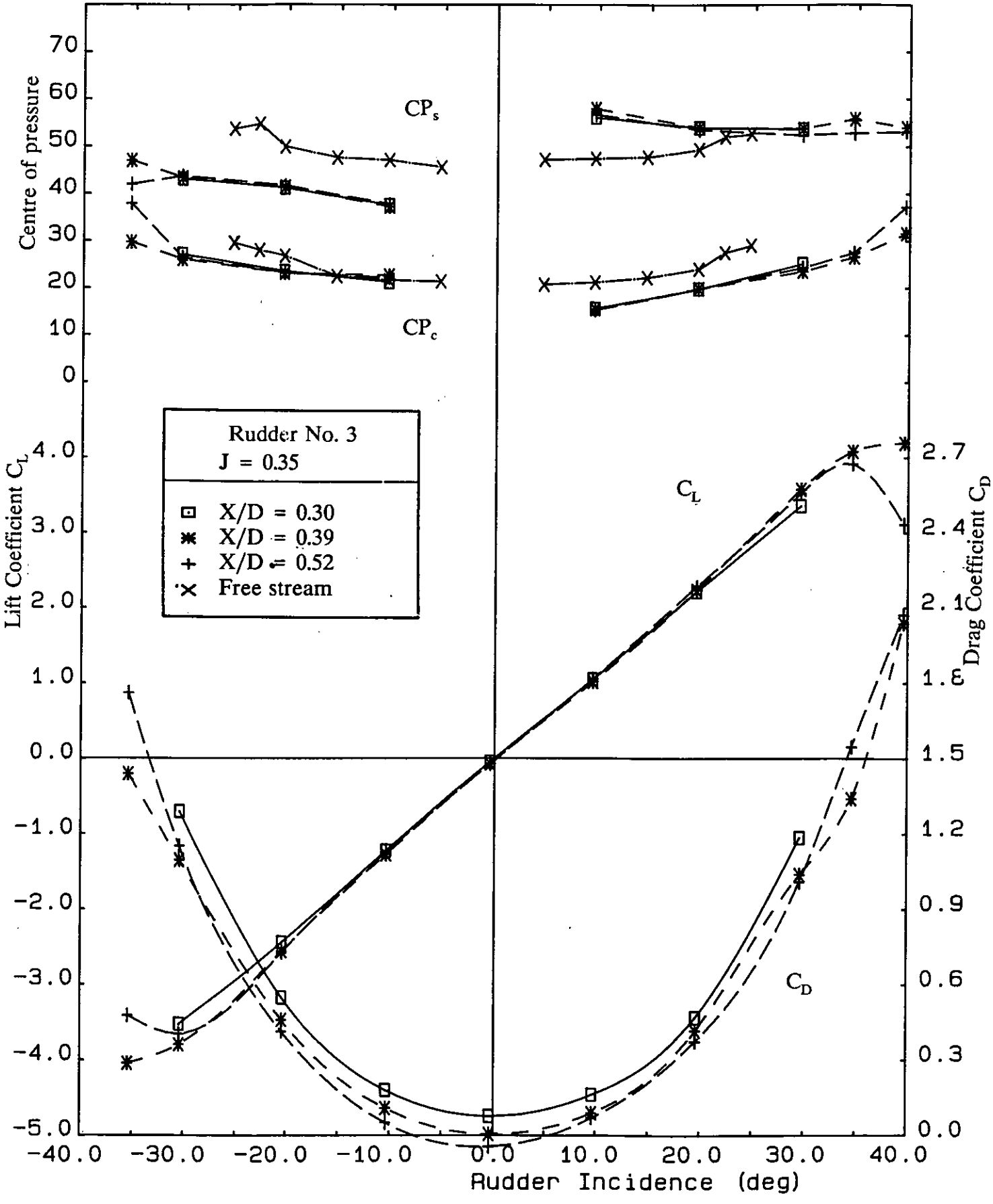

Figure 25 Effect of Longitudinal Separation on the Performance Characteristic of All-Movable Rudder No.3 with a propeller advance ratio of 0.35

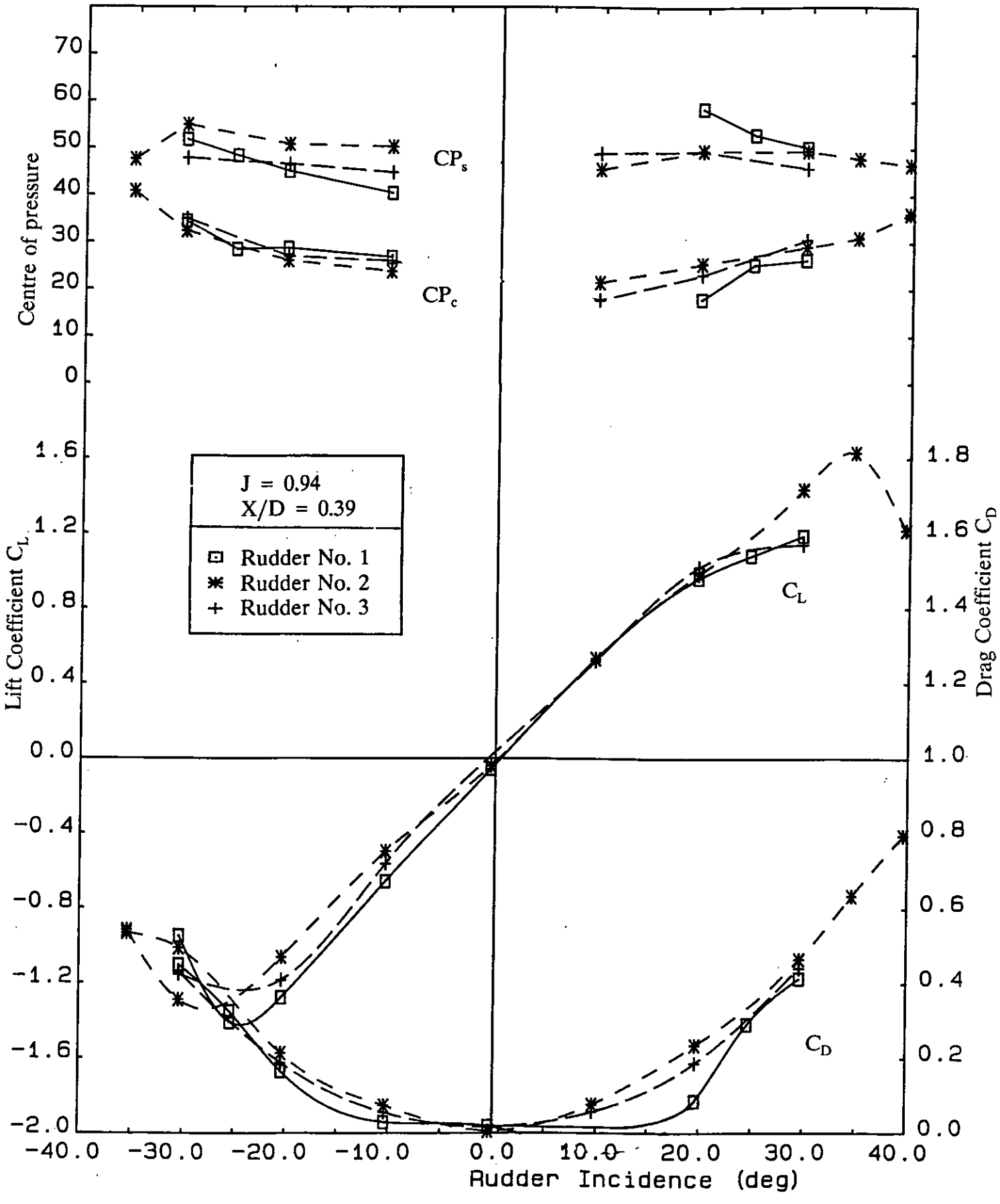

Figure 26 Comparison of the Performance characteristics of three All-Movable Rudders at an advance ratio of 0.94

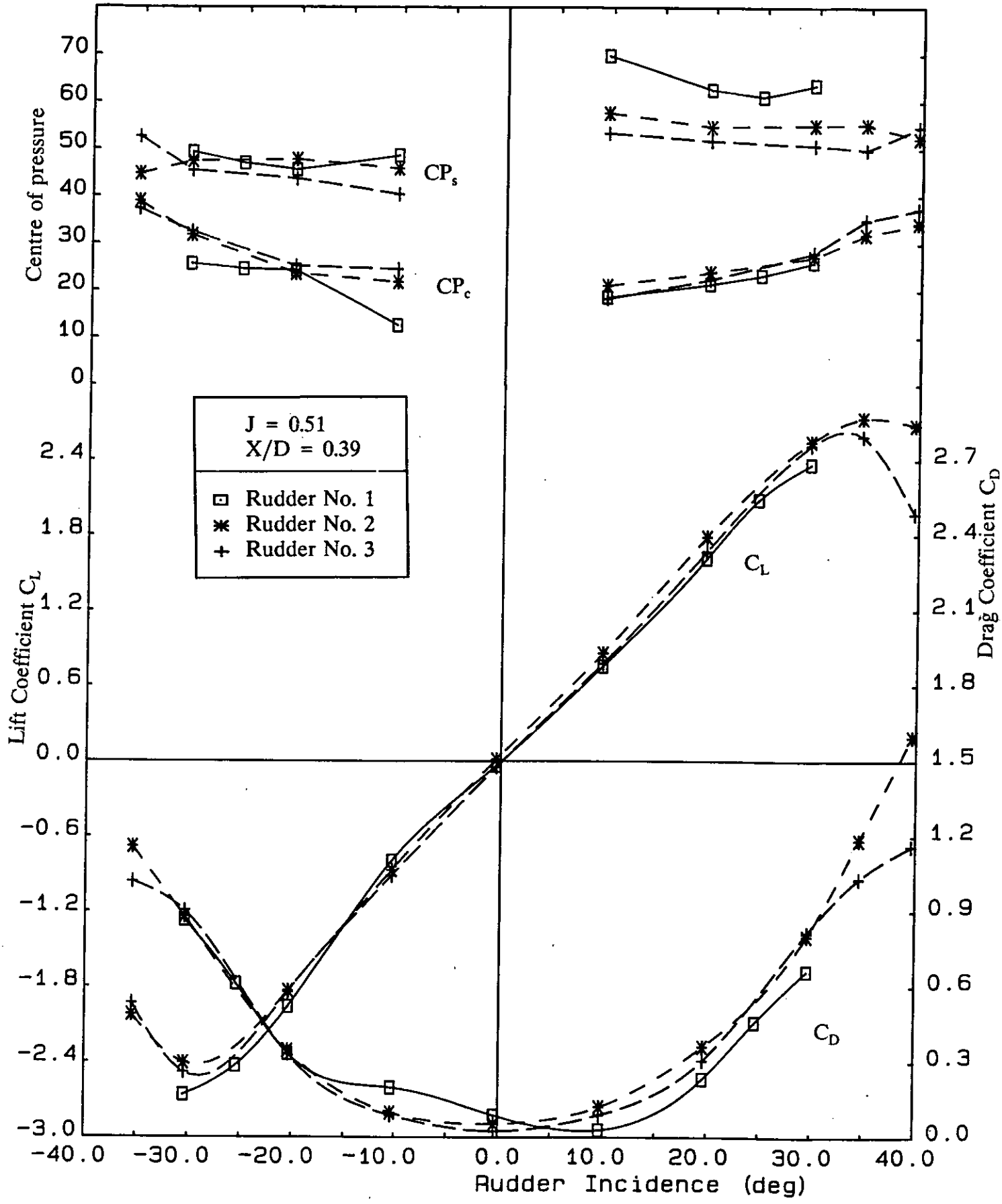

Figure 27 Comparison of the Performance characteristics of three All-Movable Rudders at an advance ratio of 0.51

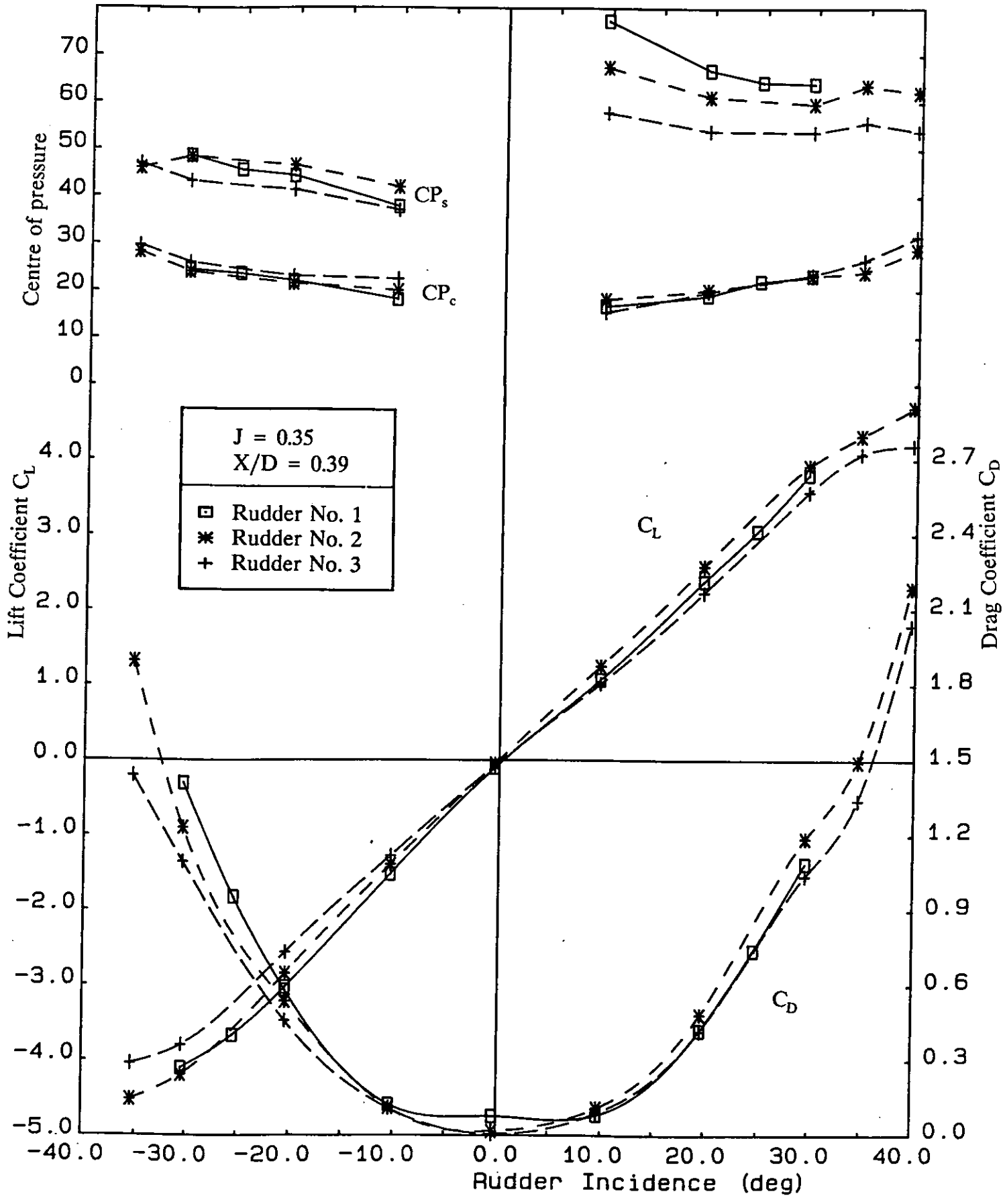

Figure 28 Comparison of the Performance characteristics of three All-Movable Rudders at an advance ratio of 0.35

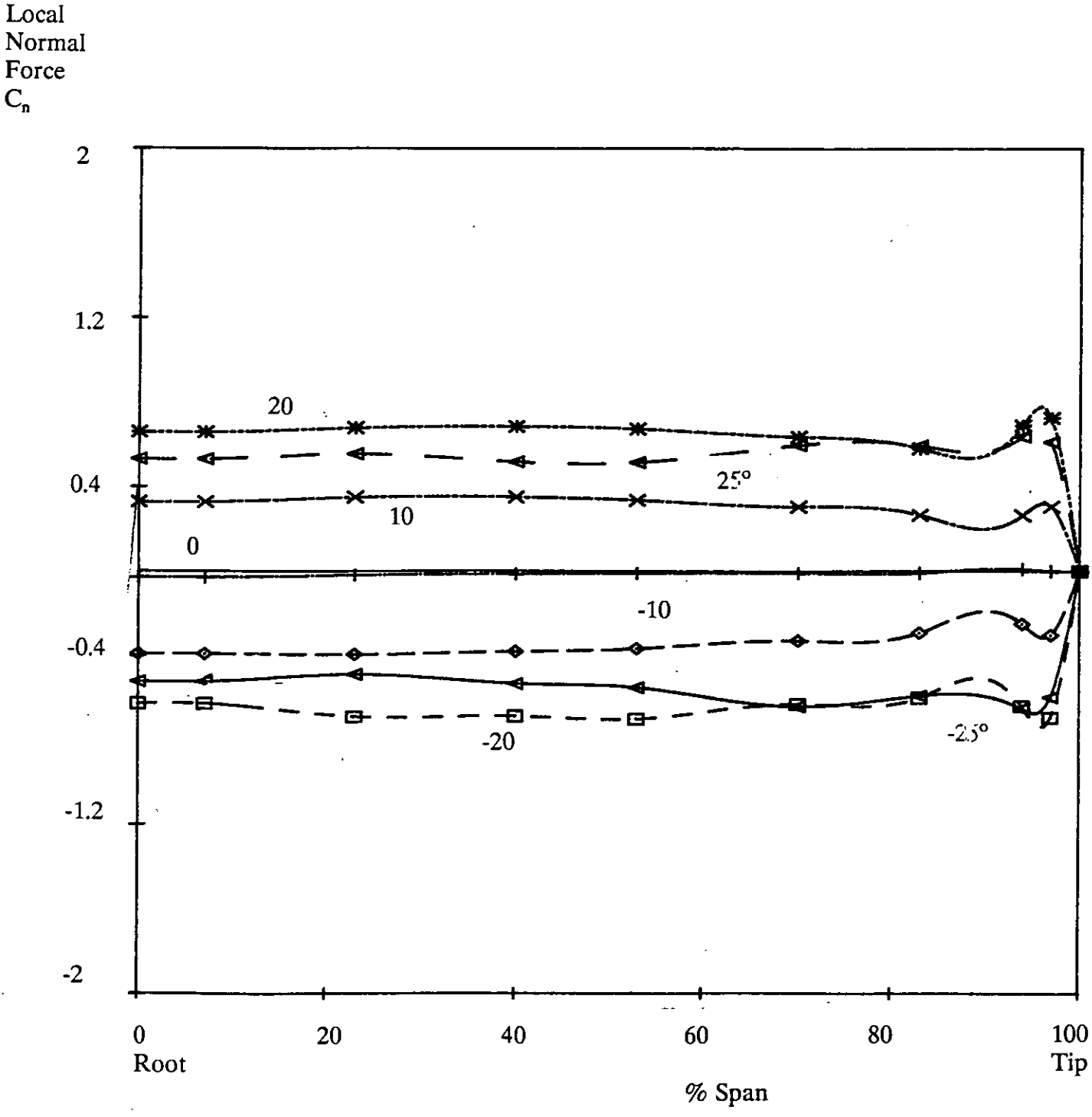

Figure 29 Freestream variation of spanwise distribution of local section C_N with incidence for All-Movable Rudder No.2

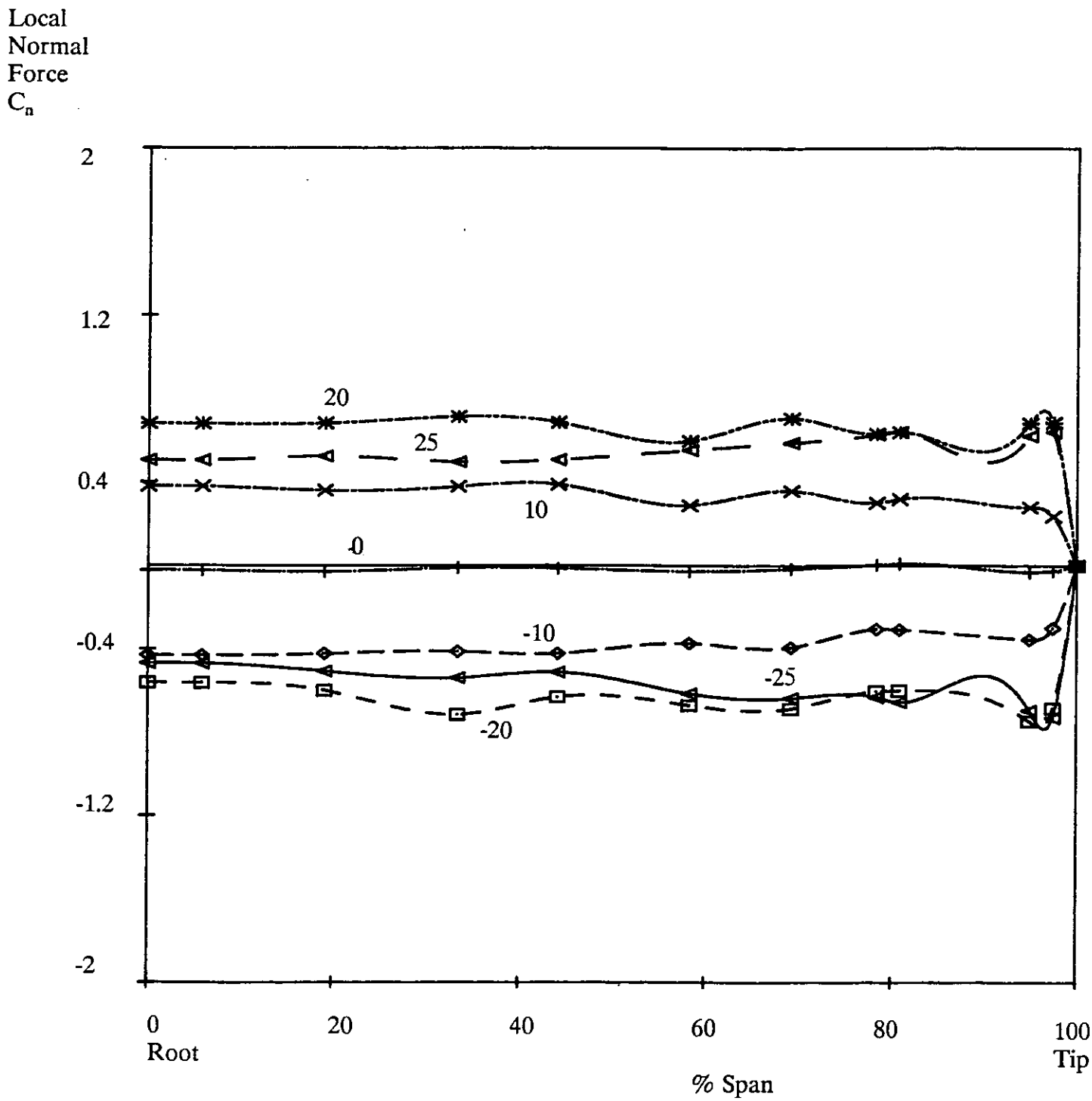

Figure 30 Freestream variation of spanwise distribution of local section C_N with incidence for All-Movable Rudder No.3

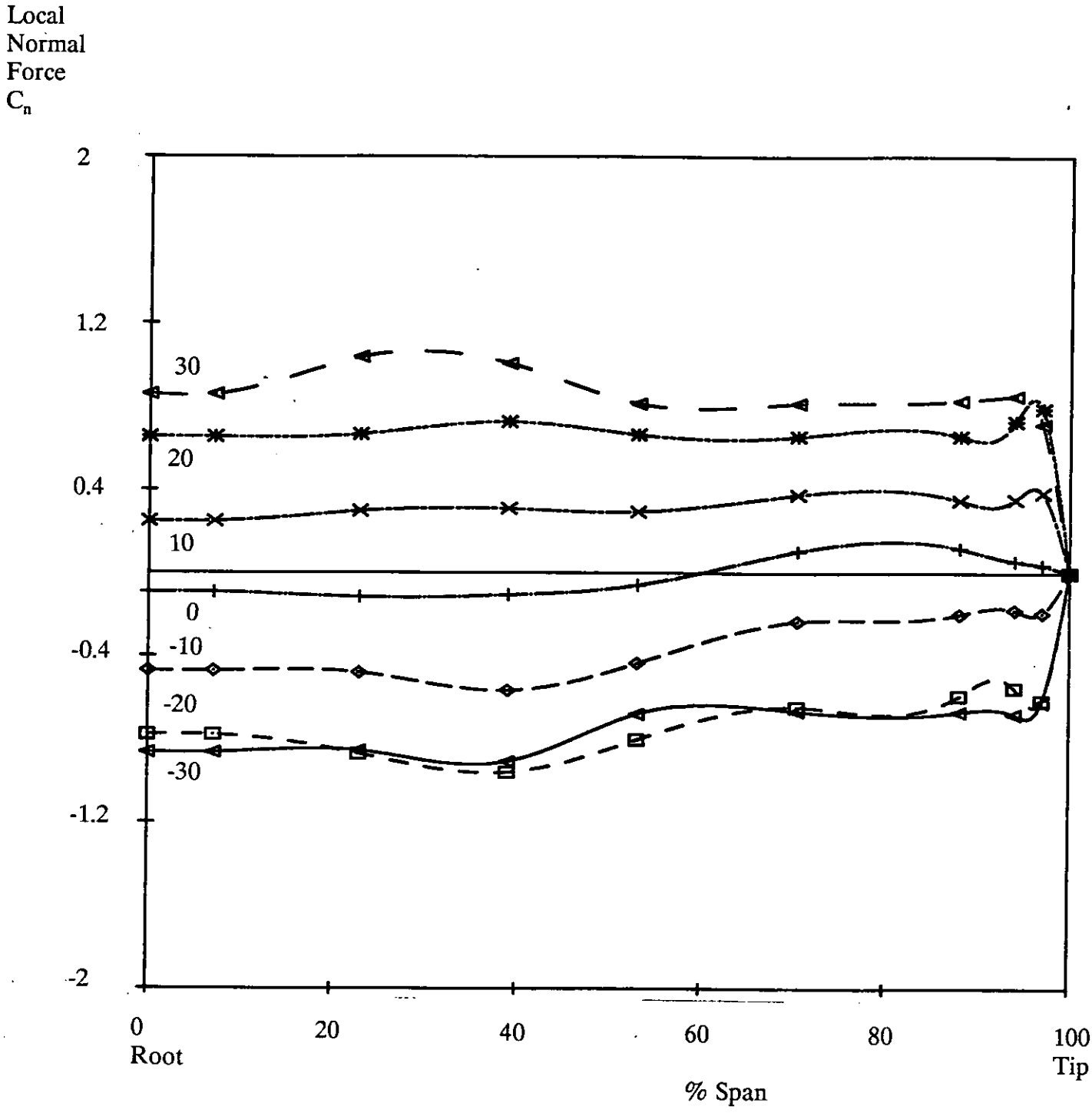

Figure 31 Variation of Spanwise Distribution of Local Section C_N with Incidence for All-Movable Rudder No.1 at a Propeller Advance Ratio of 0.94

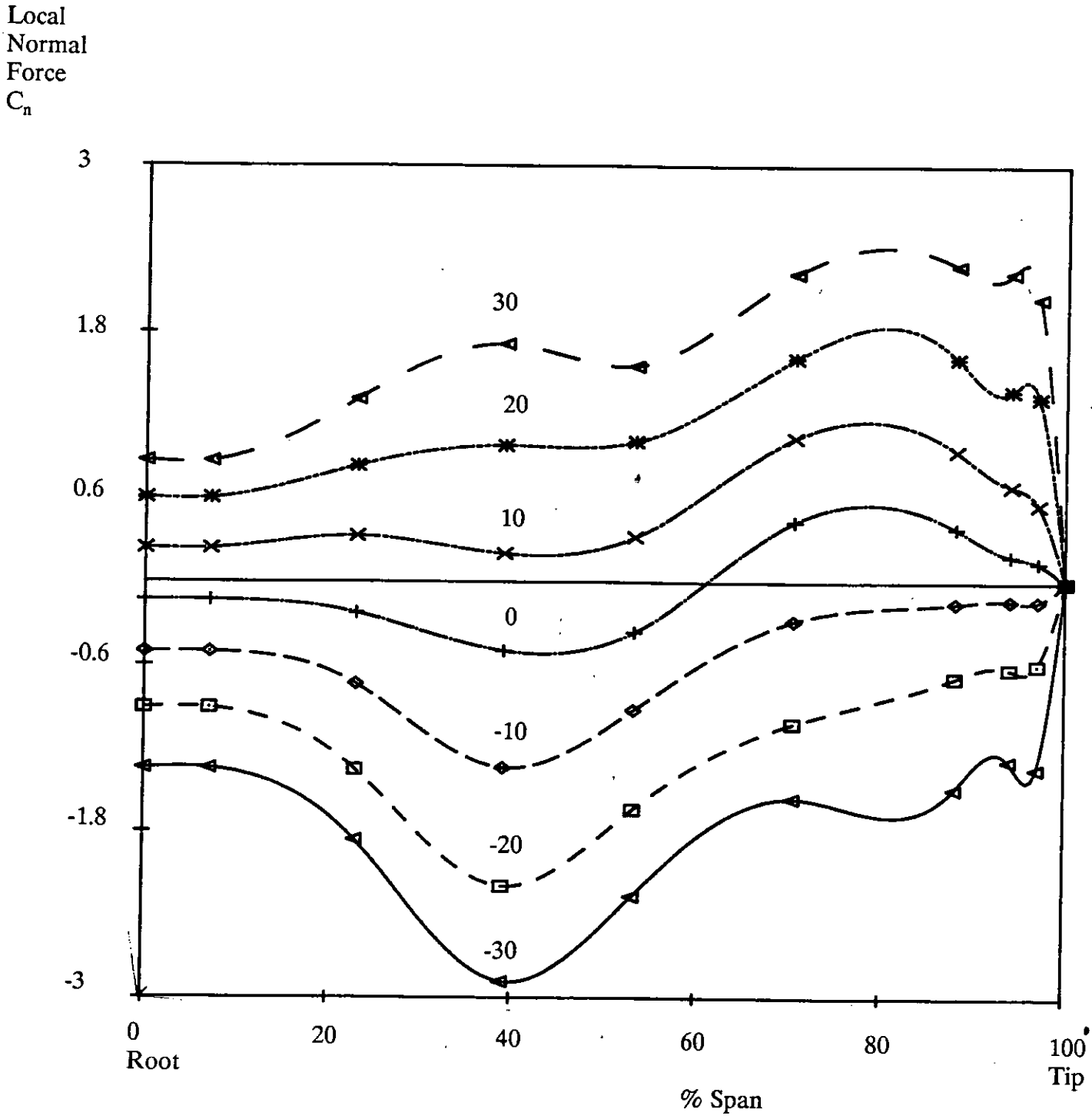

Figure 32 Variation of Spanwise Distribution of Local Section C_N with Incidence for All-Movable Rudder No.1 at a Propeller Advance Ratio of 0.51

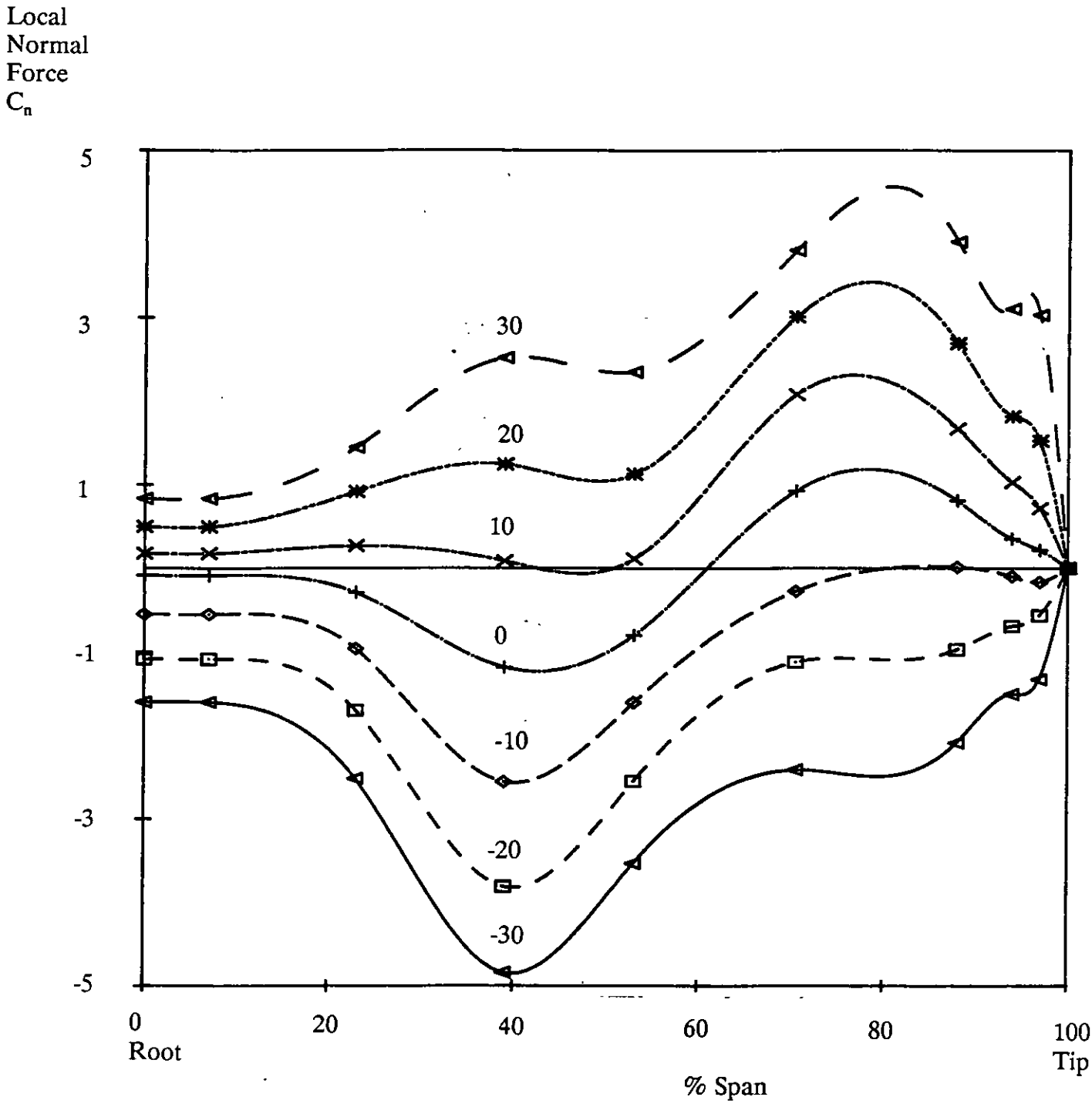

Figure 33 Variation of Spanwise Distribution of Local Section C_N with Incidence for All-Movable Rudder No.1 at a Propeller Advance Ratio of 0.35

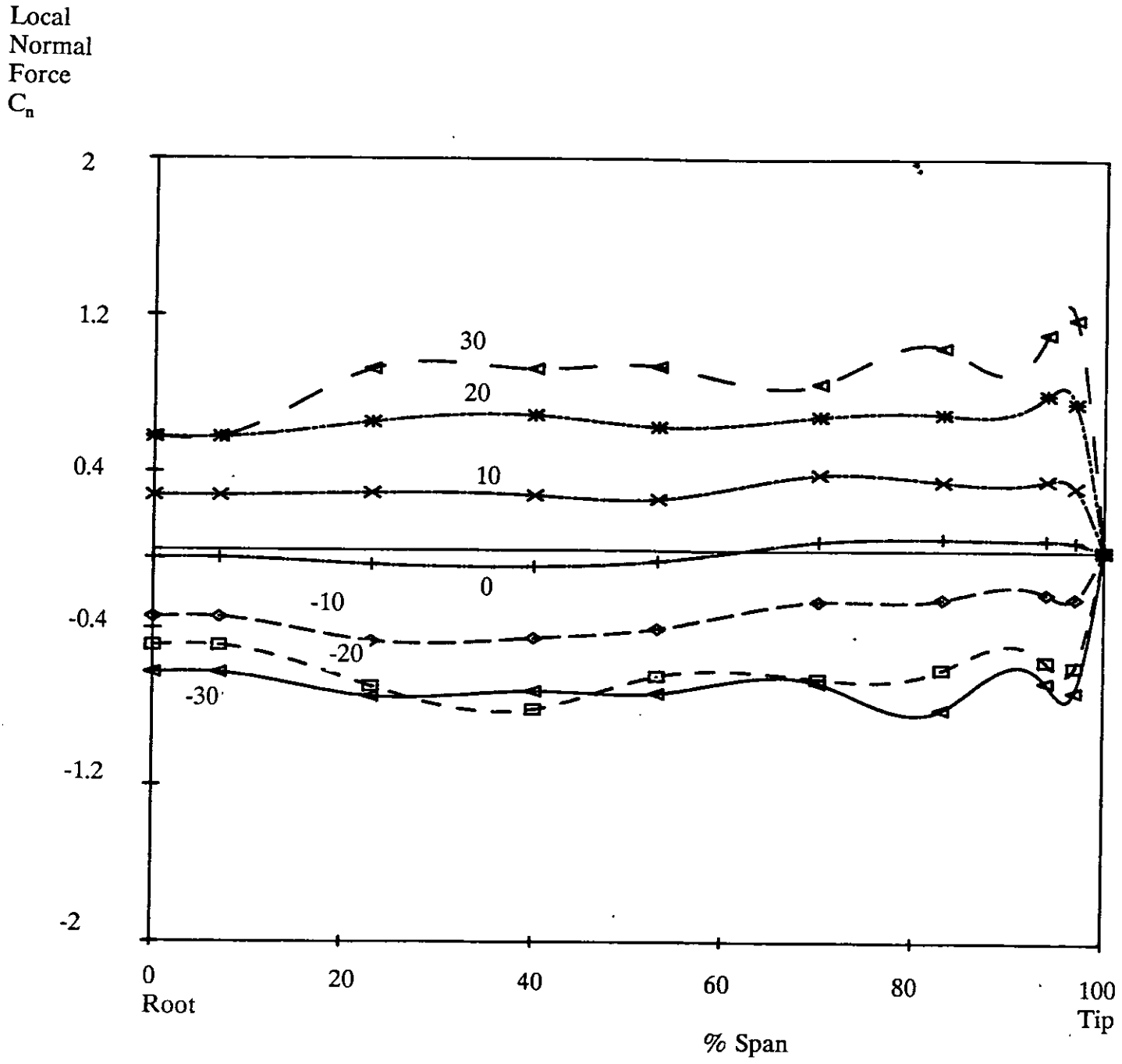

Figure 34 Variation of Spanwise Distribution of Local Section C_N with Incidence for All-Movable Rudder No.2 at a Propeller Advance Ratio of 0.94 and Longitudinal Separation of X/D=0.3

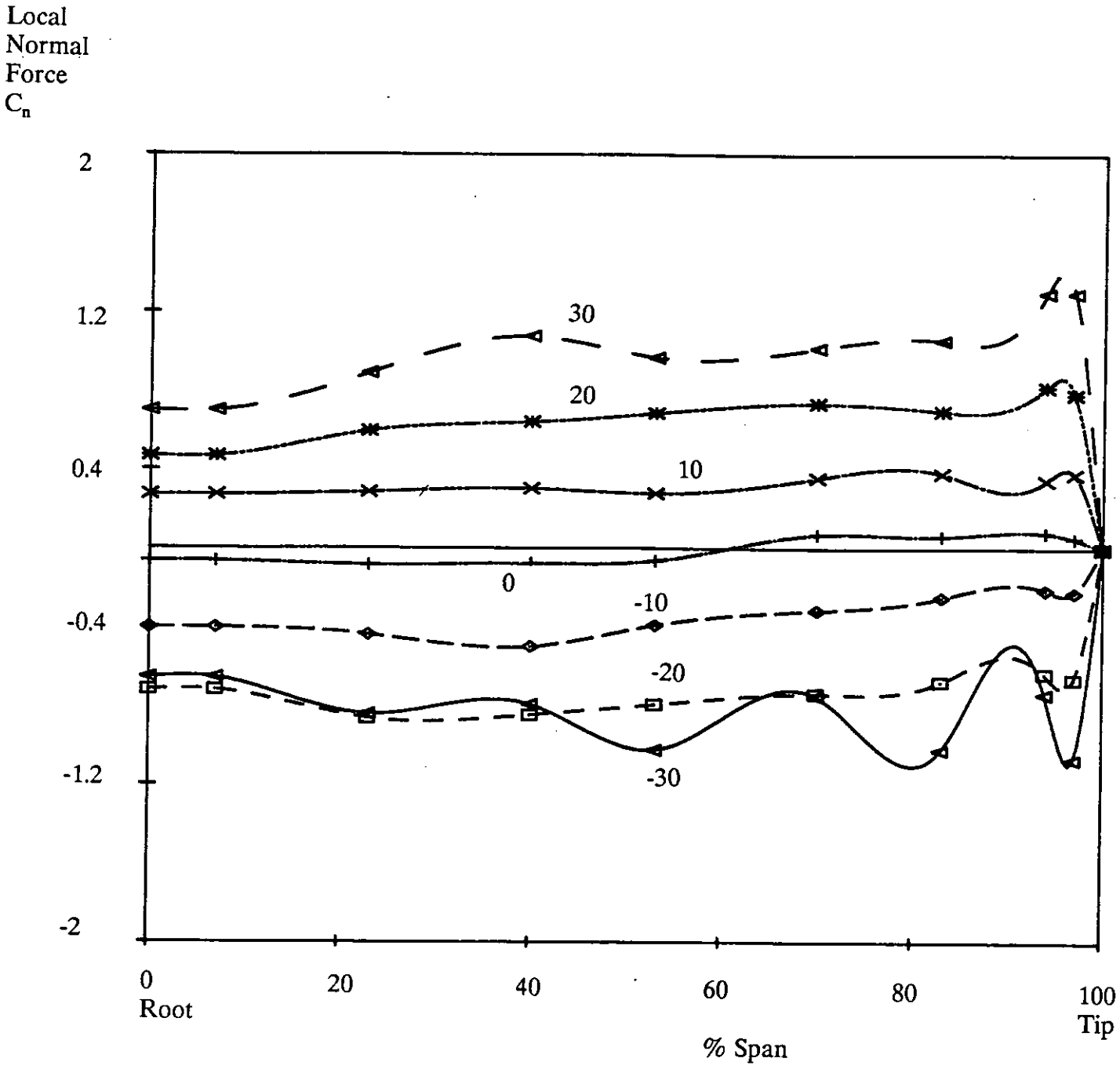

Figure 35 Variation of Spanwise Distribution of Local Section C_N with Incidence for All-Movable Rudder No.2 at a Propeller Advance Ratio of 0.94 and Longitudinal Separation of X/D=0.39

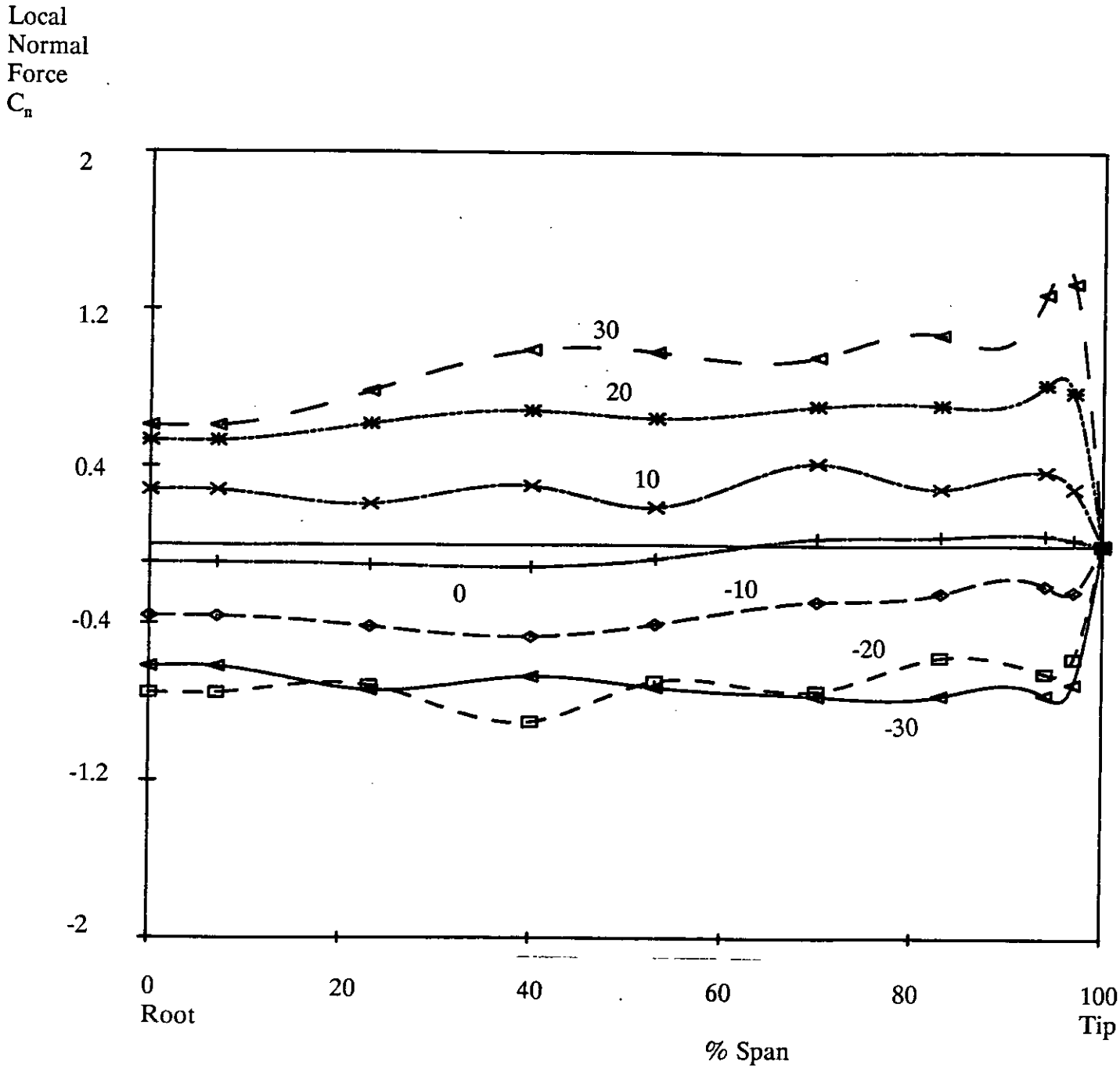

Figure 36 Variation of Spanwise Distribution of Local Section C_N with Incidence for All-Movable Rudder No.2 at a Propeller Advance Ratio of 0.94 and Longitudinal Separation of X/D=0.52

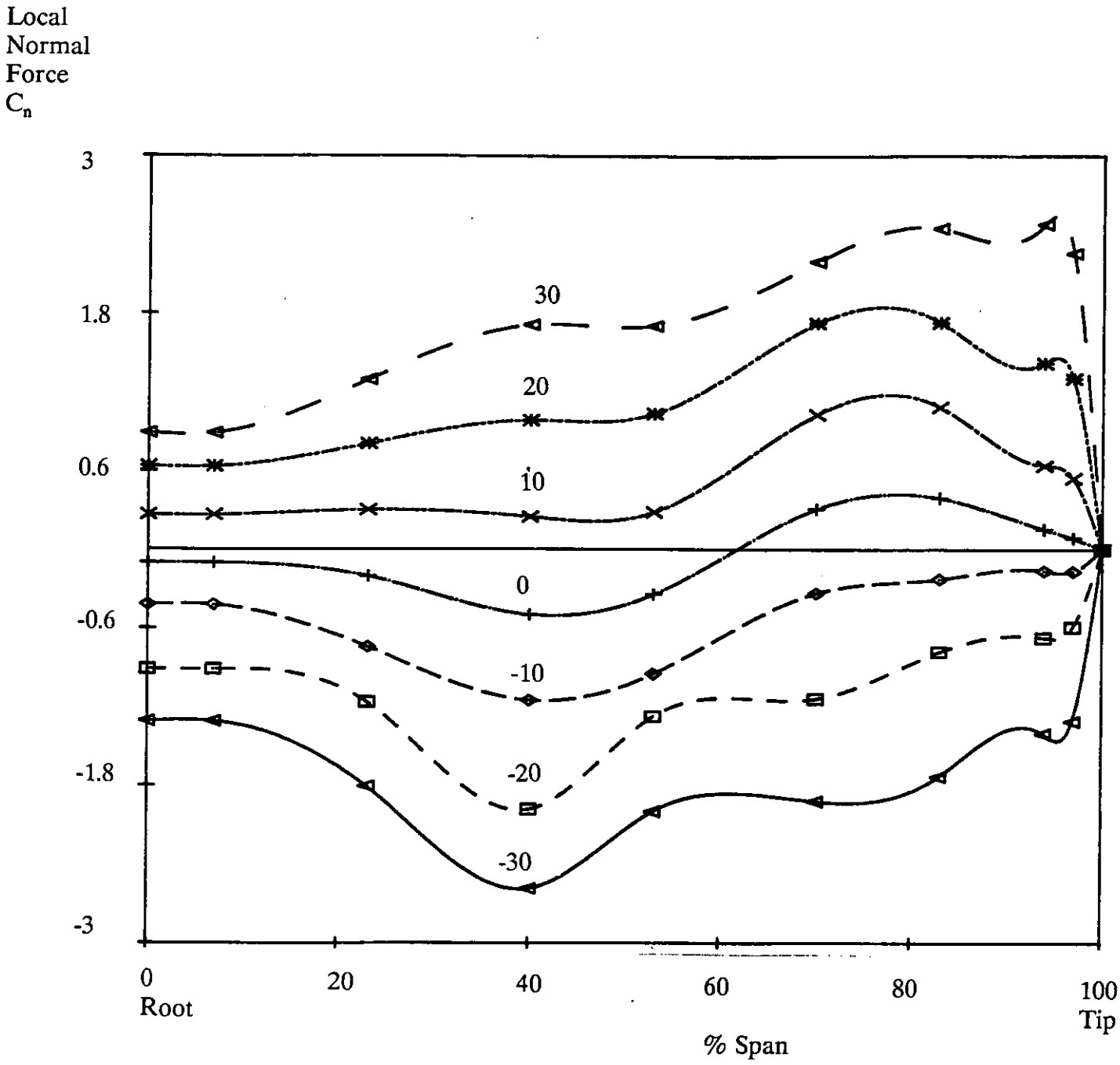

Figure 37 Variation of Spanwise Distribution of Local Section C_N with Incidence for All-Movable Rudder No.2 at a Propeller Advance Ratio of 0.51 and Longitudinal Separation of X/D=0.3

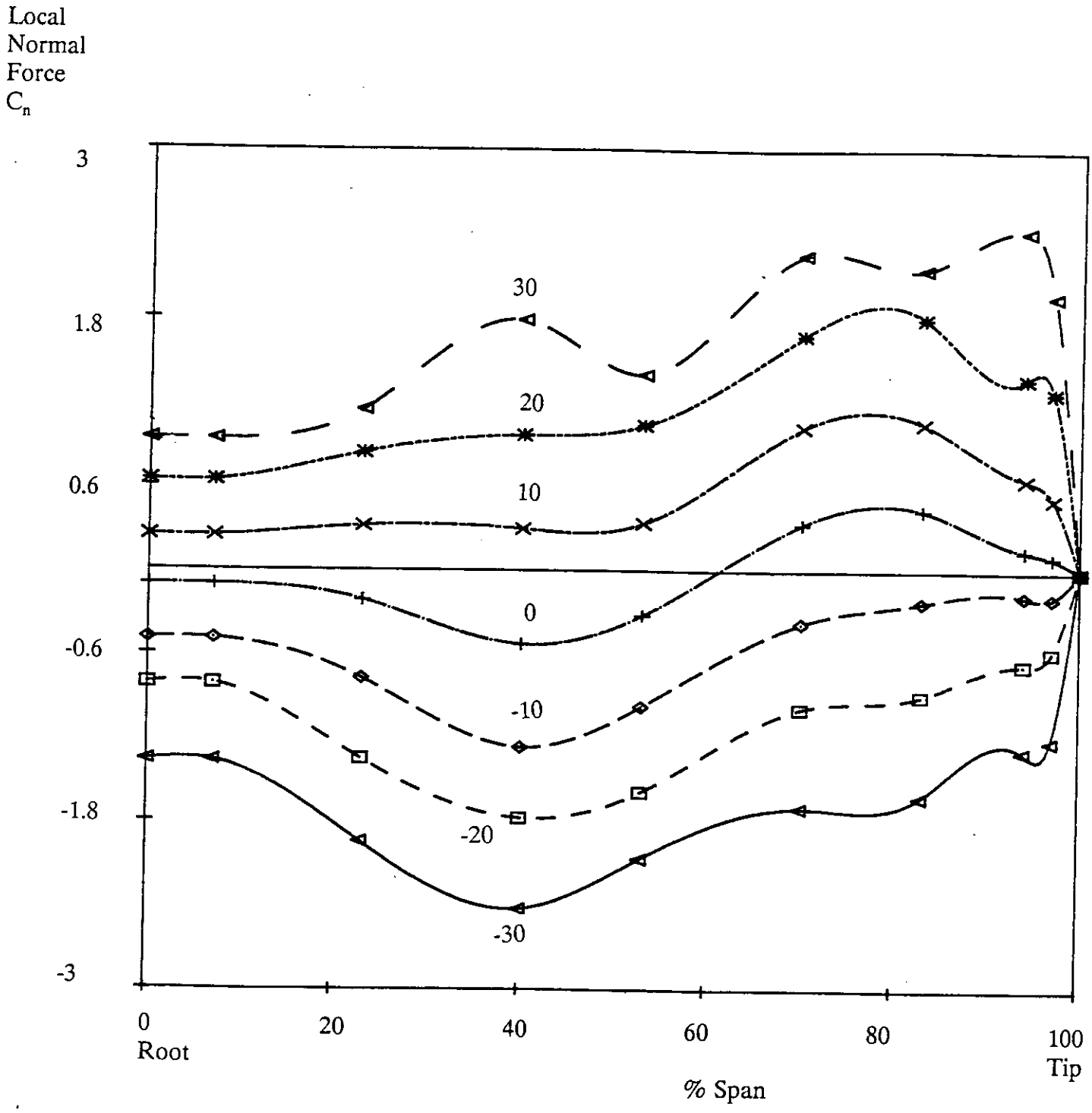

Figure 38 Variation of Spanwise Distribution of Local Section C_N with Incidence for All-Movable Rudder No.2 at a Propeller Advance Ratio of 0.51 and Longitudinal Separation of X/D=0.39

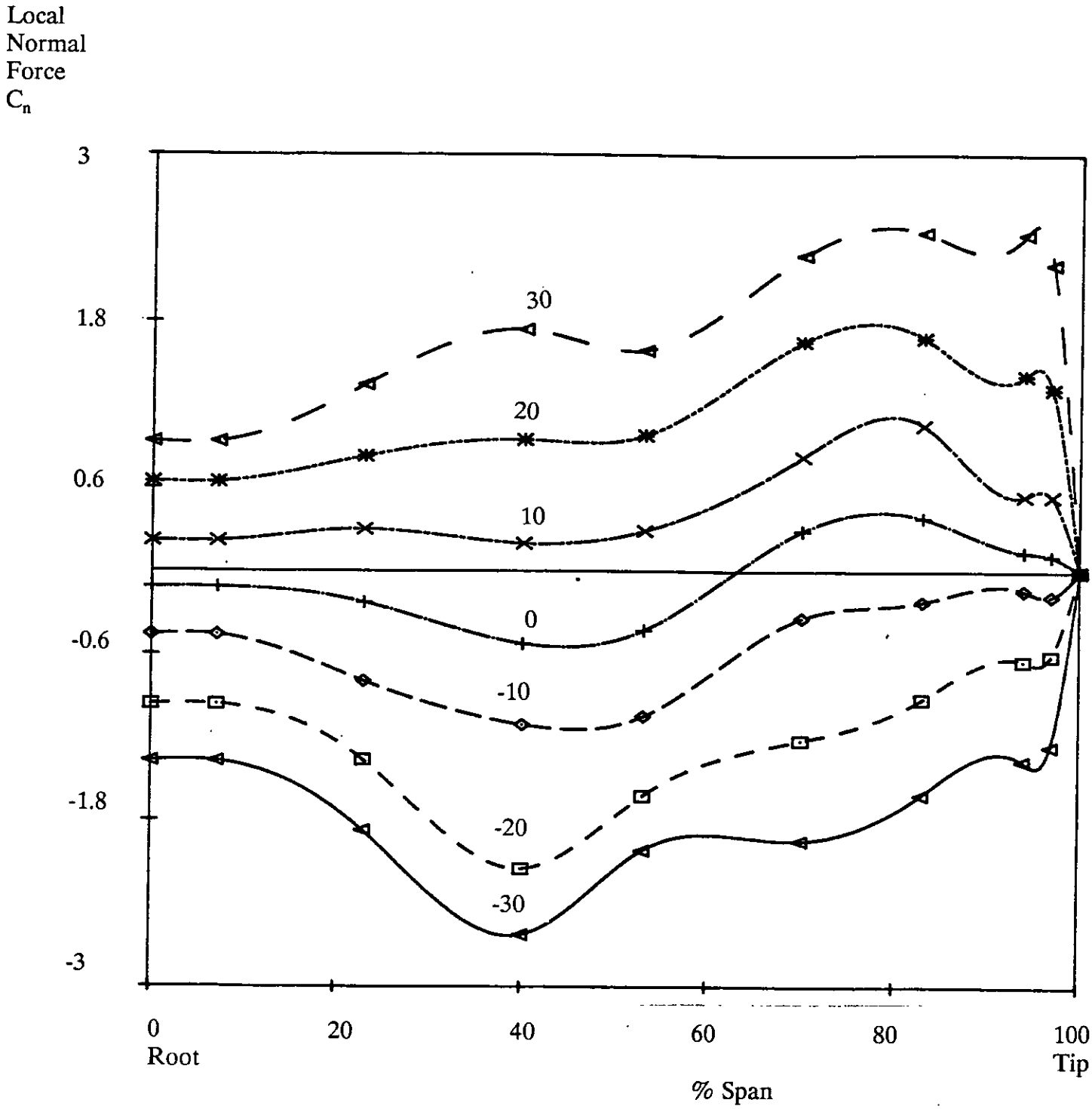

Figure 39 Variation of Spanwise Distribution of Local Section C_N with Incidence for All-Movable Rudder No.2 at a Propeller Advance Ratio of 0.51 and Longitudinal Separation of X/D=0.52

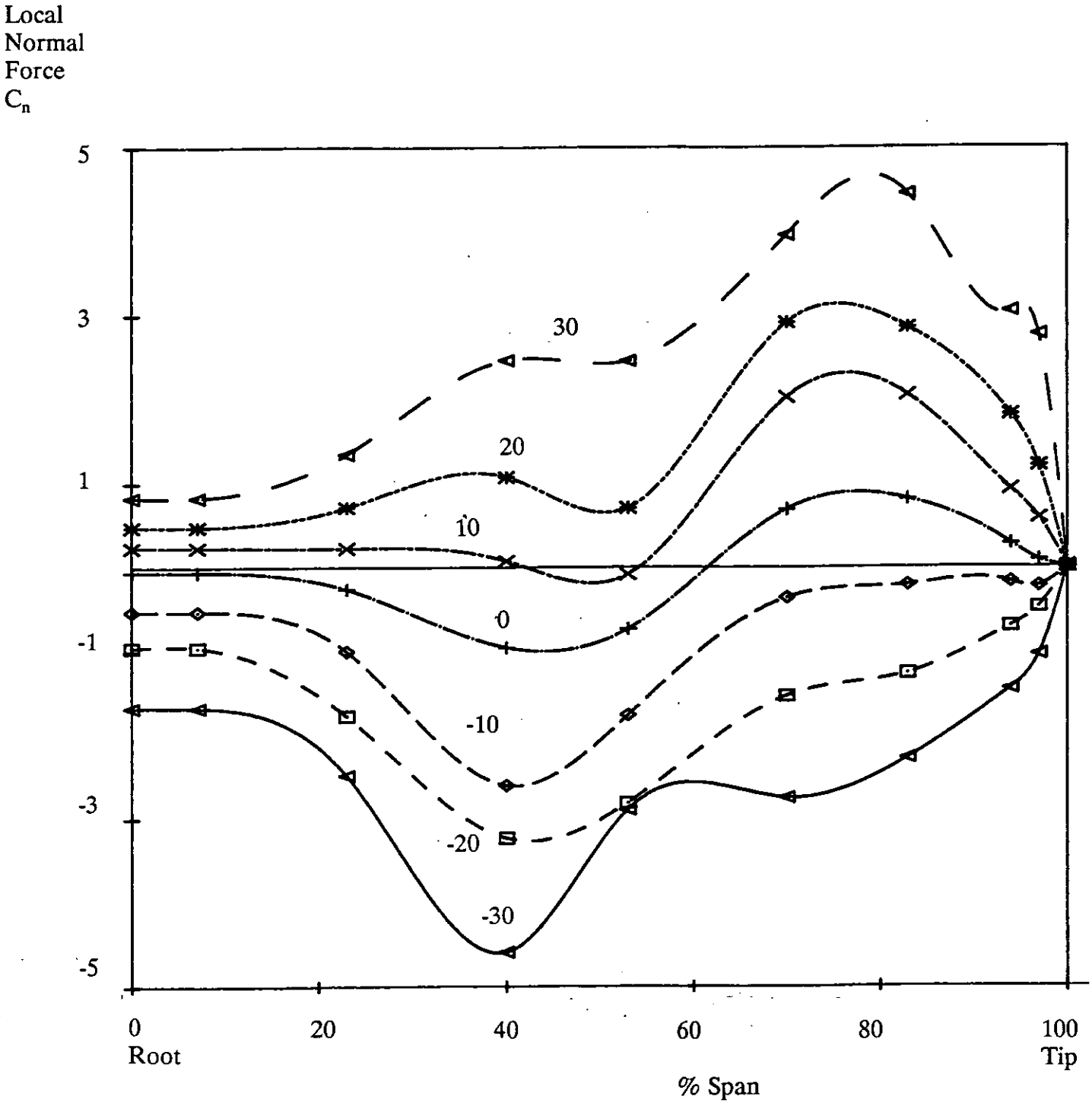

Figure 40 Variation of Spanwise Distribution of Local Section C_N with Incidence for All-Movable Rudder No.2 at a Propeller Advance Ratio of 0.35 and Longitudinal Separation of X/D=0.3

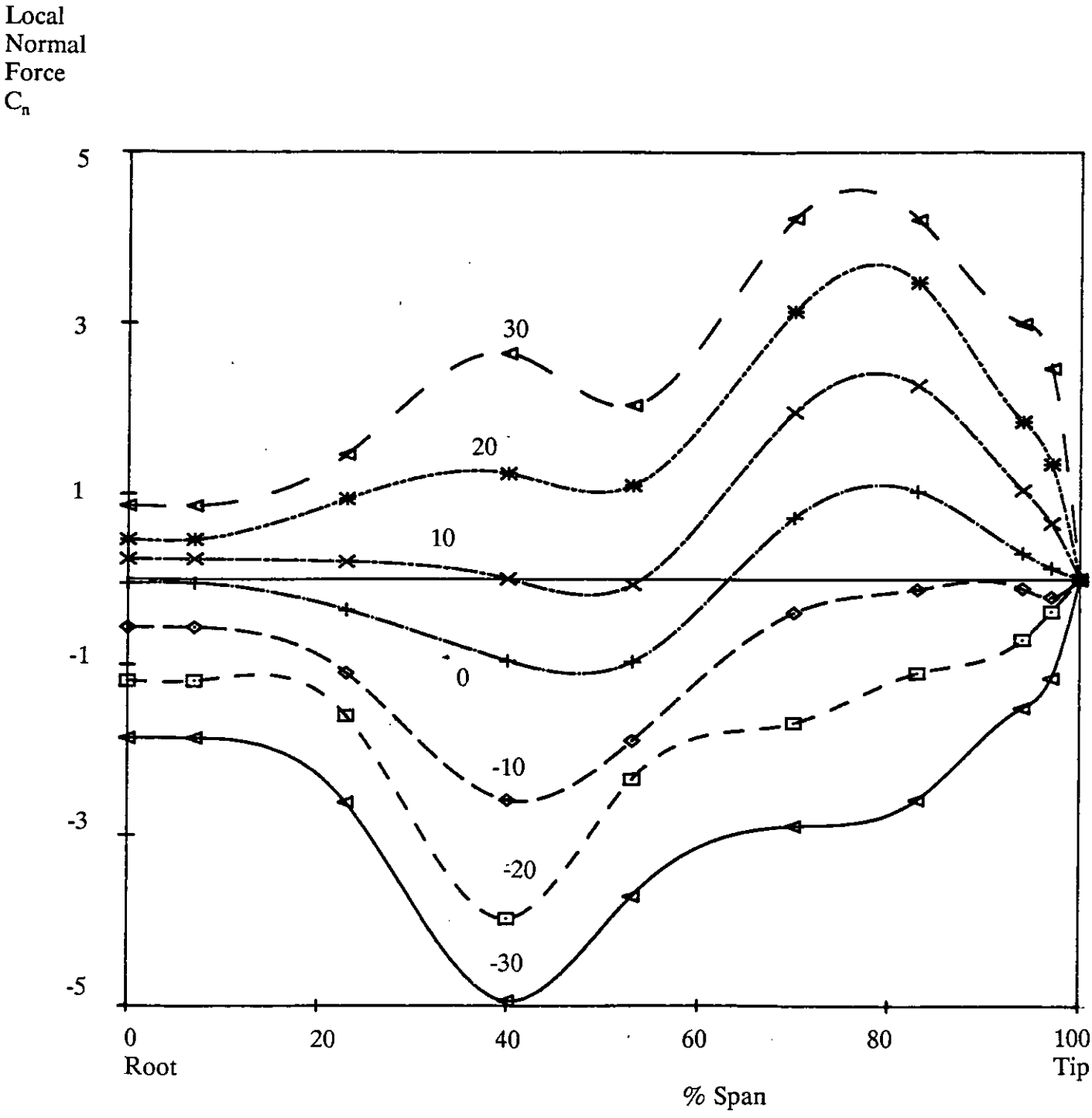

Figure 41 Variation of Spanwise Distribution of Local Section C_N with Incidence for All-Movable Rudder No.2 at a Propeller Advance Ratio of 0.35 and Longitudinal Separation of X/D=0.39

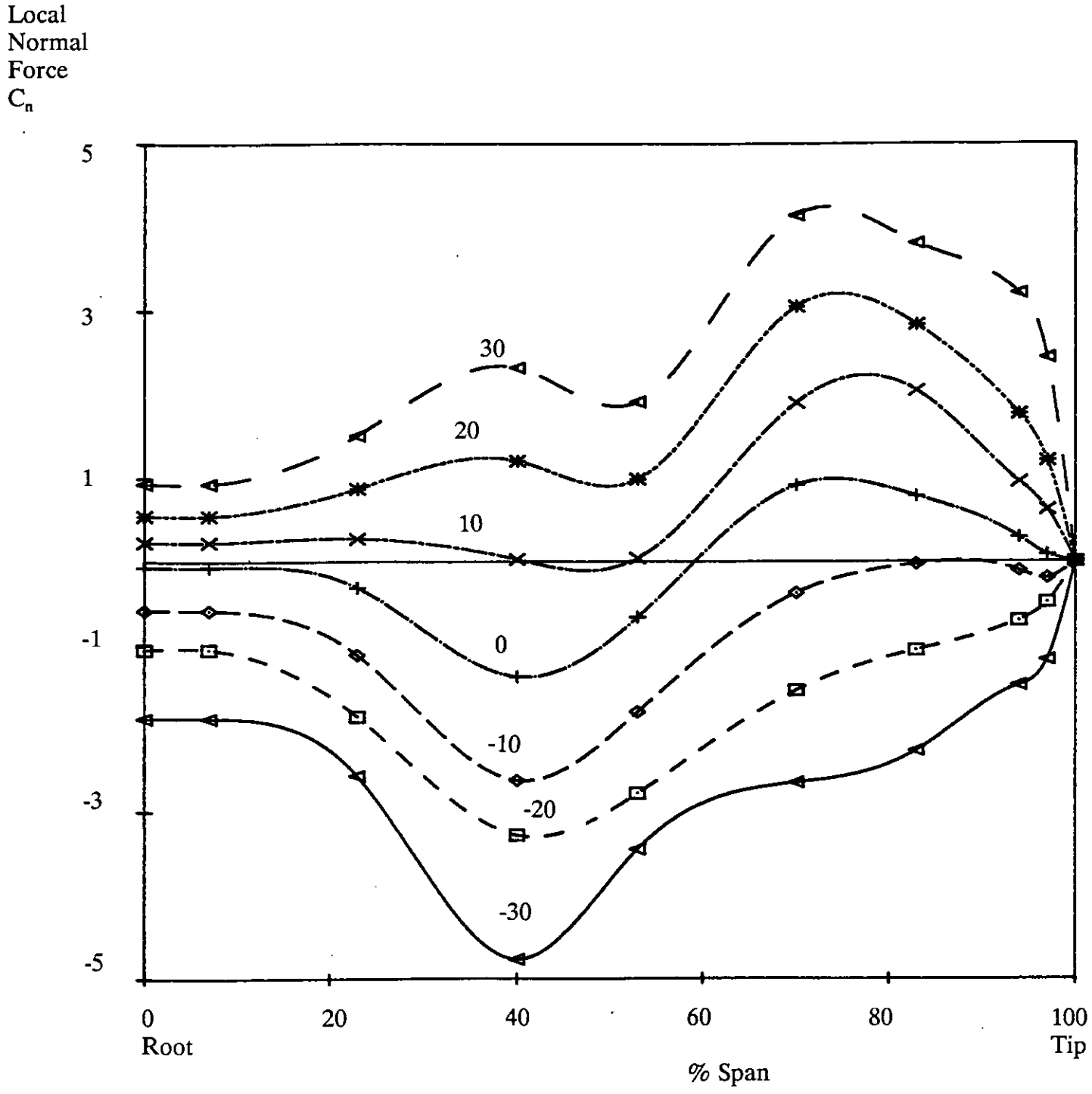

Figure 42 Variation of Spanwise Distribution of Local Section C_N with Incidence for All-Movable Rudder No.2 at a Propeller Advance Ratio of 0.35 and Longitudinal Separation of X/D=0.52

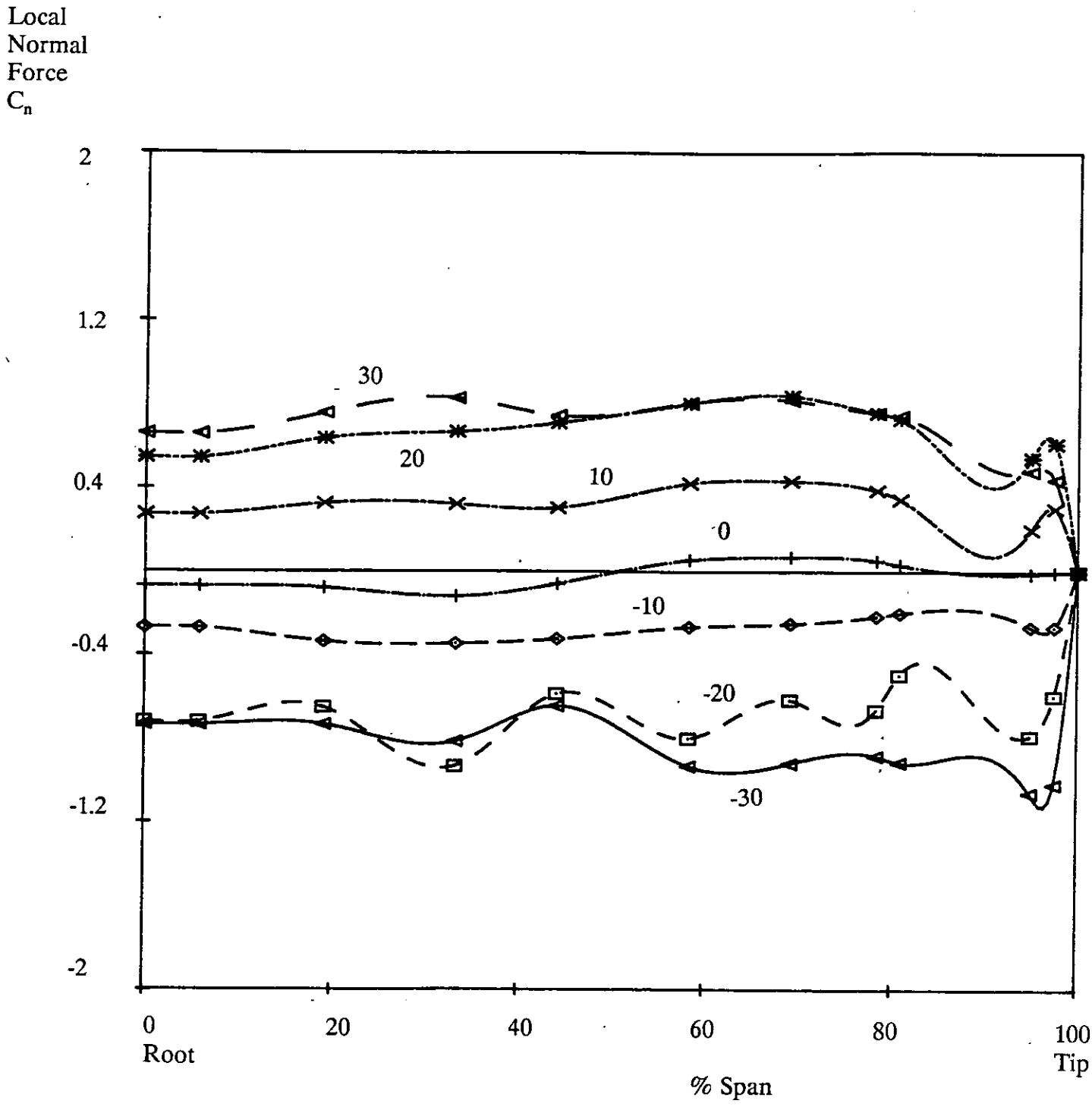

Figure 43 Variation of Spanwise Distribution of Local Section C_N with Incidence for All-Movable Rudder No.3 at a Propeller Advance Ratio of 0.94 and Longitudinal Separation of X/D=0.3

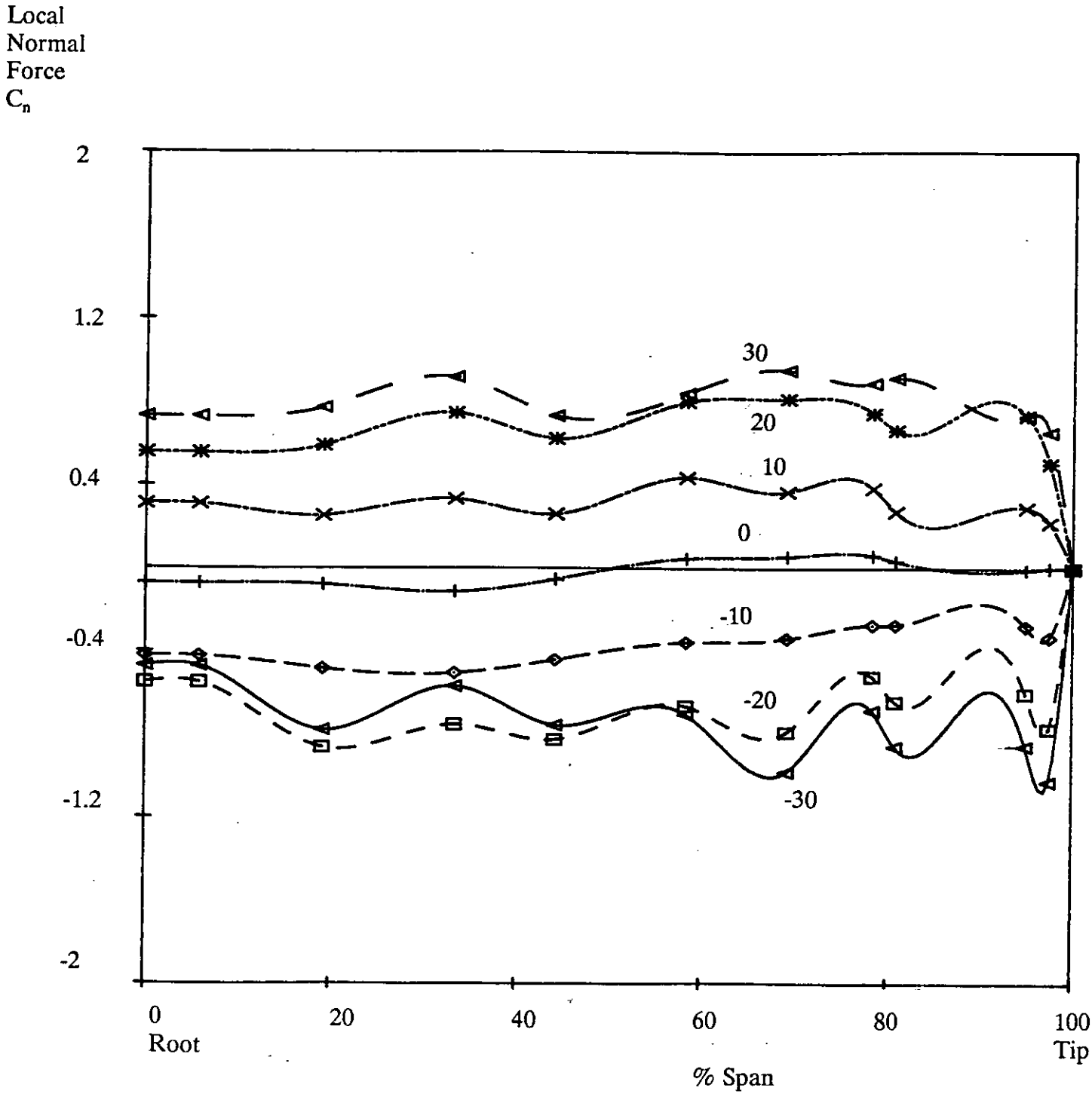

Figure 44 Variation of Spanwise Distribution of Local Section C_N with Incidence for All-Movable Rudder No.3 at a Propeller Advance Ratio of 0.94 and Longitudinal Separation of X/D=0.39

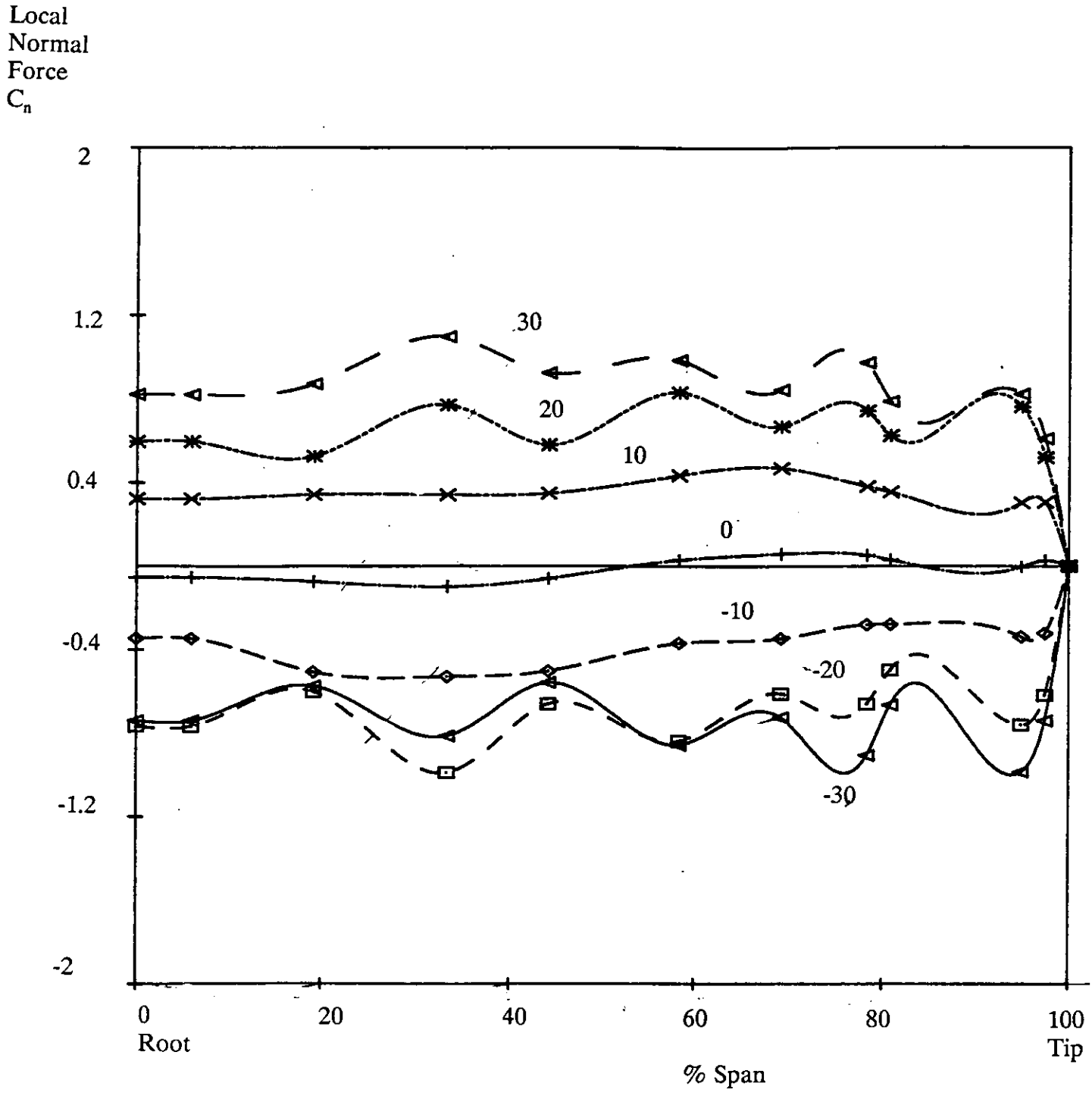

Figure 45 Variation of Spanwise Distribution of Local Section C_N with Incidence for All-Movable Rudder No.3 at a Propeller Advance Ratio of 0.94 and Longitudinal Separation of X/D=0.52

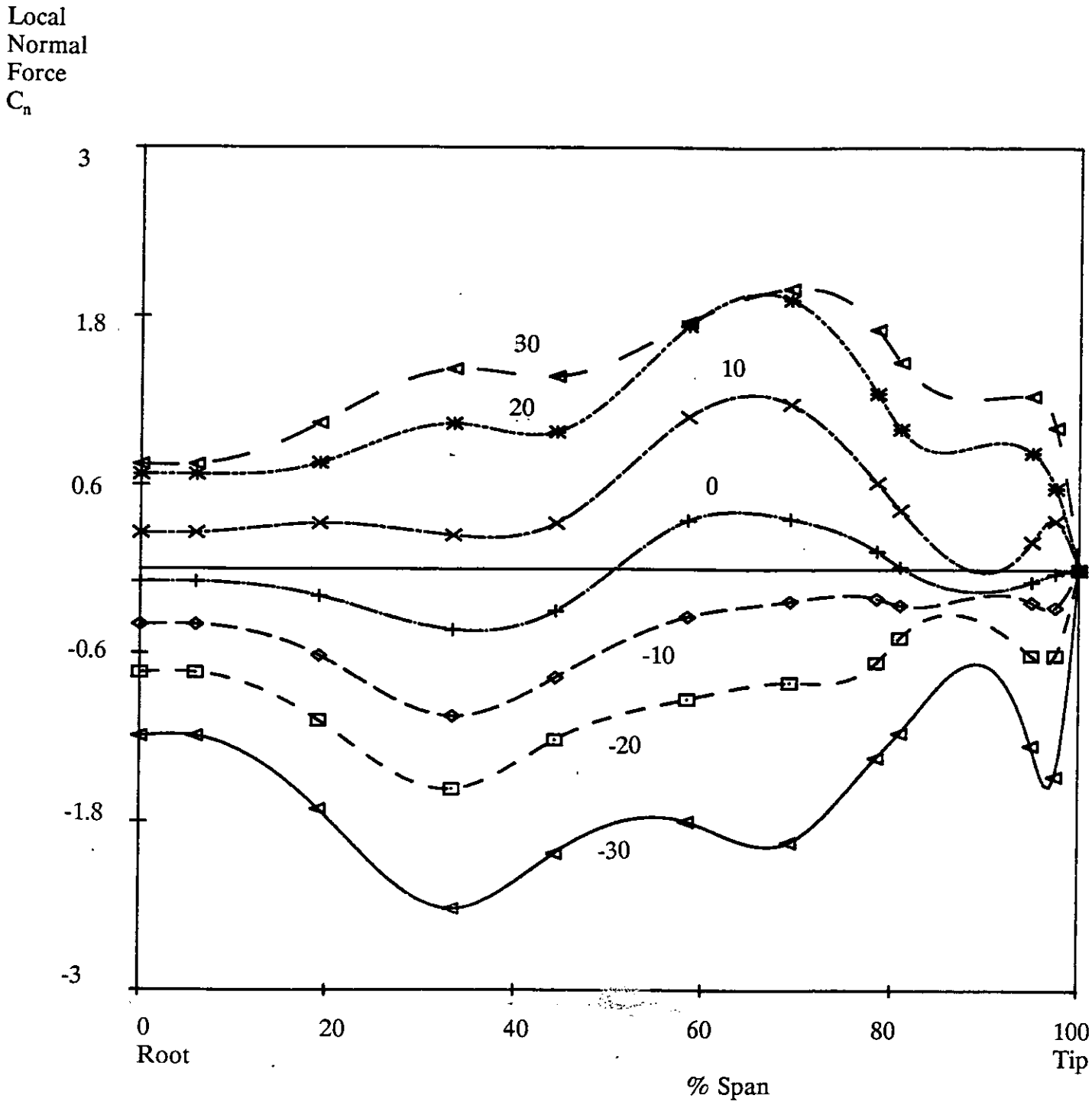

Figure 46 Variation of Spanwise Distribution of Local Section C_N with Incidence for All-Movable Rudder No.3 at a Propeller Advance Ratio of 0.51 and Longitudinal Separation of X/D=0.3

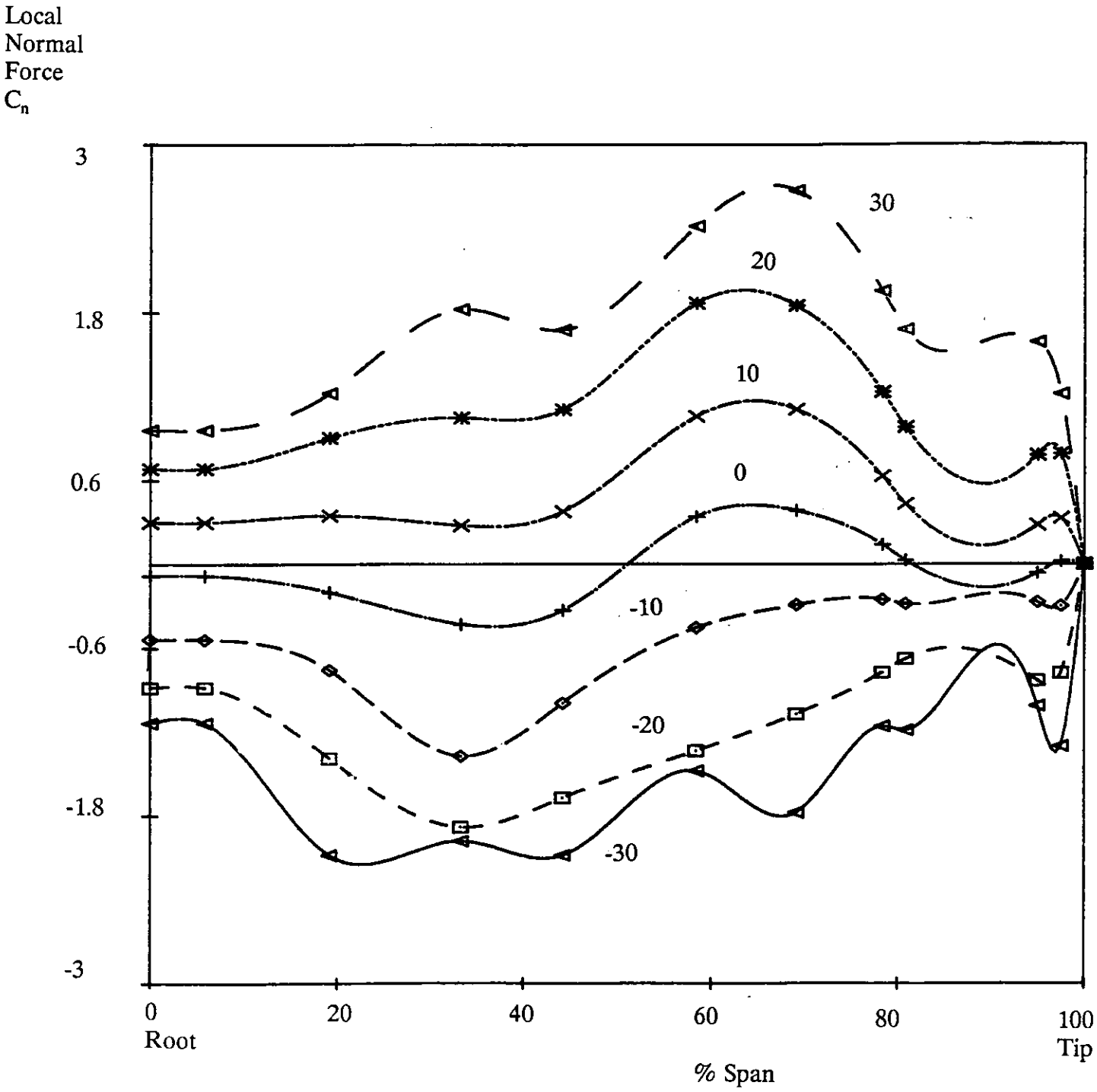

Figure 47 Variation of Spanwise Distribution of Local Section C_N with Incidence for All-Movable Rudder No.3 at a Propeller Advance Ratio of 0.51 and Longitudinal Separation of X/D=0.39

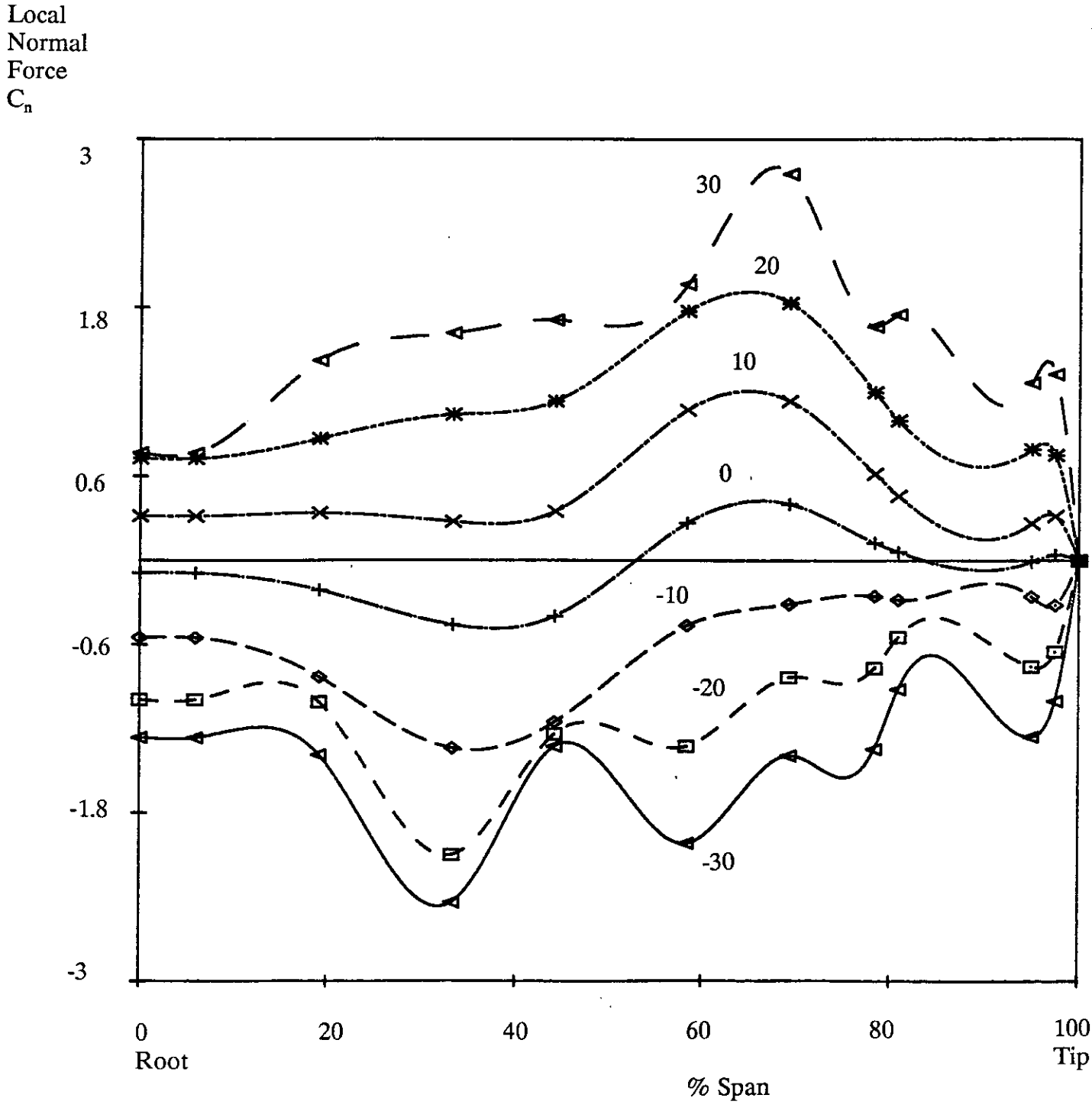

Figure 48 Variation of Spanwise Distribution of Local Section C_N with Incidence for All-Movable Rudder No.3 at a Propeller Advance Ratio of 0.51 and Longitudinal Separation of X/D=0.52

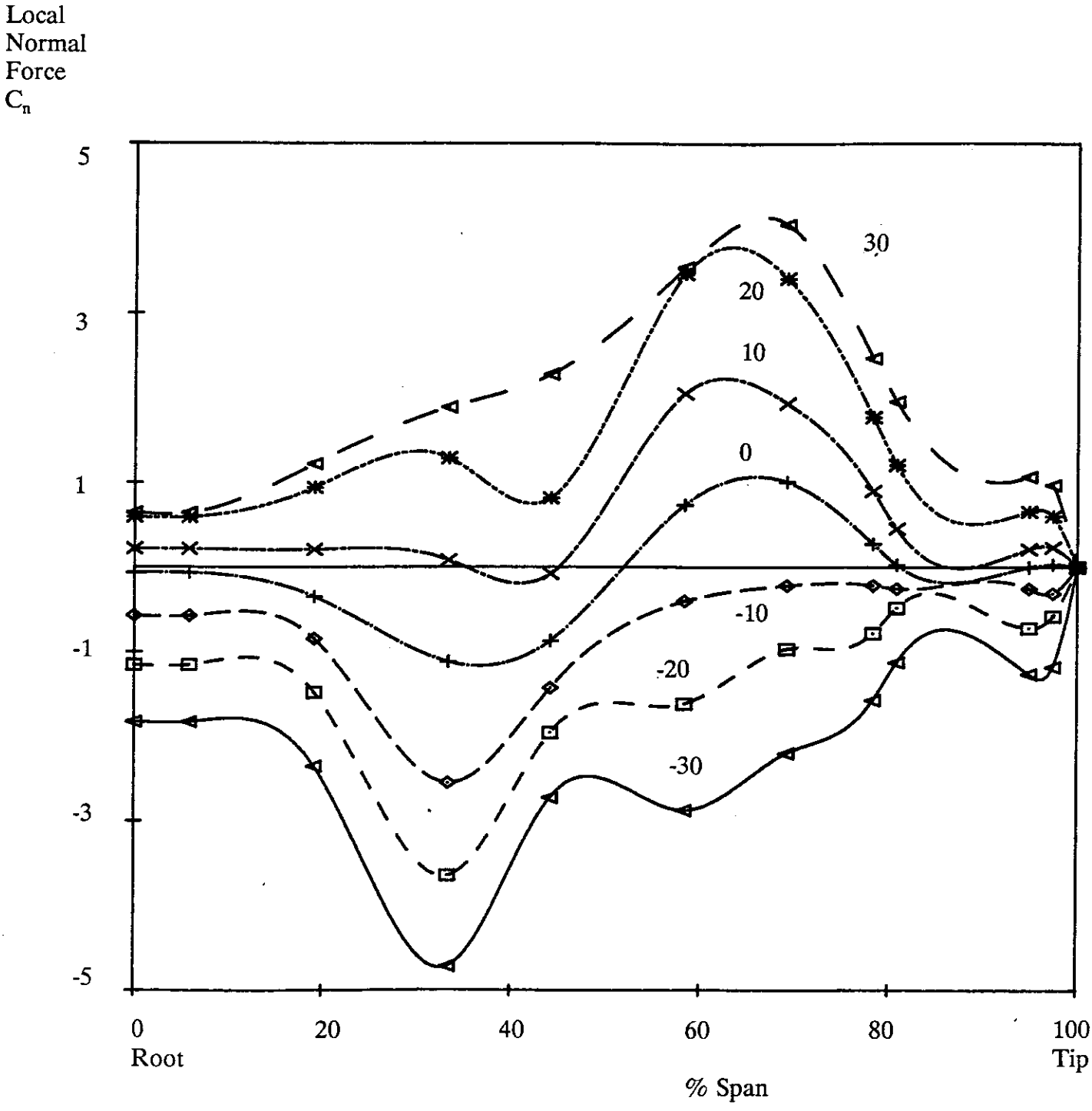

Figure 49 Variation of Spanwise Distribution of Local Section C_N with Incidence for All-Movable Rudder No.3 at a Propeller Advance Ratio of 0.35 and Longitudinal Separation of X/D=0.3

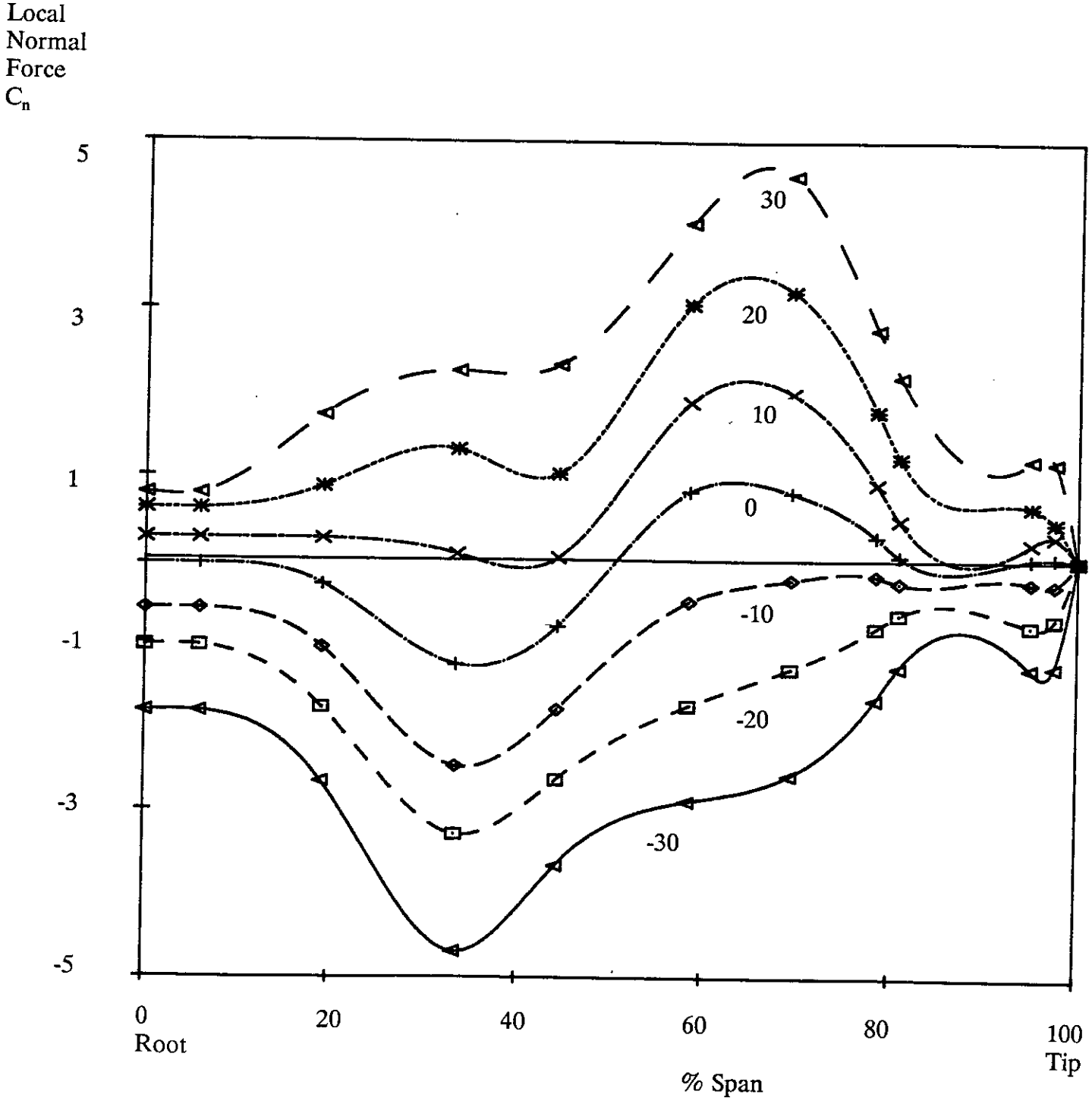

Figure 50 Variation of Spanwise Distribution of Local Section C_N with Incidence for All-Movable Rudder No.3 at a Propeller Advance Ratio of 0.35 and Longitudinal Separation of X/D=0.39

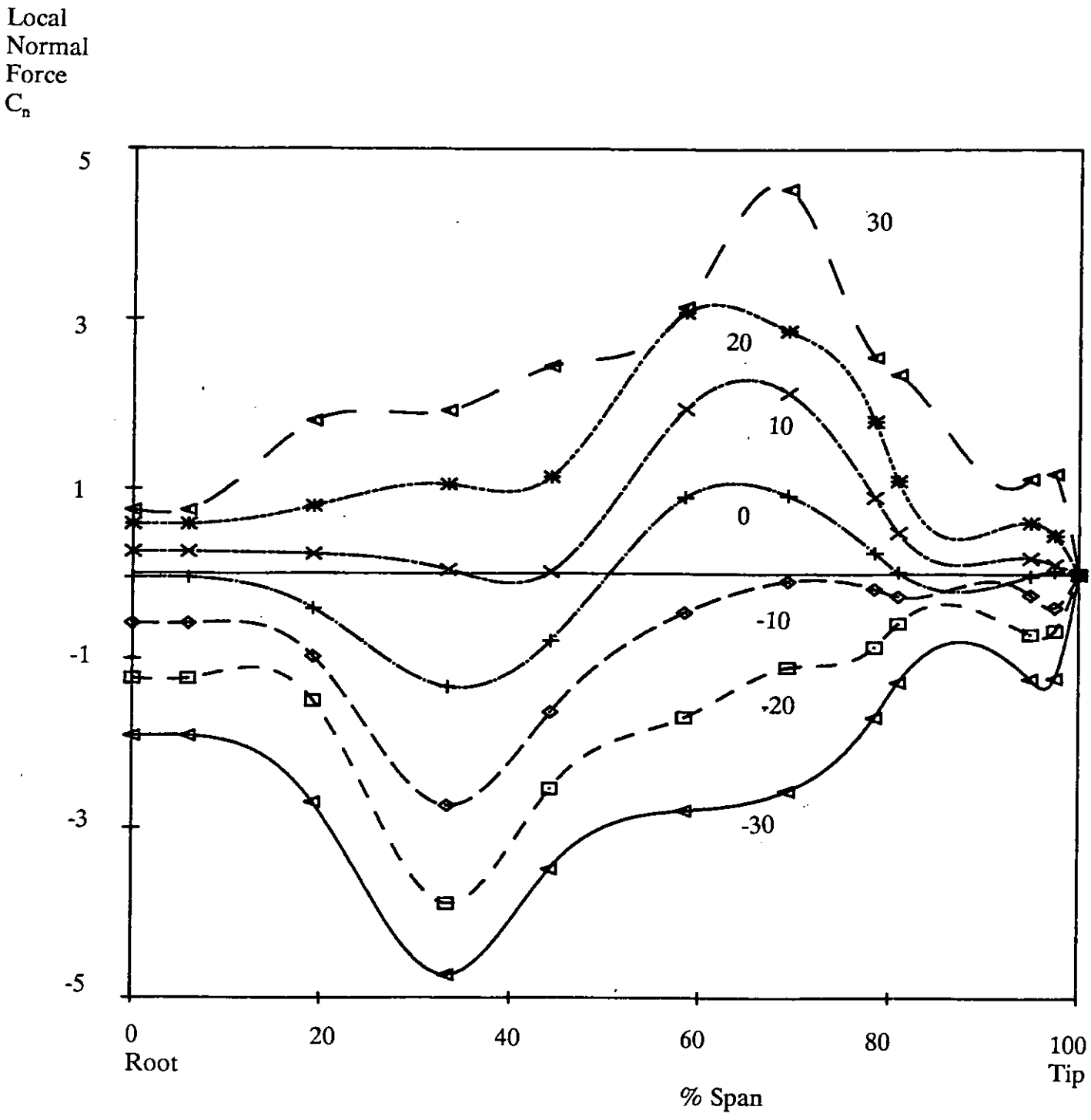

Figure 51 Variation of Spanwise Distribution of Local Section C_N with Incidence for All-Movable Rudder No.3 at a Propeller Advance Ratio of 0.35 and Longitudinal Separation of X/D=0.52

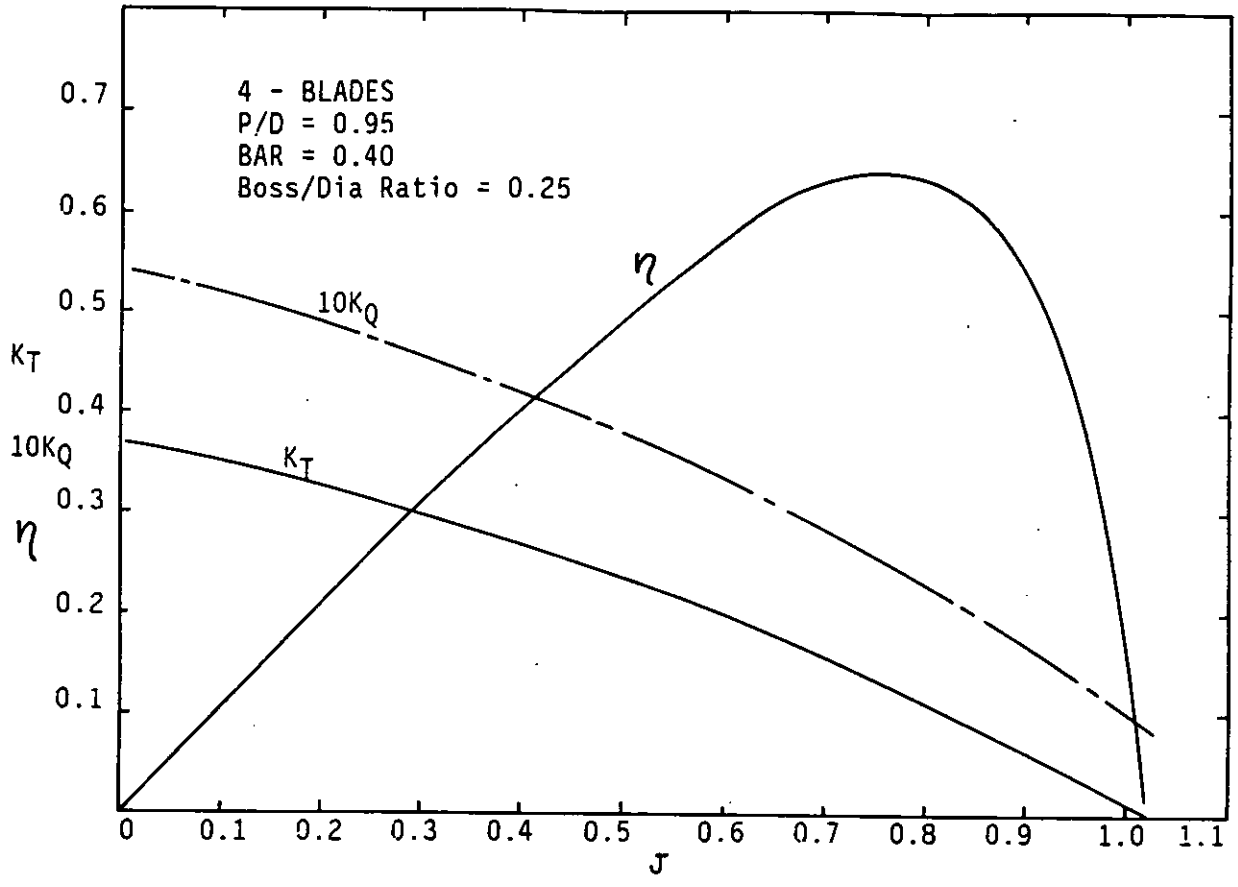

Figure 52 Freestream (Open Water) propeller characteristic of modified Wageningen B4.40 at a mean Pitch Ratio of 0.95

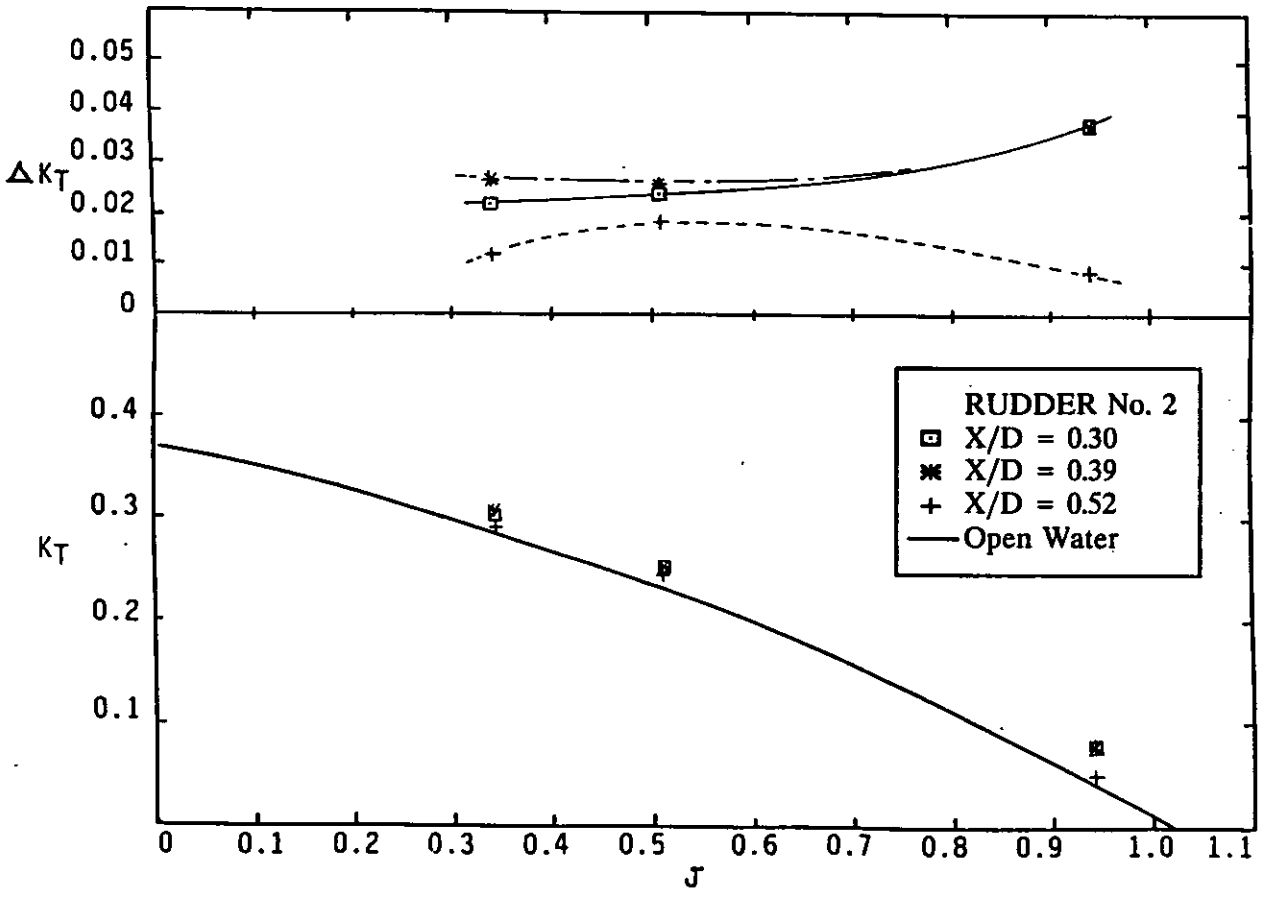

Figure 53 Comparison of The Propeller Thrust K_T against advance ratio for three longitudinal separations of All-Movable Rudder No.2

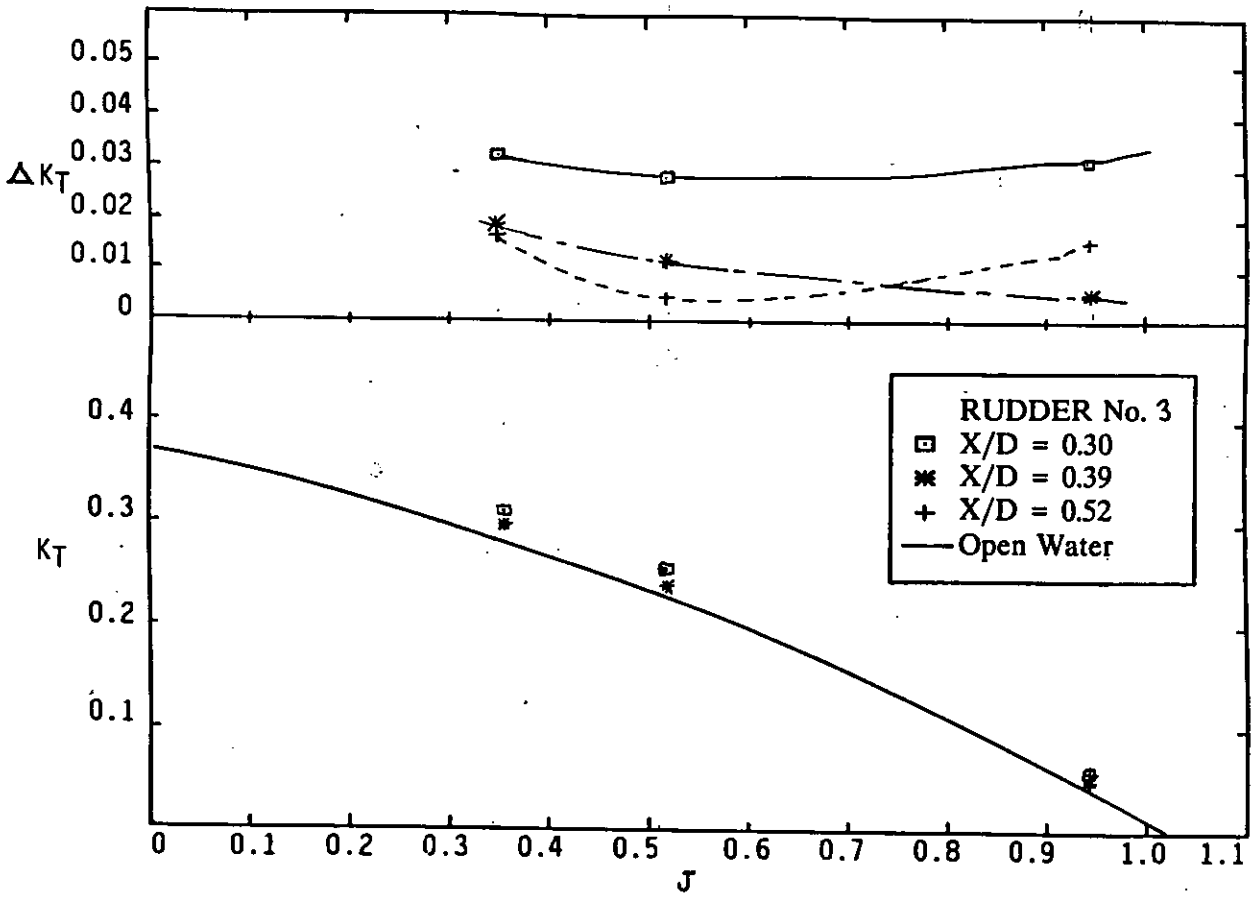

Figure 54 Comparison of The Propeller Thrust K_T against advance ratio for three longitudinal separations of All-Movable Rudder No.3

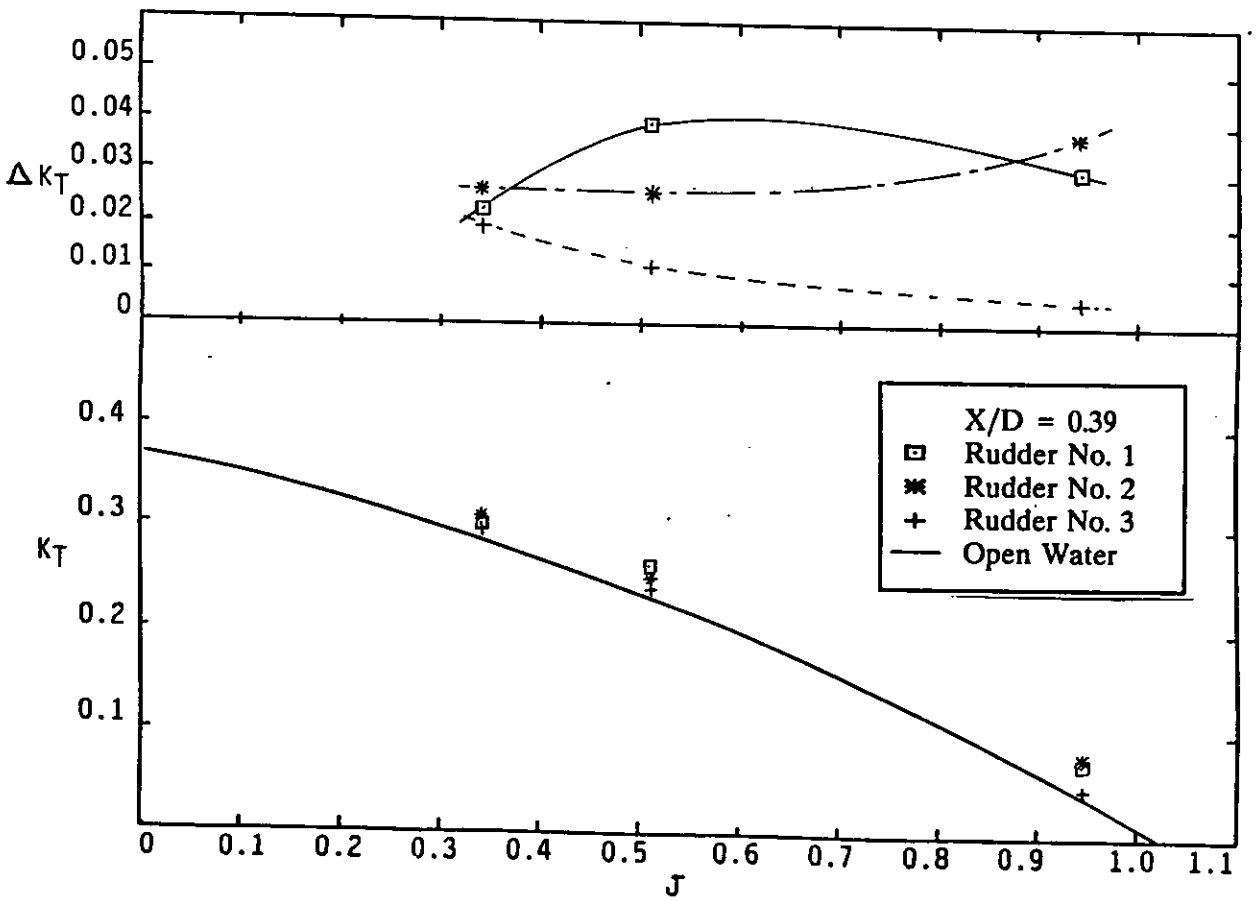

Figure 55 Comparison of The Propeller Thrust K_T against advance ratio for the three All-Movable Rudders.

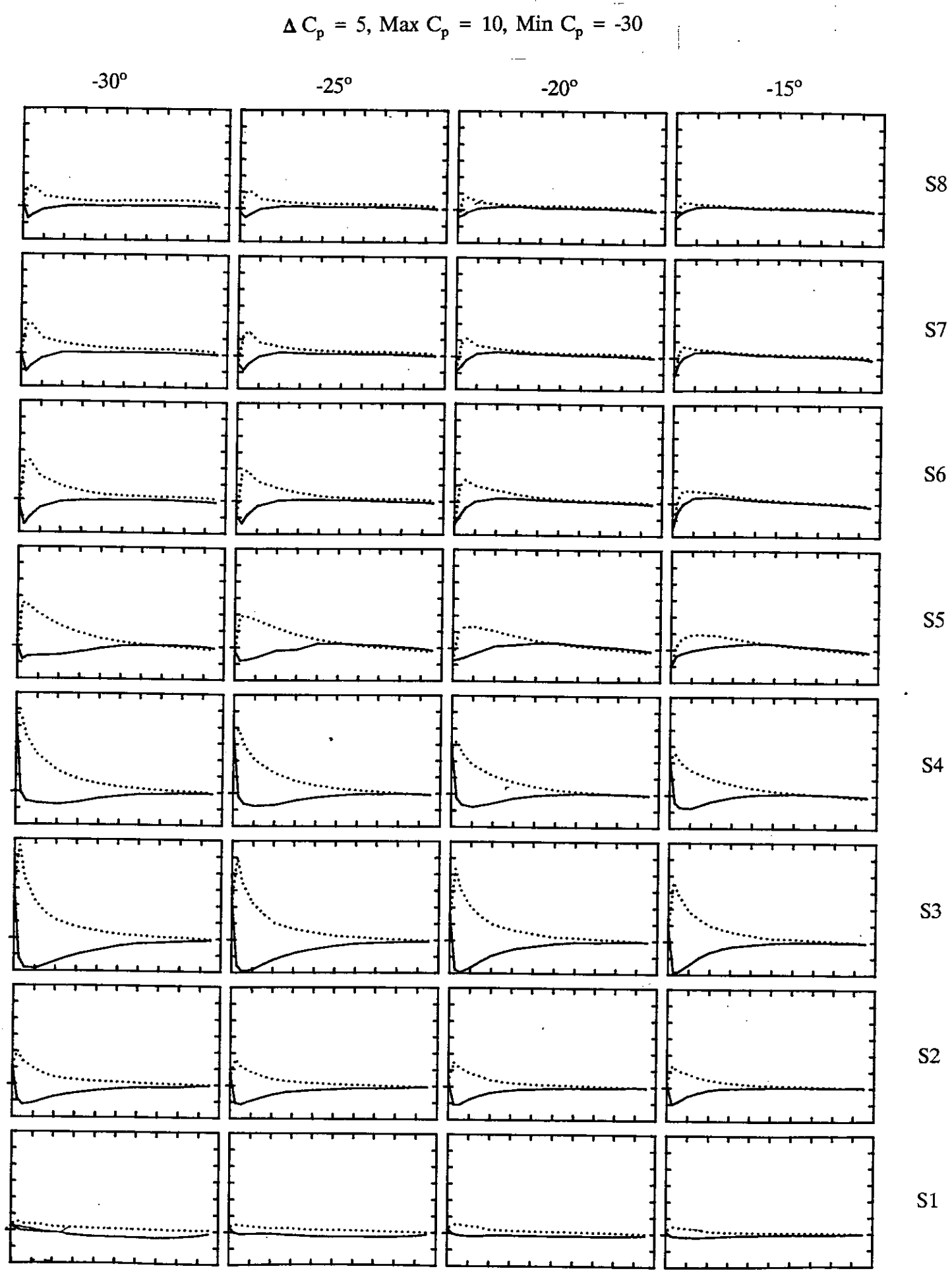

Figure 56 Chordwise pressure distributions at 8 spanwise positions for Rudder No. 1 at J=0.35 for incidence of -30°,-25°,-20°,-15°,-10°,0°,10°,15°,20°,25°,30°.

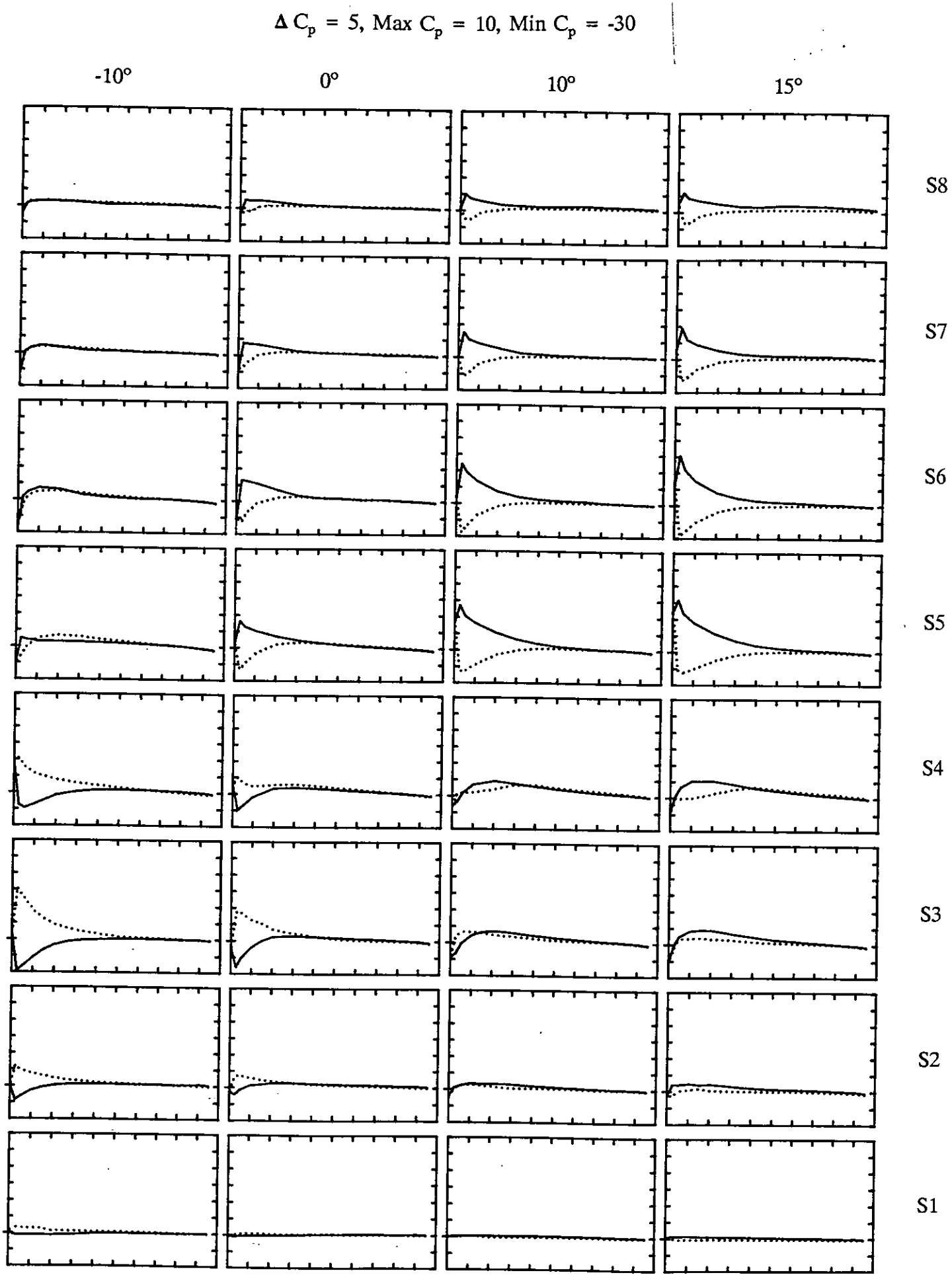

Figure 56 cont.

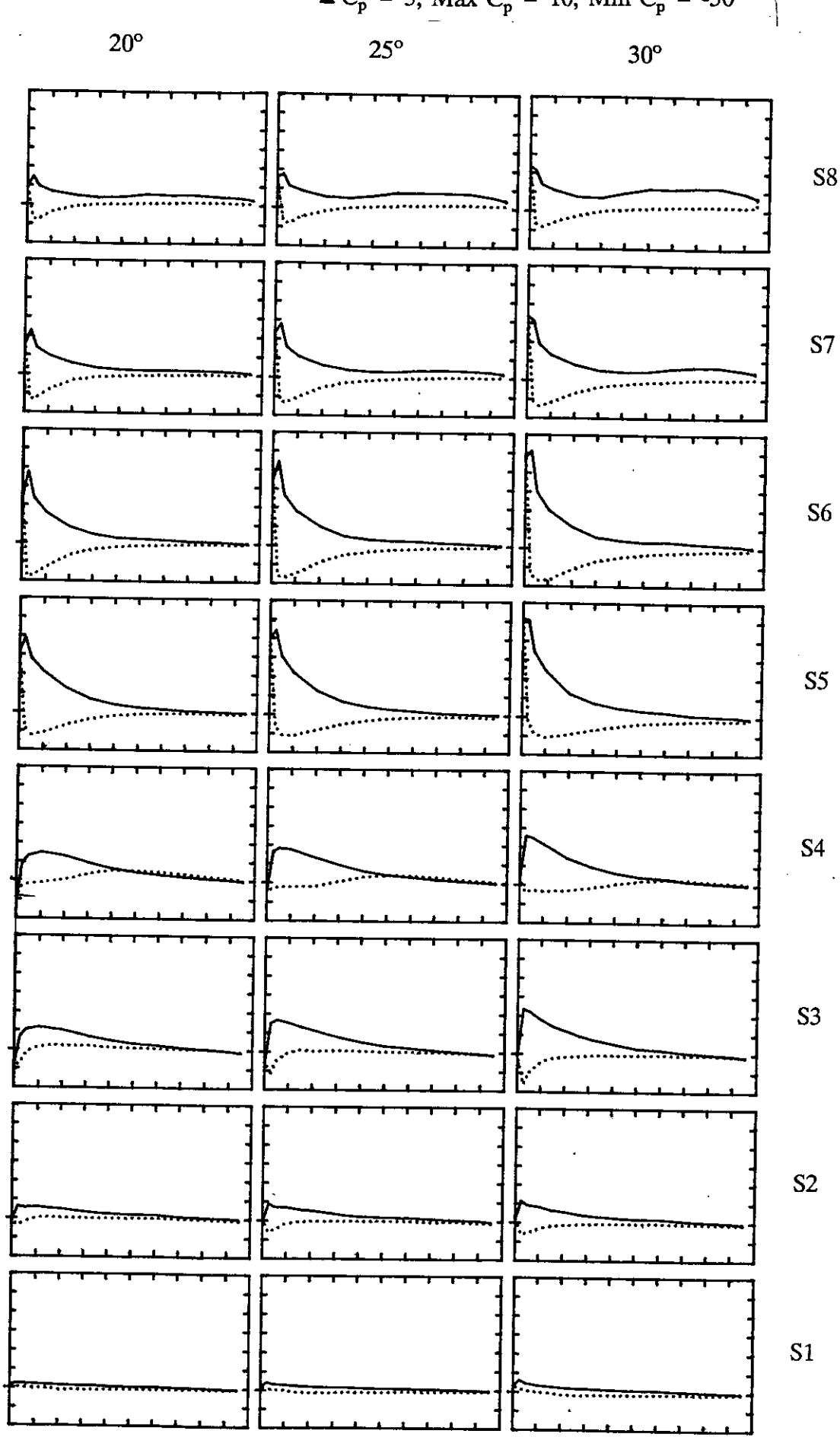

Figure 56 cont.

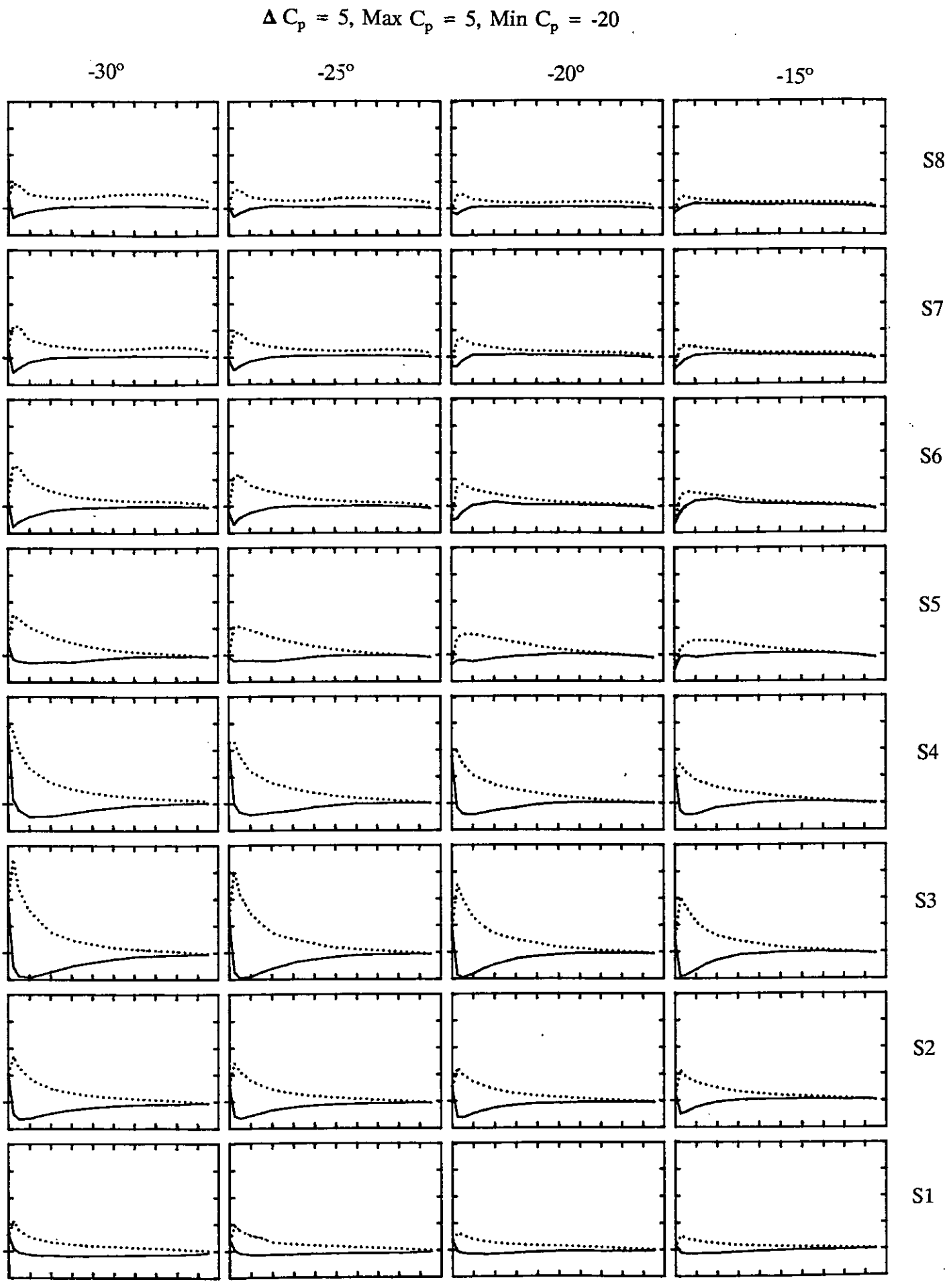

Figure 57 Chordwise pressure distributions at 8 spanwise positions for Rudder No. 1 at J=0.51 for incidence of -30°,-25°,-20°,-15°,-10°,0°,10°,15°,20°,25°,30°.

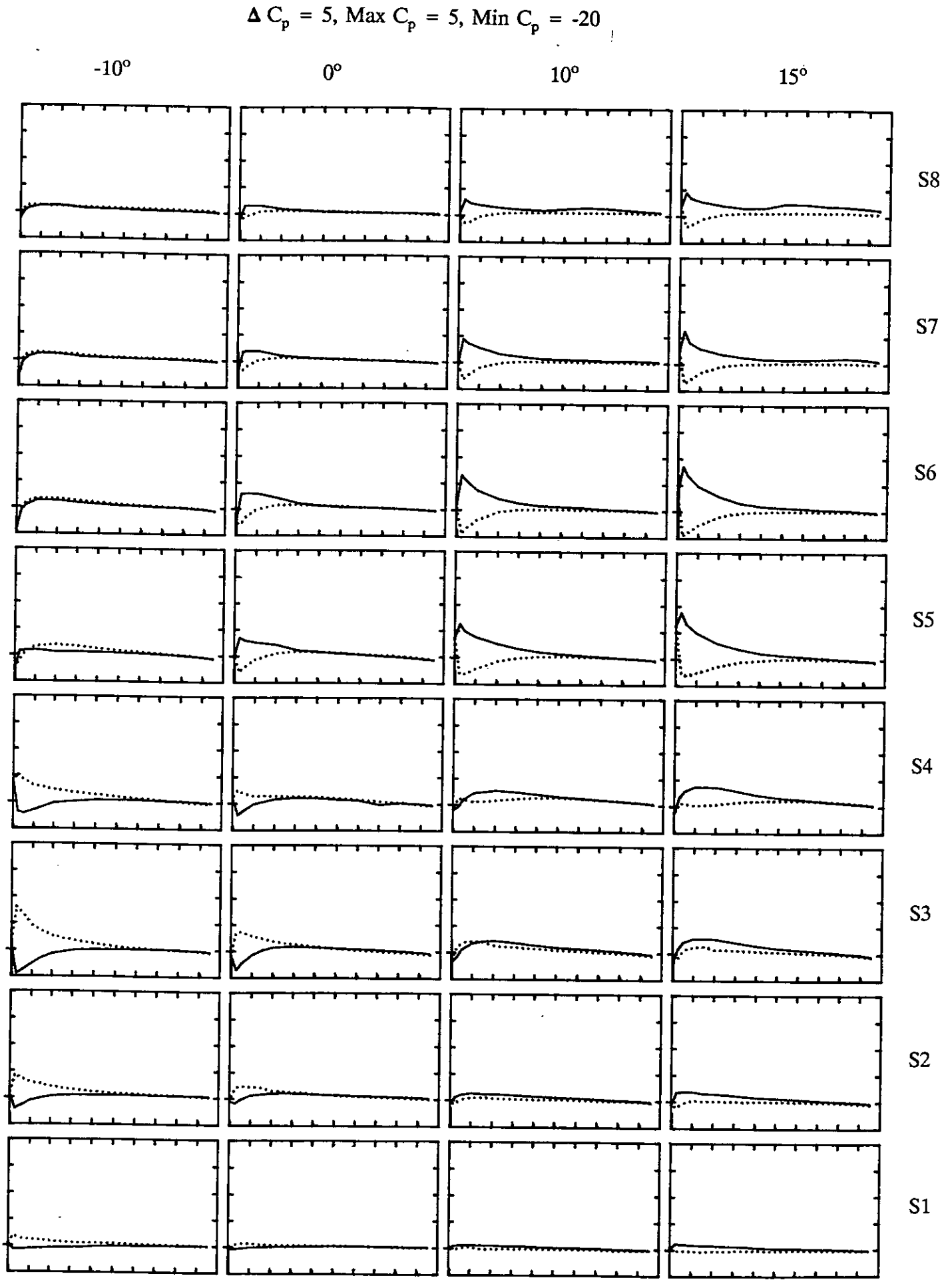

Figure 57 cont.

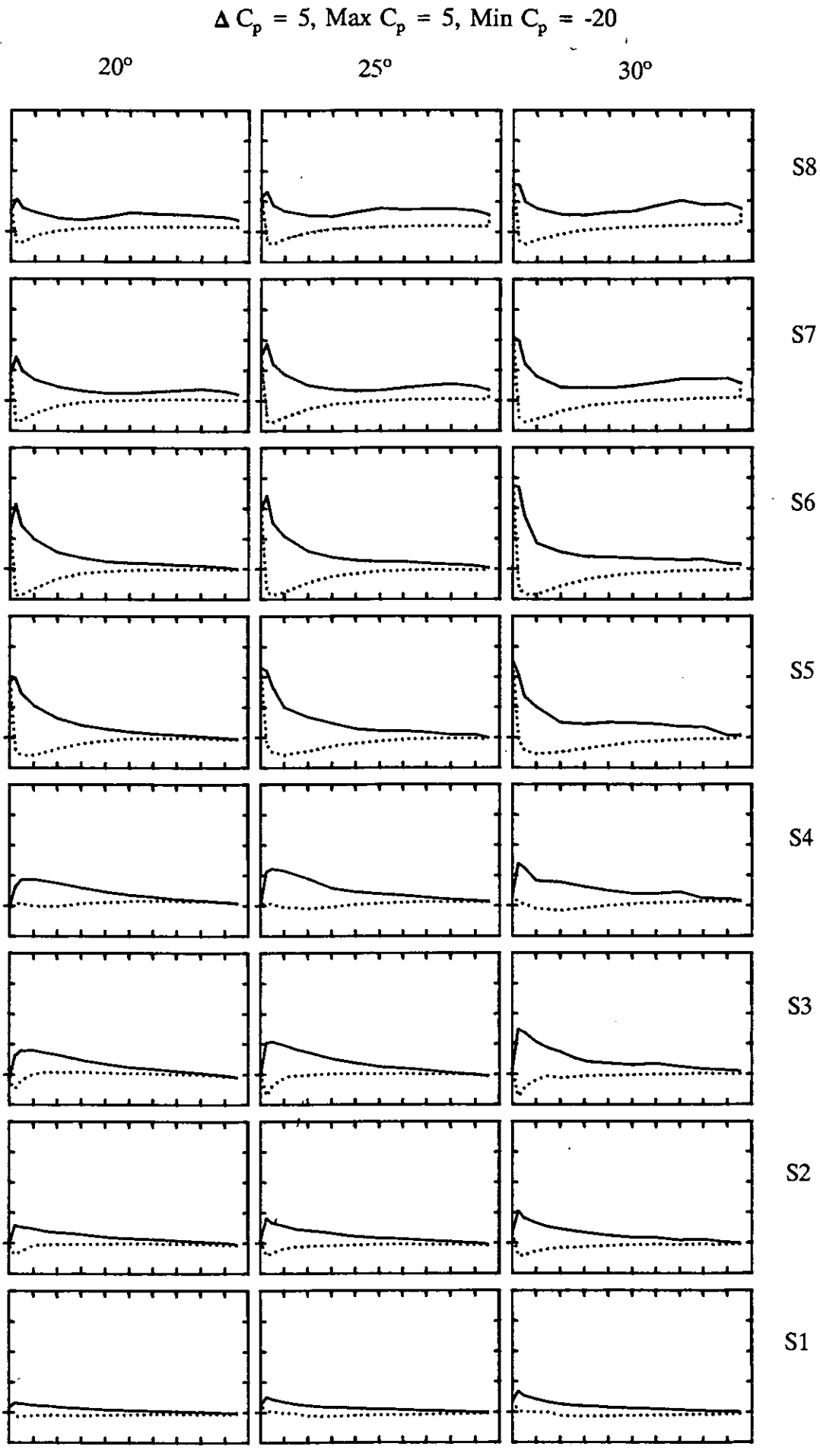

Figure 57 cont.

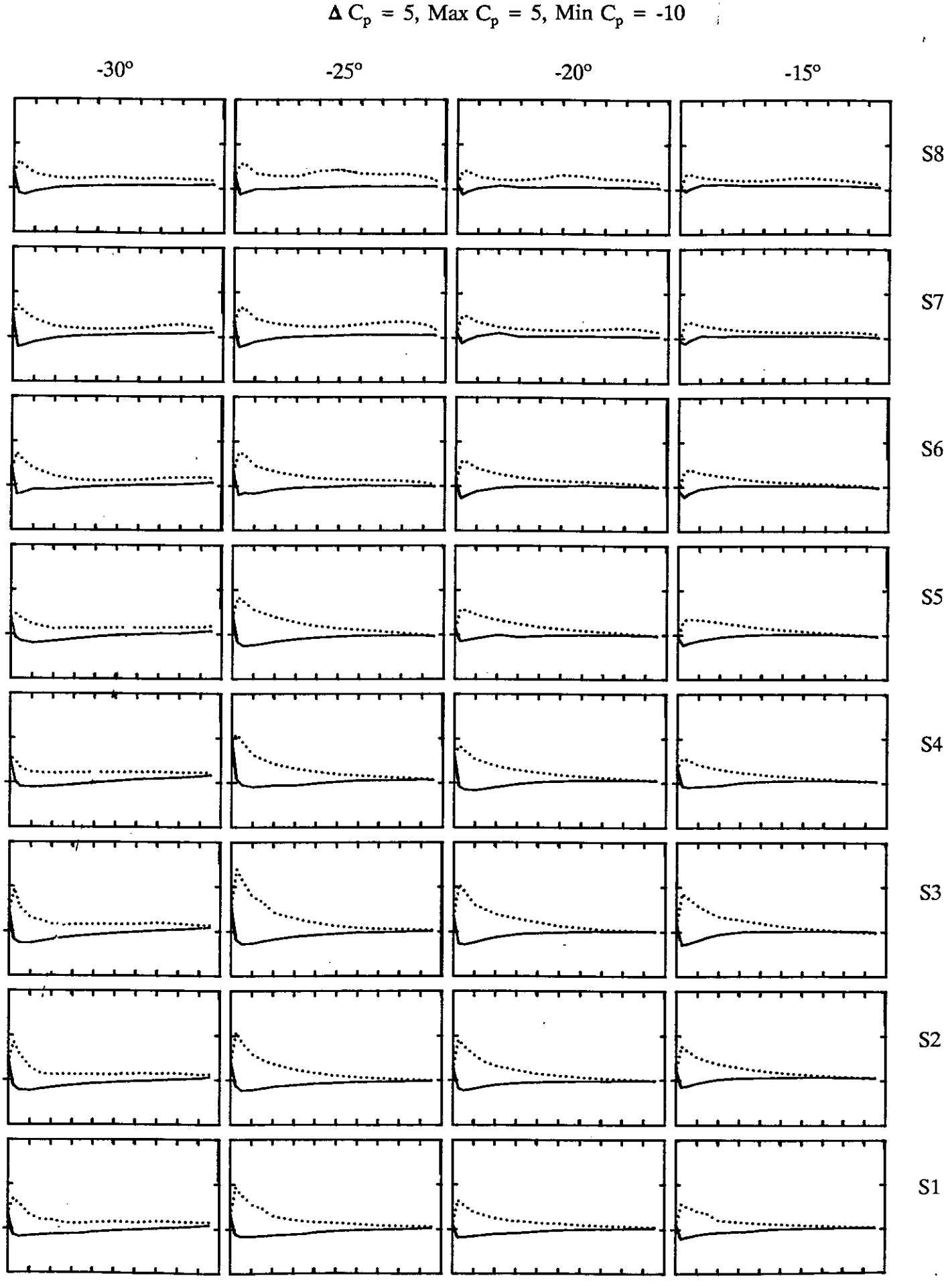

Figure 58 Chordwise pressure distributions at 8 spanwise positions for Rudder No. 1 at J=0.94 for incidence of -30°,-25°,-20°,-15°,-10°,0°,10°,15°,20°,25°,30°.

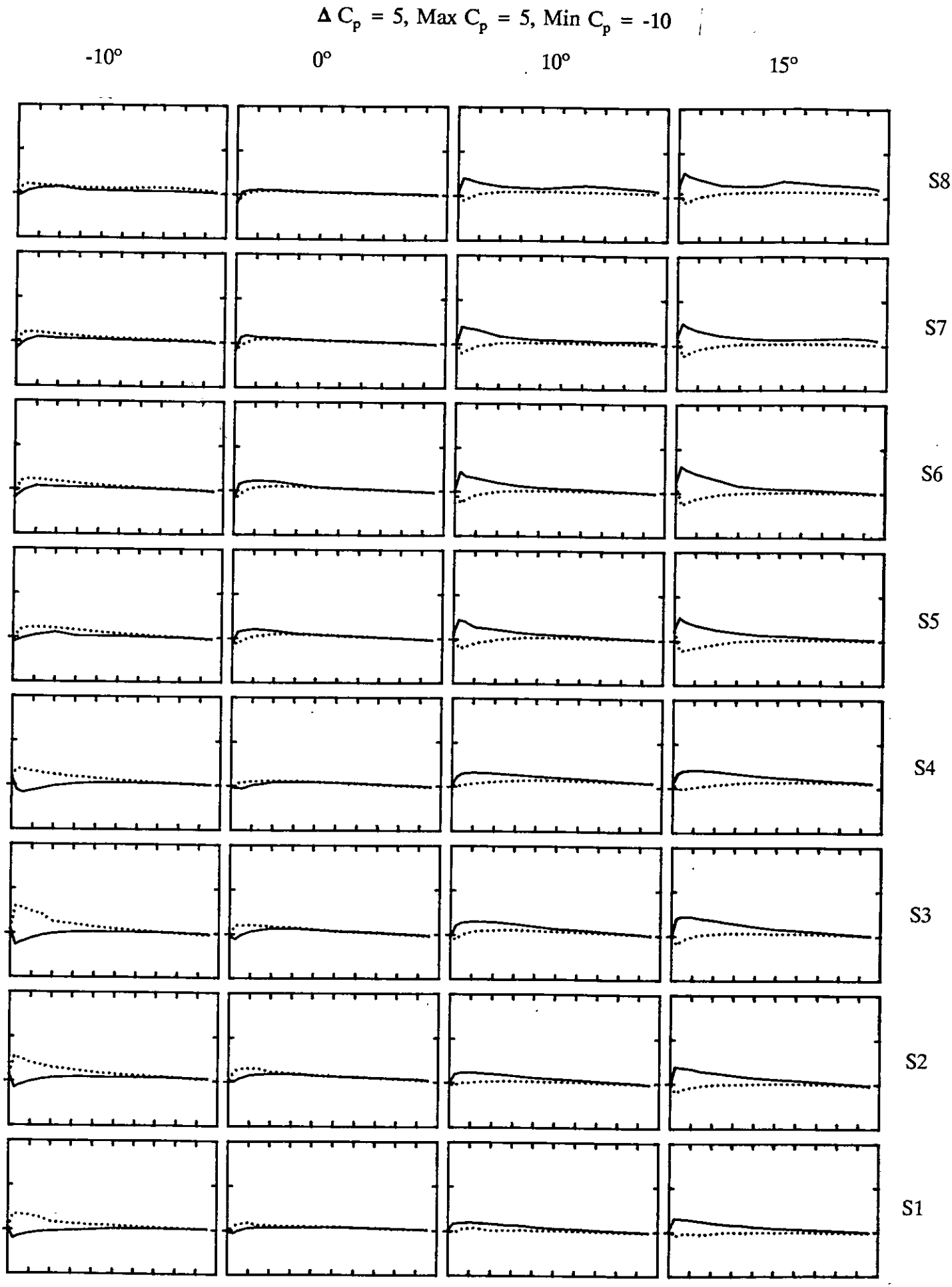

Figure 58 cont.

$\Delta C_p = 5$, Max $C_p = 5$, Min $C_p = -10$

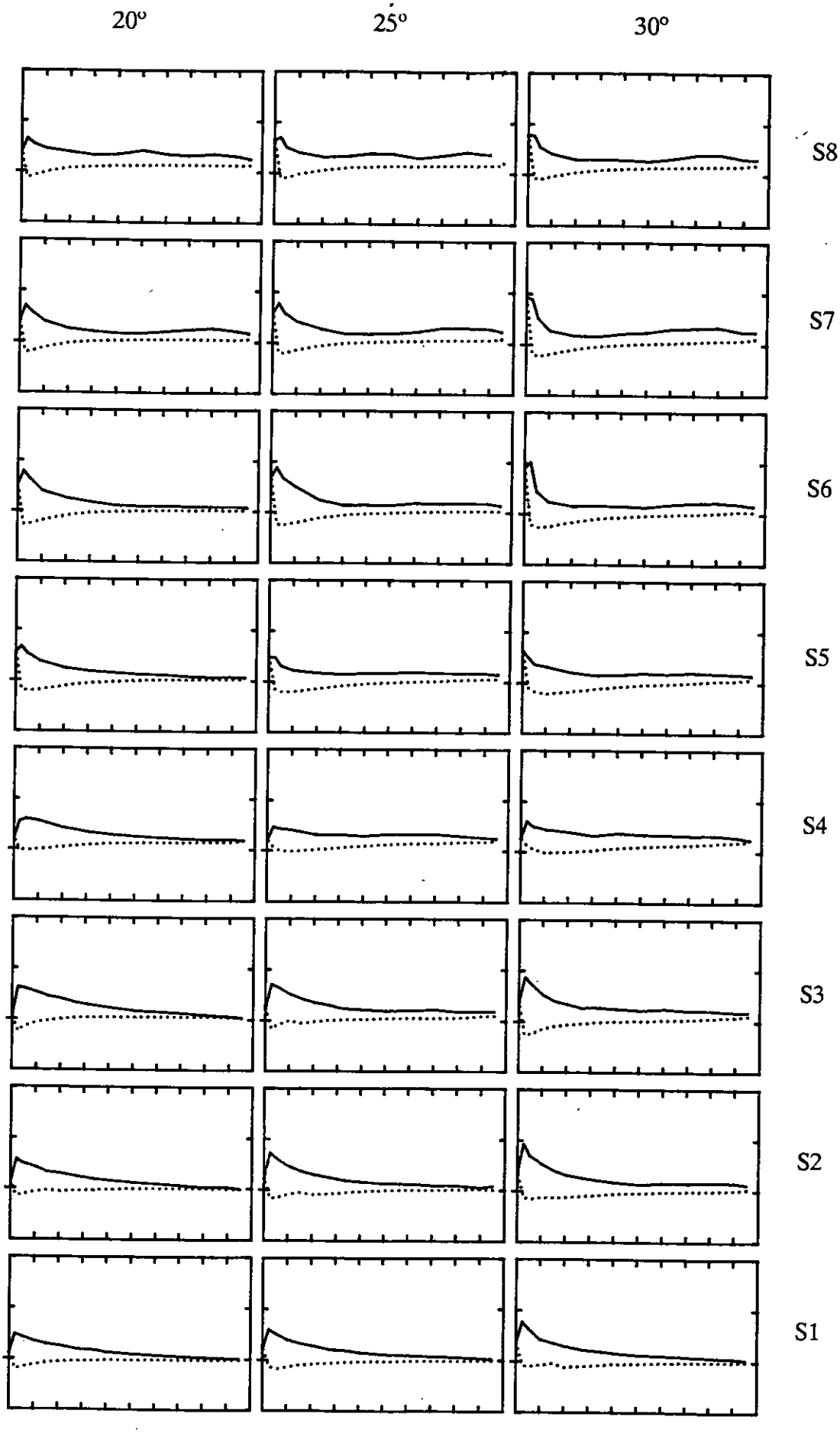

Figure 58 cont.

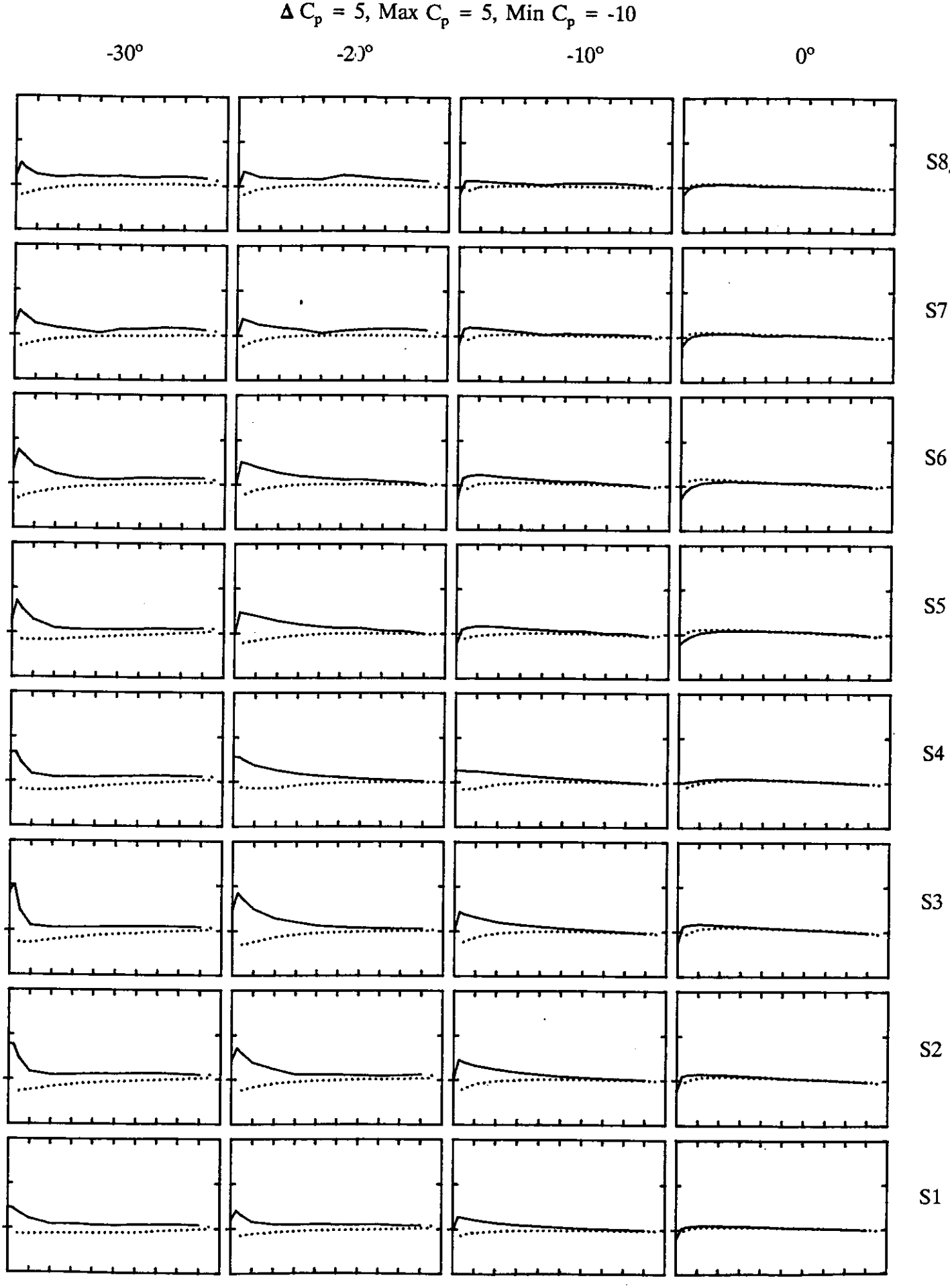

Figure 59 Chordwise pressure distributions at 8 spanwise positions for Rudder No. 2 at J=0.94 for X/D=0.3 at incidence of -30°,-20°,-10°,0°,10°,20°, and 30°.

$\Delta C_p = 5$, Max $C_p = 5$, Min $C_p = -10$

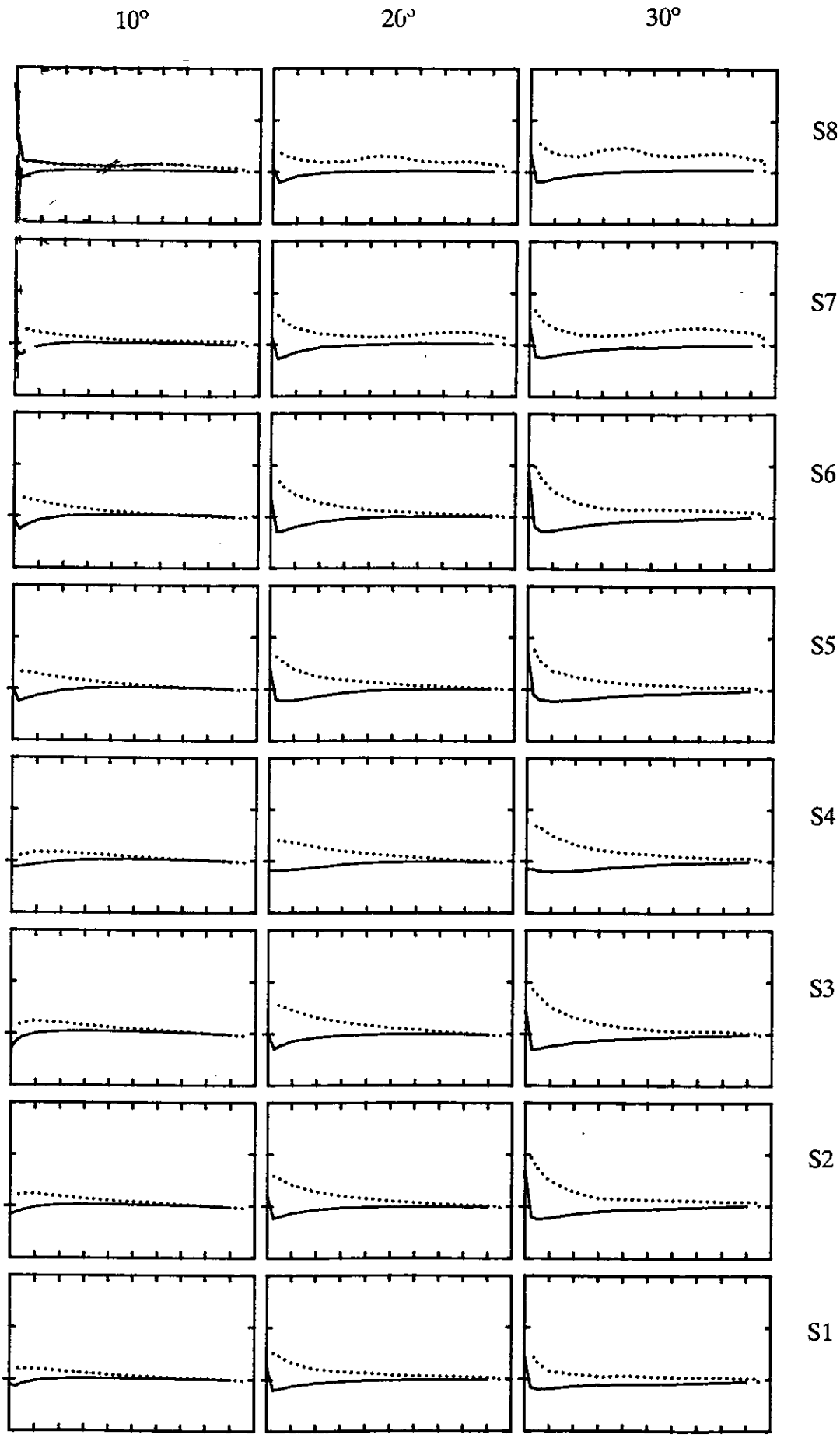

Figure 59 cont.

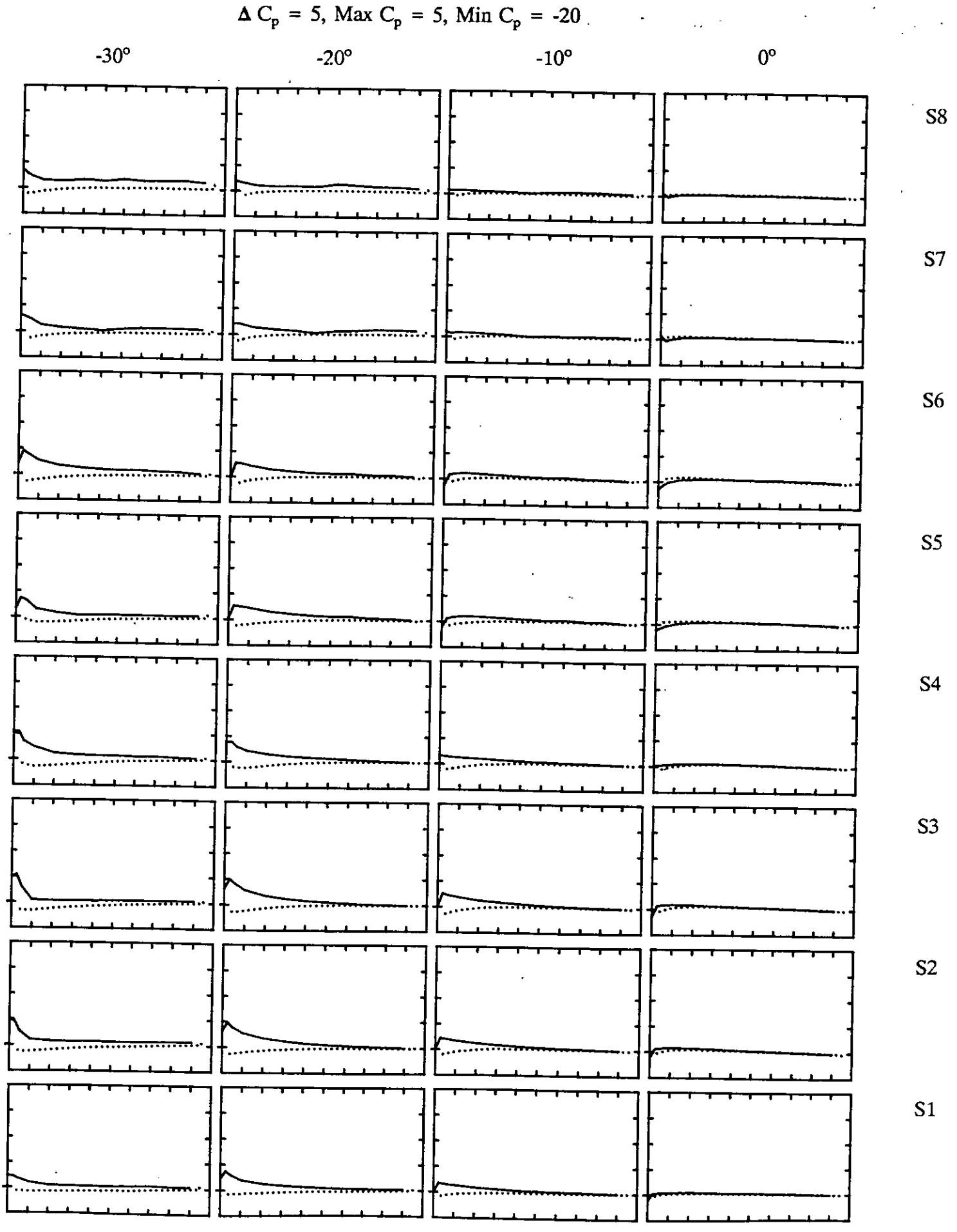

Figure 60 Chordwise pressure distributions at 8 spanwise positions for Rudder No. 2 at J=0.94 for X/D=0.39 at incidence of -30°,-20°,-10°,0°,10°,20°, and 30°.

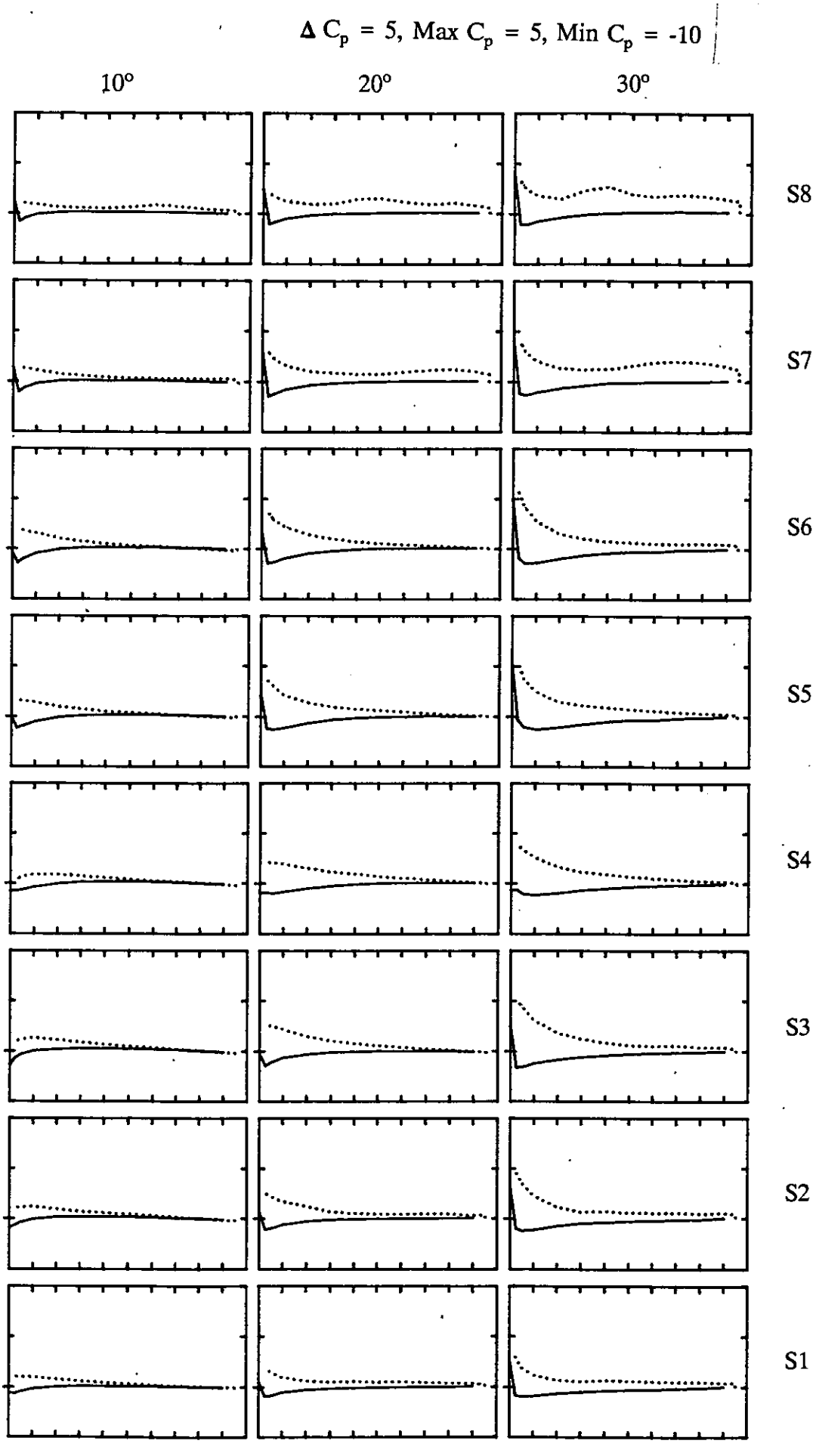

Figure 60 cont.

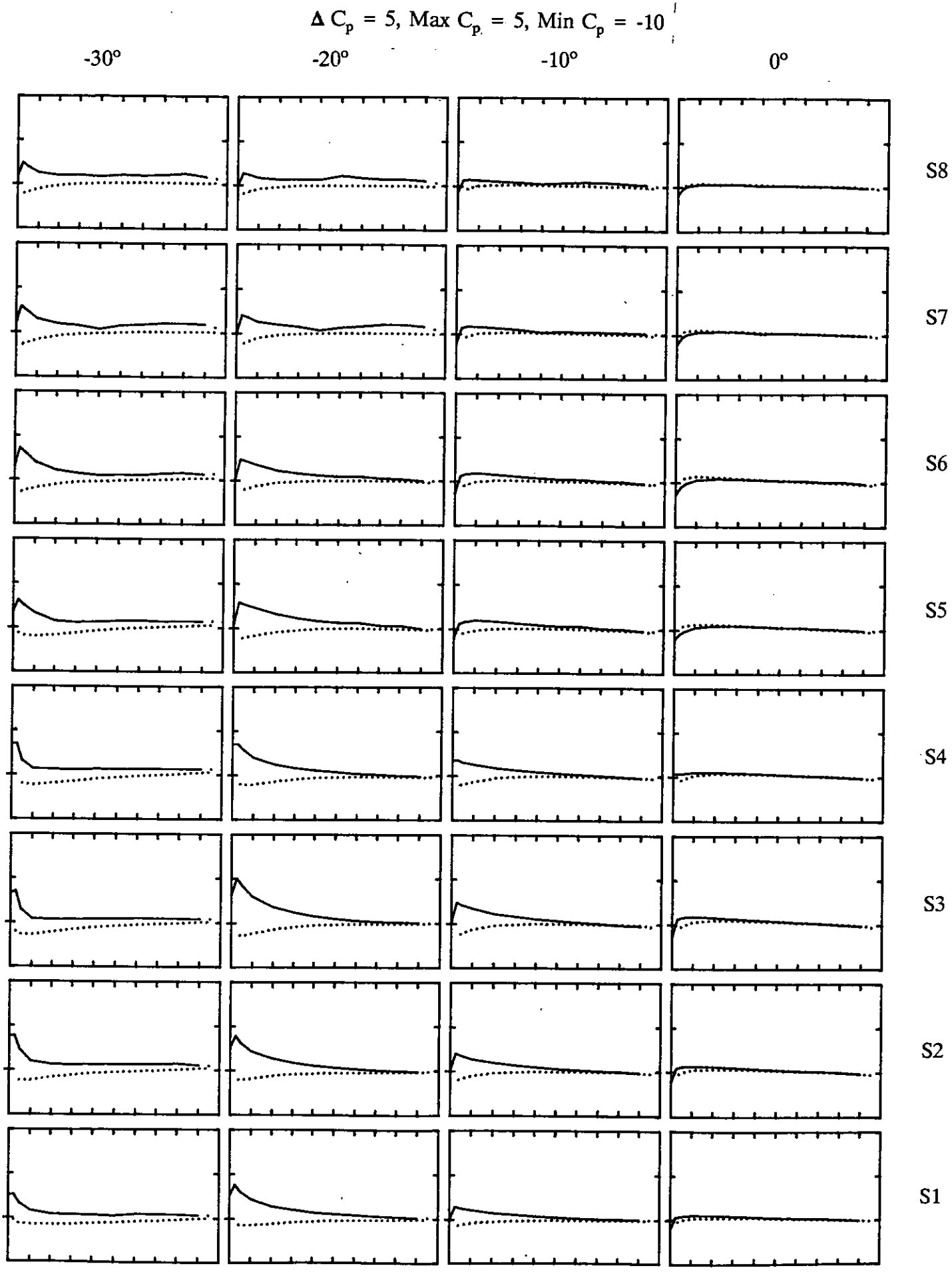

Figure 61 Chordwise pressure distributions at 8 spanwise positions for Rudder No. 2 at J=0.94 for X/D=0.52 at incidence of -30°,-20°,-10°,0°,10°,20°, and 30°.

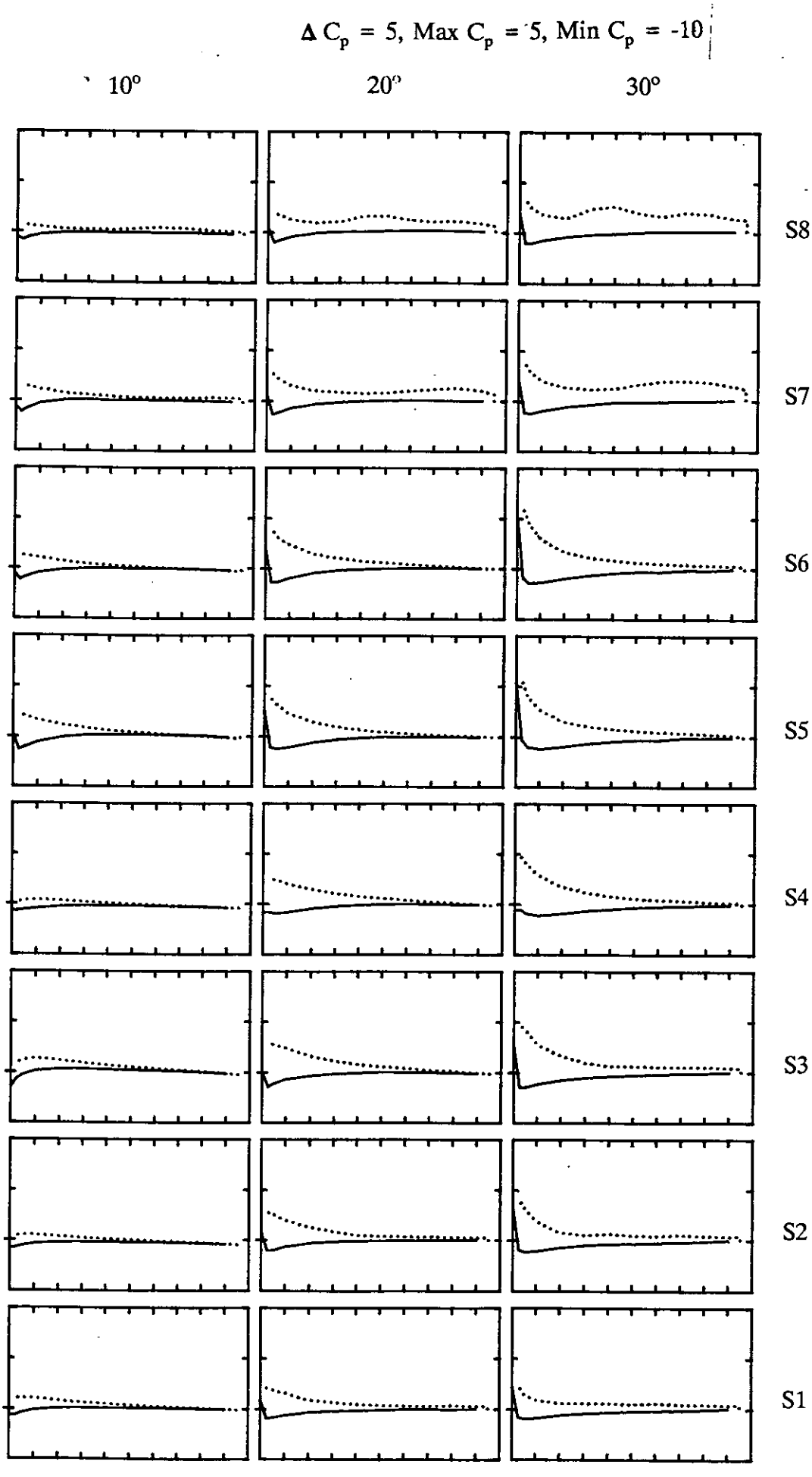

Figure 61 cont.

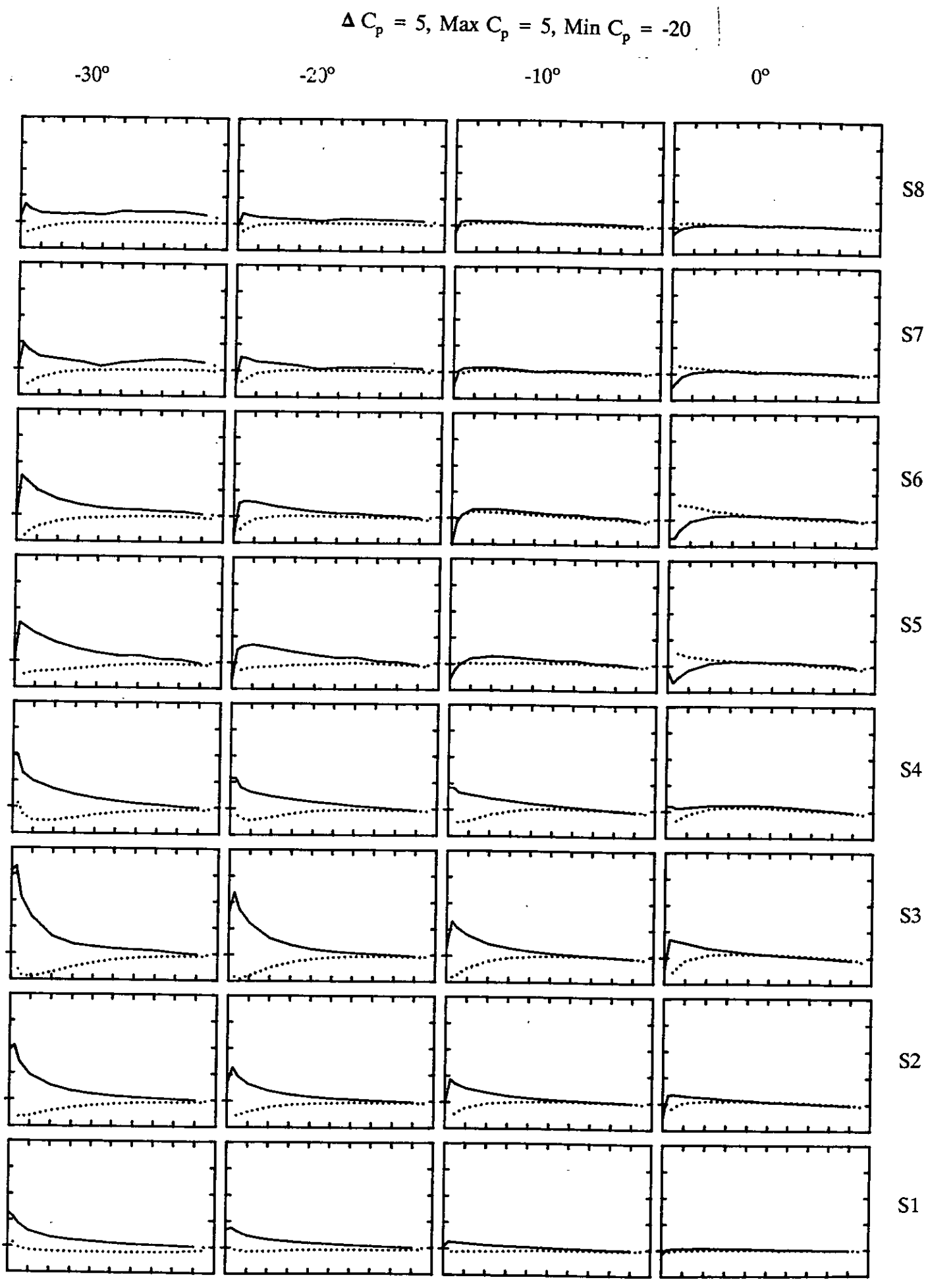

Figure 62 Chordwise pressure distributions at 8 spanwise positions for Rudder No. 2 at J=0.51 for X/D=0.3 at incidence of -30°,-20°,-10°,0°,10°,20°, and 30°.

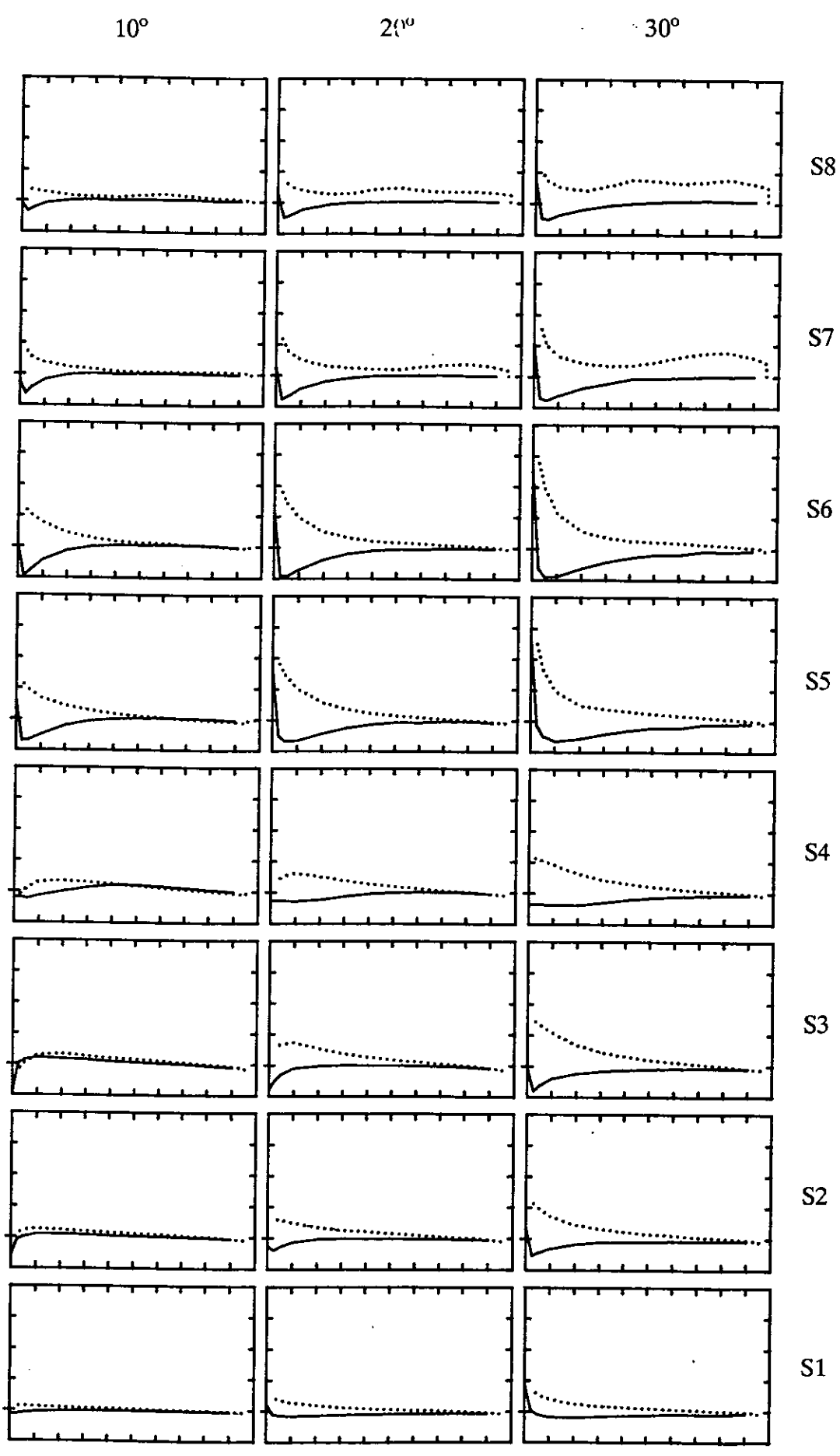

Figure 62 cont.

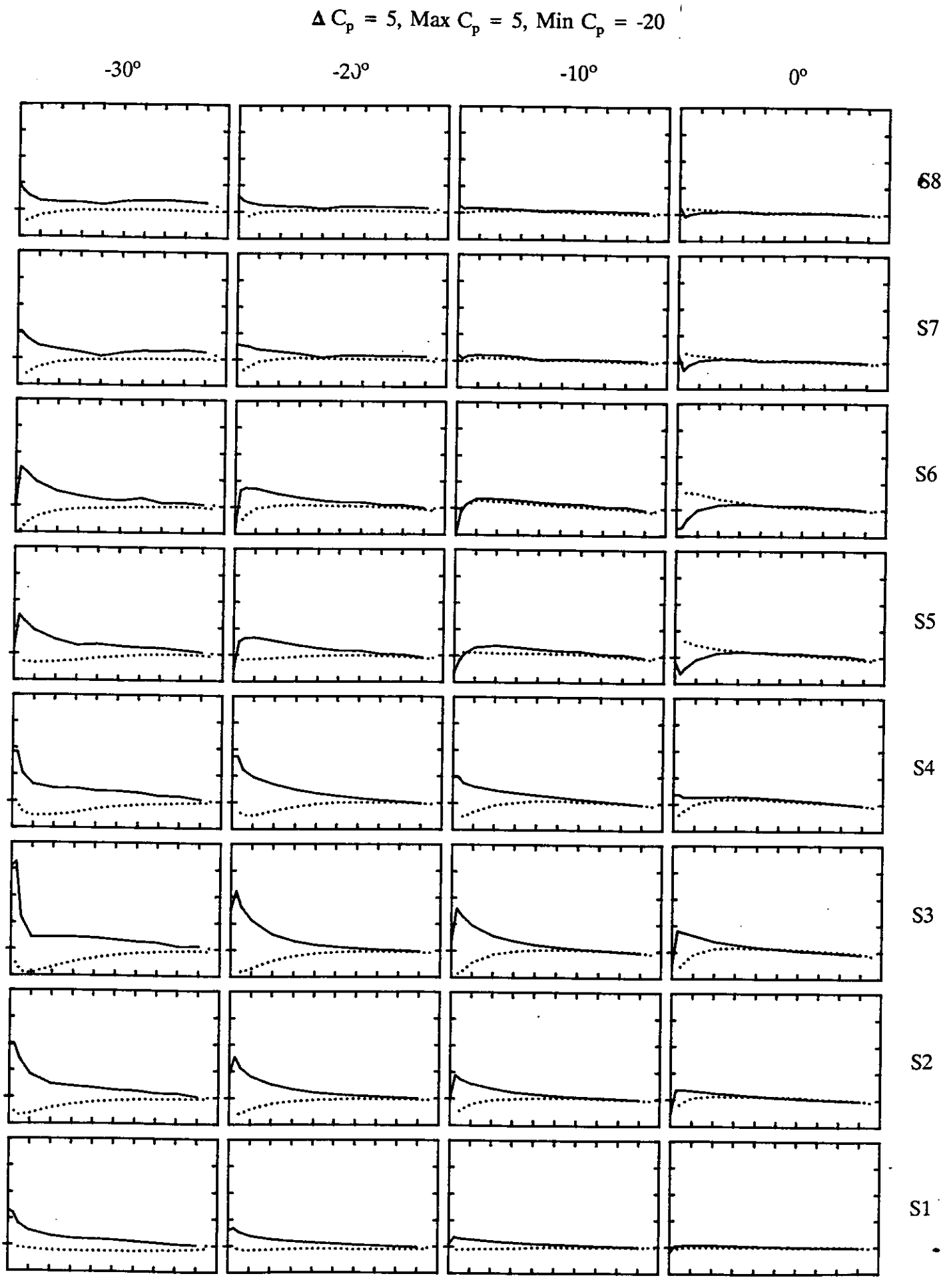

Figure 63 Chordwise pressure distributions at 8 spanwise positions for Rudder No. 2 at J=0.51 for X/D=0.39 at incidence of -30°,-20°,-10°,0°,10°,20°, and 30°.

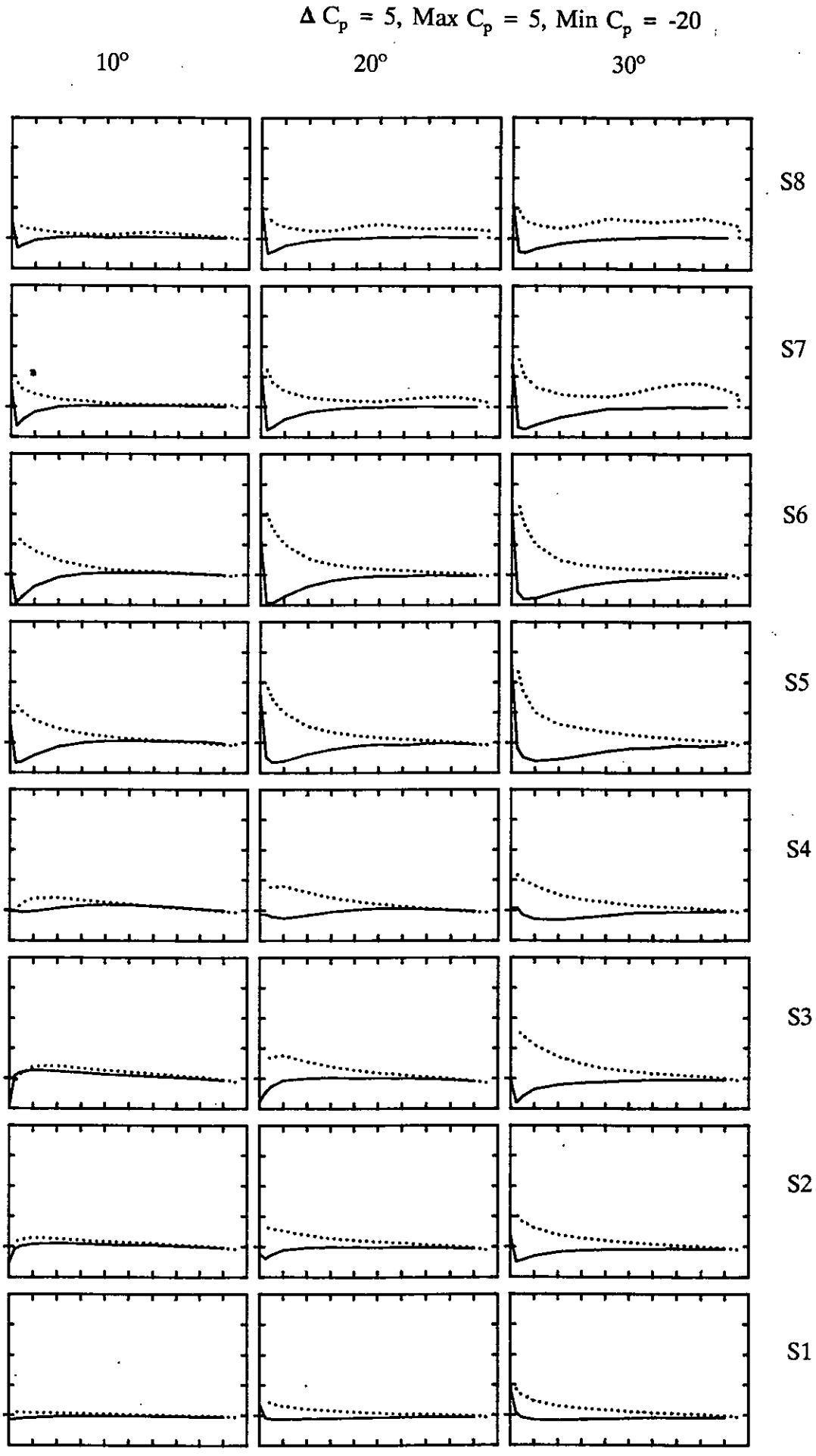

Figure 63 cont.

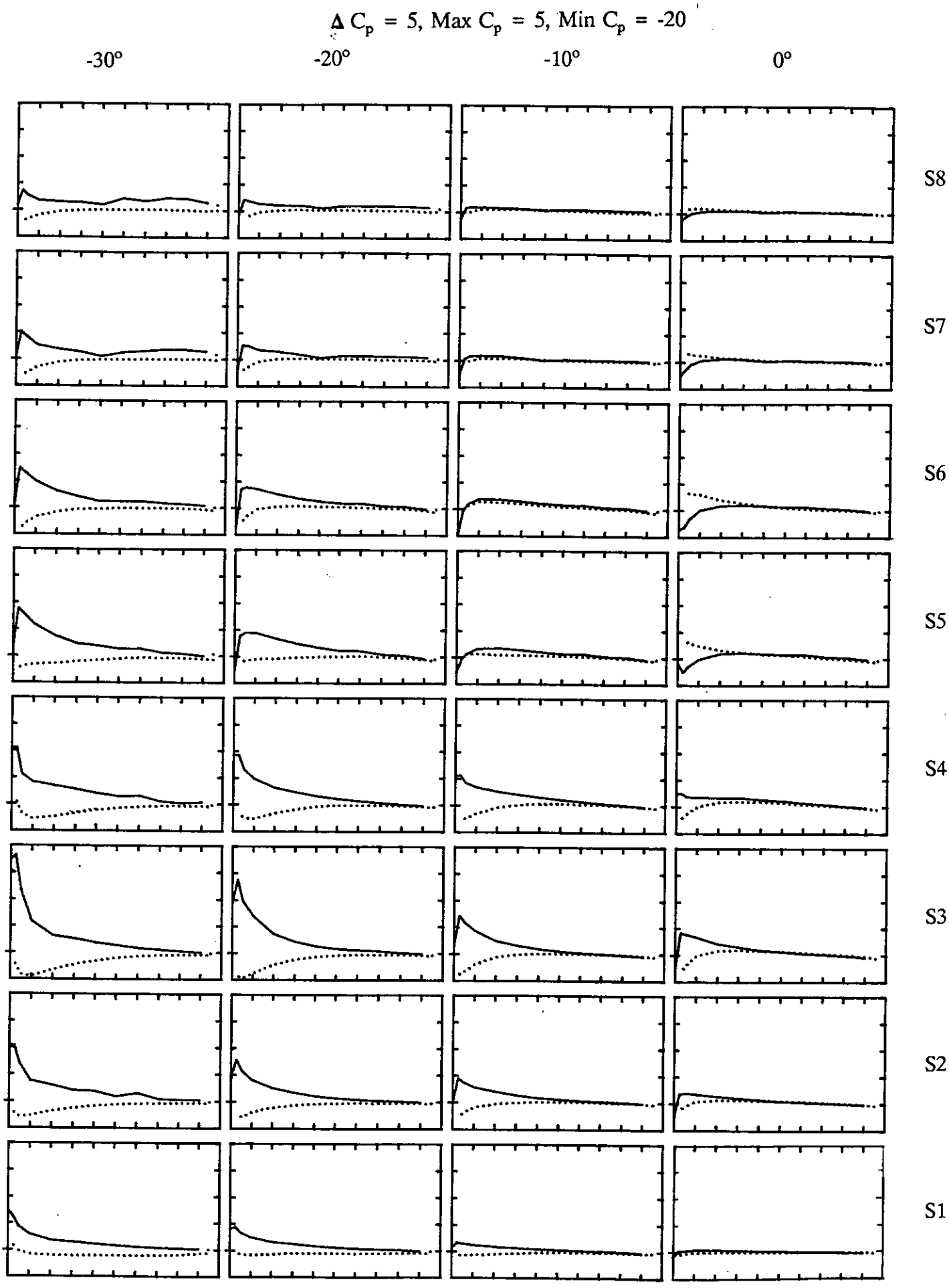

Figure 64 Chordwise pressure distributions at 8 spanwise positions for Rudder No. 2 at J=0.51 for X/D=0.52 at incidence of -30°,-20°,-10°,0°,10°,20°, and 30°.

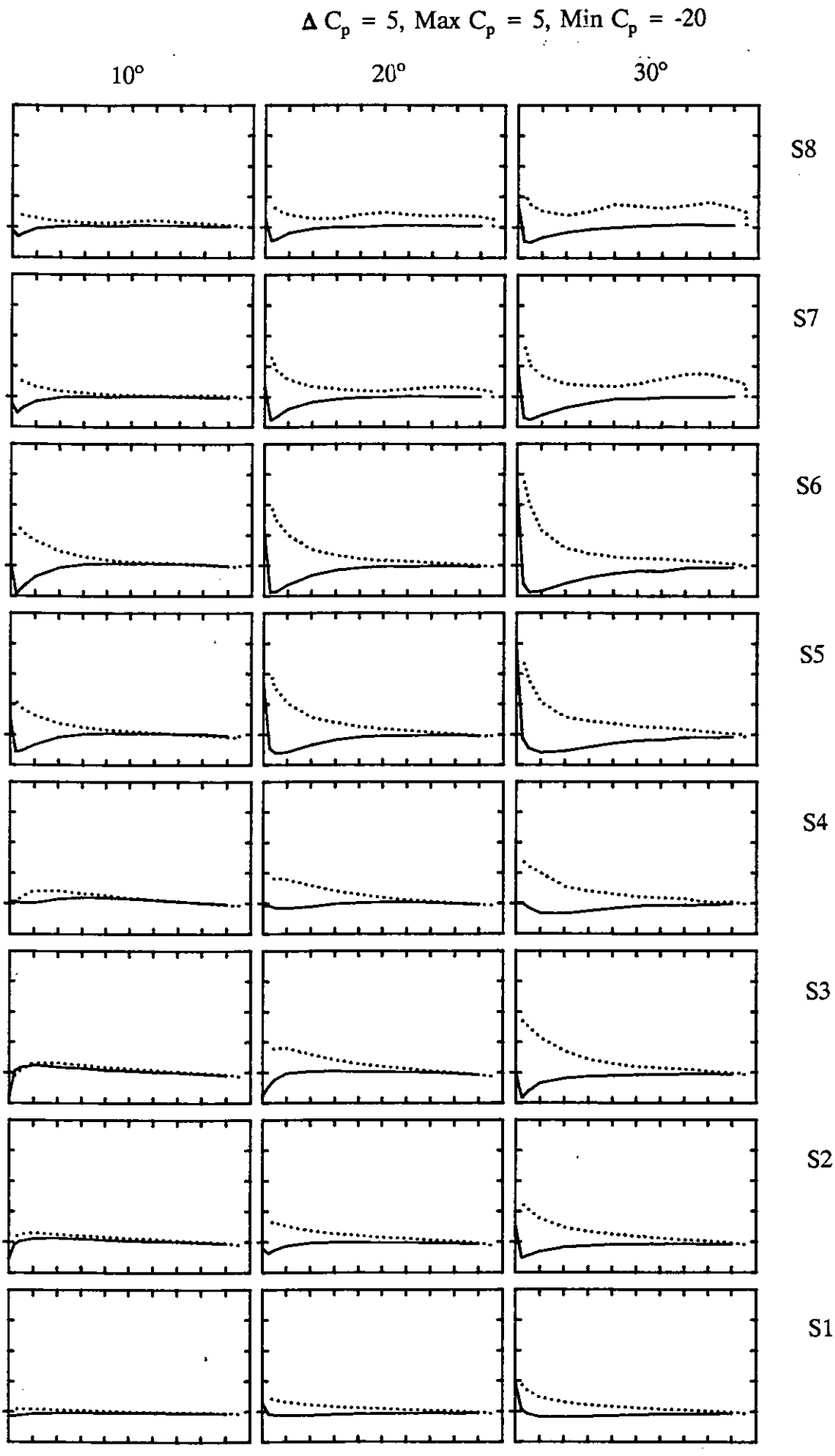

Figure 64 cont.

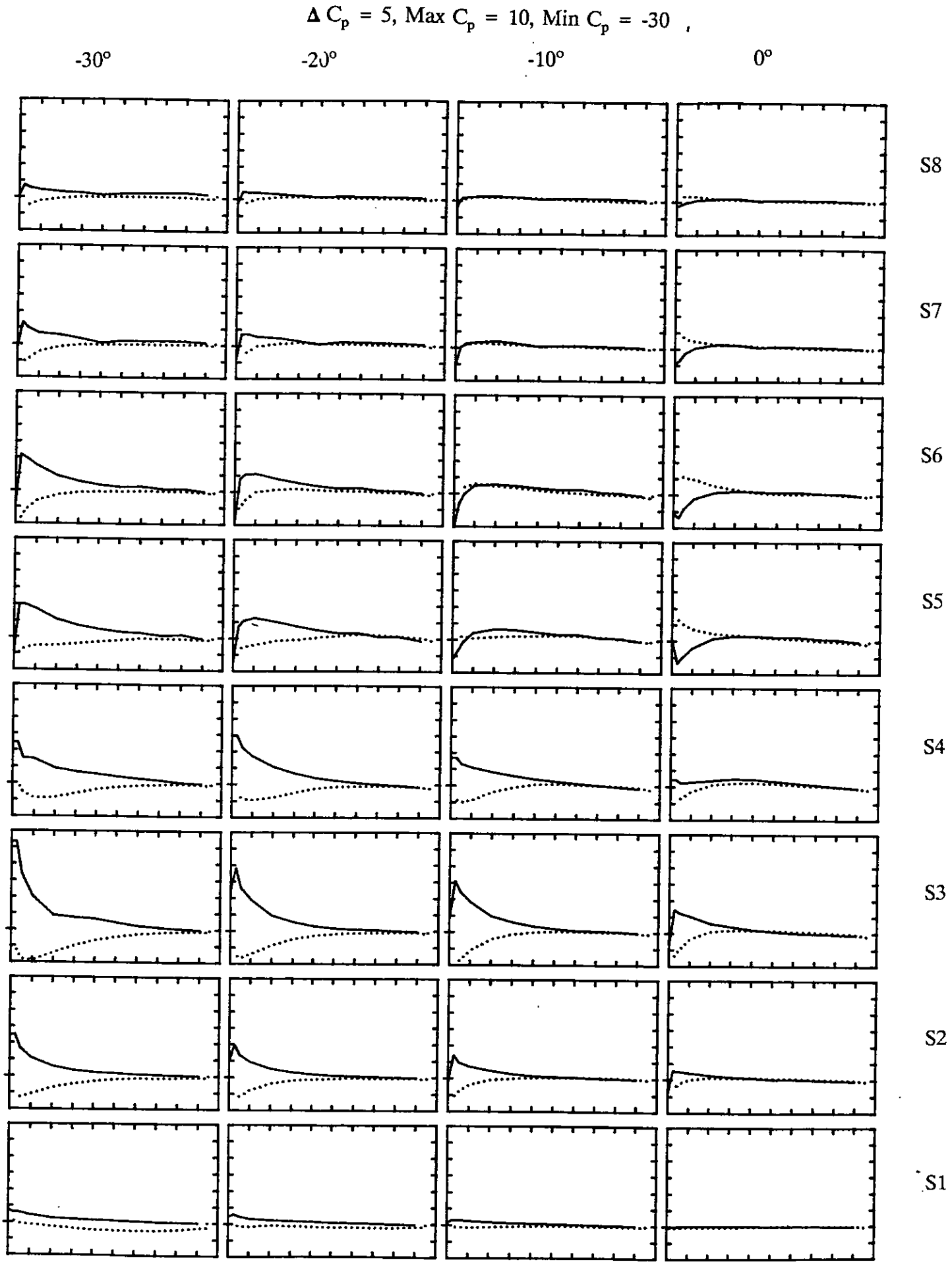

Figure 65 Chordwise pressure distributions at 8 spanwise positions for Rudder No. 2 at J=0.35 for X/D=0.3 at incidence of -30°,-20°,-10°,0°,10°,20°, and 30°.

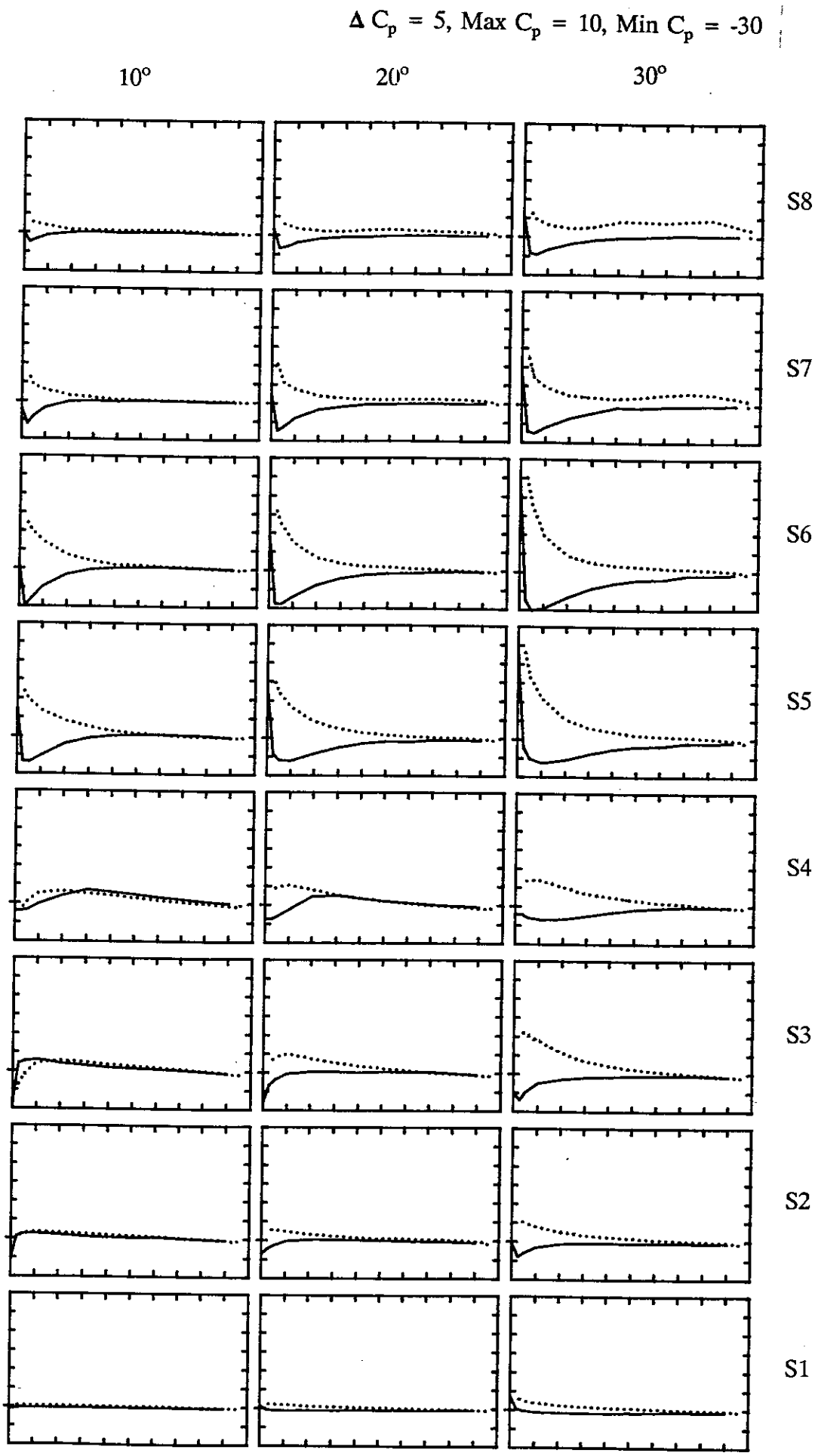

Figure 65 cont.

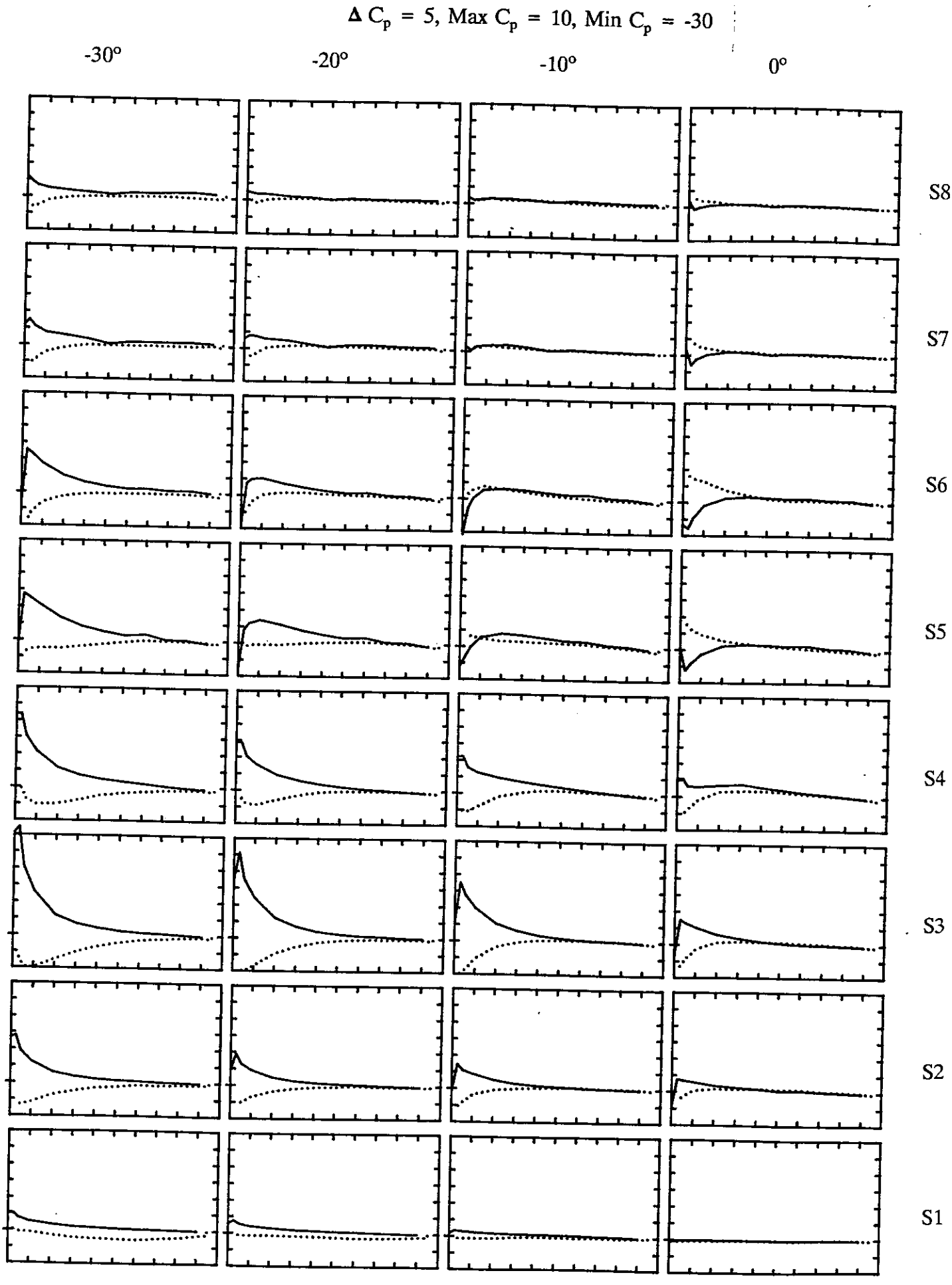

Figure 66 Chordwise pressure distributions at 8 spanwise positions for Rudder No. 2 at J=0.35 for X/D=0.39 at incidence of -30°,-20°,-10°,0°,10°,20°, and 30°.

$\Delta C_p = 5$, Max $C_p = 10$, Min $C_p = -30$

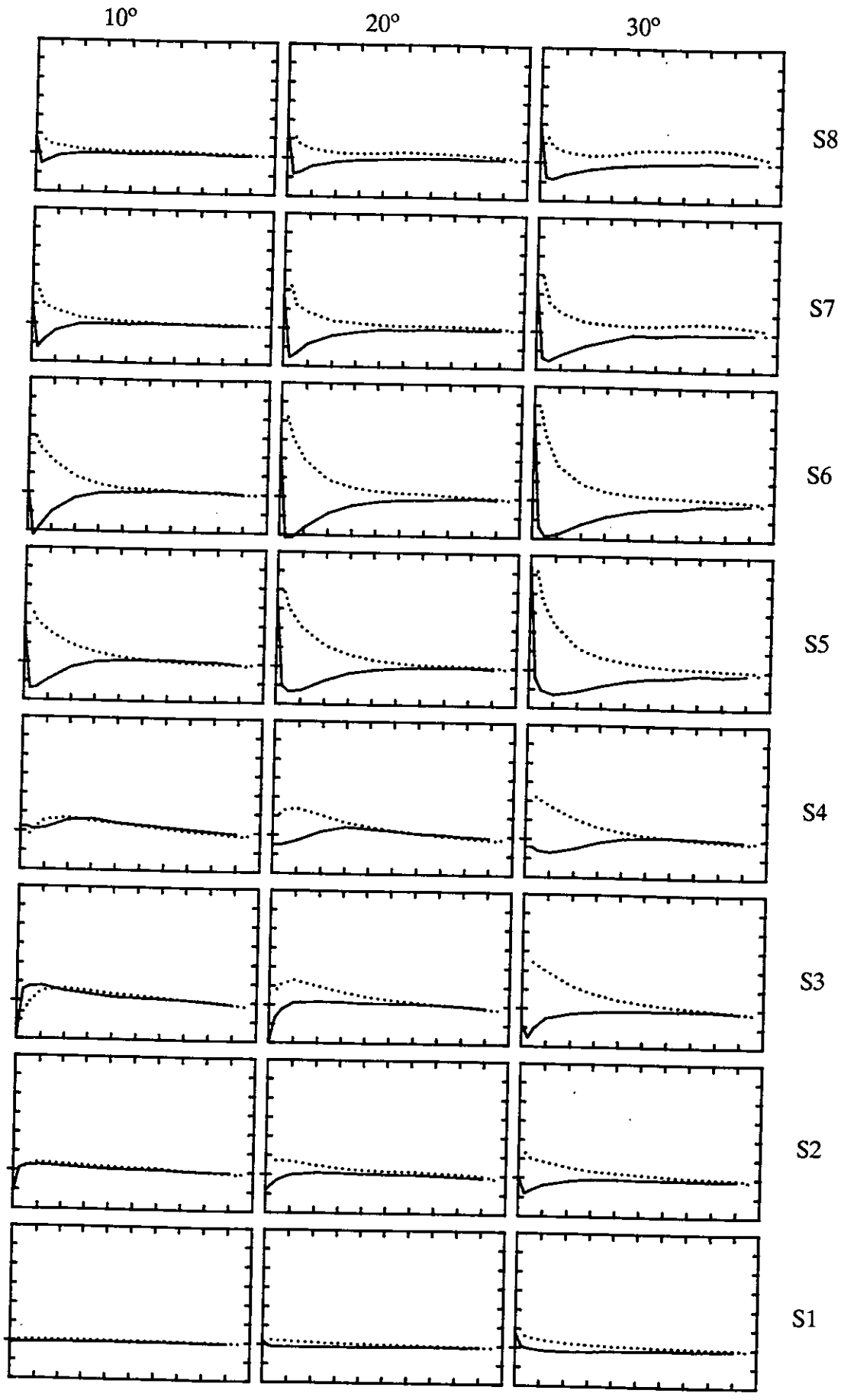

Figure 66 cont.

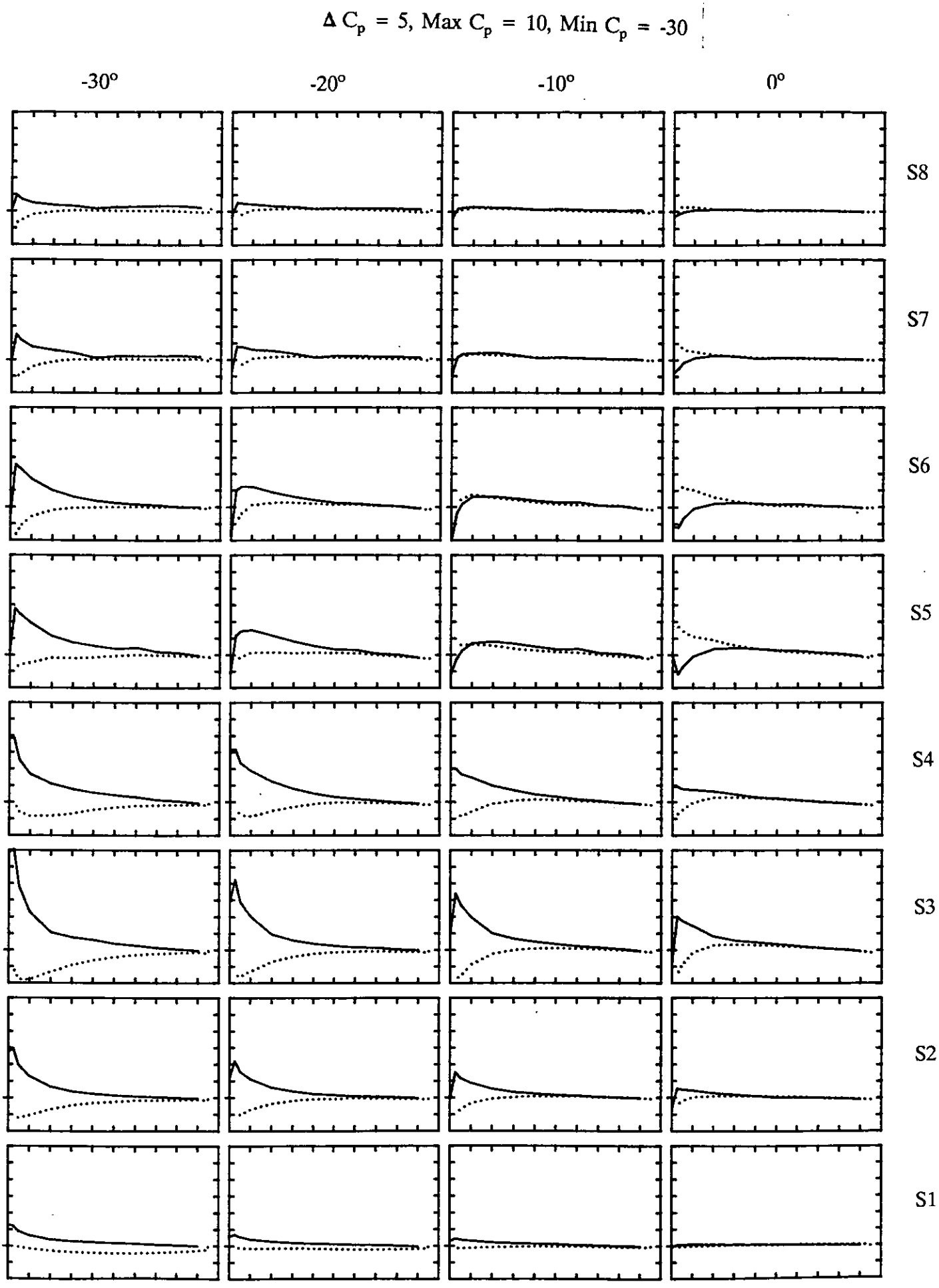

Figure 67 Chordwise pressure distributions at 8 spanwise positions for Rudder No. 2 at J = 0.35 for X/D = 0.52 at incidence of -30°,-20°,-10°,0°,10°,20°, and 30°.

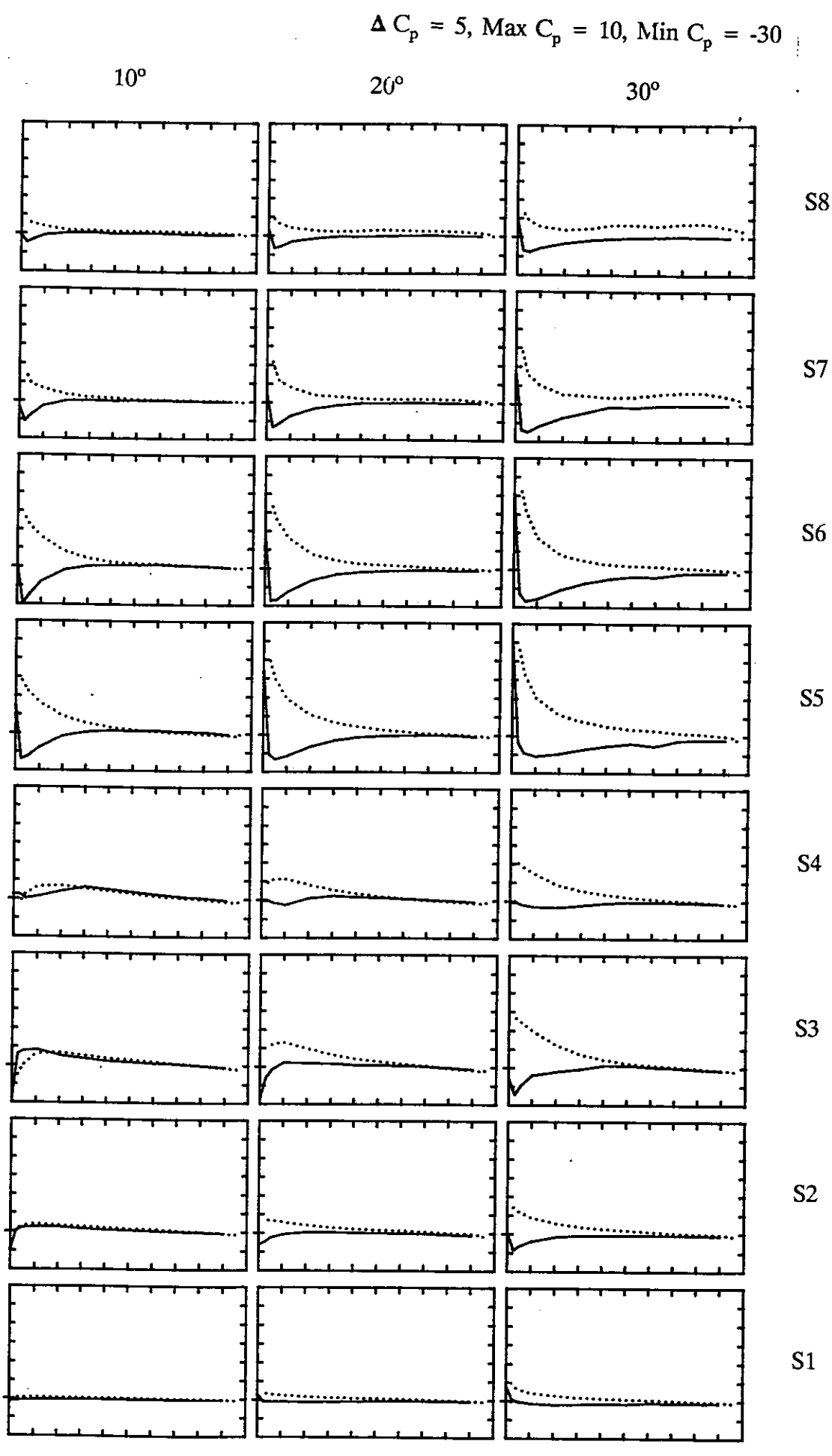

Figure 67 cont.

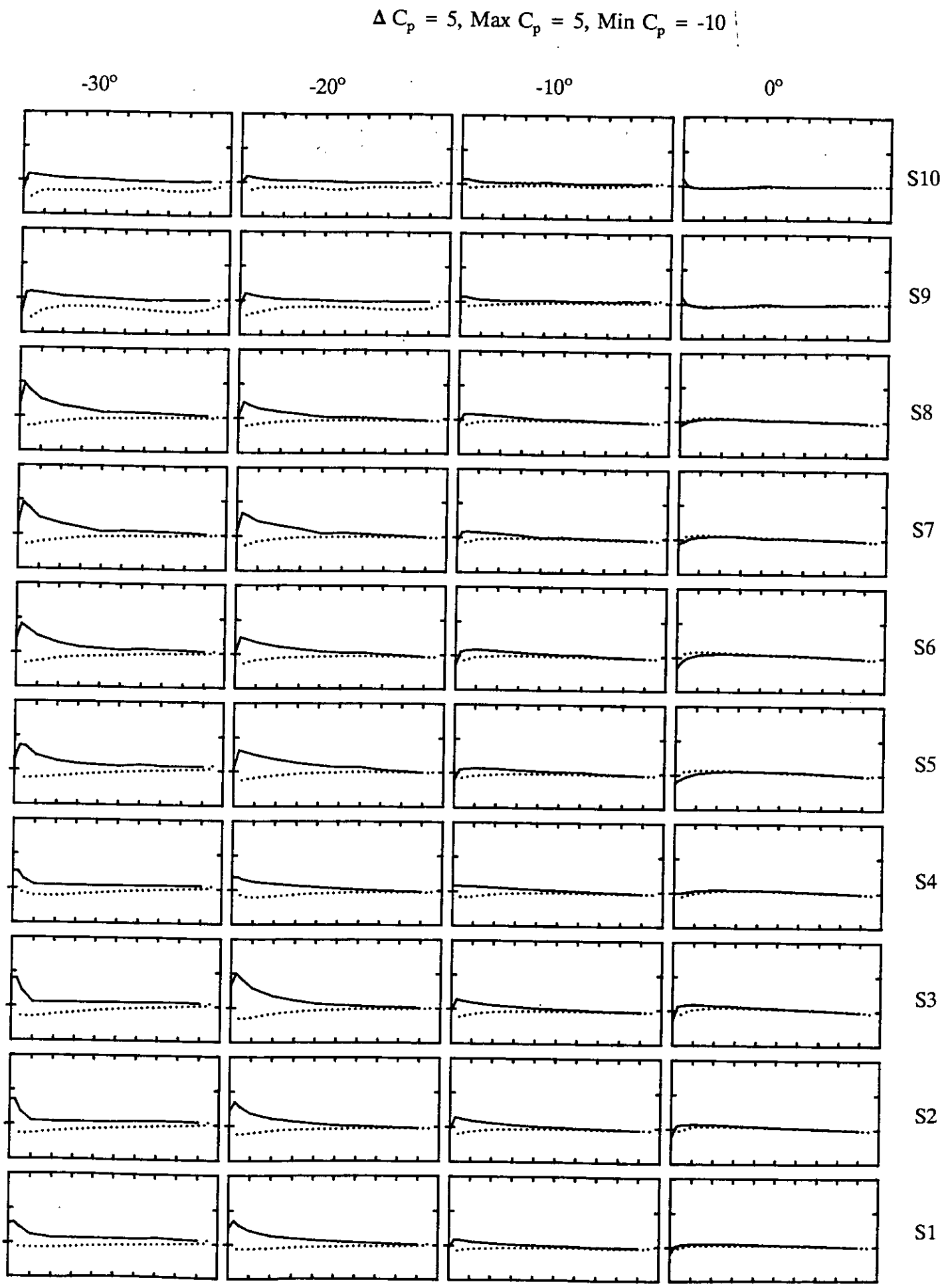

Figure 68 Chordwise pressure distributions at 10 spanwise positions for Rudder No. 3 at J=0.94 for X/D=0.3 at incidence of -30°,-20°,-10°,0°,10°,20°, and 30°.

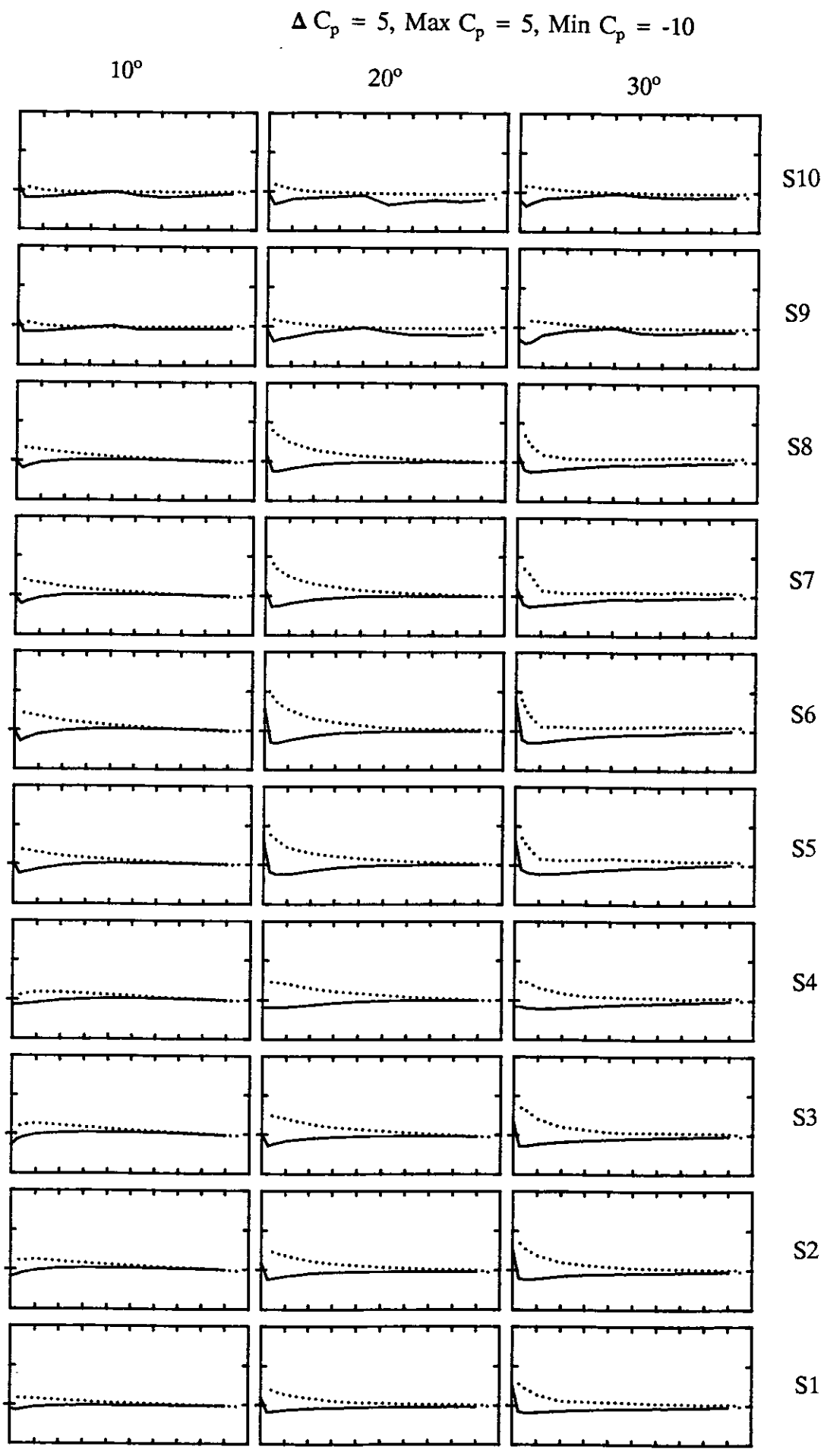

Figure 68 cont.

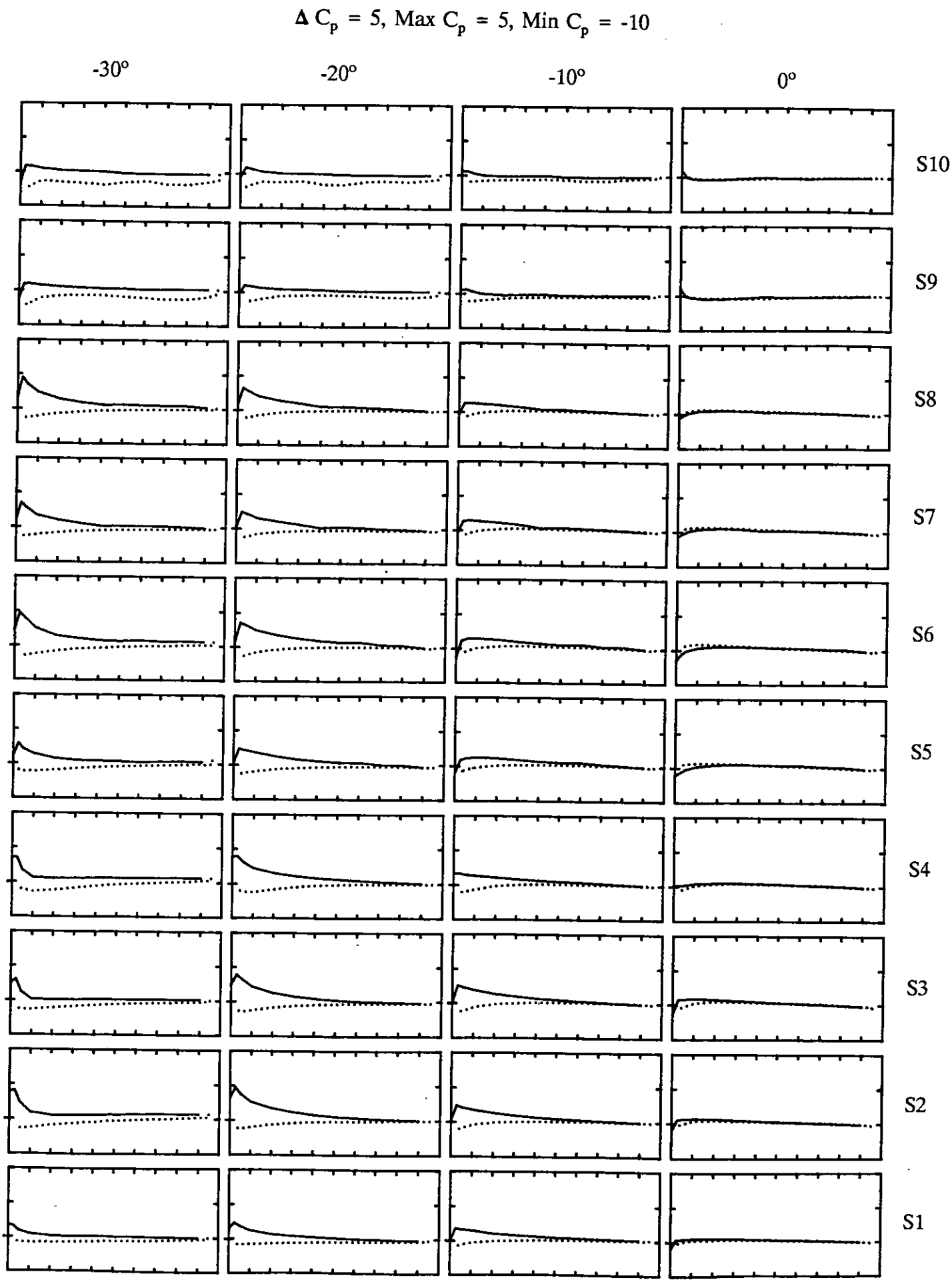

Figure 69 Chordwise pressure distributions at 10 spanwise positions for Rudder No. 3 at J=0.94 for X/D=0.39 at incidence of -30°,-20°,-10°,0°,10°,20°, and 30°.

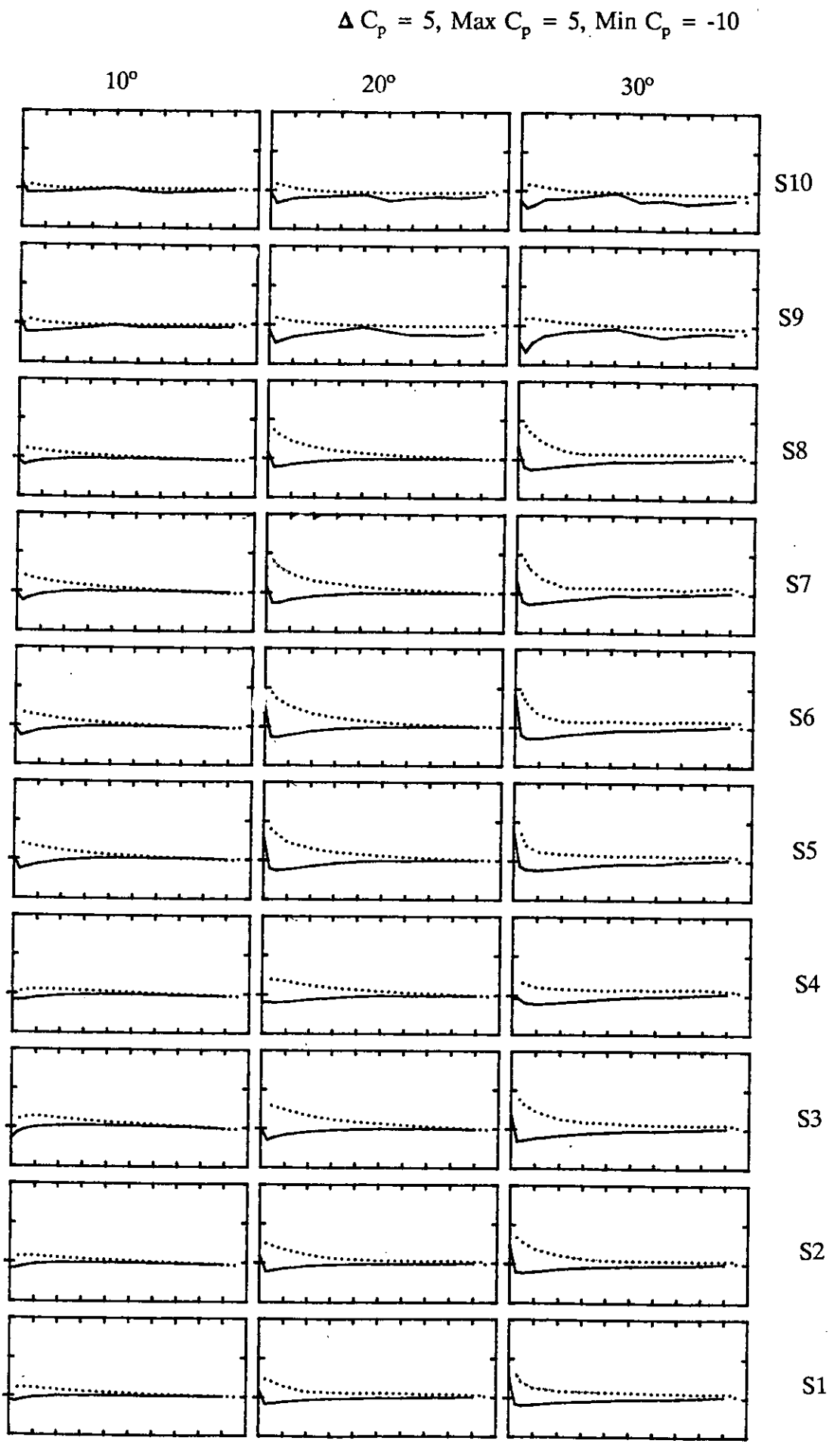

Figure 69 cont.

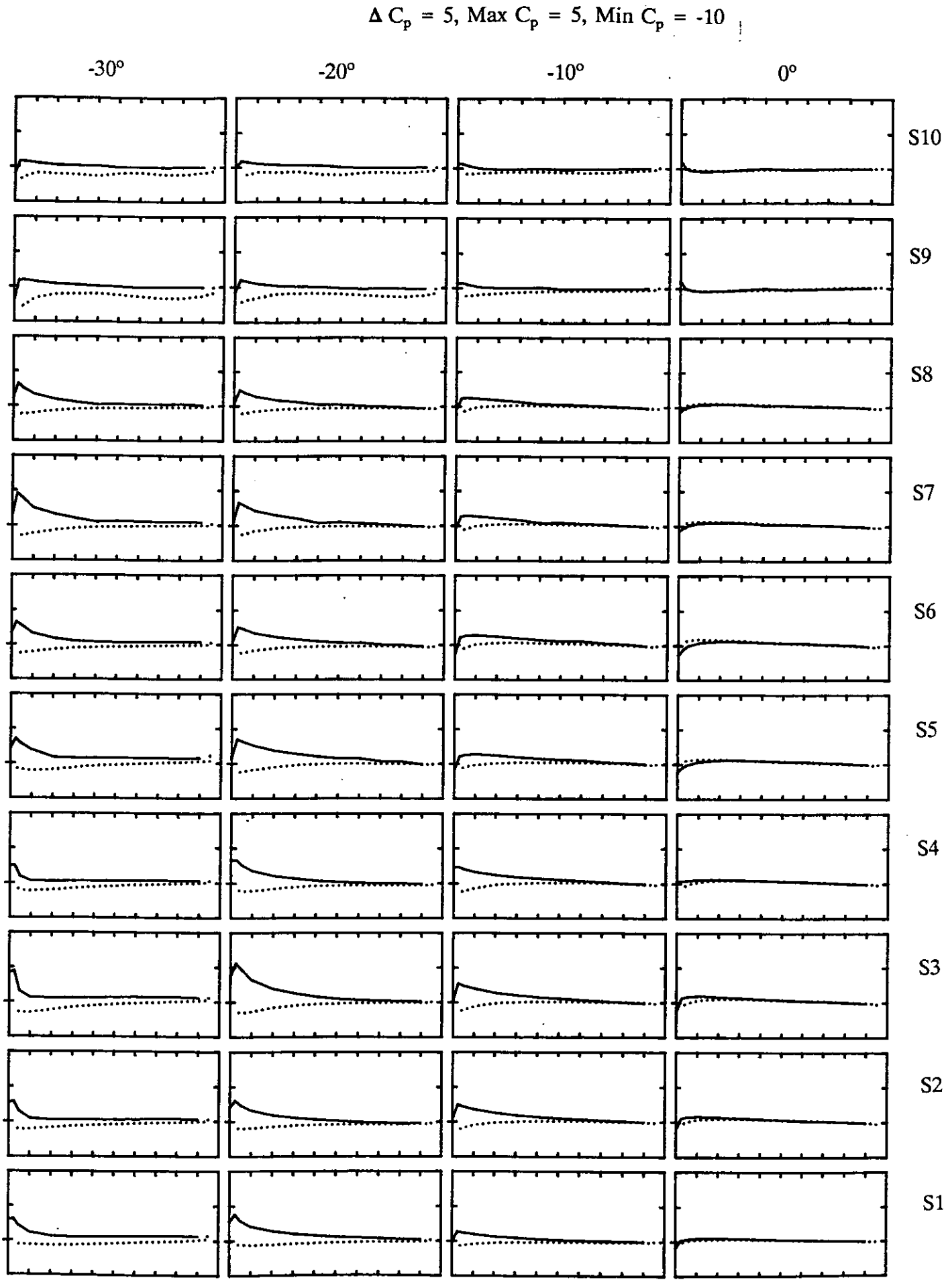

Figure 70 Chordwise pressure distributions at 10 spanwise positions for Rudder No. 3 at J=0.94 for X/D=0.52 at incidence of -30°,-20°,-10°,0°,10°,20°, and 30°.

$\Delta C_p = 5$, Max $C_p = 5$, Min $C_p = -10$

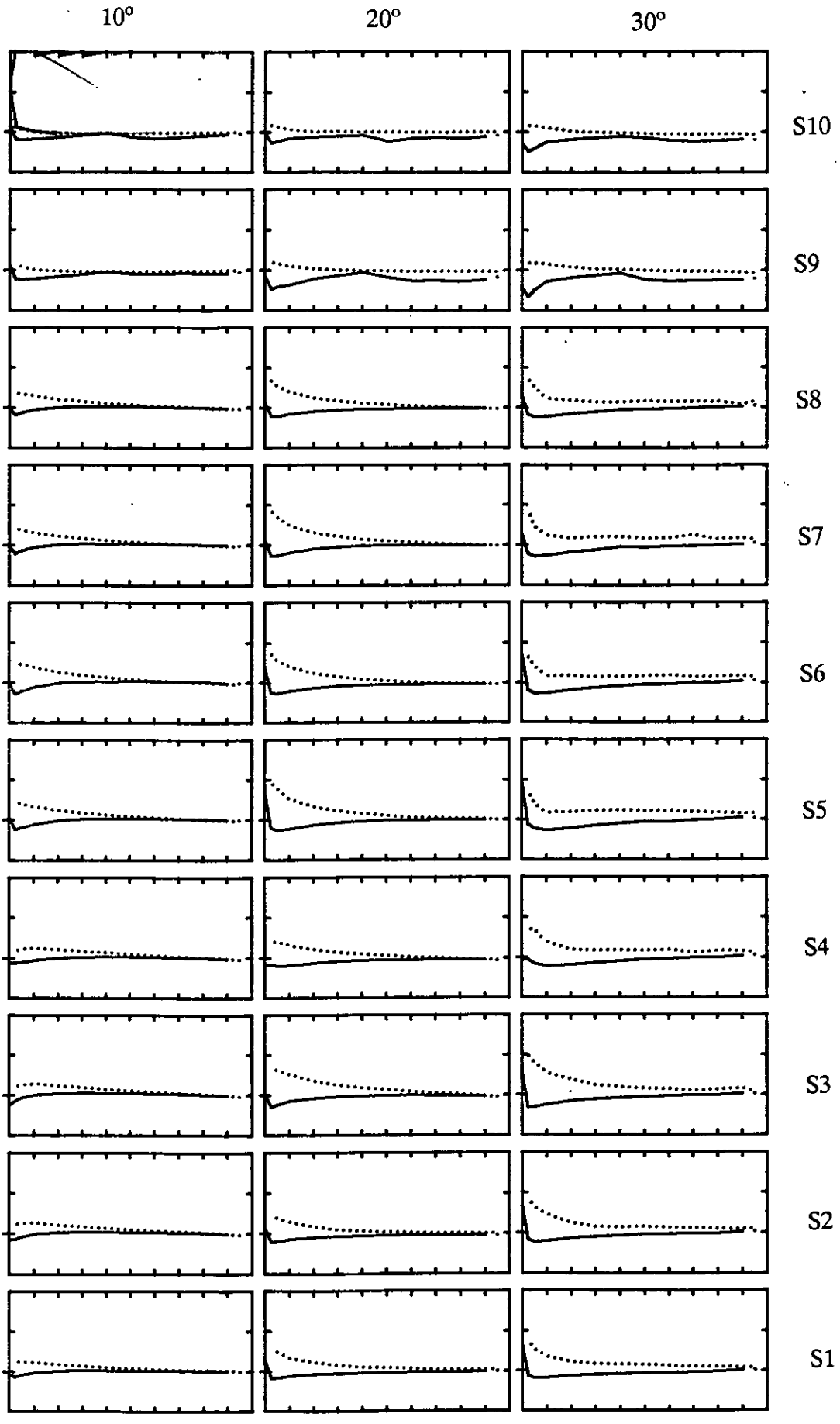

Figure 70 cont.

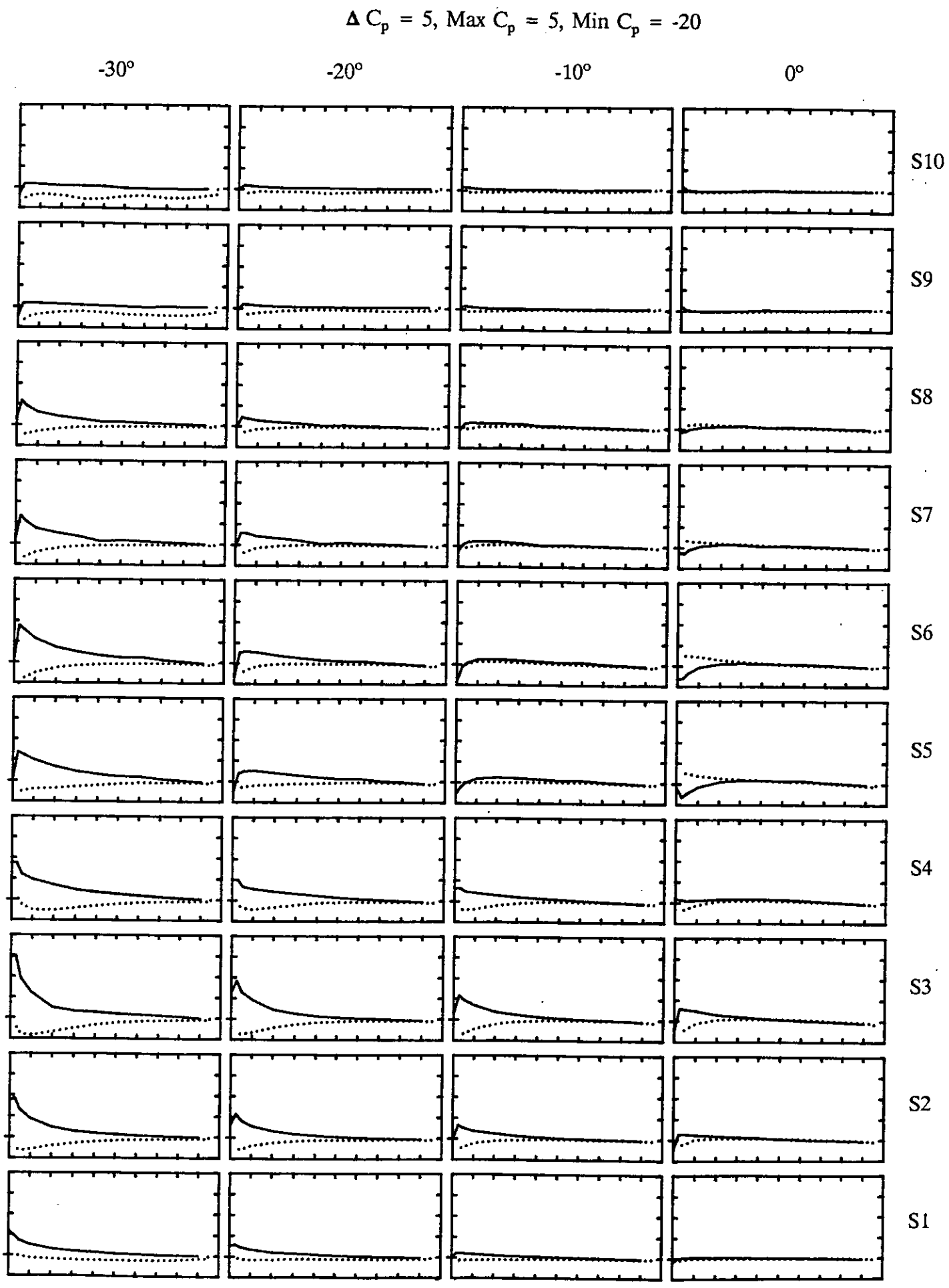

Figure 71 Chordwise pressure distributions at 10 spanwise positions for Rudder No. 3 at J=0.51 for X/D=0.3 at incidence of -30°,-20°,-10°,0°,10°,20°, and 30°.

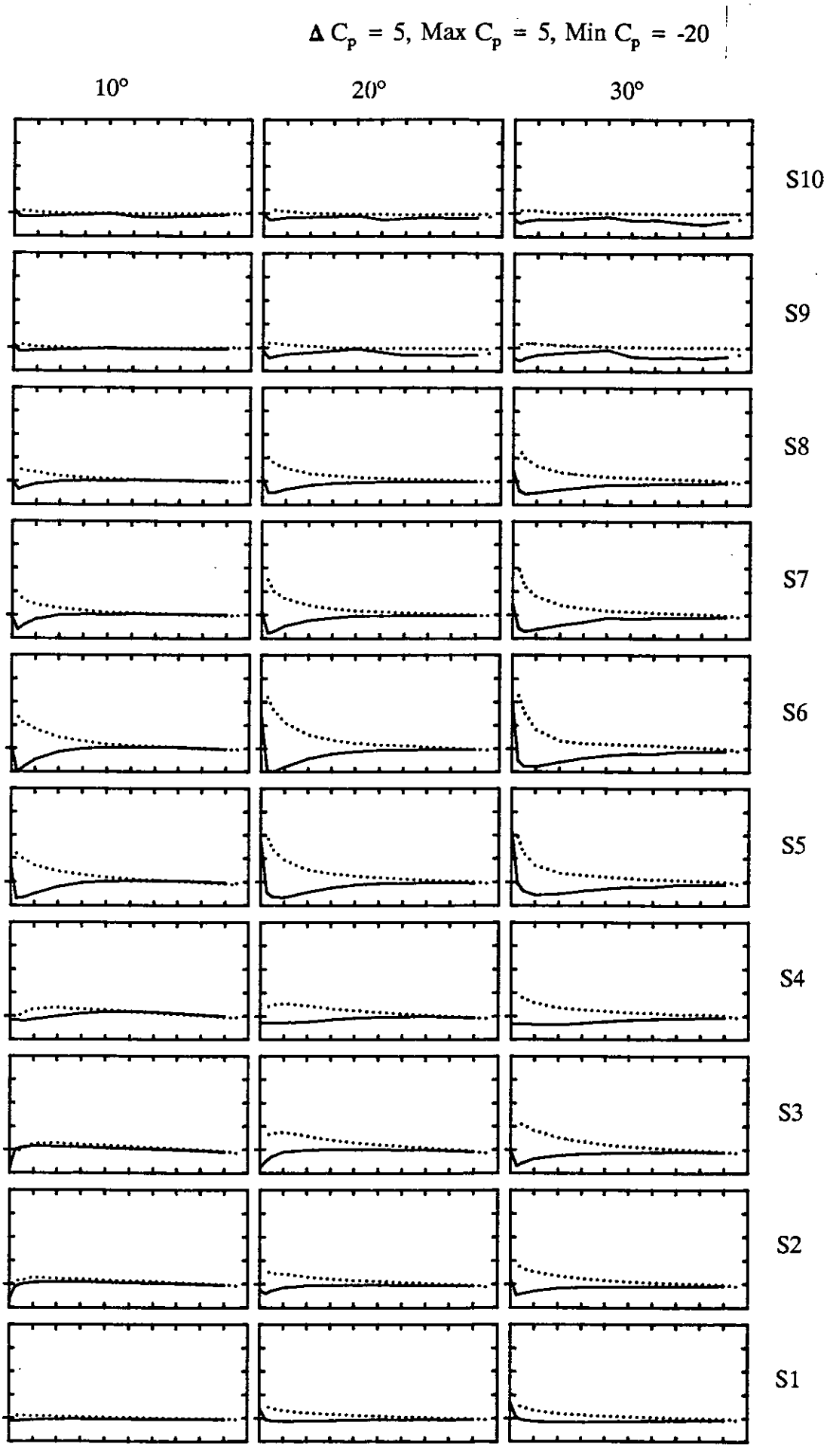

Figure 71 cont.

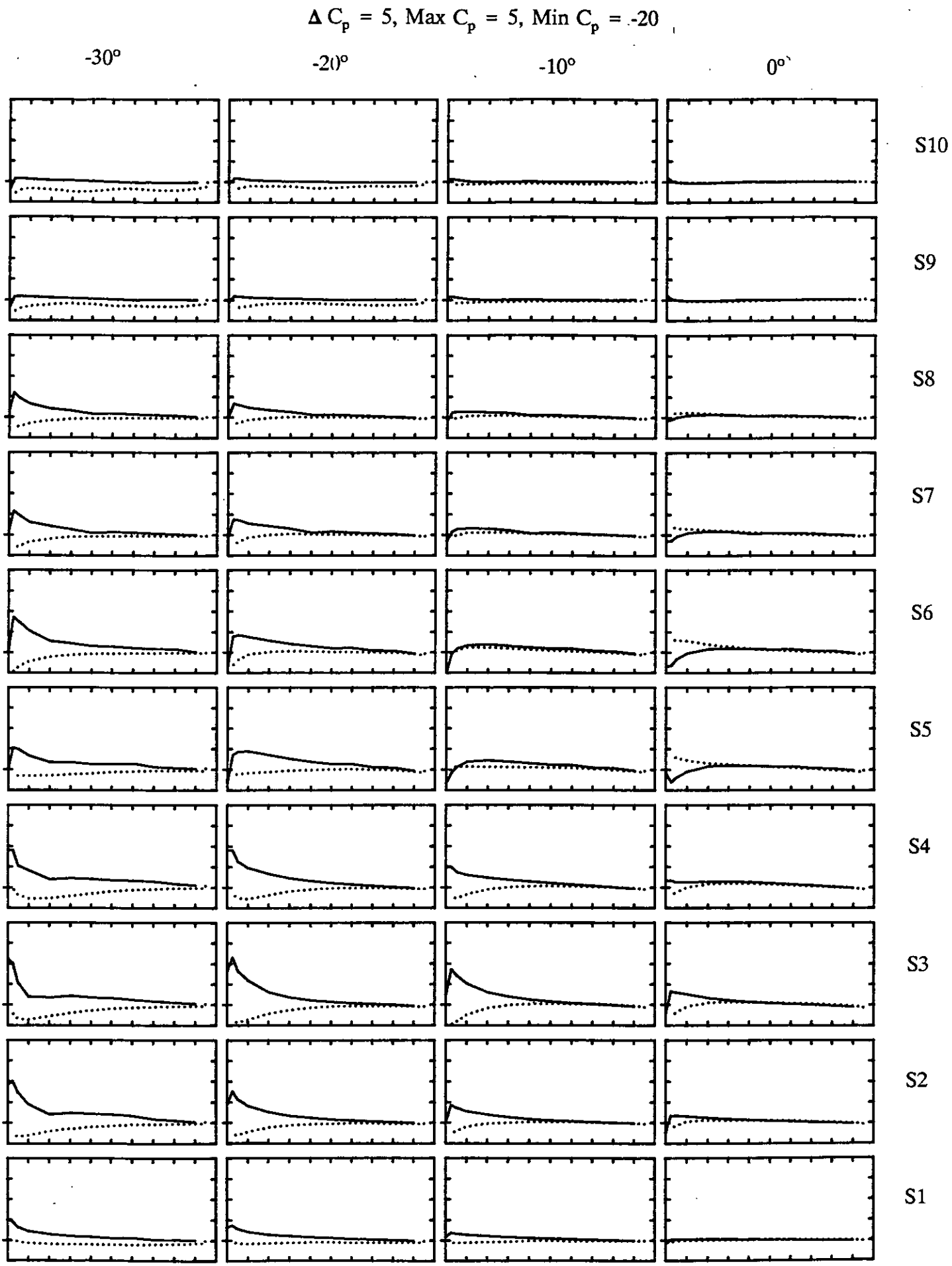

Figure 72 Chordwise pressure distributions at 10 spanwise positions for Rudder No. 3 at J=0.51 for X/D=0.39 at incidence of -30°,-20°,-10°,0°,10°,20°, and 30°.

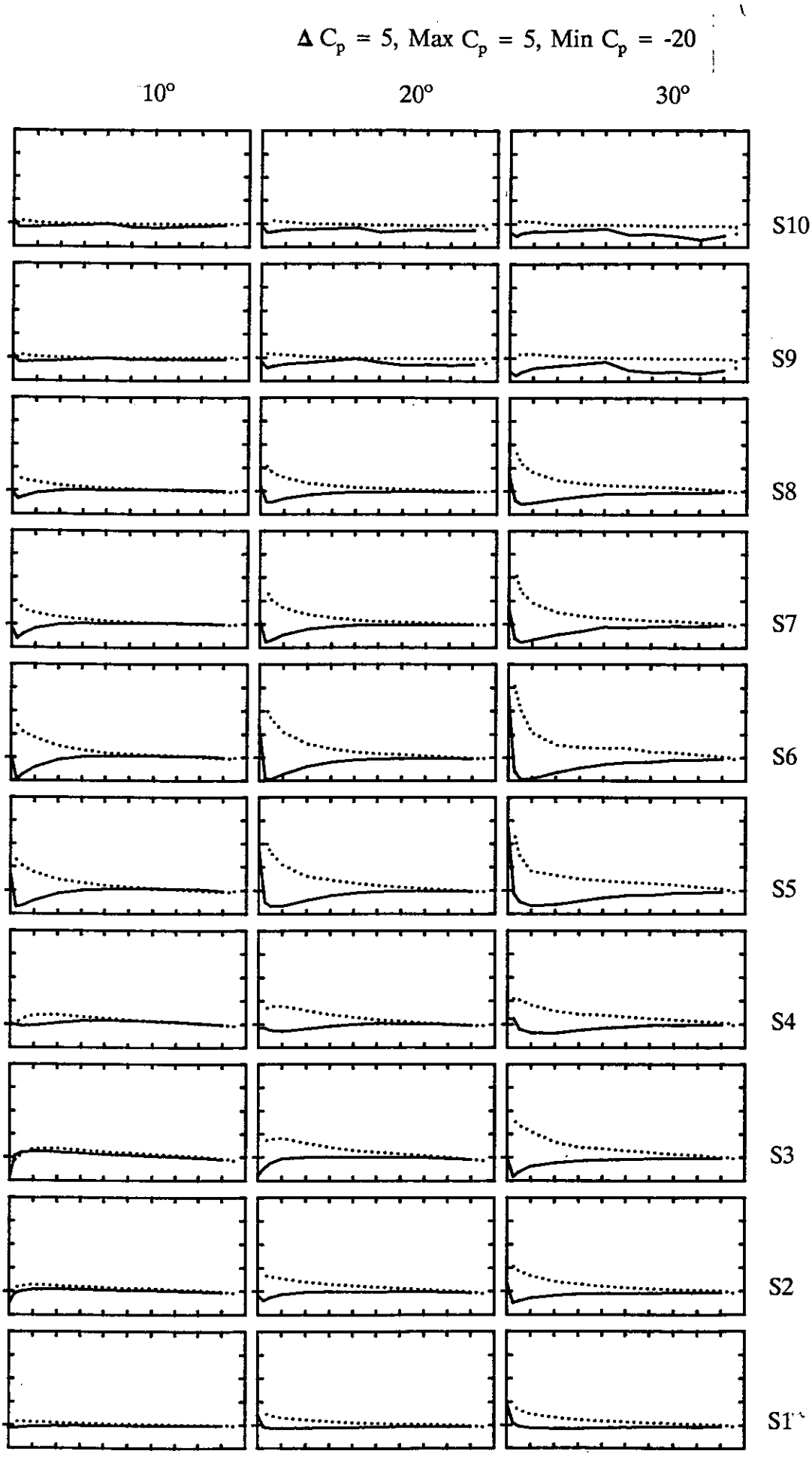

Figure 72 cont.

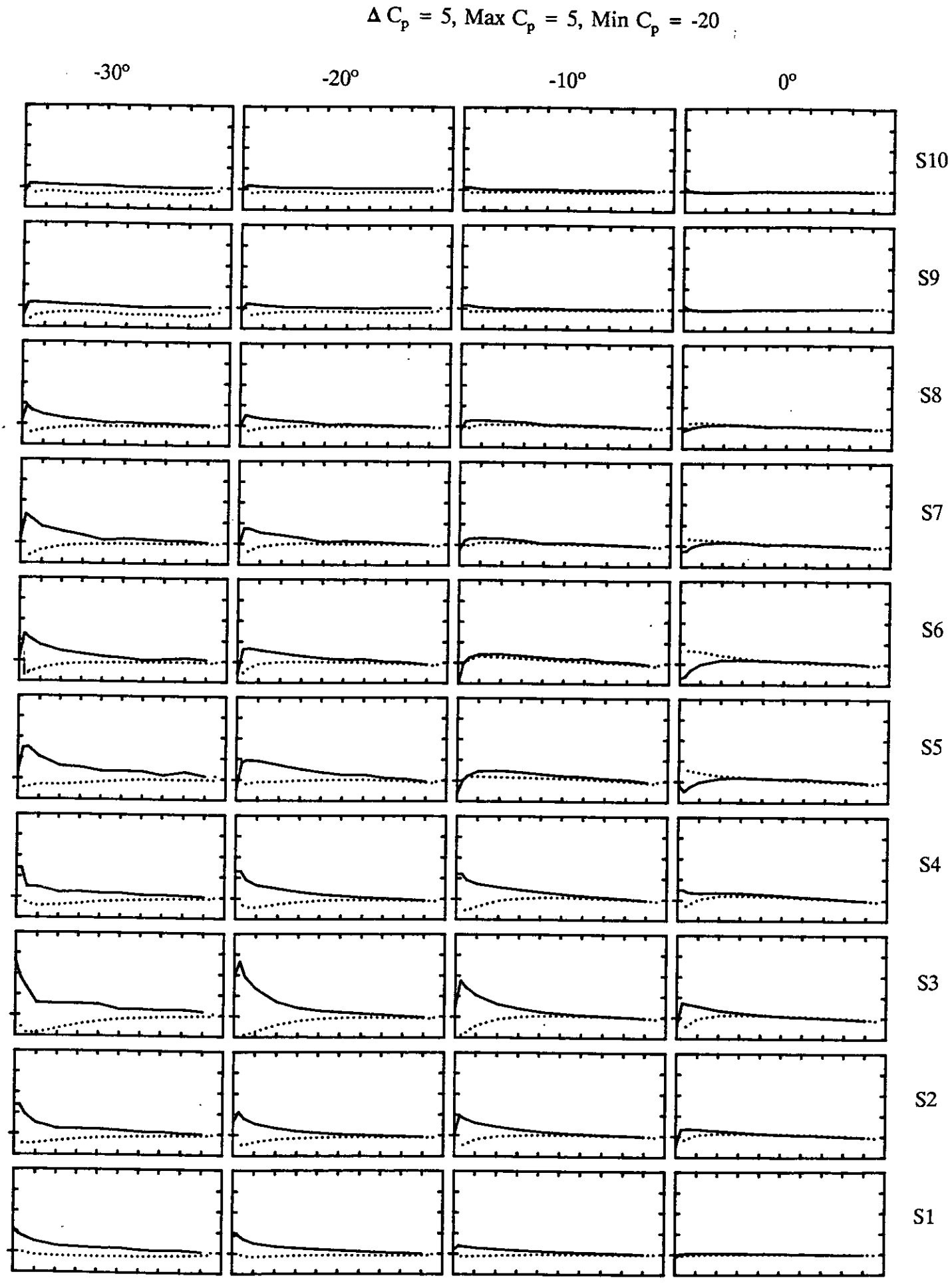

Figure 73 Chordwise pressure distributions at 10 spanwise positions for Rudder No. 3 at J=0.51 for X/D=0.52 at incidence of -30°,-20°,-10°,0°,10°,20°, and 30°.

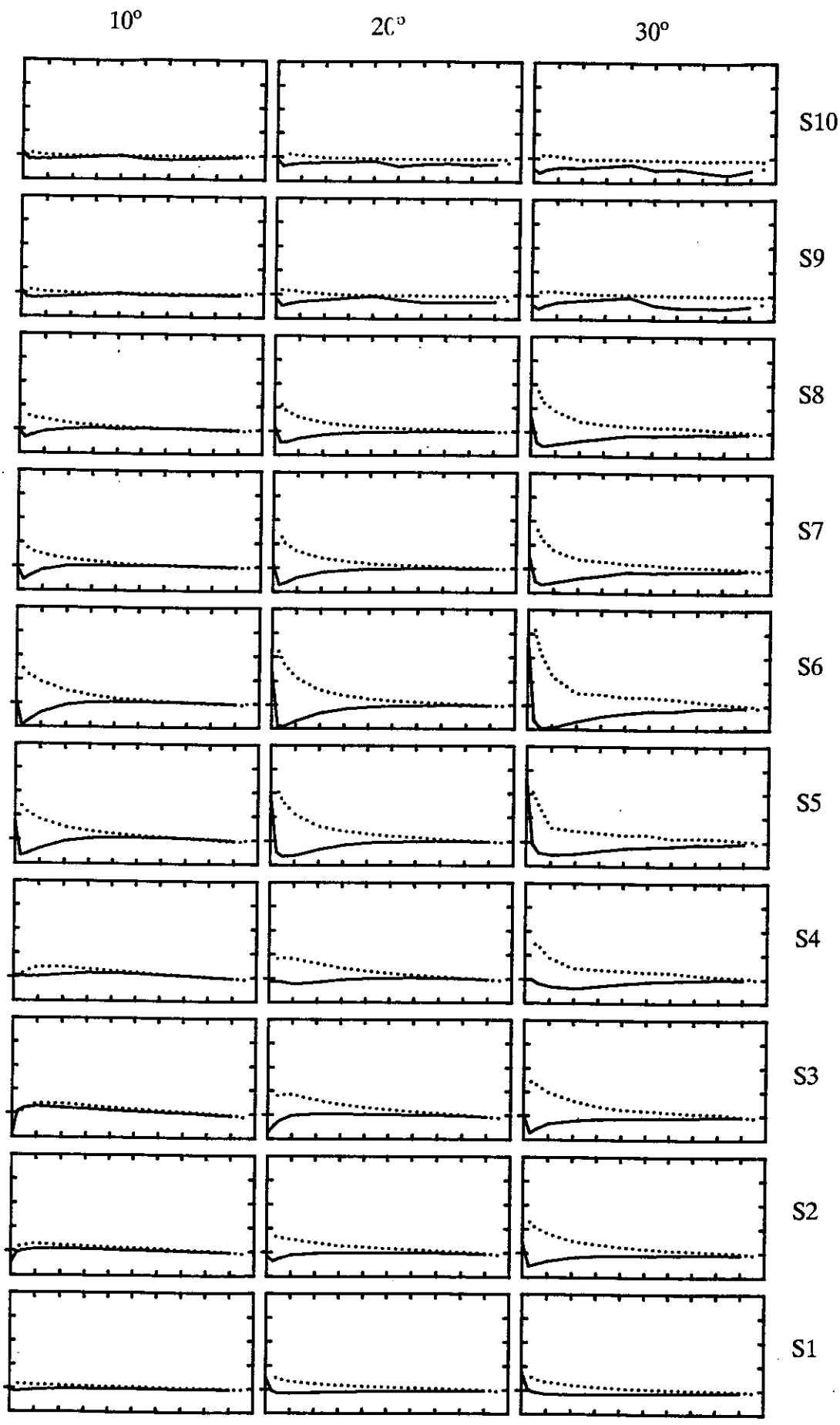

Figure 73 cont.

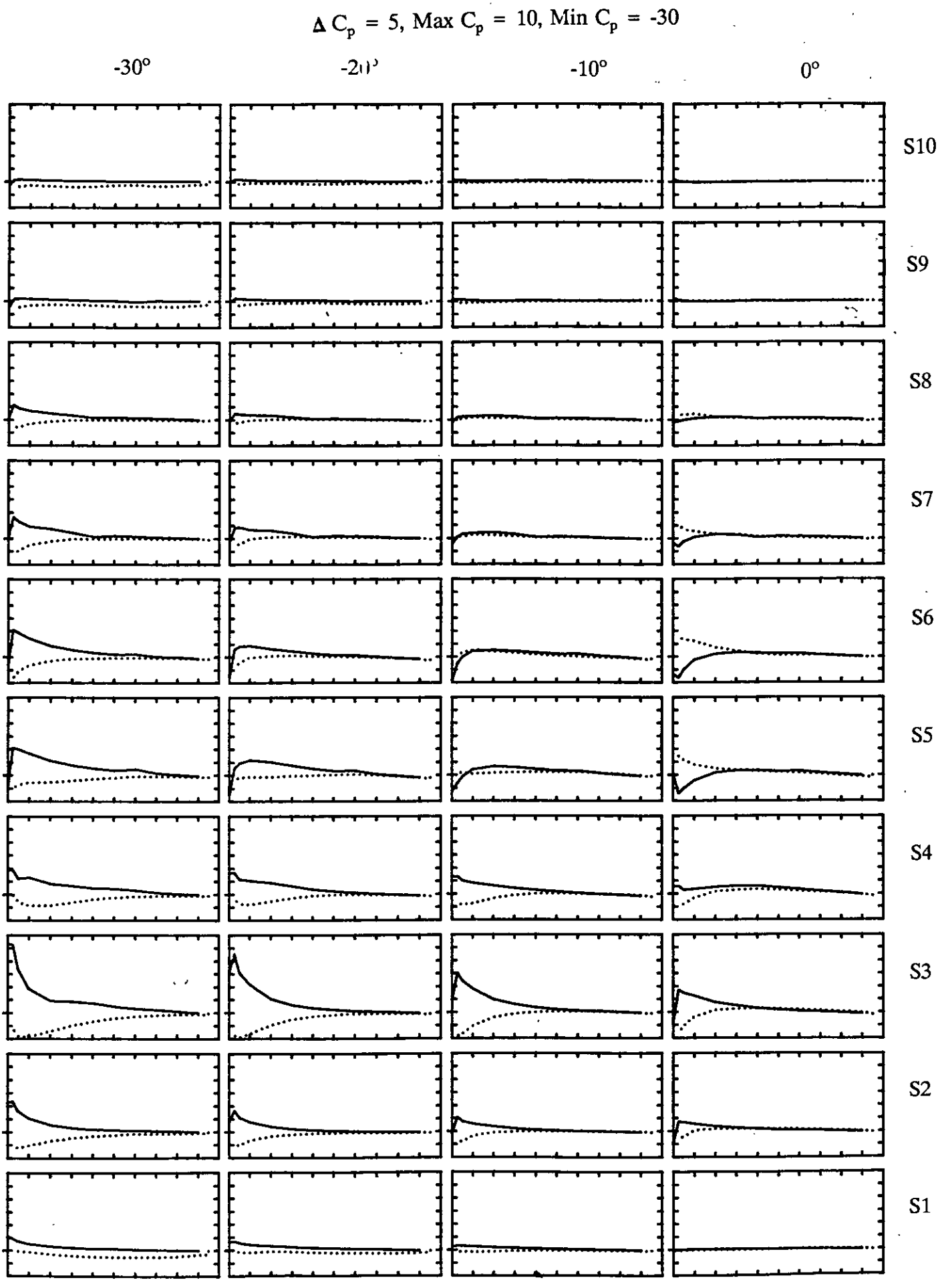

Figure 74 Chordwise pressure distributions at 10 spanwise positions for Rudder No. 3 at J=0.35 for X/D=0.3 at incidence of -30°,-20°,-10°,0°,10°,20°, and 30°.

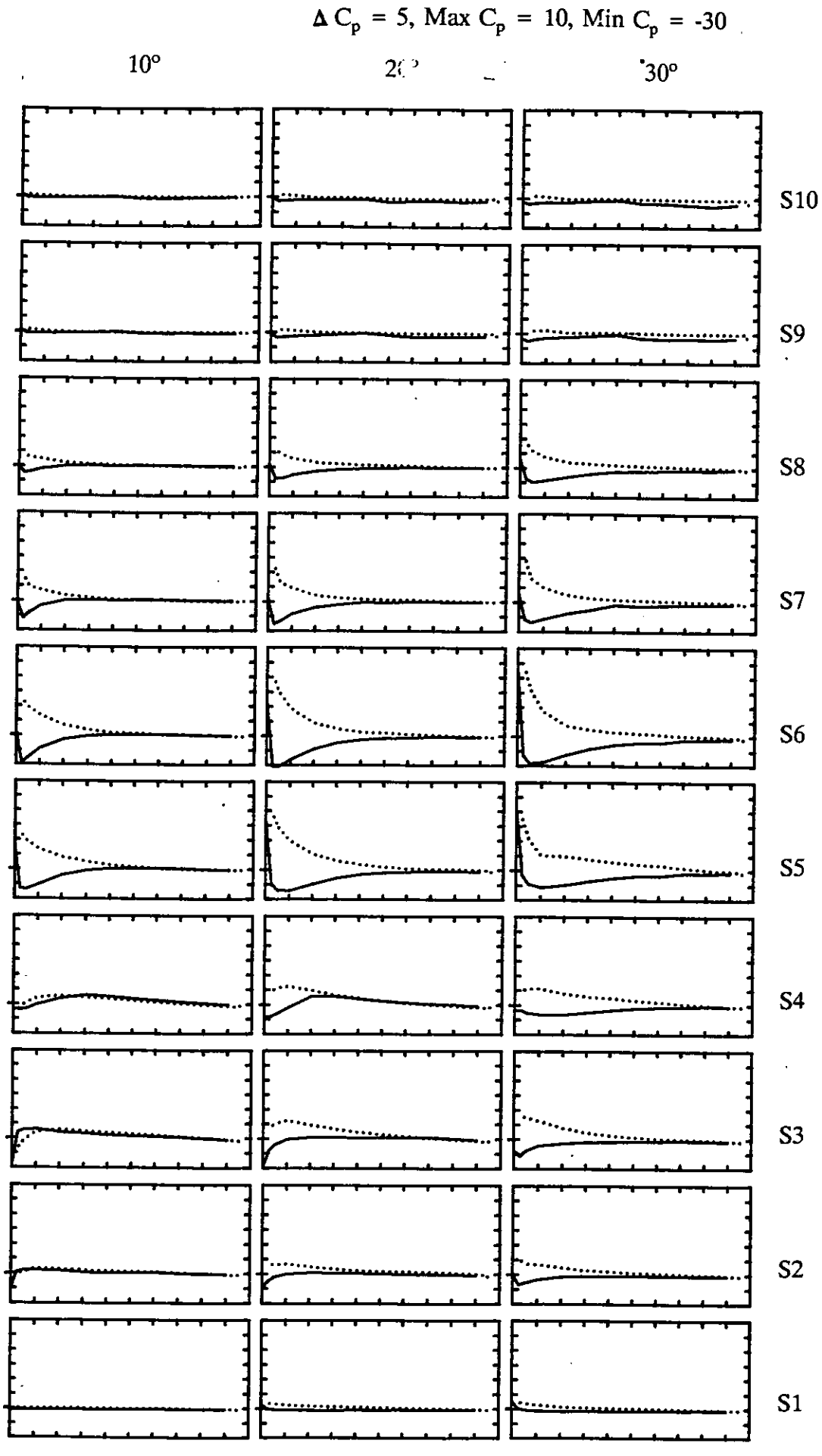

Figure 74 cont.

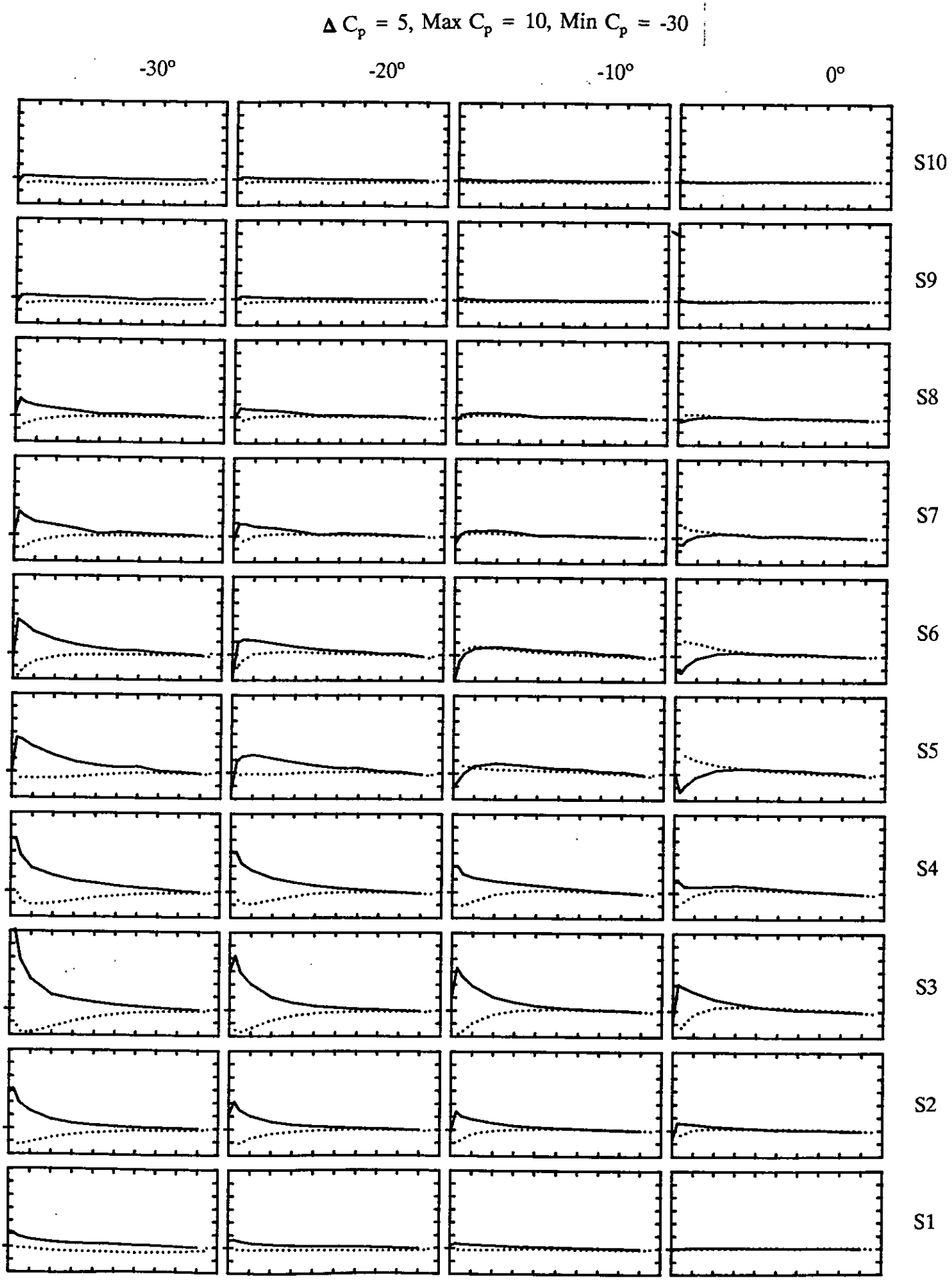

Figure 75 Chordwise pressure distributions at 10 spanwise positions for Rudder No. 3 at J=0.35 for X/D=0.39 at incidence of -30°,-20°,-10°,0°,10°,20°, and 30°.

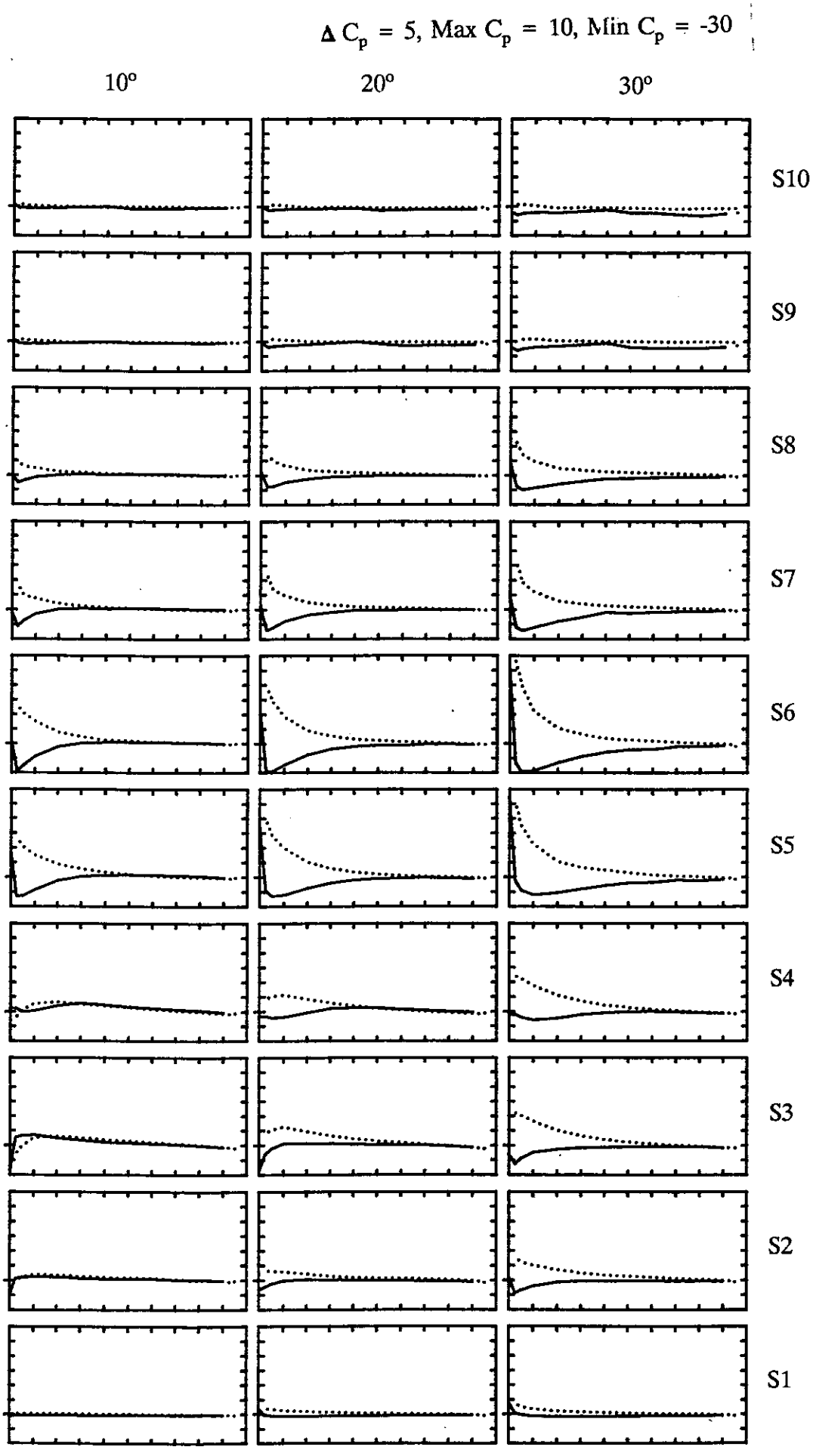

Figure 75 cont.

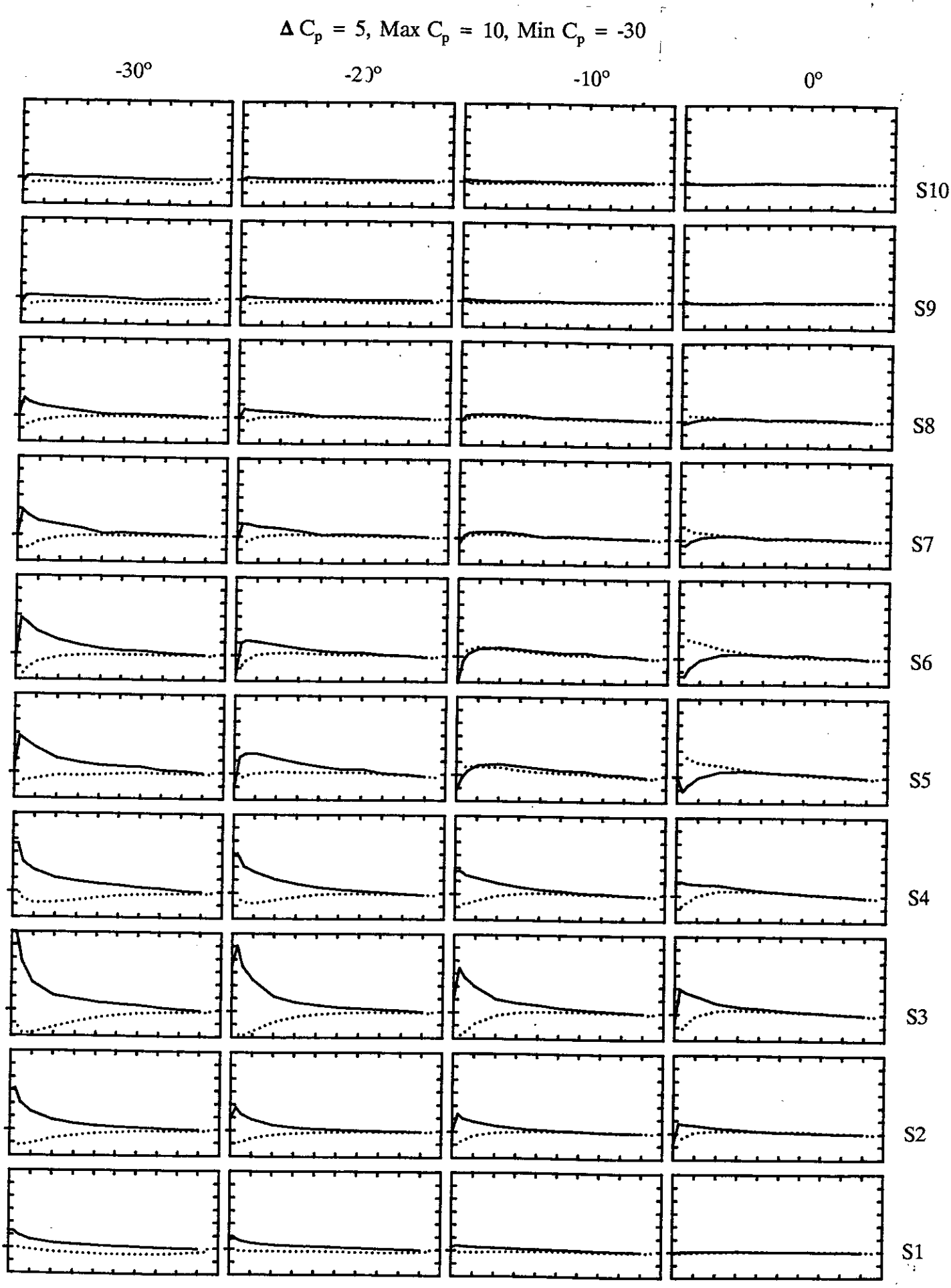

Figure 76 Chordwise pressure distributions at 10 spanwise positions for Rudder No. 3 at J=0.35 for X/D=0.52 at incidence of -30°,-20°,-10°,0°,10°,20°, and 30°.

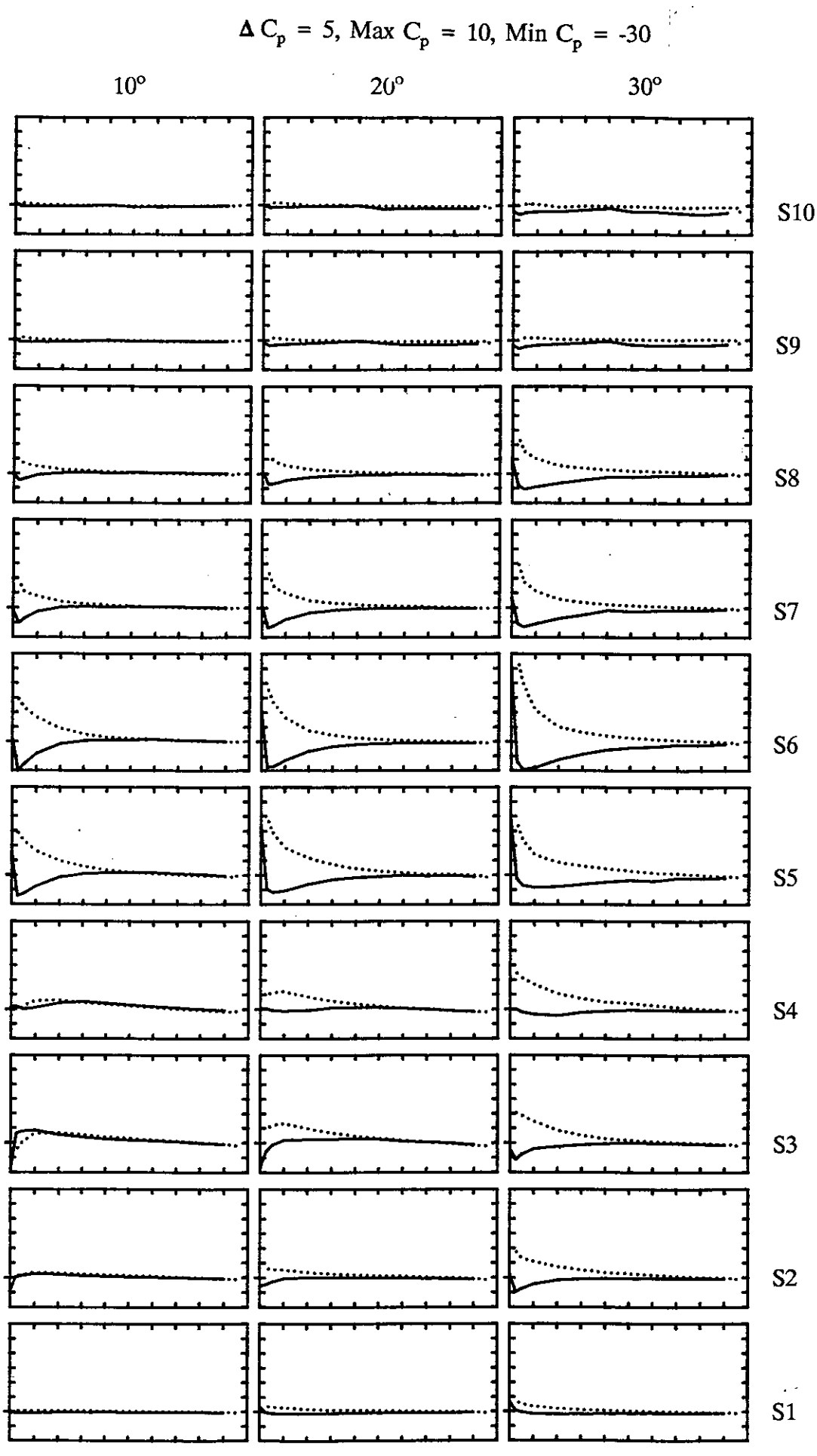

Figure 76 cont.